REWAS 2016

Towards Materials Resource Sustainability

Editors:

Randolph E. Kirchain
Bart Blanpain
Christina Meskers
Elsa Olivetti
Diran Apelian
John Howarter
Anne Kvithyld
Brajendra Mishra
Neale R. Neelameggham
Jeff Spangenberger

TMS

Springer


REWAS
2016
Towards Materials
Resource
Sustainability

TMS2016

145th Annual Meeting & Exhibition

FEBRUARY 14-18 DOWNTOWN NASHVILLE, TENNESSEE MUSIC CITY CENTER

New proceedings volumes from the TMS2016 Annual Meeting:

- 7th International Symposium on High-Temperature Metallurgical Processing
- CFD Modeling and Simulation in Materials Processing 2016
- Characterization of Minerals, Metals, and Materials 2016
- Energy Technology 2016: Carbon Dioxide Management and Other Technologies
- EPD Congress 2016
- Light Metals 2016
- Magnesium Technology 2016
- Rare Metal Technology 2016
- REWAS 2016
- Shape Casting: 6th International Symposium
- TMS 2016 Supplemental Proceedings

REWAS 2016

Towards Materials Resource Sustainability

Proceedings of a symposium sponsored by
the Recycling and Environmental Technologies Committee, the Materials and Society Committee, the Extraction & Processing Division, and the Light Metals Division of
The Minerals, Metals & Materials Society (TMS)

held during

TMS2016
145th Annual Meeting & Exhibition

FEBRUARY 14-18 DOWNTOWN NASHVILLE, TENNESSEE MUSIC CITY CENTER

Edited by:

Randolph E. Kirchain, Bart Blanpain, Christina Meskers, Elsa Olivetti, Diran Apelian, John Howarter, Anne Kvithyld, Brajendra Mishra, Neale R. Neelameggham, and Jeff Spangenberger

Editors

Randolph E. Kirchain
Bart Blanpain
Christina Meskers
Elsa Olivetti
Diran Apelian
John Howarter
Anne Kvithyld
Brajendra Mishra
Neale R. Neelameggham
Jeff Spangenberger

ISBN 978-3-319-48618-5 ISBN 978-3-319-48768-7 (eBook)
DOI 10.1007/978-3-319-48768-7

Chemistry and Materials Science: Professional

Published by Springer International Publishers, Switzerland, 2016
Reprint of the original edition published by John Wiley & Sons, Inc., 2016, 978-1-119-22581-2

Printed on acid-free paper

This Springer imprint is published by Springer Nature
The registered company is Springer International Publishing AG
The registered company address is: Gewerbestrasse 11, 6330 Cham, Switzerland

TABLE OF CONTENTS
REWAS 2016

Enabling & Understanding Sustainability - Ferrous & Non-ferrous Metals Processing

Understanding & Enabling Sustainability - (Rechargeable) Batteries

Enabling & Understanding Sustainability - Rare Earth Element Applications

Enabling & Understanding Sustainability - Building Materials & Slag Valorization

Designing Materials and Systems for Sustainability

Understanding & Enabling Sustainability - Light Metals Recycling & Waste Valorization

Poster Session

EDITORS

Randolph E. Kirchain's research and teaching aim to improve materials-technology decisions by characterizing the economic and environmental impact of those decisions. That impact may derive from changes in the performance of the products into which those materials are transformed and/or in the systems in which they are produced, used, and eventually discarded. Dr. Kirchain has authored over 100 publications in refereed journals and conferences. He has been awarded the American Iron and Steel Institute's Top Technical Achievement Award, the General Motors Technical Achievement Award, and the TMS Recycling Technology Award. Currently, Dr. Kirchain serves as the co-director of the MIT Concrete Sustainability Hub.

Bart Blanpain is a full professor at the department Materials Engineering of KU Leuven (Belgium) where he is coordinator of the 'High Temperature Processing and Industrial Ecology' research group and the head of the 'Sustainable Metals Processing and Recycling' division division. He obtained an M.Sc. in Metallurgical Engineering (KU Leuven) and an M.Sc. and Ph.D. in Materials Science and Engineering (Cornell University). His research areas are high temperature metals production and refining, metallurgical slag engineering, and resource recovery and recycling. He is also a co-director for the I/UCRC 'Center for Resource Recovery and Recycling' and is a co-editor-in-chief for the *Journal of Sustainable Metallurgy*.

Christina Meskers is senior manager and leading the Market Intelligence and Business Research team at Umicore Precious Metals Refining in Hoboken, Belgium. She is responsible for monitoring and assessing medium and long term market and policy developments, and for collaborative (research) projects in this domain. Part of her activities is bringing Umicore's ideas and expertise on closed loop material cycles, recycling, and sustainability forward in numerous interactions with stakeholders in industry, research, and government. Meskers co-authored the United Nations' International Resource Panel report "Metal Recycling - Opportunities, Limits, Infrastructure" (2012), among other publications.

Dr. Meskers completed her Ph.D. in metallurgy at Delft University of Technology in 2008. In 2008 she was a recipient of the Young Leader Award of The Minerals, Metals & Materials Society (TMS) Extraction and Processing Division. She currently serves as member of the TMS Recycling Committee, Materials and Society Committee, and Public and Governmental Affairs Committee.

Elsa Olivetti is the Thomas Lord Assistant Professor in the Department of Materials Science and Engineering at MIT. She received her B.S. in Engineering Science from the University of Virginia and her Ph.D. in Materials Science from MIT working on development of nanocomposite electrodes for lithium-ion rechargeable batteries. Olivetti joined MIT's faculty in 2014 where her current research focuses on improving the environmental and economic sustainability of materials in the context of rapid-expanding global demand. Olivetti leverages machine learning as well as data mining coupled with engineering and macroeconomic models to determine the scaled impact of novel materials and processes.

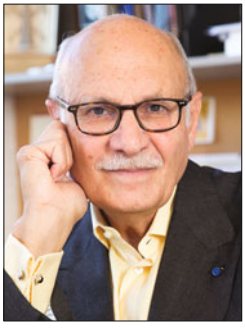

Diran Apelian is the Alcoa-Howmet Professor of Engineering and Founding Director of the Metal Processing Institute (MPI) at Worcester Polytechnic Institute (WPI). He received his B.S. degree in metallurgical engineering from Drexel University in 1968 and his doctorate in materials science and engineering from MIT in 1972. He worked at Bethlehem Steel's Homer Research Laboratories before joining Drexel University's faculty in 1976. At Drexel he held various positions, including professor, head of the Department of Materials Engineering, associate dean of the College of Engineering, and vice-provost of the university. He joined WPI in July 1990 as Provost. In 1996 he returned to the faculty and leads the activities of the Metal Processing Institute.

Dr. Apelian is credited with pioneering work in various areas of solidification processing and powder metallurgy – specifically in molten metal processing, aluminum alloy development, plasma deposition, spray casting/forming, and semi-solid processing of metals. During the last decade, he has worked on sustainable development issues, and particularly, resource recovery, reuse, and recycling. Apelian is the recipient of many distinguished honors and awards – national and international; he has over 600 publications to his credit; and he serves on several technical, corporate and editorial boards. During 2008/2009, he served as President of TMS. Apelian is a Fellow of TMS, ASM, and APMI, and he is a member of the National Academy of Engineering (NAE) and the Armenian Academy of Sciences.

John Howarter is an assistant professor in materials engineering at Purdue University, with a joint appointment in environmental and ecological engineering. His research interests are centered on the synthesis, processing, and characterization of polymers and nanocomposite materials for sustainability applications including water treatment, thermal management in electronic devices, and material design for recycling and value recovery.

Anne Kvithyld is a senior research scientist at SINTEF, Norway, where she has been since 2007. Her research interests are centered around production of metals, in particular refining and recycling. She earned her Ph.D. entitled "Thermal decoating of aluminium scrap" in 2003. She has been a Visiting Post.Doc at Colorado School of Mines, USA and was the winner of the 2011 Vittorio de Nora Award for Environmental Improvements in Metallurgical Industries.

Brajendra Mishra is the Kenneth G. Merriam Distinguished Professor of Mechanical Engineering and Assoc. Director of the Metal Processing Institute at the Worcester Polytechnic Institute (WPI). Dr. Mishra is the Director of the National Science Foundation's Industry/University Collaborative Research Center on Resource Recovery & Recycling – the first National Center of its kind. Mishra received his Bachelor of Technology degree in Metallurgical Engineering from the Indian Institute of Technology in Kharagpur, India and his M.S. and Ph.D. in Materials Science from the University of Minnesota in Minneapolis. Prior to joining WPI, Mishra was a Professor of Corrosion and Physico-chemical Processing in Metallurgical & Materials Engineering at the Colorado School of Mines (CSM) where he also served as the Associate Director of the Kroll Institute for Extractive Metallurgy. Dr. Mishra has over 25 years of research experience in materials recovery and recycling, molten salt pyrometallurgy and electrochemistry and has many contributions to the application of these technologies to materials development and processing.

Dr. Mishra has authored over 500 technical publications in refereed journals and conference proceedings. He holds six patents and has authored/edited 19 books. Dr. Mishra is a member of TMS, ASM International, and NACE. He is a Fellow of ASM (2001) and TMS (2016). Mishra received the Distinguished Service Award from The Minerals, Metals & Materials Society (2010) and the highest award of Honorary Membership from the Indian Institute of Metals (2008). Mishra served as the 2006 President of The Mineral, Metals & Materials Society (TMS) and the 2011 President of the American Institute of Mining, Metallurgical & Petroleum Engineers (AIME). Dr. Mishra received the Presidential Citation of AIME in 2015.

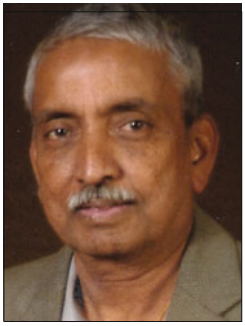

Neale R. Neelameggham is 'The Guru' at IND LLC, involved in Technology marketing and international consulting in the field of light metals and associated chemicals [boron, magnesium, titanium, lithium, and alkali metals], rare earth elements, battery and energy technologies, etc. He was a visiting expert at Beihang University of Aeronautics and Astronautics, Beijing, China, and a plenary speaker at the Light Metal Symposium in South Africa – on low carbon dioxide emission processes for magnesium.

He has over 38 years of expertise in magnesium production and was involved in process development of its startup company NL Magnesium through to the present US Magnesium LLC, Utah from where he retired in 2011. He is developing thiometallurgical processes – a new concept of using sulfur as the reductant and or fuel. He has authored a 21st century convective heat transfer model of continued global anthropogenic warming moderated by excess precipitation – based on thermal emissions independent of energy conversion source – fuel or renewable resources.

Dr. Neelameggham holds 16 patents and applications. He has served in the Magnesium Committee of LMD since its inception in 2000, chaired in 2005, and in 2007 he was made a permanent co-organizer for the Magnesium Technology Symposium. He has been a member of the Reactive Metals Committee, Recycling Committee, and Titanium Committee, and has been Program Committee Representative of LMD and LMD council.

Dr. Neelameggham was the inaugural chair, when in 2008, LMD and EPD created the Energy Committee, and has been a co-organizer of the Energy Technology symposium through the present. He received the LMD Distinguished Service Award in 2010. While he was the chair of Hydro and Electrometallurgy committee he initated the Rare Metal Technology symposium in 2014. He is co-organizer for the 2016 symposiums on Magnesium Technology, Energy Technology, Rare Metal Technology and light metals section of REWAS 2016.

Jeff Spangenberger is an engineering specialist, Sr at Argonne National Laboratory with a B.S. in chemical engineering from Iowa State University. Working in the Energy Systems Division's Process Technology Group, Spangenberger has lead research activities ranging in scale from bench top testing through full scale plant installations and process efficiency studies. While he works to find ways of reducing energy demands in many energy intensive processes, much of his work relates to the separation and recovery of materials in waste streams destined for landfill. This research has resulted in the conceptualization, design,and construction of equipment, pilot scale processes and industrial scale plants resulting in numerous patents and awards.

REVIEWERS

Randolph Kirchain

Bart Blanpain

Jeffrey Spangenberger

Elsa Olivetti

Anne Kvithyld

John Howarter

Gabrielle Gaustad

Dirk Verhulst

Cem Tasan

Naiyang Ma

Christina Meskers

Neale Neelameggham

Enabling & Understanding Sustainability - Ferrous & Non-ferrous Metals Processing

REWAS 2016: Towards Materials Resource Sustainability
Edited by: Randolph E. Kirchain, Bart Blanpain, Christina Meskers, Elsa Olivetti, Diran Apelian, John Howarter, Anne Kvithyld, Brajendra Mishra, Neale R. Neelameggham, and Jeff Spangenberger
TMS (The Minerals, Metals & Materials Society), 2016

RECYCLING OF POLY-METALLIC RESIDUES FROM METAL INDUSTRY – CURRENT STATUS AND FUTURE DEVELOPMENTS

Jürgen Antrekowitsch[1]

[1]Christian Doppler Laboratory for Optimization and Biomass Utilization in Heavy Metal Recycling, Montanuniversitaet Leoben, Franz-Josef-Str. 18, Leoben, 8700, Austria

Keywords: multi metal recovery, residues, lead, zinc, zero waste

Abstract

Within the last years it has become a mutual business to look at different residues, either dumped or continuously produced, trying to utilize them as secondary resources. Especially those from Zinc-, Lead- and Copper production are well known for carrying different valuable metals in parallel but also highly disturbing impurities. Therefore, as a matter of environmental considerations as well as economic issues, process development has to be carefully done to allow feasible treatment concepts. The paper gives an overview on characteristics, available amounts and possible routes for the treatment of such poly-metallic materials. Beside this it describes how present minor metals can contribute to an economic processing. Furthermore, the option for a "zero-waste" solution and with this a complete remediation of potential dumps is discussed. Finally, the paper draws an outlook on how a successful recycling of these residues could contribute to the base metals production in future.

Introduction

For many decades various residues from metal production, such as slags, dust and sludge have been seen as wastes which were dumped as a matter of course. Except the companies nobody really recognized that often hazardous wastes went to landfilling in an amount, which is more or less similar to the metal production itself or even higher. In the eighties and nineties first environmental concerns led to the situation that a bit more attention was paid on such dumps. Nevertheless, missing technologies as well as low metal prices were responsible for the still rather low interest. During the last years more and more the strategy of multi-metal-recovery, not only for primary ores but also for secondary materials came up. Together with elevated metal prices and the need for special metals in various high sophisticated technologies more and more attention was paid to such residues. However, the situation still shows low recycling rates and huge amounts of yearly dumped residues.

Multi-metal-containing residues

When screening the metallurgical area, first of all residues out of the lead, zinc and copper industry show this special character due to the treated ores which are well known for containing a high number of valuable metals in parallel. This circumstance can be shown in the so called Reuters Wheel were the main ore with its associated elements is described (figure 1).

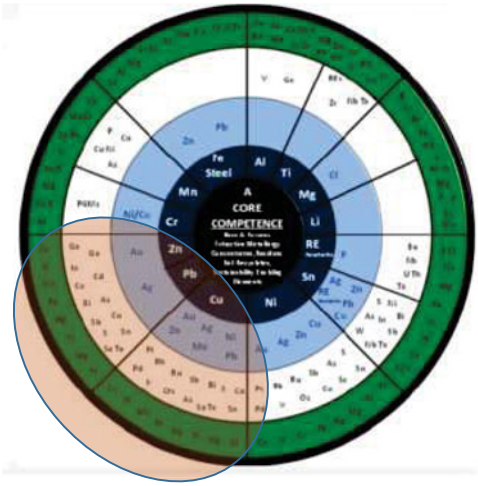

Figure 1: Main metals in nonferrous industry and their associated elements [1]

Some of the displayed metals are already recovered in a certain amount by the primary metallurgical process but a lot of them end up in different waste streams of the particular process. Very often sludge from hydrometallurgical operations and dust from pyrometallurgical ones offer a high number of contained metals. The same situation becomes evident for some recycling processes, where high diversified and contaminated scraps are used, such as car bodies or especially electronic scrap. In the following picture some examples are shown (figure 2), which on the one side illustrate the possible recoverable elements but also the high overall amount that is present.

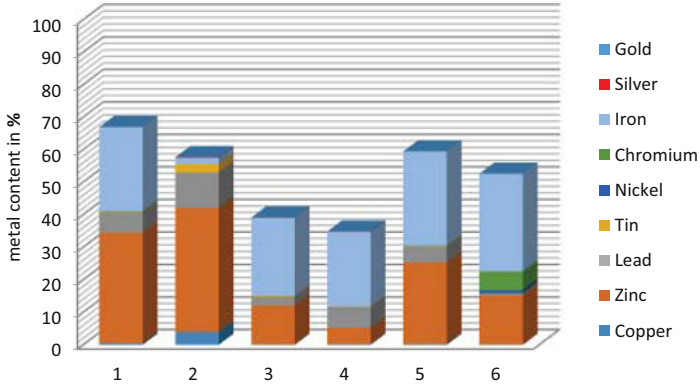

Figure 2: Examples for different residues with their metal content (except PGM)
1 Electric Arc Furnace steel mill Dust,2 Dusts from copper recycling, 3 Slags from lead industry, 4 Jarosite from zinc industry, 5 Dusts from cupola furnaces, 6 Stainless steel production dust

Beside dust and sludge also slags have to be considered but often do not show such high metal contents due to the situation that slags have been mixed in a certain extant with other phases like liquid metal or matte and therefore lost most of their valuables, if the process was carried out in a successful way.

The State of the art of multi metal recycling out of complex residues

As stated in the introduction, one main reason why recycling rates of the described complex residues are relatively low is that with most of the running processes, only one or maybe two (this case is still rare) contained valuable metals are recovered, generating again high volumes of residues which still contain value. Beside the main metals Zn, Pb, Cu and Fe within the technological developments of the last decades, other rare elements have become the focus of recycling. Especially in zinc and lead concentrates, precious metals (especially Ag) and others such as In, Ge or Ga can be found but were left unaccounted especially in the treatment of residues. Nevertheless, the general intention should be to recover the base metals simultaneously [2]. It was found, however, that particularly the precious metals must be taken into account because they are present in many such residues and even in the case of low percentages, due to their high value, it must be the objective to recover them as efficiently as possible.
Of course for some of the described residues process concepts are already existing, but at the end their worldwide recycling rates (overall recycling) show still low values partly far below 50 %.
Typical reasons for the missing success of existing processes are:

- relatively low yields
- recovery of only one metal
- low product quality anf generation of huge amounts of new residues
- problems with refractory lining
- necessity to transport the material to centralized recycling units
- dependency on environmental legislation of the particular country
- economic viable only because of high treatment fees
- difficulties in the collection of the materials

In the following chapter one possibility of such multi-metal containing wastes which is mainly dumped is described concerning its characteristic and a possible way how a multi-metal recycling could be realized.

Examples for the characteristic of multi metal containing residues

In hydrometallurgical processes precipitation and cementation are often used to get rid of undesired elements. However this creates huge amounts of waste material which is often dumped under special conditions due to its hazardous character.
One of these materials is the so-called jarosite, a typical residue from primary zinc winning, which nowadays is done mainly by leaching and electro winning. During iron precipitation from the leach prior to the cementation and electro winning, this jarosite is generated by increasing the pH value and the addition of oxidizing reagents and sodium or ammonium. In the course of this precipitation, this complex jarosite is formed which contains remaining zinc and very often lead and silver. A second option would be goethite precipitation which is not so often applied as jarosite.

Thermochemical software generally does not provide the complex compounds formed here in their database, and X-ray diffraction is, in most of the cases, also impossible to interpret - even for the elements with higher concentrations - due to missing databases for the formed compounds. Therefore, it is mandatory to combine different analytic principles to distinguish between the various types of jarosites which are formed according to the mineralogical compound

$AB_3(SO_4)_2(OH)_6$ where

A is: H_3O^+, Na^+, K^+, NH_4^+, Ag^+, Li^+, Ti^+, Rb^+, ½ Hg^{2+} or ½ Pb^{2+}

B is: Fe^{2+}, Zn^{2+}, Cu^{2+} or Al^{3+}

In the industry, typical types are ammonium jarosite and sodium jarosite, which are reported in literature to be of the form

$[Ag_{0,001}Na_{0,07}K_{0,02}Pb_{0,007}(NH_4)_{0,59}(H_3O)_{0,31}]\cdot Fe_3(SO_4)_2(OH)_6$ and

$[Na_{0,675}Ag_{0,005}(H_3O)_{0,32}]\cdot Fe_3(SO_4)_2(OH)_6$ respectively [3].

Depending on the industrial process, especially if a lead-silver separation is done or not, the jarosites can contain higher amounts of these two metals. In the case of silver, it is a question of how it was bound before the leaching step. Some Ag-compounds are soluble and will end up as silver jarosite during iron precipitation while if it occurs as Ag or Ag_2O it remains solid during leaching and could be separated with other insoluble compounds like SiO_2, forming the well-known lead-silver residue from hydrometallurgical zinc production. However, this separation is either not done at all or done inefficiently at a lot of different sites, so that the residue dumped today still contains these valuable metals, without exception.
With a combination of differential thermo analysis, ICP and scanning electron microscopy it was possible to evaluate and calculate the occurring types of jarosites as well as other components in different samples. An example for a sodium jarosite mixed with a residue from a direct leaching process is shown in Table 1.

Tab. 1: Calculated composition based on analytical findings for a sodium jarosite

Parameter	Value [%]	Parameter	Value [%]	Parameter	Value [%]
$2K[Fe_3(SO_4)_2(OH)_6]$	3.05	MnO	0.05	$CuSO_4$	0.34
$2Na[Fe_3(SO_4)_2(OH)_6]$	27.94	$CaSO_4$	17.47	H_2SO_4	10.79
$2H_3O[Fe_3(SO_4)_2(OH)_6]$	10.61	MgO	0.05	ZnSO4	4.24
Ag (various compounds)	0.018	Al_2O_3	1.20	FeS_2	3.01
$PbSO_4$	8.79	SiO_2	1.80	Rest	~10.00

The following picture gives an overview about hydrometallurgical produced zinc, nowadays the main route for zinc winning, and with this a potential to find jarosites and goethites with remarkable contents of valuable metals. Especially in Europe as well as in Australia some of the goethite ponds can be found but still represent a minority compared to jarosite (Europe).

Figure 3: Hydrometallurgical zinc production, data extracted from [4]

Out of this data and the fact that roughly 600 kg to 1000 kg per ton of zinc are produced, it can be easily calculated that yearly about 7 to 9 Mio tons of leaching residues are generated containing metal values in the range of several hundred million USD [1] [5].
In general only a few concepts for reprocessing are existing showing typical disadvantages like mentioned above.
One new concept was developed by the chair of nonferrous metallurgy, Montanuniversitaet Leoben in Austria together with the company Railly&Hill and Befesa. This process idea is somehow a little bit more complex due to three combined steps but would allow at the end the recovery of different valuable metals mainly via a liquid lead bath. A rough process scheme is given in figure 4. Trials in lab-scale as well as technical scale (50-100 kg/batch) showed high recovery rates as well as a moderate energy consumption, if the pre-treatment and the metallurgical treatment are combined in a reasonable way. Lead and zinc were recovered to more than 90 % and also the silver recovery reached values above 90 %. The typical products out of such a recycling process are listed below:

- Zinc oxide, received by reduction and subsequent volatilization, containing maybe also a certain amount of indium
- Lead bullion, containing the reduced lead as well as silver and other lead soluble metals
- Remaining slag, widely free of heavy metals

One important step that would increase considerably the economy of such a concept is the possible concentration of valuable metals by means of beneficiation. For this some first promising results have been received but investigations are still in progress to verify and optimize these ideas.
Nevertheless, the applicability of such a concept depends on the detailed metallurgical route from where the residue is generated from and the environmental legislation in the particular country.

Figure 4: Possible process scheme for multi-metal recovery out of jarosites

The viability of the described concept is first of all dependent on the following major factors:

- The amount of valuable metals, especially silver
- The possibility to make use of an existing sulfuric acid plant
- The LME notation of the valuable metals
- The accessibility of the dump

With the presented example jarosite, a zero waste scheme is difficult to realize. Nevertheless, it was investigated, if also an iron reduction and with this the generation of a more clean slag could be realized. The results did not show a full reduction of the iron but in parallel other heavy metals were brought down to a rather low level. Therefore it could be assumed that, even though iron reduction requires a lot of energy, a best case, where the slag could find utilization in dike- and road-construction or maybe sand-blasting, could be realized. Trials in this field were done in 100 kg-scale and have to be verified in larger scale. Also it has to be calculated, if such a concept is economical or if it would make more sense to landfill the remaining slag.

Within the investigations also a model for economic verification has be established and different dumps worldwide have been investigated. Within this evaluation high promising dump sites as well as residues of poor quality were detected.

The developed concept was only investigated for jarosite-type zinc leach residues. Theoretically it can be also applied for goethite-type materials. Of course in this case some different boundary conditions have to be considered. On the one side, there are less sulfur components on the other side the amount of the mentioned valuable metals is often different. For example in goethite-type processes Indium often is already removed. In general for such goethite-residues more often already developed treatment scenarios can be found compared to jarosite.

Summary

Different wastes from metallurgical industry which were mainly dumped in the past are containing interesting amounts of various important metals interesting for future recycling. Nevertheless, it is necessary to realize a type of process which is able to recover as many metals as possible in parallel. As shown with the example jarosite from zinc industry it might be possible to realize an

economic concept combining metallurgical and mineral processing steps. With advanced research, higher metal prices and stricter environmental legislation residues such as dust, sludge and slags from zinc, lead and copper industry will more and more play an important role in the field of secondary resources.

Acknowledgments

The present work has been funded by the Austrian Federal Ministry of Science, Research and Economy.

References

[1] Reuter M.: Outotec and Sustainability, Pesentation, 2011

[2] Steinlechner S., J. Antrekowitsch: Concepts for the Simultanous Recovery of Valuable Metals from Zinc Bearing Residues. Proc. of Earth2011 - The 11th International Symposium on East Asia Resource Recycling Technology (2011), Kaohsiung, Taiwan, 733 – 736

[3] Salinas E., et.al: Characterization and alkaline decomposition–cyanidation kinetics of industrial ammonium jarosite in NaOH media, Hydrometallurgy 60 (2001), 237-246

[4] Zinc online data base, International Lead and Zinc Study Group, ILZSG, Lisbon, 2015

[5] Pawlek F.: Metallhüttenkunde, Walter de Gruyter, Berlin-New York, 1983

REWAS 2016: Towards Materials Resource Sustainability
Edited by: Randolph E. Kirchain, Bart Blanpain, Christina Meskers, Elsa Olivetti, Diran Apelian, John Howarter, Anne Kvithyld, Brajendra Mishra, Neale R. Neelameggham, and Jeff Spangenberger
TMS (The Minerals, Metals & Materials Society), 2016

BAUXITE RESIDUE FOR PHOSPHORUS REMOVAL FROM WASTE WATER

Gamini Mendis[1], Amanda Brock[2], Kai Gao[1], Indrajeet Chaubey[2,3,4], Ron Turco[5], John Howarter[1,3]

[1]School of Materials Engineering, Purdue University, West Lafayette, IN

[2]School of Agricultural and Biological Engineering, Purdue University, West Lafayette, IN

[3]Division of Environmental and Ecological Engineering, Purdue University, West Lafayette, IN

[4]Department of Earth and Atmospheric Science, Purdue University, West Lafayette, IN

[5]Department of Agronomy, Purdue University, West Lafayette, IN

Keywords: Bauxite residue, phosphate recovery, waste water

Abstract

Phosphorus compounds have been used in a wide variety of industrial and agricultural applications. However, they have also been shown to cause eutrophication in water systems. It is important that the phosphorus is removed from water systems and potentially reclaimed for reuse. One potential phosphorus capture material is bauxite residue. Bauxite residue is a waste product from the Bayer process of aluminum production. The residue is kept in large, alkaline holding pools where it remains unused. Through processing, bauxite residue has been shown to remove phosphorus compounds from waste water. Here, bauxite residue is modified and processed, and the structure-properties relationships are investigated. The effects of microstructure and chemical composition on the removal of phosphorus from water are examined and methods for bauxite valorization are discussed.

Introduction

Current agricultural practices require the use of large amounts of phosphate-based fertilizer to increase crop yields. Unused phosphate is washed away by rainwater and ends up in large bodies of water, such as rivers and lakes. Bacteria and algae feed on the phosphate and multiply, causing algae blooms and the depletion of O_2 in the water. This results in the widespread death of aquatic life due to asphyxiation. There is a general need for phosphate capture/sequestration technologies that can be cheaply implemented in existing agricultural systems.

Phosphorus is found in aqueous environments as several competing structures, according to pH. At pH <7, orthophosphate or monobasic phosphate is the dominant phosphate species[1]. As pH

increases above 7, pyrophosphate or dibasic phosphate becomes the primary phosphate, and other phosphates such as tripolyphosphate significant minor species. In the specific agricultural breeder system examined here, pH ranges from 6.09 to 7.45, and orthophosphate is the largest fraction (50%) of the 5.52 mg/L phosphate in solution.

One possible phosphate capture technology utilizes bauxite residue (BR), a combination of hematite, alumina, lime and silica among other trace oxides. Bauxite residue, or red mud, is produced in excess of 70 million tons per year as an industrial byproduct of the Bayer process of alumina production[2,3]. BR has been used in heavy metal extraction, metal feedstock applications, wastewater treatment, cement aggregate and polymer filler applications, and as a construction material, however these solutions are not yet commercially viable[4].

Bauxite residue is sequestered through segregation in large red mud reservoirs, where it remains perpetually. This method of disposal is potentially hazardous[4]; bauxite residue contains low concentrations of heavy metals and naturally occurring radioactive materials, is very alkaline (pH 10-12.5[5]) and in its native state, prevents the growth of plants. However, bauxite residue has a high cation exchange capacity, allowing the facile replacement of salts with phosphate molecules[5,6]. Phosphate capture in bauxite residue occurs through two processes: the formation of apatite from CaO and the formation of a ligand between the phosphate and the iron oxide. Apatite formation is promoted at lower pH (~1-5), whereas iron-phosphate interactions occur at higher pH[7]. This exchange can be promoted further at moderate pH (6-8)[6], usually through the process of acid washing the red mud [5,6,8]. The effects of pH, concentration, and processing conditions of various bauxite and/or bauxite phosphate systems are well described in literature [2,7,9–13].

The application of bauxite residue in farmland wastewater applications has been explored in depth by Summers, et al. through a series of studies in a sandy region of Pinjarra, Western Australia. They found that the addition of bauxite residue to sandy regions increased water retention (10-35%) and phosphate retention (70%)[14] for two years after application while decreasing phosphorous concentration in drainage water by up to 75%[15]. Furthermore, they determined that the phosphate was made biologically available to subterranean clover for the duration of the study, which increased clover yield [16].

Here, a possible phosphate sequestration technology is demonstrated, which uses heat treated bauxite powder, and has high water uptake and good phosphate capture rates. X-ray diffraction shows high structural conversion to α-hematite. Measurement of the phosphate uptake indicates that upwards of 70% removal of the phosphate in a 5 mg/L solution occurs. This technology enables farmers to extract phosphate content from wastewater runoff and may enable phosphate recovery from bauxite residue in the future.

Procedure

Bauxite residue was received from a corporate sponsor. The bauxite residue was dried at 100 °C in an oven for 12 hours to remove water, then was crushed and sieved to a 106 μm -212 μm particle size. The particles of bauxite residue were heated in an alumina crucible using a 5 °C/min ramp

rate and were held at 900°C or 1000°C for 10 hours in air. The samples were allowed to slow cool to room temperature.

X-ray diffraction was used to characterize the structure of the bauxite residue. A D-8 Focus X-ray diffraction machine (Bruker, Madison, WI, USA) with a copper K-α source (1.5418 nm wavelength) was used to scan from 20° to 70° using a 1°/min scan rate.

Phosphate uptake testing was performed to examine the phosphate removal of the bauxite residue powder. Bauxite residue (0.1 g/L, 1 g/L, 10 g/L) was deposited in 30 mL of DI water with 5 mg/L orthophosphate solution.

The concentration of phosphate after the addition of the bauxite residue was determined by using a SpectraMax Plus UV-vis spectrometer (Molecular Devices, Sunnyvale, CA, USA) with a method as reported previously [17]. Bauxite powder treated phosphate solutions were subjected to centrifuge for 20 mins to sediment the bauxite particles. After sedimentation, 20 ml upper clear solution was transferred to a 125 ml Erlenmeyer flask. The phosphate testing reagent was made using the previously reported formula [17] and 4 ml of this testing reagent was added to the phosphate solution to be measured. The color of the solution was allowed to develop for at least 15 mins before being tested on the UV-vis spectrometer with the adsorption reading being set at 882 nm. Reference used on UV-vis spectrometer was made by mixing the blank testing reagent in the same manner using distilled water.

Experimental Results and Discussion

X-ray diffraction was used to examine the temperature evolution of the Bauxite residue crystal structure (Figure 1). At room temperature, the bauxite residue contained Hematite, Quartz and Andradite. At higher temperatures, the Quartz and Andradite peaks disappear [18]. A Calcium Aluminum Oxide family of peaks appear at 900ºC, but the only identifiable peak at 1000ºC was that of Hematite. The broad amorphous peak between 25-35º is likely due to the presence of aluminosilicate glasses; the intensity of the amorphous peak increases at higher temperature, suggesting the formation of more glassy material at elevated temperature.

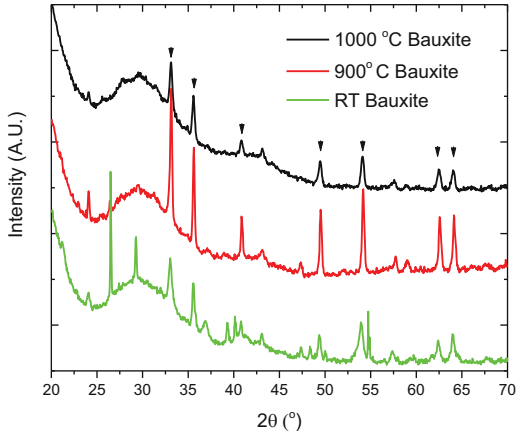

Figure 1: X-ray diffraction (Cu-Kα) spectra of bauxite residue heated in air to different temperatures. The arrows indicate the peak position of the α-hematite phase.

The increase in the hematite phase is desirable for phosphate recovery. Hematite is able to form strong complexes with phosphates. Therefore it is expected that the 1000ºC samples will remove the highest amount of phosphorus.

Phosphate uptake testing was performed using 5 mg/L orthophosphate, according to standard amounts of phosphate found in wastewater. The stock solution of 5 mg/L had an absorbance of 0.73, as shown in Table 1. Moderate phosphate removal was observed using RT bauxite residue, as indicated by the decrease in absorption of the indicator solution, which scaled with the amount of bauxite residue used. At 900ºC and 1000ºC, the absorption of phosphorus was greatly increased at 10 g/L bauxite residue in water.

Table 1: Phosphate absorption of bauxite residue specimen

	RT BR	*900ºC BR*	*1000ºC BR*
0.1 g/L	0.714	0.733	0.738
1 g/L	0.683	0.743	0.732
10 g/L	0.550	0.210	0.166
Phosphorus content at 10 g/L BR	3.76 mg/L	1.43 mg/L	1.13 mg/L

The high phosphate uptake behavior of the 900ºC and 1000ºC samples was expected. Increased hematite fraction enables higher surface adsorption of the phosphate. The mechanism of

One explanation of the lack of phosphate absorption at low concentration is that the dried bauxite residue powder absorbed water from the solution, which increased the concentration of phosphate in solution.

The capture of the phosphate by the bauxite residue is pH dependent. After phosphorus recovery, the bauxite has the potential to be acid- or base-treated to recover the phosphate for other industrial uses. Future work will examine the viability of this recovery mechanism.

Conclusions

Bauxite residue was dried and heat treated to change the predominant phases. Heat-treated bauxite residue contains higher fractions of Hematite, which is able to remove 80% of phosphorus from water.

References

[1] S. Yeoman, T. Stephenson, J.N. Lester, R. Perry, The removal of phosphorus during wastewater treatment: a review., Environ. Pollut. 49 (1988) 183–233. doi:10.1016/0269-7491(88)90209-6.

[2] Y. Liu, C. Lin, Y. Wu, Characterization of red mud derived from a combined Bayer Process and bauxite calcination method., J. Hazard. Mater. 146 (2007) 255–61. doi:10.1016/j.jhazmat.2006.12.015.

[3] Y. Pontikes, C. Rathossi, P. Nikolopoulos, G.N. Angelopoulos, D.D. Jayaseelan, W.E. Lee, Effect of firing temperature and atmosphere on sintering of ceramics made from Bayer process bauxite residue, Ceram. Int. 35 (2009) 401–407. doi:10.1016/j.ceramint.2007.11.013.

[4] C. Klauber, M. Gräfe, G. Power, Bauxite residue issues: II. options for residue utilization, Hydrometallurgy. 108 (2011) 11–32. doi:10.1016/j.hydromet.2011.02.007.

[5] W. Huang, S. Wang, Z. Zhu, L. Li, X. Yao, V. Rudolph, et al., Phosphate removal from wastewater using red mud., J. Hazard. Mater. 158 (2008) 35–42. doi:10.1016/j.jhazmat.2008.01.061.

[6] Y. Li, C. Liu, Z. Luan, X. Peng, C. Zhu, Z. Chen, et al., Phosphate removal from aqueous solutions using raw and activated red mud and fly ash., J. Hazard. Mater. 137 (2006) 374–83. doi:10.1016/j.jhazmat.2006.02.011.

[7] Y. Zhao, Q. Yue, Q. Li, B. Gao, S. Han, H. Yu, The regeneration characteristics of various red mud granular adsorbents (RMGA) for phosphate removal using different desorption reagents., J. Hazard. Mater. 182 (2010) 309–16. doi:10.1016/j.jhazmat.2010.06.031.

[8] Y. Zhao, J. Wang, Z. Luan, X. Peng, Z. Liang, L. Shi, Removal of phosphate from aqueous solution by red mud using a factorial design., J. Hazard. Mater. 165 (2009) 1193–9. doi:10.1016/j.jhazmat.2008.10.114.

[9] G. Akay, B. Keskinler, U. Danis, Phosphate Removal From Water By Red Mud, Water Res. 32 (1998) 717–726.

[10] B. Koumanova, M. Drame, M. Popangelova, Phosphate removal from aqueous solutions using red mud wasted in bauxite Bayer's process, Resour. Conserv. Recycl. 19 (1997) 11–20. doi:10.1016/S0921-3449(96)01158-5.

[11] Y. Zhao, Q. Yue, Q. Li, X. Xu, Z. Yang, X. Wang, et al., Characterization of red mud granular adsorbent (RMGA) and its performance on phosphate removal from aqueous solution, Chem. Eng. J. 193-194 (2012) 161–168. doi:10.1016/j.cej.2012.04.040.

[12] Y. Zhao, Q. Yue, Q. Li, Q. Li, B. Gao, S. Han, et al., Influence of sintering temperature on orthophosphate and pyrophosphate removal behaviors of red mud granular adsorbents (RMGA), Colloids Surfaces A Physicochem. Eng. Asp. 394 (2012) 1–7. doi:10.1016/j.colsurfa.2011.11.013.

[13] Q. Yue, Y. Zhao, Q. Li, W. Li, B. Gao, S. Han, et al., Research on the characteristics of red mud granular adsorbents (RMGA) for phosphate removal., J. Hazard. Mater. 176 (2010) 741–8. doi:10.1016/j.jhazmat.2009.11.098.

[14] R.N. Summers, N.R. Guise, D.D. Smirk, Bauxite residue (red mud) increases phosphorus retention in sandy soil catchments in Western Australia, Fertil. Res. 34 (1993) 85–94. doi:10.1007/BF00749964.

[15] R.N. Summers, J.D. Pech, Nutrient and metal content of water, sediment and soils amended with bauxite residue in the catchment of the Peel Inlet and Harvey Estuary, Western Australia, Agric. Ecosyst. Environ. 64 (1997) 219–232. doi:10.1016/S0167-8809(97)00040-6.

[16] R.N. Summers, M.D.. Bolland, M.. Clarke, Effect of application of bauxite residue (red mud) to very sandy soils on subterrnean clover yield and P response, Aust. J. Soil Res. (2001).

[17] J. Murphy, J.P. Riley, A modified single solution method for the determination of phosphate in natural waters, Anal. Chim. Acta. 31 (1962) 31–36.

[18] V. Sglavo, R. Campostrini, S. Maurina, G. Carturan, M. Monagheddu, G. Budroni, et al., Bauxite "red mud" in the ceramic industry. Part 1: thermal behavior, J. Eur. Ceram. Soc. 20 (2000) 235–244.

REWAS 2016: Towards Materials Resource Sustainability
Edited by: Randolph E. Kirchain, Bart Blanpain, Christina Meskers, Elsa Olivetti, Diran Apelian, John Howarter, Anne Kvithyld, Brajendra Mishra, Neale R. Neelameggham, and Jeff Spangenberger
TMS (The Minerals, Metals & Materials Society), 2016

MODELING THE ELECTROMAGNETIC PROCESSING OF RECYCLED SILICON DUST

G. Djambazov[1], K. Pericleous[1], V. Bojarevics[1], M. Forzan[2], F. Dughiero[2]

[1]University of Greenwich, Park Row, London, SE10 9LS, United Kingdom
[2]Universita degli Studi di Padova, Via 8 Febbraio 1848, 2, Padova, 35122, Italy

Keywords: Silicon recycling, electromagnetic separation, induction melting

Abstract

The kerf waste from the sawing of PV silicon wafers is pelletized and then remelted in an induction furnace. The furnace has a square cross-section quartz crucible, surrounded by graphite susceptors and heated by an induction coil that enables directional solidification of the new ingot. Top and bottom 'pancake' coils provide additional temperature control. Once melted, silicon becomes electrically conductive and subject to stirring by induction. To recycle the silicon, particulate impurities (due to the sawing, condensed silicon oxides or carbides) need to be removed. Flow control and the electromagnetic Leenov-Kolin force are used to expel particulates, through a novel dual frequency induction scheme. Three-dimensional numerical modeling captures the electromagnetic, fluid-flow and heat-transfer effects in this problem, in a multi-physics finite volume computational framework. Results are presented for typical electromagnetic, velocity and force fields and conclusions are drawn about the expected effectiveness of the electromagnetic separation system which is still under construction.

Introduction

The process of solar grade silicon production from SiO_2 is energy intensive (typically 50 kWh/kg [1]) and harmful to the environment. Yet, 40% –50% of this valuable product material is lost into sawdust (kerf loss) during wafering [2, 3]. It is desirable to remelt the sawdust in a process which also removes impurities. Various laboratory methods, e.g. chemical treatment, heavy fluid centrifugation, electric field, phase-transfer, organic solvers separation, have been tried for removing the SiC particles from the kerf silicon [2]. The emerging technology, Fixed Abrasive Sawing, which uses diamond particles (instead of SiC) fixed to a cutting wire to slice the silicon feedstock presents an opportunity for industrial-scale recycling [3]. The kerf loss from this process can be pelletized and then remelted and overheated in a vacuum induction furnace to remove organics and the silicon dioxide which inevitably forms during the sawing [4]. This leaves about 200 ppm of diamond particles. If left untreated, formation of silicon carbide and precipitation during crystallisation is to be expected. The scheme proposed in the EU SIKELOR project [4] involves the careful control of induction currents which penetrate the melt to direct non-conducting particles towards the walls of the crucible using the electromagnetic Leenov-Kolin force [5] and so can aid the separation of the particles from the bulk of the melt [6, 7].

The investigated design of an induction furnace (iDSS which is under construction) aims to produce solar grade multi-crystalline silicon blocks cast in commercial sizes. It has a square cross-section quartz crucible which is surrounded by graphite susceptors forming an air-tight and thermally-insulated block [8]. On the outside, the block is surrounded by six water-cooled induction coils which can be independently switched on and off. That enables directional

solidification of the new ingot. Top and bottom 'pancake' coils provide additional temperature control. Once melted, silicon becomes electrically conductive and therefore subject to stirring by the electromagnetic Lorentz force. A novel dual frequency induction scheme is investigated. Low frequency and high frequency electrical currents are simultaneously applied to the coils. The low frequency current induces stirring of the silicon melt while the high frequency current heats the melt through the graphite susceptors. This is possible because the higher electrical resistance of the graphite allows the low-frequency magnetic field to penetrate the silicon charge with sufficient strength. The following sections present the mathematical model of the dual frequency induction and the computed results for a given scenario of the switching of the coils for directional solidification.

Mathematical and Numerical Model

A new formulation [9] of the electromagnetic field equations is used which allows the computational domain to cover only the inside of the furnace and not the surrounding space. Pseudo-steady solutions are obtained for the unknown vector of the induced electric field $\boldsymbol{E}$ with its real (R) and imaginary (I) parts for a fixed angular frequency ω by solving six scalar equations:

$$\nabla^2(\overrightarrow{E_{R,I}} - \nabla\varphi_{R,I}) = \pm\mu\sigma\omega(\overrightarrow{E_{I,R}} - \nabla\varphi_{I,R}) \quad (1)$$

where μ and σ are the magnetic permeability of the diamagnetic materials and their electrical conductivity. In the conducting parts of the domain, charge continuity is ensured by solving two auxiliary equations for the parts of a scalar electric potential: $\nabla^2\varphi_{R,I} = \nabla\cdot\overrightarrow{E_{R,I}}$. The induced magnetic field $\boldsymbol{B}$ is recovered from the solved electric field using Faraday's law:

$$\omega\,\overrightarrow{B_{R,I}} = \mp\nabla\times\overrightarrow{E_{I,R}}. \quad (2)$$

Boundary conditions on the external surfaces of the graphite susceptor box include the contributions to the local values of the magnetic field components by both the applied and the induced currents. Those contributions are calculated from the Biot-Savart integral [9]. Zero normal current conditions are imposed on the surfaces between conducting and non-conducting parts of the domain. The electrical current induced in the conducting liquid and solid objects is $\vec{J} = \sigma(\vec{E} - \nabla\varphi)$; the electromagnetically generated instantaneous Lorentz force $\boldsymbol{F}$ and Joule heat Q are $\vec{F} = \vec{J}\times\vec{B}$ and $Q = J^2/\sigma$. Time-averaging these sinusoidal quantities yields the mean (pseudo-steady) values $\vec{F}_{mean} = 0.5\left(\overrightarrow{J_R}\times\overrightarrow{B_R} + \overrightarrow{J_I}\times\overrightarrow{B_I}\right)$ and $Q_{mean} = (J_R^2 + J_I^2)/2\sigma$. The mean force is responsible for the flow in the liquid and Joule heat is released in both the liquid silicon and in the graphite susceptors which then transfer the heat by thermal radiation and conduction to the quartz crucible and the silicon charge.

Fluid Flow and Turbulence. Mass continuity in the liquid is achieved by ensuring the velocity $\boldsymbol{u}$ satisfies $\nabla\cdot\vec{u} = 0$ which is an implicit equation for the pressure p also appearing in the momentum equations [10]. The driving Lorentz force appears as a source term in the momentum equations. The effective viscosity which is responsible for the resistance to the flow includes the mixing action of turbulence (in spreading momentum between faster and slower fluid regions). The standard in CFD k-ε model of turbulence is used with logarithmic-law wall functions on solid surfaces bounding the liquid. The numerical method used to solve the electromagnetic, fluid-flow and turbulence model equations is based on cell-centered discretization and velocity-pressure coupling is accomplished with the SIMPLE procedure and the Rhie-Chow interpolation scheme [10].

Forces on Particles. As a first approximation, only the two main forces acting on the particles are considered – namely the Leenov-Kolin force and fluid drag. The Leenov-Kolin force is a

direct consequence of the Lorentz force $\boldsymbol{F}$ acting on the conducting liquid surrounding the non-conducting particle. It is caused by the pressure gradient across the particle as current is diverted around it and is oppositely directed to the Lorentz force vector: $\overrightarrow{F_E} = -V_P \frac{3}{2} \vec{F}_{mean}$, V_p being the volume of the particle. This formula is valid for alternating currents and magnetic fields [11]; the original Leenov-Kolin expression [5] derived for direct current is two times weaker and has a coefficient $\frac{3}{4}$.

The fluid drag force is expressed as $\overrightarrow{F_D} = C_D \rho_L \frac{A}{2} (\vec{u} - \overrightarrow{u_P}) \, |\vec{u} - \overrightarrow{u_P}|$ where A is the cross-section area of the particle, $\boldsymbol{u}_p$ is the particle velocity and ρ_L is the density of the liquid. The drag coefficient is $C_D = \frac{24}{Re}(1 + 0.15Re^{0.687})$ [12]. The maximum drag occurs when the particle is held stationary by the combination of Leenov-Kolin and adhesion forces, i.e. when $\overrightarrow{u_P} = 0$. Since the aim is to predict whether the Leenov-Kolin force will be sufficiently strong to counteract the drag, the adhesion forces are not included in the force balance calculation.

Computational Domain. After the initial melting of the silicon pellets, the liquid level reaches about 230 mm from the bottom of the crucible and its upper part remains empty. So we assume the top coil is no longer needed and is switched off. The electrical current in the bottom coil [6] is also switched off but its water flow remains on, thus allowing the bottom to become a heat sink promoting the directional solidification from the bottom up. Figure 1 shows the remaining six side coils with their leads and the sealed graphite furnace box.

Preliminary simulations have shown that the effect of the leads can be ignored because their magnetic field cancels out (the same currents flowing in opposite directions) and the six turns (which can be independently switched on and off) can be represented in the model as exactly symmetrical. Since the furnace geometry is also symmetrical, it is enough to model only one quarter which allows much shorter computational times. At the same time, for the calculation of the magnetic field, the currents in the whole furnace and of the whole coil are taken into account in the Biot-Savart integrals.

Results and Discussion

Simulations were carried out for three different positions of the solidification front in order to reveal how the forces on the particles change during the directional solidification of the ingot: initial state – all liquid, 55 mm from the bottom and 110 mm from the bottom (see Figure 2).

The step of 55 mm was chosen because that is the vertical spacing of the side coils and the following scenario of successive switching off of these coils was assumed: When the silicon charge is all liquid, all six coils are active; when the solid front rises by 55 mm, the current in the lowest turn is switched off; when the solid front reaches 110 mm, the second coil turn from the bottom is also switched off; etc.

Two frequency combinations were examined for each of the front positions: (a) only high-frequency 2350 Hz current is supplied to the active coils and (b) both the high frequency and a low frequency of 120 Hz are provided by a special power supply. This is done with the following facts in mind: The magnetic field induced by the high frequency has shallow penetration and produces a lot of heat mainly in the graphite susceptors but is also responsible for the strong Lorentz (hence, Leenov-Kolin) force in a thin boundary layer in the silicon at the

crucible walls, while the magnetic field of the low-frequency current penetrates deep into the melt and is responsible for its stirring.

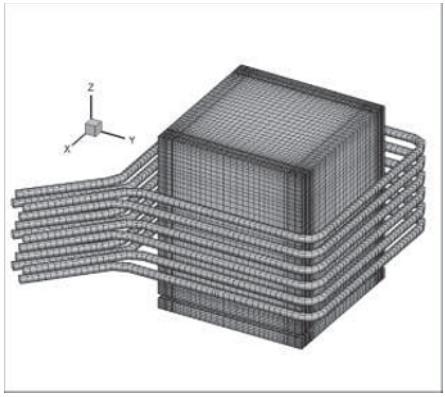

Figure 1. Overview of iDSS furnace mesh with side coils

Two important aspects of the purification process occur simultaneously during the directional solidification of the silicon ingot: *stirring* of the melt, so that particulate impurities are taken from the bulk to the walls of the holding vessel (crucible) and *entrapment* of the particles by the Leenov-Kolin force at the walls. (These contaminated sides of the solidified ingot can be sliced off, leaving the purified bulk.) Good stirring is achieved with higher liquid velocities (mainly driven by the Lorentz force) and more vigorous turbulent mixing indicated by the 'effective turbulent viscosity' (enut) calculated via the turbulence model. A special 'separation criterion' was defined to indicate the strength of the particle entrapment – the dot product of the Leenov-Kolin force and the fluid drag force:

$$dotp = \frac{\overrightarrow{F_E} \cdot \overrightarrow{F_D}}{s^2} \tag{3}$$

where s is a scaling factor which is chosen as the maximum value of the magnitude of the Leenov-Kolin force $\boldsymbol{F}_E$ in the liquid part of the computational domain. Where the dot product is positive, the flow helps push the particles towards the entrapment zones; in regions of negative dot product, the flow takes the particles back to the bulk of the melt.

Particle sizes of 100 μm (shaded contours) and 10 μm (line contours at 'dotp' values 0, 1 and 2) are considered for comparison (on the left) in Figure 2. The displayed cross-sections are 4 mm from the crucible wall (x = 200 mm). On the right, the corresponding turbulent mixing contours and liquid velocity vectors are shown for cross-sections through the middle of the domain.

It can be seen the addition of the low frequency in (b) enhances the mixing substantially which is good for taking the non-conducting particles out of the bulk but, at the same time, makes the entrapment zones more patchy leading to non-uniform concentrations of the particles near the walls of the vessel, i.e. at the sides of the ingot. The prescribed low-frequency component of the coil current in this simulation had an amplitude of 1000 A; naturally this can be reduced so that good mixing is retained but more uniform separation is achieved at the same time.

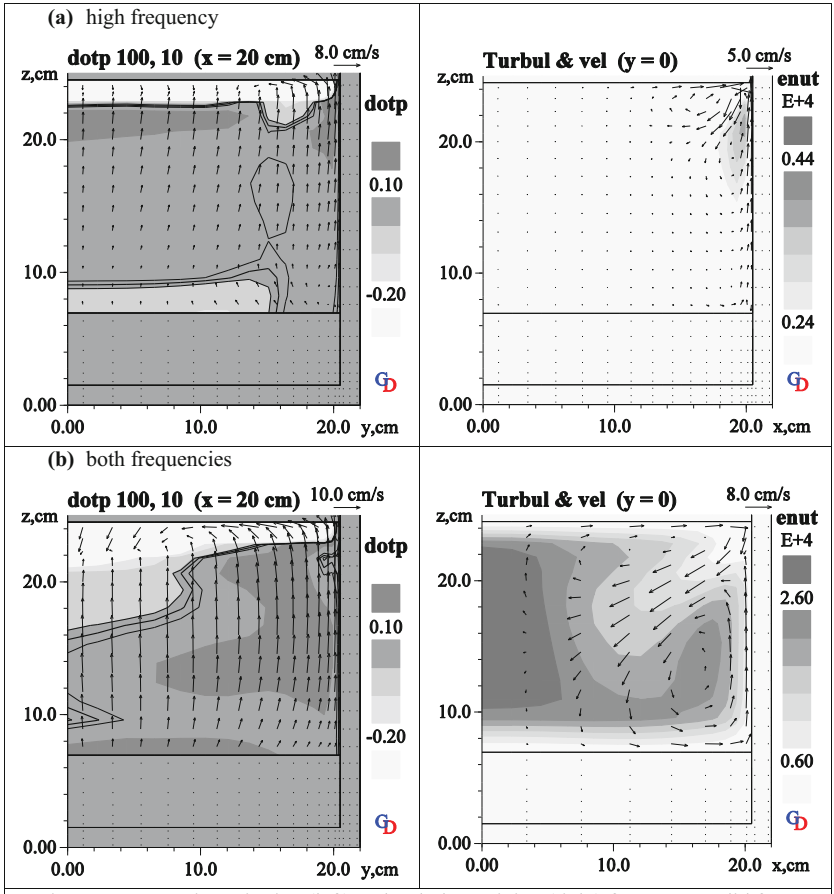

Figure 2. Separation criterion (left) and turbulent mixing (right) for 55 mm solid front

Conclusions

A computational numerical model based on solving partial differential equations for the electric field vector in induction furnaces with one or two imposed frequencies addresses the problem of impurity expulsion from recycled PV silicon. The use of dual frequencies (low and high) provides a measure of independent control between heating, stirring and separation. Further work is in progress to optimise the process.

Acknowledgements

This work is financed by SIKELOR [2] - a project funded by the 7th Framework Programme of the European Commission, sub-programme: ENV.2013.6.3–1, project reference 603718.

References

1. J.O. Odden, G. Halvorsen, H. Rong, and R. Gløckner, "Comparison of the energy consumption in different production processes for solar grade silicon," Silicon for the Chemical and Solar Industry IX conf. Oslo, Norway, 2008.

2. Peng-fei Xing, Jing Guo, Yan-xin Zhuang, Feng Li and Gan-feng Tu, "Rapid recovery of polycrystalline silicon from kerf loss slurry using double-layer organic solvent sedimentation method," *International Journal of Minerals, Metallurgy and Materials*, **20**, (10), (2013), 947–952. DOI: 10.1007/s12613-013-0819-z

3. I. Lombardi et al. "High yield recycling process of silicon kerf from diamond wire wafering," Proceedings of the 24th European Photovoltaic Solar Energy Conference, Hamburg, Germany, 21-25 September 2009.

4. SIKELOR. Silicon kerf loss recycling. www.sikelor.eu

5. D. Leenov and A. Kolin, "Theory of electromagnetophoresis". *Journ. Chem. Phys*., **22** (4), (1954), 683-688.

6. H.K. Moffatt, and A. Sellier, "Migration of an insulating particle under the action of uniform ambient electric and magnetic fields. Part 1. General theory," *J. Fluid Mech*., **464**, (2002), 279–286.

7. S. Taniguchi, N. Yoshikawa, and K. Takahashi, "Application of EPM to the separation of inclusion particles from liquid metal," *The 15th Riga and 6th PAMIR Conference on Fundamental and Applied MHD*, A. Alemany, Ed., Salaspils Institute of Physics, Riga, Latvia, 2005, p. 55. http://pamir.sal.lv/2005/cd/vol.I/riga-pamir-vol.I-55.pdf

8. F. Dughiero, M. Forzan, C. Pozza, and A. Tolomio. "Experimental results in industrial environment of the i-DSS furnace." Conference: Modelling for Electromagnetic Processing, Hannover, Germany, 2014. http://www.sikelor.eu/publications

9. G. Djambazov, V. Bojarevics, K. Pericleous, N. Croft. "Finite volume solutions for electromagnetic induction processing." *Applied Mathematical Modelling* **39** (2015) 4733–4745.

10. PHYSICA Theory Manual. http://staffweb.cms.gre.ac.uk/~physica/phy3.11/theory/

11. V. Bojarevics and K. Pericleous. "Particle tracking during melting and solidification in the presence of AC magnetic field of various configurations." Proceedings 8th Int. Conf. Electromagnetic Processing of Materials, 2015, Cannes, France.

12. M. Cross, T. N. Croft, G. Djambazov and K. Pericleous. "Computational modelling of bubbles, droplets and particles in metals reduction and refining." *Applied Math. Modelling*, **30**, 1445–1458, 2006.

REWAS 2016: Towards Materials Resource Sustainability
Edited by: Randolph E. Kirchain, Bart Blanpain, Christina Meskers, Elsa Olivetti, Diran Apelian, John Howarter, Anne Kvithyld, Brajendra Mishra, Neale R. Neelameggham, and Jeff Spangenberger
TMS (The Minerals, Metals & Materials Society), 2016

POTENTIAL CONTRIBUTION TO THE SUPPLY OF SILVER BY THE RECYCLING OF INDUSTRIAL RESIDUES FROM Zn, Pb AND Cu PLANTS

Stefan Steinlechner[1]

[1]Chair of Nonferrous Metallurgy, University of Leoben
Franz-Josef-Str. 18, Leoben, 8700, Austria/Europe

Keywords: Industrial wastes, recycling, silver, precious metals

Abstract

The focus of recycling processes for industrial residues from lead, zinc and copper industry in the past was mainly on the recovery of the base metals. Silver, gold or also PGMs are well-known valuable side elements in the corresponding ores and with this significant contents can be found in some of the residues but were not recovered in the past. Therefore, the recovery of for instance silver is highly interesting, beside the above described base metals to contribute to the overall economy of a potential recycling process, although they occur in much smaller quantities in materials like tailings, sludge, slags or dusts. As an example, the annually produced and mainly dumped amount of zinc leach residues contains roughly 500 tons of silver beside lead, zinc and others. Therefore, the present paper tries to answer how recycling of such industrial residues can contribute for example to the supply of silver or also other precious metals.

Introduction

To maintain as well as improve the quality of life especially raw materials play a crucial role. Due to not evenly distributed resources worldwide, often discrepancies between supplier and consumers of metals are the result. Especially the industrialized countries consume high amounts of technologically important metals, like silver but also PGM or indium, etc. in for instance the electronic industry or food industry. At the moment, the element silver, compared to PGMs, Indium, Germanium, etc. is not declared as critical in the EU. Nevertheless, the silver demand is forecasted to steadily grow due to its application in electronic industry. A critical aspect in this context is the fact that silver mainly is produced as a by-product of other metals. Table 1 summarizes this circumstance for silver and other minor metals present in the same carrier metal, next to the source of by-product, the share of production in case that there are more than one and its share on the total revenue.
By looking at the table, the supply from primary ore obviously does not correlate with the demand of the critical metal itself. Moreover, it is linked to the production amount of the main metal (lead, zinc, copper or gold), carrying the side element silver. Taking this circumstance into account it becomes obvious that also the by-products and waste streams arising from this industry are potentially carrying those metals.

Table 1: Summary of selected minor metals and their production route from primary metals. Critical materials defined by the EU are underlined. [1, 2]

By-product Metal	Sources of Production	Share of Production	Recovery Efficiencies	Max. Share of Total revenues
Germanium	Zinc	70 %	≈12 %	≈2 %
	Coal	25 %	-	-
Gold	Primary	≈90 %	-	-
	Copper	≈10 %	>99 %	≈20 %
Indium	Zinc	100 %	25-30 %	≈3 %
Silver	Lead-Zinc	≈35 %	>95 %	≈45 %
	Primary	≈30 %	-	-
	Copper	≈23 %	>99 %	≈25 %
	Gold	≈12 %	-	-

By-products and residues from lead, zinc and copper production

Following the residues/by-products generated during zinc, lead and copper production are described and their potential to contribute to the silver supply is summarized.

Residues from hydrometallurgical zinc production

The hydrometallurgical route processes the major part of sulfidic or oxidic zinc ore today. Although several new technologies were implemented, like the direct leaching of sulfidic ore or the solvent extraction, two main routes can be differed in the hydrometallurgical zinc winning. The following figure illustrates the conventional two-step leaching and the one-step leaching under moderate acidity, applied in case of low iron containing zinc ores (see figure right side).

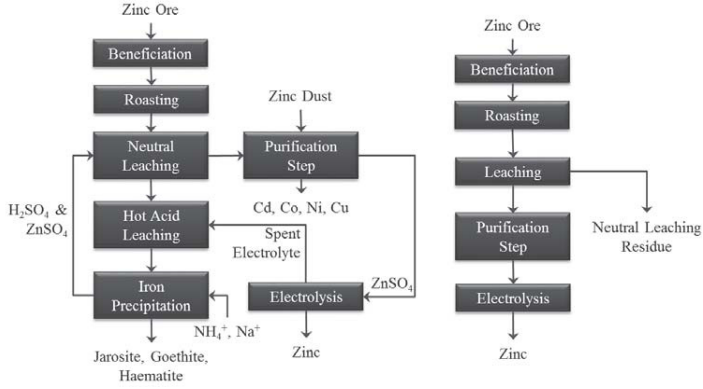

Figure 1: Left: Typical zinc production flow sheet by neutral- and hot acid-leaching, Right: One-step leaching carried out for low iron containing ores

The first step before the leaching is typically a roasting. By this, a zinc ferrite is formed in case of present iron in the ore, making the hot acid leaching step necessary to keep zinc losses low.

Due to the fact zinc ores always contain certain amounts of lead, silver and in some cases also other precious metals, which are not soluble under this moderate leaching conditions, the neutral leaching residue is the outlet for those metals [3] in case of the one-step concept. In this case 600-700 kg neutral leach residue is generated per ton of zinc, with silver contents of up to 0.1 % Ag.
In case of higher iron containing ores, formed zinc-ferrite is present and leads to the necessity of a hot-acid leaching. This additional step typically done to keep zinc losses because of hardly soluble zinc-ferrite spinel, low. In case that there is no separate filtration step for the hot-acid-leaching residue, which carries typically lead, silver and SiO_2, the iron is directly precipitated onto the remaining material and therefore the lead, silver is contained in the iron-residue. In addition, used calcine from the roaster for pH adjustment during the precipitation introduces lead and silver as well as zinc in the jarosite residue. Typically, the iron precipitate can be utilized in case of a precipitation as goethite but not in case of jarosite, leading to huge dumps worldwide filled with jarosite residues. Even in case of a lead-silver separation a certain amount of silver and lead can be found as a result of the utilized roasted ore (calcine) used for pH adjustment. Literature reports that 500-600 kg Jarosite per ton of zinc are generated with up to 230 ppm Ag [4, 5] in this residue next to also present indium and possible other precious metals. Own investigations showed up to 300 ppm of silver and Indium in investigated dried filter cakes.

Slags from primary lead production

Different lead production routes are available depending on the ore type. Below figure summarizes the general ways of direct production and the processing of mixed lead/zinc ores in a shaft furnace.

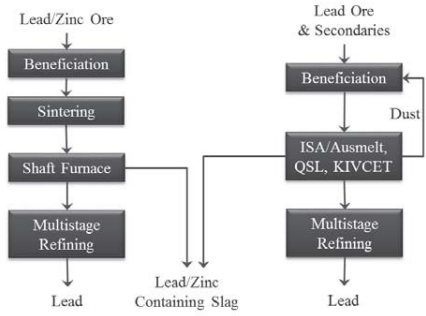

Figure 2: Overview of lead production routes

In case of a lead/zinc concentrate, the typical way is the route via the shaft furnace, producing zinc as well as lead in the so-called Imperial Smelting process. An average composition of a slag obtained from an IS furnace is shown in the table below.

Table 2: Average composition of generated slag from an IS furnace [6, 7, 8]

	Zn [%]	**Pb [%]**	**Cu [%]**	**S [%]**	**FeO [%]**	**SiO_2 [%]**	**CaO [%]**
Slag	6-9	0-2.5	0-0.6	0-3.6	37-45	15-19	13-21

The ratio between reducing agent and zinc has to be kept at a certain level to avoid the reduction of the iron in the charge. This leads to losses of lead and zinc in the slag. As accompanying elements of lead, the silver is well known and can be found partly also in the slags of the process. Own investigations showed silver contents up to 150-200 ppm per ton of material. In average, the generated amount of slag is 0.65 to 1.00 times the amount of produced zinc [6, 7, 8].
In case of low zinc containing lead ores, the lead is the only product without zinc as a direct by-product. This can be carried out for instance in shaft furnaces with a pre-sintering step or in QSL-, Ausmelt- or other direct production furnaces. Nevertheless, up to 3 % of zinc in the ore is contained in the raw material, which is not recovered and with this has to be removed from the process stream. This can be done for instance with the generated slag, by keeping the reduction potential in the furnace low so that the zinc-oxide is not reduced and stays in the taped slag. Literature states that a content of above 11 % zinc oxide in the taped slag is required to economically process the slag in an additional step, the slag fuming, for a recovery of zinc as zinc oxide. In case of lower amounts of zinc in the slag, it was dumped [7].
However, dumps with zinc contents up to 15 % exists next to significant amounts (up to 6 %) of lead and with this silver. The amount of generated slag per ton of lead fluctuates from lead production site to site because of different ores, facilities and with this recovery rates between 400-600 kg per ton.

Copper production

Especially in the copper production a wide range of materials, like precious metals containing electronic scrap next to other kinds of copper scrap are recycled. Due to the mentioned processing of complex materials (WEEE, shredder material, different sludge, etc.) an major input of other elements like zinc, lead, tin, halogens but also precious- and minor metals is the result. With the aim of producing high grade copper, those “impurities” have to be removed by generated slag-, dust- or slime phases during the smelting, reduction and converting step or also in the electrolysis. As consequence these elements enriche in those phases and can form valuable “residues”.
Related to the utilized raw material, the secondary copper production can be divided in four main steps, the melting and reduction, the converting, the fire refining and the electrolytic refining step. The figure below show a principal flow sheet of a secondary copper plant with integrated lead and tin recovery. Depending on the grade of material, the charging takes place in different steps. This offers a wide range of possible raw materials to be recycled. An internal recycling of the generated slag keeps the copper content low. Nevertheless, some plants do a reprocessing to recover also small remaining copper droplets. However, a huge amount is dumped without treatment and therefore could be potential for copper, gold and silver recovery. The generated anode slime in electro refining is typically processed in precious metal sites, so that it does not show new potential. However, especially the first two stages are emitting up to 60 kg dust per ton of produced copper, which show high contents of the valuable metals. One reason for this are present halogens, by for instance flame retardant introduced by charged PCBs or other plastics (insulations of wires), which form volatile metal halides, collected in the end in the bag house filters. By this mechanism zinc, lead and also indium are removed mainly by vaporization but also precious metals are partly evaporated as halides next to the mechanical carry over. This leads to strongly fluctuating chemical compositions of the dust, depending on the charged raw material, used process technology and operation parameters [9, 10].

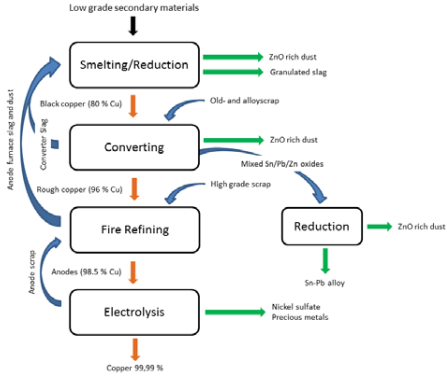

Figure 3: Principle flow sheet of a secondary copper production [9]

Especially the content of the minor metals cannot be predicted exactly. The following Table 3 gives an overview about a typical composition of the main elements in copper smelter flue dust.

Table 3: Composition of a typical flue dust from secondary copper production in [%] [9, 10]

Zn	Pb	Sn	Cu	Cl	Br	F	S	Fe	CaO	SiO_2
35-45	10-15	2-5	2-6	3-5	3-6	0.5-1	1-2	1-4	2-3	1-3

Metals like zinc, lead, tin and copper can be identified as valuable main fraction in the dust, but next to that up to 800 ppm silver beside gold and PGMs are present, due to carry-over as well as formed volatile compounds. Although there is a zinc content of up to 50 % it is not possible to use this material directly in the primary zinc production. The main reason are the halogen compounds, which would disturb the electro winning process significantly. Moreover, the presence of high lead, tin and copper contents leads to higher effort and additional problems in the zinc winning. Nevertheless, these dusts are showing high potential concerning the secondary production of precious metals [9, 10].

Conclusions to the status and potential of residue recycling

Especially ores from zinc, lead and copper industry carry silver, gold, PGMs or also indium etc. as valuable side elements. With this, the residues from that industry sector show specifically potential to contribute to the future silver and other precious metals supply. Next to residues which are inefficiently treated or dumped, also a lot of by-products, like solution cleaning residues from zinc industry, anode slime from copper industry or by-products from lead refining, are utilized already or further processed. Nevertheless also in this area optimization potential is still here. Table 4 summarizes the main by-products and residues generated in copper, zinc and lead industry, whereof the origin was already described in the previous chapters.
On the one hand the complexity of the material and with this expensive processes but on the other hand also the fact that in various processes only one metal is considered to be recovered, is the reason why still today some of the mentioned materials are dumped.

Table 4: Status of precious metals recycling out of residues from lead, zinc and copper industry

Base Metal	Copper	Zinc	Lead
Mainly recycled	Anode slimes	Neutral leach residues Goethite	Matte
Generally not recycled	Slags from 1st step Dusts from various steps	Jarosite	Slag Speiss

Although the typical amount of minor elements in those materials is very low, in some cases only ppm, they can contribute a lot to the possible overall revenue of recycling concepts for those residues. Table 5 summarizes this circumstance and estimates the amount of silver contained in the discussed untreated residues of the lead, zinc and copper industry.

Table 5: Potential sources of precious metals and estimated amount of silver in untreated residues from copper, lead and zinc industry

untreated material	amount	silver	potential for:	
	in 1 000 t	in t	gold	PGMs
Jarosite	4 000	800	Yes (low)	
Goethite	400	100		
Neutral leaching residues	200	200	Yes (low)	Yes (low)
Dust from sec. copper industry	100	50	Yes	Yes
Lead slag	3 000	150		

It can be summarized that the potentially recovered silver from untreated residues is 1 300 tons of Ag annually, which would represent 5.1 % of the worldwide mine production. Even not considered is the amount of additional potential in different mine wastes. The average contents of gold and PGMs are relatively difficult to estimate in these residues, which is the reason why it is only mentioned in what residues there is a potential. Nevertheless, it was shown that there is high potential of different secondary resources to contribute to the silver as well as other precious metals supply in future.

Acknowledgement

The authors want to thank the Austrian Research Promotion Agency (FFG) and the Federal Ministry of Science, Research and Economy (BMWFW) for the financial support.

References

[1] World Survey Silver 2014, published by Thomas Reuters, London, ISSN: 2372-2312.
[2] Study on Critical Raw Materials at EU Level. http://ec.europa.eu/DocsRoom/documents/5605/attachments/1/translations/en/renditions/native [Accessed 5th March 2015]
[3] J. E. Dutrizac, J. L. Jambor: Jarosite and their application in hydrometallurgy, Reviews in Mineralogy and Geochemistry, 01/2000, Volume 40(1), 405-452.
[4] A. Roca, J. Viñals, M. Arranz,J. Calero: Characterization and alkaline decomposition/cyanidation of beudantite–jarosite materials from Rio Tinto gossan ores, Canadian Metallurgical Quarterly, Volume 38, Issue 2, April 1999, 93–103
[5] Haisheng Han, Wei Sun, Yuehua Hu, Baoliang Jia, Honghu TangSchool: Anglesite and silver recovery from jarosite residues through roastingand sulfidization-flotation in zinc hydrometallurgy, Journal of Hazardous Materials 278 (2014) 49–54
[6] Graf G.: Ullmann Zinc, Ullmann's encyclopedia of industrial chemistry, Vol. A28 (2003) 509–530.
[7] Pawlek F.: Metallhüttenkunde, Walter de Gruyter, Berlin, Germany, New York, N.Y., 1983.
[8] Krajewski W., Krüger J.: Schlacken und Steinbildung bei der thermischen Blei- und Blei-Zink-Erzeugung, Schlacken in der Metallurgie 1 (1984) 147–160.
[9] M. Ayhan, Das neue HK-Verfahren für die Verarbeitung von Kupfer-Sekundärmaterialien, Intensivierung metallurgischer Prozess: Heft 87 der Schriftenreihe GDMB, 2000, 197-207
[10] M.E. Schlesinger et al, Extractive Metallurgy of Copper 5th edition, 2011, Elsevier

REWAS 2016: Towards Materials Resource Sustainability
Edited by: Randolph E. Kirchain, Bart Blanpain, Christina Meskers, Elsa Olivetti, Diran Apelian, John Howarter, Anne Kvithyld, Brajendra Mishra, Neale R. Neelameggham, and Jeff Spangenberger
TMS (The Minerals, Metals & Materials Society), 2016

THERMODYNAMIC ANALYSIS OF ZINC STATUS IN THE UPSTREAM EAF OFFGAS CLEANING SYSTEMS ASSOCIATED WITH IN-PROCESS SEPARATION OF ZINC FROM EAF DUST

Naiyang Ma[1]

[1]ArcelorMittal Global R&D - East Chicago Laboratories; 3001 E Columbus Dr.; East Chicago, IN 46312, USA

Keywords: Electric arc furnace dust; Zinc; Recycling; In-process separation; Thermodynamics

Abstract

Electric arc furnace dust is a listed hazardous solid waste and is thus subjected to a high treatment cost. Development of cost-effective technologies to recycle the dust is always a challenge. There are two critical problems in existing recycling practices of electric arc furnace dust: (1) iron in the dust is not recovered and is lost in slags or residues; (2) recovery of zinc from zinc-lean electric arc furnace dust is more costly. Strategy of in-process separation of zinc from electric arc furnace dust, being aimed at producing two recyclable electric arc furnace offgas byproduct streams, zinc-rich one and iron-rich one, has been recently proposed to attack these two problems. However, suitability of facilitating this strategy in electric arc furnace offgas cleaning systems has been questioned. In this study, thermodynamic analysis on zinc status in the upstream electric arc furnace offgas cleaning systems was carried out to examine possibilities of applying in-process separation strategy in producing cleaner byproducts of both zinc-rich dust and iron-rich dust for complete recycling of the electric arc furnace dust.

Introduction

Due to high flexibility, strong capability of recycling scrap, low energy consumption and low CO_2 emissions, electric arc furnace (EAF) steelmaking has grown greatly in the worldwide range. At present, about 63% steel in the United States, 50% steel in Europe and 29% steel worldwide are produced by electric arc furnaces.[1-3] However, along with steel production, electric arc furnaces also generate EAF dust. EAF dust generation rate varies from furnace to furnace, depending on raw materials, steel grades and operating conditions. On average, EAF dust generation rate is about 15 kg per ton steel.[4-6] In 2014, steel production was 88.3 million tons in the United States and 1,661.5 million tons globally.[7] Therefore, it can be estimated that in 2014, EAF dust generation was about 834,000 tons in the United States and 7.23 million tons worldwide, respectively.

EAF dust is a listed hazardous solid waste in most of the countries on this planet. There are generally two methods which are allowed for treating the hazardous EAF dust. One is to chemically stabilize the EAF dust first and then dispose the treated dust at well-lined landfills. The other is to send the EAF dust to zinc recyclers if the EAF dust contains sufficiently high level of zinc.

However, there are a series of critical issues with current EAF dust treatment. First, treating EAF dust with both landfilling and recycling is rather expensive and has imposed a heavy financial burden on EAF steelmaking companies. Technologies are badly needed for relieving EAF

steelmaking companies from this heavy financial burden. Next, most of the existing EAF dust recycling processes do not recover iron from the EAF dust. Iron values are totally lost in slags or residues. Third, in order to profitably recycle EAF dust, zinc concentration in EAF dust must be high enough. Otherwise, EAF dust recyclers will not accept the EAF dust unless EAF steelmakers are willing to pay higher fees.

In order to resolve above-mentioned issues, EAF steelmakers might take two measures. One is to reduce the generation of the dust, and the other is to increase zinc concentration in the dust. These two measures are often closely related. For electric arc furnaces with given raw materials, high zinc concentration in EAF dust often corresponds to low EAF dust generation rate.

Full recycling of EAF dust back into EAF furnaces has been widely developed and tested for achieving both increase of zinc concentration in shipped EAF dust and decrease of shipped EAF dust quantity.[8-10] However, the full recycling of EAF dust back into EAF furnaces can cause significant increase of energy consumption, limited zinc enrichment and possible deterioration of steel quality due to zinc build-up in the furnaces.[11] Therefore, full recycling of EAF dust back into EAF furnaces is hardly financially justified.

In-process separation strategy has been recently proposed to separate EAF dust into zinc-rich portion and iron-rich portion in EAF offgas cleaning systems so that the zinc-rich EAF dust can be sold to zinc market for a profit and the iron-rich EAF dust can be recycled back into EAF furnaces.[12] With in-process separation, EAF dust is fully recycled, and both zinc value and iron value are utilized. Since only zinc-rich dust will be shipped out, the total quantity of EAF dust will decrease significantly. In addition, due to zinc enrichment in the shipped EAF dust, recycling of zinc-lean EAF dust will no longer be a problem. The key factor in in-process separation is to find a cost-effective separator which can be installed in the upstream EAF offgas cleaning system for effective separation of zinc from rest of the EAF dust.

Two methods have been derived to enable in-process separation of zinc from rest of the EAF dust in EAF offgas cleaning systems. [12] One is to keep EAF offgas at high temperature and to use a high-temperature dust collector to capture EAF dust so that zinc vapor can bypass the high-temperature dust collector and precipitate in low-temperature dust collectors in the downstream EAF offgas cleaning systems. The other method is to quench EAF offgas from very high temperature at high cooling rate so that zinc vapor can be oversaturated and form tiny particles. A dust collector can be designed in such a way that zinc-rich tiny particles will bypass the dust collector while iron-rich large particles will be retained in the dust collector.

Whether there exists a region in EAF offgas cleaning systems where EAF offgas is under appropriate conditions for in-process separation of zinc from EAF dust becomes a critical point for applying in-process separation strategy in separating zinc from rest of the EAF dust. Thus, the possibility for implementing in-process separation in the EAF offgas cleaning systems has been questioned due to being afraid off early formation of zinc ferrite in EAF offgas cleaning systems. [13]

In the rest of this paper, EAF offgas cleaning systems will be reviewed first, then thermodynamic analysis will be carried out for evaluating stability of zinc vapor in an EAF offgas cleaning system, and eventually conclusion will be reached.

OFFGAS CONDITIONS IN AN EAF OFFGAS CLEANING SYSTEM

EAF offgas before the slip gap of elbow has the most favorable conditions for facilitating in-process separation of zinc from rest of the EAF dust. In literature, measurement by Kleimt et al. represents offgas conditions in this region.[14] In Kleimt's measurement, a water-cooled sampler was positioned in the top of inside EAF furnace near the offgas exit. The offgas was continuously analyzed with a mass spectrometer. Measured results in a whole heat are shown in Figures 1-2. One can see that gas composition and temperature vary over the whole heat, but O_2 is always near depletion. Overall, the offgas conditions can be represented in two regions. One region is before the second scrap charge and the other is after the second scrap charge. In the first region, offgas temperature is about 1400 ˚C and CO/CO_2 is about 4. In the second region, the offgas temperature is around 1480 ˚C and CO/CO_2 is about 3.5. O_2 concentration is near zero and hence it will not be considered in later thermodynamic analysis.

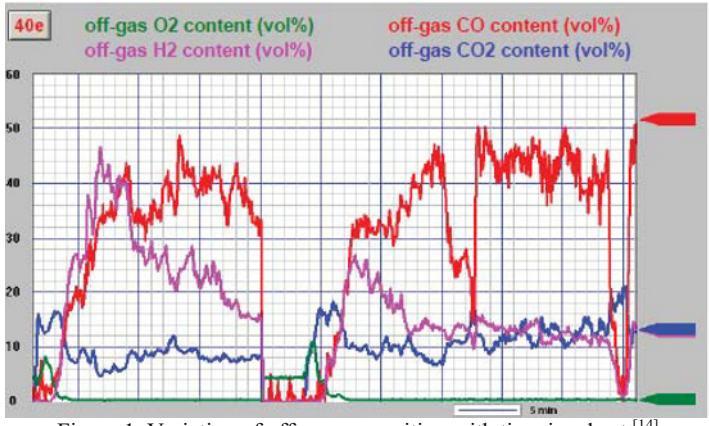

Figure 1. Variation of offgas composition with time in a heat [14]

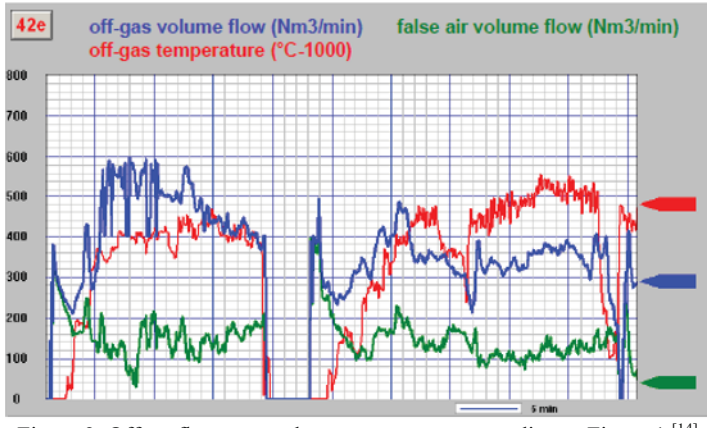

Figure 2. Offgas flow rate and temperature corresponding to Figure 1 [14]

According to Kleimt et al., "false air" in Figure 2 was entrained air in the sampling system, not in the furnace.[14] Due to thermodynamics, as long as there is sufficient CO in the offgas, O_2 concentration should be rather low in the offgas.

STABLE STATUS OF ZINC IN THE REGION NEAR OFFGAS EXIT

Zinc in the offgas near the furnace exit could be vapor Zn, solid ZnO or solid $ZnFe_2O_4$. The following reactions might occur

$$Zn(g) + CO_2 = ZnO(s) + CO, \quad (1)$$

$$3/4Zn(g) + 1/2Fe_3O_4 + CO_2 = 3/4ZnFe_2O_4(s) + CO. \quad (2)$$

Gibbs free energy changes of above reactions can be calculated by the following formulae

$$\Delta G_1 = \Delta G_1^0 + RT \ln(\frac{CO/CO_2}{p_{Zn}}), \quad (3)$$

$$\Delta G_2 = \Delta G_2^0 + RT \ln(\frac{CO/CO_2}{p_{Zn}^{3/4}}), \quad (4)$$

where ΔG_i^0 is standard Gibbs free energy change for reaction i, i=1, 2, R is gas constant, T is temperature in K, CO/CO_2 is ratio of CO Vol. % to CO_2 Vol. %, and p_{Zn} is zinc vapor partial pressure in the gas.

According to thermodynamics principal, if $\Delta G_i < 0$, reaction i proceeds to right hand side, and zinc vapor is not stable, can be oxidized and forms ZnO or $ZnFe_2O_4$; if $\Delta G_i = 0$, reaction i reaches equilibrium; if $\Delta G_i > 0$, reaction i proceeds to left hand side, zinc vapor is stable, and zinc oxides (ZnO or $ZnFe_2O_4$), if there are any, can be reduced and forms zinc vapor.

HSC 5.1 has been used to calculate the standard Gibbs free energy changes of reactions 1-2. Gas conditions demonstrated in last section has been used. Assume zinc vapor partial pressure in the gas changes from 10^{-5} atm to 10^{-1} atm. The calculated results of Gibbs free energy changes for reactions 1-2 are shown in Figures 3.

From Figure 3, one can see that under the considered gas conditions, Gibbs free energy changes for reactions of forming zinc oxides are all far greater than zero. Therefore, it can be inferred that zinc vapor is stable and prevails in EAF offgas near the furnace exit. If there is any ZnO or $ZnFe_2O_4$ in the offgas near the furnace exit, it will be reduced into zinc vapor by CO.

This calculation shows that EAF offgas near the furnace exit is under favorable conditions for in-process separation of zinc from rest of the EAF dust. After offgas exits into the elbow before the slip gap, the offgas temperature might decrease, but the gas composition might keep unchanged. Variation of Gibbs free energy changes with temperature for reactions 1-2 under the conditions of this calculation has been also calculated and the results are shown in Figure 4.

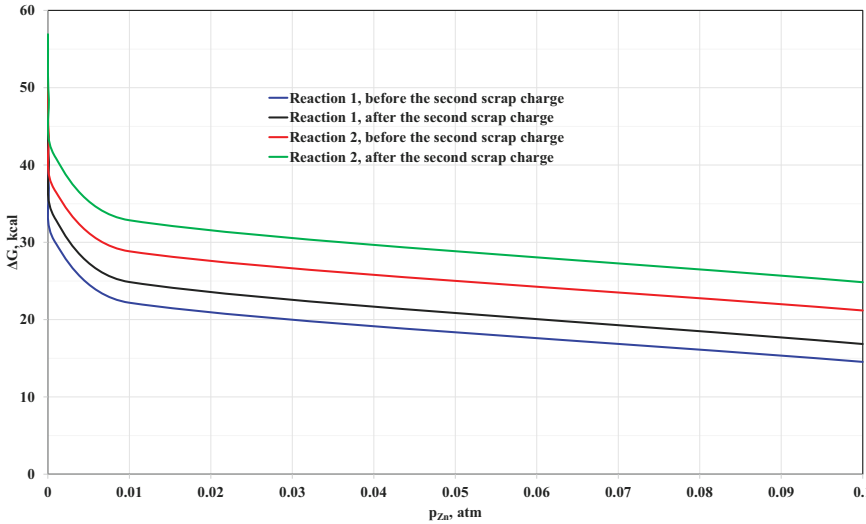

Figure 3. Gibbs free energy changes for reactions of forming zinc oxides

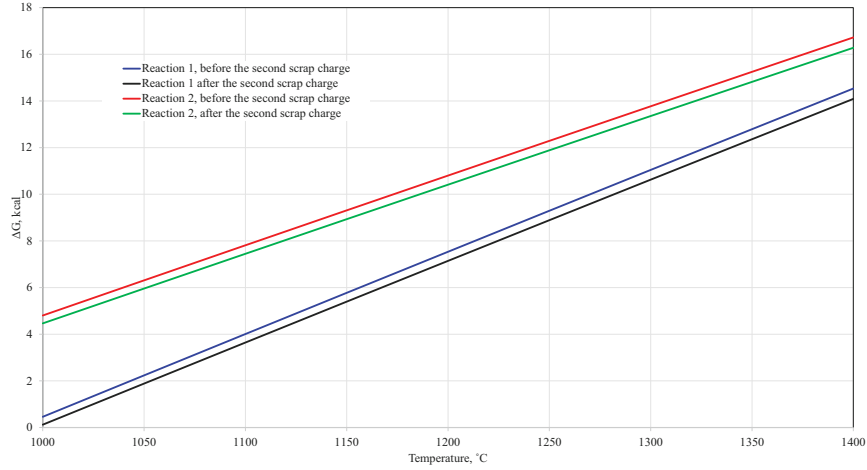

Figure 4. Gibbs free energy changes for reactions 1 and 2 versus temperature, assuming p_{Zn} 0.1 atm

One can see that even at as low as 1000 ˚C, zinc vapor is still stable, and zinc oxides, if there are any, can be reduced into zinc vapor in the offgas. This might be the reason why a scrap preheater can achieve up to 20% reduction of EAF dust generation, [15] and why a technology of separating zinc from EAF dust by a coke-bed filter integrated with a zinc condenser was developed. [16]

CONCLUSIONS

Thermodynamic analysis has demonstrated that zinc vapor is stable in the region from EAF offgas exit to the slip gap. Offgas conditions in this regions are favorable to reducing zinc oxides, like ZnO and ZnFe2O4, if there is any, into zinc vapor. In-process separation of zinc from EAF dust can be facilitated in this region. A high temperature separator can be installed in this region for separation of zinc from rest of the EAF dust.

REFERENCES

[1] USGS, *Mineral Commodity Summaries - Iron and Steel*, 2015. Website: http://minerals.er.usgs.gov/minerals/pubs/commodity/iron_&_steel/mcs-2015-feste.pdf. Accessed on August 31, 2015.

[2] Bouwen met Staal, *Production Routes for Steel*. Website: http://www.sustainableinsteel.eu/p/531/production_routes_for_steel.html. Accessed on August 31, 2015.

[3] World Steel Association, *Resource Efficiency*. Website: https://www.worldsteel.org/steel-by-topic/sustainable-steel/environmental/efficient-use.html. Accessed on August 31, 2015.

[4] AISI, *Steel Technology Roadmap – Iron Unit Recycling,* US Department of Energy, 2001. Website: http://www1.eere.energy.gov/industry/steel/pdfs/roadmap_chap3.pdf, pp. 65 – 66. Accessed on August 31, 2015.

[5] International Iron and Steel Institute, The Management of Steel Industry By-products and Waste, International Iron and Steel Institute, Brussels, Belgium, 1994, 5-4 – 5-5.

[6] Lehigh University, Characterization, Recovery and Recycling of Electric Arc Furnace Dust, Lehigh University, Bethlehem, Pennsylvania, 1982, II-3.

[7] World Steel Association, *World Crude Steel Production – Summary*, 2015. Website: https://www.worldsteel.org/dms/internetDocumentList/press-release-downloads/2015/2014-Crude-Steel-Statistics-Tables/document/2014%20Crude%20Steel%20Statistics%20Tables.pdf. Accessed on August 31, 2015.

[8] J. Jensen and K. Wolf, Reduction of EAF Dust Emissions by Injecting It into the Furnace, *MPT-Metallurgical Plant and Technology International*, No. 3, 1997, 58-62.

[9] A. Tsubone et al., Development of EAF Dust Injection Technology in Aichi Steel, *AISTech Proceedings*, 2012, 163-172.

[10] L. Evans and J. Hogan, Recycling of EAF Dust by Direct Injection, *Electric Arc Furnace Steelmaking Conference*, ISS, 1987, 367-372.

[11] R. Pruszko et al., An Assessment of Energy, Waste, and Productivity Improvements for North Star Steel Iowa, DOE Report, 2003. Website: http://www.steelnet.org/archive/20030618.htm. Accessed on August 31,2015.

[12] N.-Y. Ma, On In-process Separation of Zinc from EAF dust, *TMS 2011 Collected Proceedings*: EPD Congress 2011, pp 947 – 952.

[13] T. Suetens et al., Formation of the $ZnFe_2O_4$ Phase in an Electric Arc Furnace Off-gas Treatment System, *Journal of Hazardous Materials*, 287(2015), 180-187.

[14] B. Kleimt et al., Application of Models for Electrical Energy Consumption to Improve EAF Operation and Dynamic Control, 8th European Electric Steelmaking Conference, Birmingham 183-197 (2005). Website: http://www.yuber.com.tr/english/yeni_pdf/EAF_Energy_Model.pdf, Accessed on September 6, 2015.

[15] EPRI Report, Electric Arc Furnace Scrap Preheating, *TechCommentary*, 2000. Website: http://infohouse.p2ric.org/ref/10/09048.pdf, accessed on September 1, 2015.

[16] S. Isozaki, *et. al*., The Technology for Direct Separation and Recovery of Iron from EAF Exhaust Gas, *La Revue De Metallurgie – CIT*, January 2002.

REWAS 2016: Towards Materials Resource Sustainability
Edited by: Randolph E. Kirchain, Bart Blanpain, Christina Meskers, Elsa Olivetti, Diran Apelian, John Howarter, Anne Kvithyld, Brajendra Mishra, Neale R. Neelameggham, and Jeff Spangenberger
TMS (The Minerals, Metals & Materials Society), 2016

EVALUATION OF REACTOR REOV-01 WITH Ti ELECTRODE FOR ELECTROCHEMICAL RECOVERY OF Ag FROM INDUSTRIAL WASTES

Pedro Alberto Ramirez Ortega[1], Victor Esteban Reyes Cruz[2], Maria Aurora Velóz Rodríguez[2] Laura Garcia Hernández[1], Diana Arenas Islas[1], Mizrraim Uriel Flores Guerrero[1] Luis Garcia L[1]

[1]Área Electromecánica Industrial, Universidad Tecnológica de Tulancingo Camino a Ahuehuetitla No. 301 Colonia Las Presas, Tulancingo, Hidalgo, C.P. 43642, México
[2]Área Academica de Ciencias de la Tierra y Materiales, Universidad Autónoma del Estado de Hidalgo, Carretera Pachuca –Tulancingo Km. 4.5, Mineral de la Reforma, Hidalgo C.P. 42184, México

Keywords: Silver Recovery. Industrial wastes, electrochemical reactor, Ti, DSA

Abstract

In this work the evaluation of a filter press type Reactor (REOV-01) with Ti electrode was realized, applied in the silver recovery from industrial wastes. Macroelectrólisis studies were performed at different flow velocities with empirical and dimensionless correlations and parameters. The results of the variation of the concentration of Ag at different flow linear velocities allowed the determination of the mass transfer coefficients of silver (order of 10exp-5) for Ti electrode, which are consistent with the literature. Chronopotentiometric studies showed that the Ti electrode performed better for the recovery of silver because to a current of -150 mA during 210 minutes was achieved 99.8% of silver recovery. The current efficiency values above 100% indicated that the electrochemical process is coupled to an electroless process. The results showed low energy consumption and high space-time yield values indicating that the REOV-01 presents an excellent performance in the recovery of silver.

Keywords: Silver recovery, Radiographic films Industrial wastes, electrochemical reactor, Ti, DSA

Introduction

Silver is used in four major areas, including the industrial, photography, jewellery and coin sectors. In recent years, the industrial sector has shown an increase in the use of silver, due to its new applications in different areas. Nevertheless in sectors such as photography the consumption of silver has declined as a result of the rise of digital photography. At the present, several countries have taken the task of recovering silver from industrial wastes, due to the economic value and environmental impact they represent. Their main sources of silver recovering are the wastes generated by the photographic sector. Various technologies have attempted to recover silver contained in these wastes; however, they have not fully satisfied with the requirements of maximum recovery, neither the environmental level (less than 5 ppm) of silver in effluents [1]. There is a large number of electrochemical reactors that can be used for various processes including Electrocell AB, FM01 and FM21-LC, which are used in laboratory studies, in pilot plants and on an industrial scale, respectively [2,3]. The reactor FM01-LC is a smaller version of the reactor FM21-SP (2100 cm^2 electrode area) developed by ICI TM [4]. This reactor has shown its versatility, allowing the use of two or three-dimensional electrodes, membranes as well as baffles and turbulence promoters that allow a favored mass transfer [5-7]. This type of reactor is the best for the most of the electrochemical processes due to its simplicity of cell construction and the application of a variety of materials for its manufacture. Furthermore, the distributions of potential and current are reasonably uniform. Therefore, in this work the use of filter press type Electrochemical reactor (called REOV-01) was considered as a unit process for the recovery of silver present in radiographic films from the photographic industry on Ti.

Materials and Methods

In this work, a filter press-type electrochemical reactor (REOV-01) was used with a system of three electrodes (working, counter and reference). The capacity of the reactor is 280 mL. The working electrode was Titanium (geometric area of 64.3 cm2), a saturated calomel electrode (SCE) as reference and a DSA mesh (Ti/RuO2) as counter electrode. The hydraulic system was especially designed to work safely the nitrate solution used to dissolve the silver of the radiographic films (denominated below as SRF). A centrifugal Marathon Electric pump (1 HP of power) was used to maintain constant recirculation of the solution SRF.

The solution used for the studies was prepared in the laboratory with nitric acid solution 5%v/v and 250 g of radiographic films, giving an initial concentration of 2100 ppm Ag^{+}. The macroelectrolysis studies were carried out to constant current during 120 minutes of electrolysis time, imposing a current of -65 mA on the titanium electrode. The electrochemical studies were carried out using a potentiostat-galvanostat PAR 263A connected to a power source KEPCO with capacity of 10 A. The used techniques were handled through the PowerSuit software provided by the same company.

Results and Materials and Methods

Figure 1 shows in logarithmic scale the decay of the normalized concentration of Ag^{+} of the solution SRF to different linear velocities, in function of electrolysis time for Ti electrode. The experiments used a current imposition of -65 mA. The experimental setup considered in this work could be identified as a continuous reactor with recirculation, where the mathematical equation that relates the concentration variation with the flow, is very particular. However, considering that the solution remains in circulation and it changes with time, in addition that the volume of the cell is way smaller compared with the volume of the container makes the reactor behave like a batch reactor.

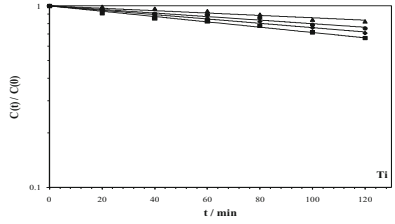

Figure 1. Log of the normalized concentration of Ag^{+} of the solution SRF in function of electrolysis time for Ti electrode to current of -65 mA and flow linear velocity range of 7.5 a 15 $Lmin^{1}$.

Figure 1 shows a linear behavior with the logarithm of the normalized concentration of Ag^{+}, respect to the electrolysis time for the four flow velocities of the solution SRF on the Ti electrode. This behavior is consistent with the mathematical model of batch reactors and indicates that the reduction of silver is controlled by mass transport. Under these conditions, the batch reactor equation to determine the mass transport coefficient is:

$$\ln\frac{C(t)}{C(0)} = -\frac{K_m A t}{V_T} \qquad (Ec.\,1)$$

Where C (t) is the concentration change respect to time, C (0) the initial concentration, Km is the mass transfer coefficient, A is the active area of electrode and V_T is the electrolyte volume.

From the value of the slope of each line (figure 1) and the equation Ec.1, the Km values for each electrode were calculated. Table 1 shows the Km values for the last three flow velocities imposed on the Ti electrode, considering that at these velocities the system is under an established flow regime. Table 1 indicates that the mass transfer coefficient (Km) for silver increases with flow linear velocities in Ti electrode.

Table 1. Mass transfer coefficient (Km) for electroactive especies of Ag^+ for Ti electrode. The evaluation of Km is made considering an area of 37.4016 cm^2.

u (m/s)	**Km** (ms^{-1})
0.43	$1.68x10^{-5}$
0.54	$2.04x10^{-5}$
0.65	$2.48x10^{-5}$

The magnitude of the mass transfer coefficients Km (10^{-5} ms^{-1}) obtained in this work is of the same order of magnitude to the ones obtained for the ferrocyanide in a reactor FM01 on Ni flat electrodes [1, 8-12]. Generally is found that for a given electrode geometry, a certain electrolyte and under certain flow conditions, the Km is obtained through the following equation:

$$K_m = \alpha \upsilon^{\beta} \qquad (Ec.2)$$

Where υ is the characteristic velocity (the electrolyte linear velocity or, the rotation velocity of a rotating electrode); the exponent β and the value of α are adjustment factors for the experimental data. For laminar flows the value of β is between 0.3 and 0.5 and higher β values are turbulent flows.

Figure 2 shows the behavior of log Km and log υ for Ti electrode on the SRF solution in logarithmic scale, the mass transfer coefficient of Ag^+ has a linear increase with increasing flow linear velocity. Experimental correlation expression is determined using the slopes in figure 2, which relates the mass transfer coefficient Km with the flow linear velocity υ and the equation Ec.2, where the β value indicates the type of flow regime in the reactor. The experimental correlations obtained for the Ti electrode is $Km = 4x10^{-5}\upsilon^{1.16}$. The β values obtained indicate that the electrochemical reactor REOV-01 operates under a fully developed turbulent flow for Ti electrode.

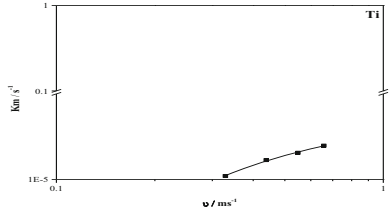

Figure 2. Variation of log Km Vs log υ to imposed a current of -65 mA on Ti electrode, during an electrolysis time of 120 minutes.

Experimental correlations with dimensionless numbers Re-Sc-Sh for the silver recovery process in the reactor REOV-01.

Km values obtained from different flow rates (table 1) are used to calculate the dimensionless numbers: Sherwood (Sh), Reynolds (Re) and Schmidt (Sc). The proposed correlation with dimensionless numbers is:

$$Sh = \boldsymbol{a} Re^{\boldsymbol{b}} Sc^{\boldsymbol{c}} \qquad (Ec.3)$$

Where **a,** is a constant of proportionality, **b** characterizes the flow regime and is assumed that **c** has a value of 1/3. The values of the constants **a**, **b** and **c** depend on both the geometry of the electrode and the flow conditions [8]. Table 2 shows the values of the physical properties of the solution used to obtain the corresponding correlations, Schmidt numbers (Sc) and the equivalent (hydraulic) diameter d_e. The diffusion coefficients values are from the literature [12] and the equivalent (hydraulic) diameter d_e of the cell was calculated using the following equation:

$$d_e = \frac{2\,B\,S}{(B+S)} \qquad (Ec.4)$$

Where S is the thickness of the electrode and B is the height of the electrode.

Table 2. Physical properties of the SRF solution used to obtain the dimensionless numbers.

Physical propieties	**Ti**	**Reference**
Kinematic Viscosity	$0.01 cm^2 s^{-1}$	(10,11)
Diffusion Coefficient of Ag (D_{Ag})	$6.10x10^{-6} cm^2 s^{-1}$	(10)
Characteristic length (d_e)	1.58cm	This work

The behavior of the logarithm of the product ShSc-0.33 and the logarithm of Re on the Ti shows the relationship $ShSc^{-0.33}$ in the last flow linear velocity. Using the slope of the curves and equation Ec.3 can be known the experimental correlations of dimensionless numbers for the Ti electrodes, this correlation is:

A304 $Sh= 0.0018Re^{1.024}Sc^{0.33}$ (Ec. 5)

Ti $Sh= 0.0012Re^{1.163}Sc^{0.33}$ (Ec. 6)

The values of the constant **a,** in both electrodes, are of the same order of magnitude. The same behavior occurs with the values of the constant b for the Ti (1.163), which confirmed that the reactor REOV-01 operates under a fully developed turbulent flow. It is important to mention, that **b** values are close to the reported in the literature [5,7].

Current efficiency ϕ^e

The values of current efficiency, ϕ^e, from the results of the macroelectrolysis studies with different flow linear velocity υ and maintaining a controlled current are shown in table 3 and were calculated using the equation Ec.7.

$$\phi^e = \frac{W_j}{W_{TOTAL}} \qquad (Ec.7)$$

Where Wj is the weight of metal j deposited and W_{total} is the weight of the deposit that should be obtained by imposing a determined current during certain time [12, 13].

Table 3 shows the weight of metal j deposited increasing respect the flow linear velocity in Ti electrode. The high current efficiency values indicated that the electrochemical process is coupled to an electroless process. This is confirmed according with the theoretical mass (W_{total}) that should be transformed by electrochemical process, which is less than the real mass (W_j) obtained from the surface during 120 minutes of electrolysis time. These results indicated that the electroless process variables affect the silver recovery. Although, the electroless process due to changing linear flow provides important information on the silver recovery, it is not the objective in this research.

Table 3. Current efficiency ϕ^e respect the weight at different flow linear velocities imposed on titanium electrode.

	Ti		
υ (ms^{-1})	$W_{theoretical}$ (g)	W_{real} (g)	ϕ^e (%)
0.328	0.523	0.517	98.7
0.438	0.523	0.523	100
0.548	0.523	0.564	107.8
0.657	0.523	0.614	117.3

Power consumption (Es) and space-time yield (ρ_{ST})

Using equations Ec.8 and Ec.9, the energy (Es) and space-time yield (ST ρ_{ST}) for silver recoveries are obtained and they are presented in Table 4.

$$E_s = -\frac{nFE_{cel}}{\phi^e} \qquad (Ec.8)$$

$$\rho_{ST} = \frac{\phi^e iM}{nFV_R} \qquad (Ec.9)$$

Where n is the number of electrons, F is the Faraday's constant, E_{cell} is the cell potential, ϕ^e is the current efficiency, M is the atomic mass and V_R is the volume of the reactor.

Table 4 shows the results of energy consumption and space-time yield ρ_{ST} for silver obtained in the reactor REOV-01 when the flow linear velocity varies in the range of 0.328 to 0.657 ms^{-1} for Ti electrode. It shows that energy consumption decreases with increasing of the flow linear velocity for electrode, while the space-time yield increases ρ_{ST}. The decrease in the consumption is due to decreased cell potential and increased current efficiency. On the other hand, the increase in space-time yield ρ_{ST} is due to the increase in current efficiency. This behavior is due to the surface changes with the silver deposit diminishing the cell potential and increasing the deposit rate.

Table 4. Energy consumption and space-time yield ρ_{ST} for silver obtained in the reactor REOV-01 when the flow linear velocity varies in the range of 0.328 to 0.657 ms^{-1} for Ti electrode, electrolysis time of 120 minutes.

	Ti	
υ (ms^{-1})	E_s ($kWhKg^{-1}$)	ρ_{ST} ($Kgs^{-1}m^{-3}$)
0.328	0.296	$2.870x10^{-5}$
0.438	0.280	$2.903x10^{-5}$
0.548	0.253	$3.134x10^{-5}$
0.657	0.222	$3.411x10^{-5}$

The results show that the electrochemical reactor REOV-01 presents a good performance for the silver recovery from radiographic films on Ti electrode, due to it complies with operational parameters of an electrochemical reactor, presents low energy consumption (about 10^{-2}), high space-time yields (about 10^{-5}) and high current efficiencies (over 100%).

Based on these results, cronopotenciométrico study was realized on titanium electrode, a current of -150 mA, over a time of 210 minutes electrolysis at a constant flow rate of 0.657 ms^{-1} (15 Lm^{-1}). This study indicated that the recovery of silver is increased, because there is a greater decrease in [Ag] SRF in solution, reaching a value silver recovery of 99.8% at a current of - 210 mA at a

time of 210 minutes; with a energy consumption Es of 0.387 KWh/kg, a current efficiency ϕ^e of 99% and a space-time yield ρ_{ST} of $6.625x10^{-5}$ kg/sm^3. This behavior indicates that during the electrolysis process is being performed massive deposit of silver on the surface of Ti electrode.

Conclusions

Concentration decrease respect to the time obtained in this study indicated that the reactor REOV-01 behaves as a Batch reactor. Furthermore, the Km values are of the order of 10^{-5} and agree with the literature [4], indicating that this type of reactor configuration with flat electrodes is a convenient way to obtain the Km. Through empirical and dimensionless equations was determined that the REOV-01 reactor operates under a fully developed turbulent flow. The similarity of the correlation coefficient **b** for both correlations (dimensionless and empirical) supports this fact. The current efficiency values were above 100% suggest that the electrochemical process is coupled to an electroless process. The magnitude of energy consumption, current efficiency and space-time yield meet the requirements necessary for the proper functioning of an electrochemical reactor, indicating the viability of using the reactor REOV-01 in the silver recovery from radiographic films. For a current of -150 mA and an electrolysis time of 210 min, silver recovery reached 99.8% on Ti electrode. Indicate that the filter press-type electrochemical reactor (REOV-01) used in this study is an excellent option for the recovery

Acknowledgments

The author Pedro A. Ramírez O, would like to express their gratitude to PROMEP for their economic support (136567).

References

1. Ramírez O.P. A, *Estudio electroquímico preliminar para depositar Ag proveniente de los desechos sólidos de la industria fotográfica y radiográfica*. Tesis de Licenciatura, UAEH, Hidalgo, México (2006).
2. K. Guenter, Silver Recycling from photographic solutions: review of the methods, Chemical Labor Betr. 32 (1981), p40-48.
3. M. I. Ismail, Electrochemical reactors, their science and technology, part A: fundamentals, electrolysers, batteries and fuel cells; Elseiver Science Publishers B. V., Ámsterdam, Holanda (1989).
4. A. A. Wragg y A. A. *Leontaritis*. Chem. Eng. J. 66 (1997)
5. D. Pletcher y F. C. Walsh. Industrial Electrochemistry, 2nd Edn., Chapman & Hall, London (1990).
6. D. A. McInnes, The Principles of electrochemistry. New York, USA (1990).
7. D. Pletcher. A First Course in Electrode Processes. RSC Publishing, UK (1991).
8. C. J. Brown, D. Pletcher, F. C. Walsh, J. K. Hammond y D. Robinson. Studies of Space-Averaged Mass Transport in the FM01-LC Laboratory Electrolyser. J. of Appl. Electrochem. 22 (1992) 631.
9. G. M. Zarkadas, A. Stergiou y G. Papanastasiou, Influence of citric acid on the silver electrodeposition from aqueous AgNO3 solutions, J. Electrochimica Acta 50 (2005) 5022-2031.
10. N. Nakiboglu, D. Toscali y I. Yasa, *Silver recovery from waste photographic films by enzematic method*, Turk J. Chem. 25 (2001) 349-353.
11. P. C. Holloway, K. P. Merriam y T. H. Etsell, *Nitric acid leaching of silver sulphide* precipitates, J. Hidrometallurgy 74 (2004) 213-220.
12. K. Jauttner, *Electrochemical techniques for a cleaner environment*, European school on electrochemical engineering, Toulouse, Francia, (1995).
13. A. J. Bard and L. R. Faulkner, Electrochemical methods: fundamentals and applications, 2nd Edn., Wiley: USA (2000).

REWAS 2016: Towards Materials Resource Sustainability
Edited by: Randolph E. Kirchain, Bart Blanpain, Christina Meskers, Elsa Olivetti, Diran Apelian, John Howarter, Anne Kvithyld, Brajendra Mishra, Neale R. Neelameggham, and Jeff Spangenberger
TMS (The Minerals, Metals & Materials Society), 2016

MINI MILL SOLUTIONS IN THE RECYCLING OF ELECTIC ARC FURNACE DUST – THE 2^{S}DR PROCESS

Gernot Rösler[1], Christoph Pichler[2], Stefan Steinlechner[2] and Jürgen Antrekowitsch[1]

[1]Christian Doppler Laboratory for Optimization and Biomass Utilization in Heavy Metal Recycling, Montanuniversitaet Leoben, Franz-Josef-Str. 18, Leoben, 8700, Austria
[2]Chair of Nonferrous Metallurgy, Montanuniversitaet Leoben, Franz-Josef-Str. 18, Leoben, 8700, Austria

Keywords: EAFD recycling, 2^{s}DR process, zero waste

Abstract

High amounts of Steel Mill Dust is produced worldwide each year. Although the Waelz kiln is the preferred route for processing these wastes, significant amounts of this residue stays untreated. Very often, the unprocessed dust gets landfilled and therefore, it is lost for the recovery of zinc and further heavy metals accompanied in the waste. An alternative way with respect to treating Electric Arc Furnace Dust would be the so called 2^{s}DR (Two step Dust Recycling) process, which allows the simultaneous recovery of high purity zinc oxide as well as iron and other heavy metals. This leads to a zero waste process, because the remaining slag is free of heavy metals which allows a utilization for e.g. construction purposes. The present publication should give an overview on the process set-up itself; moreover, achieved data from extended lab scale trials underlines the sustainability of this process.

Introduction

Producing steel in an electric arc furnace (EAF) leads to the formation of electric arc furnace dust (EAFD) at melting down steel scrap. Due to the fact that the feed material, steel scrap, is very often coated by various materials like zinc and organic layers, usually this corrosion protection gets evaporated by the applied high temperatures inside the EAF and forwarded to the filter house. Because of the fact that the steel scrap comes very often from shredded car bodies, zinc is one the major elements within the EAFD, since the feed material is usually coated with zinc. Beside zinc, iron can be found as well in a huge quantity, here, small iron droplets are formed during the essential working steps at scrap smelting that are also elevated by the off gas stream and collected in the bag house filters. Beside these two metals, which are usually bond to oxygen, some amounts of chlorine and fluorine are present in the dust. Chlorine is often connected to hydrocarbons as organochloride. Sources for detecting this element can be also found within the charged material – organic coatings of car bodies for protection purposes. Fluorine can be often associated to casting powders in the melt shop. Further elements present in the EAFD are mainly lead, sodium and potassium. The conclusion of this enumeration of metals shows that the obtained EAFD is a complex mixture of a huge quantity of elements where the elemental distribution is very unstable since the conditions are always changing and depending on the feeding of the EAF and its composition. [1–5].

A statistical literature survey shows, that in average 450 Mio. t of crude EAF steel were produced in 2014. Moreover, assuming a dust amount of 15-25 kg/t of crude steel, 6.75-11.25 Mio. t of EAFD are generated each year. Of course, the Waelz kiln process seems to be a very good option to recycle these wastes occurring, since they are labelled as “Best Available Technique” or “Best Demonstrated Available Technology” for the recovery of zinc from EAFD´s. Unfortunately, some disadvantages are known which should be mentioned in the following: [1, 6–9].

- Minimum zinc content of the feed material > 9 % to run the process, nowadays the value is set to 20 % to run the process in an economic way.
- Iron is completely lost, as well as all further heavy metals
- Halides (mostly chlorine and fluorine) accumulate in the main product, the Waelz oxide (WOX) which are dissolved when leaching it in sulphuric acid to obtain zinc again via the hydrometallurgical electrowinning route; Chlorine harms the lead made anodes and forms chlorine gas, fluorine attacks the aluminium made cathodes [3, 5, 8].
- Nowadays there is a big concern with respect to the Waelz slag which contains the whole iron. As mentioned before, several other heavy metals are associated to the slag that often can be leached very easily. That means, a utilization for construction purposes seems to be not the best way, therefore it gets more and more declared as hazardous waste. Moreover, the financial effort increases continuously which makes the dumping much expensive. [10].

Since the Waelz process is still the preferred route for processing EAFD´s, although it has some disadvantages, the search for alternative routes has to go on. Several alternative methods were invented until now, but unfortunately, none of them were successful, also because they were producing new wastes again which makes the process uneconomic.

Theoretical consideration

A huge amount of data is available concerning the chemical composition. A good example is represented in Table 1 where the range of typical dust is represented. [11–18].

Table 1: Average chemical composition of an EAFD [18]

Species	Range (Weight-%)
Zn	17-32
Pb	0.1-3
FeO	23-45
CaO	3.5-15
MgO	1.7-9
SiO_2	1-8
Cl	0.1-4
F	0.1-1.5
S	0.2-1

Beside the chemical composition of the residue, a mineralogical analysis is mandatory to characterize the present dust [19]. The phases with the highest quantity are very often Fe_3O_4, which represents very often the matrix of the residue. Moreover, ZnO, $ZnFe_2O_4$, $MgFe_2O_4$, $FeCr_2O_4$, Mn_3O_4, MgO, SiO_2, $Ca_{0.15}Fe_{2.85}O_4$ can be found in varying quantities.

The mineralogical analysis shows, that a relevant amount of zinc is bond to iron, which makes a hydrometallurgical treatment difficult, since the zinc-ferrite bonding has to be cracked, leading to a high acid consumption and elevated leaching temperatures, as it is known from the hydrometallurgical zinc winning process.
The present proposal for a sustainable recycling process is pictured in Figure 1. The dust gets pelletized in a very first step, where an addition with fluxing agents is possible. The 2^{s}DR process (Two step Dust Recycling) starts subsequently after the beneficiation of the dust. It consists – as the name suggests – of two independent steps to treat EAFD to obtain a very pure zinc oxide and an iron alloy.
After agglomeration, the first step consists of a clinkering step of the EAFD where the undesired halides are removed as well as lead and small quantities of zinc. The process is carried out at temperatures in between 1100 and 1200 °C to guarantee a good removal efficiency.
The second step is the reduction step of the 2^{s}DR process. The hot clinker is forwarded to its reduction on a carbon containing iron bath. Here, the carbon dissolved in the melt reduces the oxidic components like iron, zinc and other heavy metals. Zinc gets evaporated and reoxidized in the offgas, forming very pure ZnO. Iron sinks into the melt and is accumulated with the other metals like Cr, Ni, Mo, etc. which increases the value of the iron bath. From time to time, the furnace is tapped and the iron is solidified and utilized as alloying element in the steel mill. Finally, the slag is free of heavy metals and can be easily used for construction purposes or road construction. By applying this technique a “zero waste” process, without any new residues, is proposed. The subsequent Figure 1 shows the procedure of the process on basis of two simultaneously operated Top Blown Rotary Converters (TBRC´s). A big advantage of this process is the variability of the used furnaces. For instance, instead of a TBRC in the first step, a short rotary furnace could be used. Moreover, the second TBRC could be substituted by a Submerged Arc Furnace (SAF).
The last mentioned configuration was applied for the present publication. Instead of using a TBRC for the reducing step, a SAF was used to reduce the clinker to obtain a dust that is high in zinc and to become an iron alloy which could be sent back to the steel mill immediately.

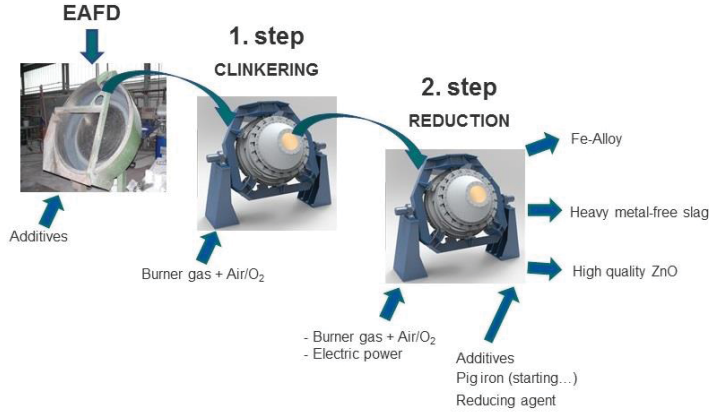

Figure 1: Draft of the 2^{s}DR process with additional agglomeration step at the beginning

The 2^{s}DR process using a TBRC and a SAF

A huge amount of tentative tests and small scale trials were performed in the past, the present paper will review the latest scale-up to 50 kg batch size by applying a TBRC for oxidizing (clinkering) and a SAF for reduction purposes. The process type using two TBRC´s, one for clinkering and one for reduction purposes, was already performed and published. [20]
As already mentioned, instead of using a second TBRC for reduction purposes, a SAF was used. To remove the undesirable halides from the EAF, a clinkering was proposed which should vaporize these elements. The experimental procedure started with heating up the TBRC at 1100 °C using a methane/oxygen burner. After reaching the temperature and a holding time to have a good temperature distribution within the refractory lining as well, the agglomerated EAFD was charged. Recent experiments show, that sufficient halogen removal needs at least 2 h. Also the "extended lab scale" trial was set to this time. The subsequent Table 2 shows the yield of the major elements obtained during this cleaning step.

Table 2: Yield of selected elements obtained at a 50 kg trial as well as the mass balance

Yield	Zn	Pb	Fe	Cl	F
[%]	85.8	70.3	94.2	<39.5	<33.8

Input Pellets [kg]	50.00
Output Pellets [kg]	44.07
Difference[kg]	5.93

It can be observed at the previous table, that there are some zinc losses, however, this quantity can be attributed to bonding of zinc with chlorine and fluorine. Moreover, almost 30 % of lead could be removed successfully, as well as the halides present in the residue. The supposed high values can be contributed to the lower measurement limit of the chemical analysis, since both elements were detected lower 0.1 % in the clinker. The hot material should be directly forwarded to the SAF in industrial scale, nevertheless, due to the fact that these experiments are still performed in a lab scale, it was not possible. The following Table 3 represents the input as well as output data of the executed SAF trial. It can be seen that the metal alloy amount increased due to the reduction of heavy metals out of the clinker and further accumulation in the iron. Furthermore, the subsequent Table 4 gives an overview on the elemental composition of the obtained products, where the success of the metallurgical treatment can be justified.

Table 3: Mass balance of the reduction trial at a 50 kg scale using a SAF

Input	[kg]	[%]	Output	[kg]	[%]
BF-Slag	10.0	19.16	Fe alloy	13.4	25.67
Pig Iron-Granules	10.0	19.16	Slag	21.3	40.80
Clinkered EAFD	20.0	38.31	Dust (incl. offgas)	17.5	33.52
Pet-coke	7.2	13.80	Sum	52.2	
Quartz	5.0	9.58			
Sum	52.2				

Table 4: Chemical analysis of the main products: dust, metal alloy and slag

Dust	ZnO	PbO	Fe_2O_3	Cl	F
[%]	98.14	0,99	0,38	0,45	0,04

Slag	ZnO	PbO	Fe_2O_3	Al_2O_3	CaO	MgO	SiO_2
[%]	0,26	0,01	3,4	11,5	22,6	6,9	42,4

Fe alloy	Zn	C	Fe	Mn
[%]	0,16	2,09	94,23	1,12

Summary and further developments

During the last years, the idea came up to invent a new way to process EAFD´s via an alternative route beside the Waelz kiln process. Since this process has some disadvantages, which will probably increase the processing costs in the coming years (e.g. for slag dumping, washing of WOX, etc. …) there will be space for new methods to treat this residue. The 2^sDR process is a potential candidate, since the plant design allows to erect this plant on-site of a steel mill, directly where the EAFD is generated. Moreover, the produced metal alloy will find its way back into the steel mill, therefore, a lot of energy can be saved. Furthermore, 2^sDR is very flexible with respect to the applied testing facilities, since the process is not designed to an explicit furnace. Flexibility is one of the major advantages of this process, also with respect to the input material. Very often, steel mills have varying feed material, therefore, also the dust composition and quantity is fluctuating.

Since the scale of the experiments is around 50 kg per batch, it is at the moment very difficult to get detailed data with respect to energy consumption. Values will be available after pilot scale trials. Theoretically, heating energy and reducing energy can be estimated by thermodynamic calculation.

Similar approaches can be assumed concerning cost calculation. The proposed cash cow will be the high quality zinc oxide, which is very low in Cl and F. Moreover, the iron alloy can be sold back internally to the steel mill, and since the obtained slag is free of heavy metals, a utilization as construction material is possible. Due to the critical situation with respect to slag handling, especially in the EU, the proposed cost planning accounts no revenues for slag utilization.

However, “extended lab scale” trials were very successful, in 2016, pilot scale trials are planned with a batch size of 500 kg to adjust the process design due to the changing behaviour because of the bigger scale. Further steps are focussed on detailed economic considerations.

Acknowledgments

The present work has been founded by the Austrian Federal Ministry of Science, Research and Economy. Moreover, the authors wish to thank Mr. Manuel Leuchtenmüller, MSc and Mr. Stefan Wegscheider, MSc for their huge contribution to this work.

References

[1] A.-G. Guézennec, J.-C. Huber, F. Patisson, P. Sessiecq, J.-P. Birat and D. Ablitzer: *Powder Technology,* 2005, 1-3, pp. 2–11.

[2] G. Ye, J. White and L.-Y. Wei, in *Global Symposium on Recycling Waste Treatment and Clean Technology, REWAS'99*, ed. Gaballah, I., Hager, J. and Solozabel, R., Minerals, Metals & Materials Society, Warrendale, PA, 1999, pp. 1503–1510.
[3] A. Zunkel, in *Third International Symposium, Recycling of Metals and Engineered Materials*, ed. Queneau, P.B. and Peterson, R.D., Minerals, Metals & Materials Society, Warrendale, PA, 1995, pp. 579–587.
[4] J. Rütten, in *3. Seminar Networking between Zinc and Steel*, ed. Harre, J., GDMB, Clausthal-Zellerfeld, 2011, pp. 77–90.
[5] S.R. Badger and W.K. Kneller, in *55th Electric furnace conference*, ed. Iron & Steel Society, Iron & Steel Society, Warrendale, PA, 1998, pp. 95–97.
[6] Integrated Pollution Prevention and Control (IPPC): *Reference Document on Best Available Techniques in the Non Ferrous Metals Industries,* 2011.
[7] worldsteel Committee on Economic Studies: *Steel Statistical Yearbook 2013,* Brussels*,* 2013.
[8] P.A. Kozlov: *The Waelz Process 2003,* Ore and metals publishing house, Moscow*,* 2003.
[9] US EPA: *Best Demonstrated Available Technology (BDAT) Background Document for K061,* 1988.
[10] H. Bartusch, A.M. Fernández Alcalde and M. Fröhling: *Erhöhung der Energie- und Ressourceneffizienz und Reduzierung der Treibhausgasemissionen in der Eisen-, Stahl- und Zinkindustrie (ERESTRE),* KIT Scientific Publishing, Karlsruhe*,* 2013.
[11] T. Sofilić, A. Rastovčan-Mioć, Š. Cerjan-Stefanović, V. Novosel-Radović and M. Jenko: *Journal of hazardous materials,* 2004, 1-3, pp. 59–70.
[12] J.G.M.d.S. Machado, F.A. Brehm, C.A.M. Moraes, C.A. dos Santos and A.C.F. Vilela: *Mat. Res.,* 2006, 1, pp. 41–45.
[13] J.G. Machado, F.A. Brehm, C.A. Moraes, C.A. dos Santos, A.C. Vilela and J. Cunha: *Journal of hazardous materials,* 2006, 3, pp. 953–960.
[14] P.J. Nolasco-Sobrinho, D.C.R. Espinosa and J.A.S. Tenório: *Ironmaking & Steelmaking,* 2003, 1, pp. 11–17.
[15] M.C. Mantovani, C. Takano and P.M. Büchler: *Ironmaking & Steelmaking,* 2004, 4, pp. 325–332.
[16] B. Garcia-Egocheaga, N. De Goicoechea and Gandiaga, in *Global Symposium on Recycling Waste Treatment and Clean Technology, REWAS'99*, ed. Gaballah, I., Hager, J. and Solozabel, R., Minerals, Metals & Materials Society, Warrendale, PA, 1999.
[17] A.M. Hagni, R.D. Hagni and C. Demars: *JOM,* 1991, 4, pp. 28–30.
[18] A. Ruh and T. Krause, in *3. Seminar Networking between Zinc and Steel*, ed. Harre, J., GDMB, Clausthal-Zellerfeld, 2011, pp. 35–46.
[19] A. Stefanova and J. Aromaa: *Alkaline leaching of iron and steelmaking dust,* Aalto University, Helsinki*,* 2012.
[20] G. Rösler, C. Pichler, J. Antrekowitsch and S. Wegscheider, *JOM*, 2014, 9, pp. 1721-1729.

Understanding & Enabling Sustainability - (Rechargeable) Batteries

REWAS 2016: Towards Materials Resource Sustainability
Edited by: Randolph E. Kirchain, Bart Blanpain, Christina Meskers, Elsa Olivetti, Diran Apelian, John Howarter, Anne Kvithyld, Brajendra Mishra, Neale R. Neelameggham, and Jeff Spangenberger
TMS (The Minerals, Metals & Materials Society), 2016

ROADMAP FOR THE LIFECYCLE OF ADVANCED BATTERY CHEMISTRIES

Timothy W. Ellis[1]
John A. Howes[2]

[1]President, RSR Technologies, Inc.,
4828 Calvert St., Dallas, TX 75247 USA
Chairman, SAE Battery Recycling Committee, & Chairman, Advanced Lead-Acid Battery Consortium

[2] Principal, Redland Energy Group, 1875 Eye St., NW, Washington, DC 20006
Vice-Chairman, American Bar Association Energy, Infrastructure and Reliability Committee

Keywords: Circular Economy, Recycling, Batteries

Abstract

Energy storage and recycling are among the most important strategies identified by governments and non-governmental organizations to confront the challenges of developing a more "circular" economy. The need for more efficient batteries to help the energy storage industry meet the changing needs of a growing world population is presenting new opportunities for metals used to make batteries. For the use of these metals to be compatible with the needs of a circular economy, recycling is key to the efficient utilization and conservation of natural resources. Some materials used in the battery industry have been adapted to the needs of a circular economy more successfully than others. Lead is the most recycled of all metals, with a battery recycling rate of 99%. The lessons learned from the utilization of a highly-recycled metal such as lead must be considered a model for the development of batteries made with other metals.

Introduction

Between now and 2050, the world's population is expected to grow from 7.7 billion to 9.5 billion. The world's middle class will grow from 23 per cent to 52 per cent. The demand for technologies to serve the needs of agriculture, manufacturing, communications, and transportation will grow exponentially. Batteries are particularly important not only because of their role in serving these growing needs, but because of the greater use of natural resources. To minimize this growing impact on natural resource demand, recycling is one of the most important strategies to confront these challenges in a more "circular" (or "restorative") economy.

Some materials used in the battery industry have been adapted to the needs of a circular economy more successfully than others. Lead is the most recycled of all metals. The recycling rate of lead (95%) exceeds the recycling rates of such metals as nickel (88%), cobalt (68%), zinc (60%), copper (53%), cadmium (15%), or lithium (1%).[i] It is important, therefore, that lessons learned from a highly-recycled metal such as lead be considered a model for the development of batteries made with other metals.

Changing consumer needs and the battery industry

The world's economy has evolved, for the most part, in a "linear" fashion in which goods produced from natural resources were simply incinerated or disposed of in landfills. Most governments, especially in the developing world, did little to encourage or mandate changes in disposal patterns. Pollution caused by such disposal practices is a matter of record.

Yet, a number of industries (such as lead, aluminum, copper and steel) with leaders aware of the need for effective resource management have developed recycling processes into successful businesses. They all have demonstrated that recycled materials can be economically competitive with materials extracted from natural resources.

Recycling at battery end-of-life

Until recently, the rechargeable battery industry was largely a "static" one, serving starter-lighting-ignition (SLI) functions in vehicles, along with deep-cycle batteries for motive power applications and standby storage. Now, batteries are needed for more rapid discharge-recharge and they must be lower weight and lower cost. They also must be produced in accordance with principles of environmental stewardship. Hence, the need for effective and profitable recycling.

An economically viable recycling industry for lead-acid batteries has existed for more than 100 years, but has not for lithium batteries. Instead, the lithium industry is promoting the "second use" of batteries when they are no longer suitable for use in hybrid or electric vehicles. Lithium batteries can be "remanufactured" or "repurposed" for use in less demanding applications such as stationary power sources.[ii] While this certainly extends the useful life of lithium-ion batteries, it still does not address the question of what to do with them when they no longer are useful in any function. As a result, recycling remains the best long-term answer to lithium batteries.[iii]

Ultimately, as the use of lithium batteries continues to grow, their status under the Resource Conservation and Recovery Act of 1975 (RCRA) will become an important issue. Under RCRA, the U.S. Environmental Protection agency sets standards for the management of hazardous waste. Lead-acid batteries are tightly regulated under RCRA and also by individual states. Lithium batteries in large format applications, however, are not.[iv] This likely will change as the volume of large format lithium-ion batteries grows and/or incidents of battery failures increase.[v]

There is a crucial economic relationship between the value of a battery when purchased by a consumer and the value of a battery when purchased by a recycler. Recyclers of materials, such as secondary lead smelters, are paid for tons processed. The greater the tonnage recycled, the larger the facilities that can be supported. The lower the cost of tons produced, the more competitive recycled metals are against metals produced from primary sources.

Batteries are sold to the consumer as highly engineered devices with very high material performance requirements. To a recycler, however, the end-of-life value of the battery is predicated on the value of elements recovered from the battery. Commodities markets set both the value of the scrap and the value of metal emerging from the recycling process. Market volatility is a fact of life in both values. The lead-acid industry is better able than competing

chemistries to manage the risk volatility associated with buying scrap, operating a smelter, and selling recycled metal in a highly competitive market.

The recycling process for lead-acid is straightforward because its success has long been established in high volume markets like automotive, industrial and motive power. For more than a half century, lead-acid batteries have set a remarkable record for recycling efficiency. In the western world the collection and recycling rate of lead-acid batteries is in the high 90% range. Nearly 90% of new lead-acid batteries are made from recycled materials with no government subsidies required. Lead-acid recycling is a profitable business throughout North American and Europe and the fact that it has remained so has kept jobs in those regions.

The importance of recycling needs to be clearly understood. As a matter of sound public policy, the disposal of hazardous wastes into landfills is to be avoided wherever possible. But, accomplishing that objective is a challenge better met by some industries than others.

The closed loop model:

- Batteries are produced, sold, used and collected at their end-of-life.
- Recyclers separate the battery materials (metal, acids, containers, etc.).
- The separated materials are recycled and sold to battery producers.
- Prices charged for recycled materials produced in this closed loop are competitive with primary (or "virgin") materials. The cost of recycling is rolled into the retail battery price.

How recyclers make profits:

- Recyclers make a profit when the price of the finished product they sell to battery producers is higher than the price they pay for batteries at their end-of-life (scrap).
- Sufficient production volume generates revenue to support the enterprise.

Ideally, the metals recovered through recycling should be as usable and economically competitive with metals extracted from natural resources as the world moves toward a "circular economy." Recycling is preferred to "down-cycling" in which recovered metals are often used in purposes such as road slag because their value is below that of metals from virgin resources. That is the challenge facing metals used in batteries that seek to compete against lead-acid.

No other battery chemistry can make the same claims of profitability and environmental stewardship as lead-acid batteries, which for the most part are made with the same materials in a design that has stood the test of time for more than 150 years. Batteries made with other chemistries, however, are a different story.

Lithium batteries, for example, are made from a collection of metal oxides and/or phosphates with multiple combinations of manganese, cobalt, nickel, iron, titanium, etc. in the cathode and anode materials. Carbon based materials are also present as graphite for anodes or as part of the electrolyte systems. While each of these base elements is relatively inexpensive, it is the engineering required to design and manufacture the batteries that accounts for their high cost. As a result, materials extracted from lithium-ion cells at their end-of-life, if they pass certain criteria,

can be used for road/concrete aggregate, but little else. The lithium has been "downcycled" because its value to battery manufacturers is considerably lower than "virgin" lithium.

Nickel metal hydride (NiMH) cells are in a similar situation as Li-ion although the NiMH chemistry is not as potentially powerful. From the perspective of recycling, the fact that NiMH batteries are comprised mostly of nickel is a good start. However, the addition of lanthanides (rare earths) and other "transition" metals to the hydrogen storage alloys used in the cathode adds complexity to the design. Recovery of the lanthanides is troublesome as they are oxidized in the recycling process. The reprocessing of these elements back into commercially usable metals is very difficult, one that requires fluoride salts and metallothermic reduction with calcium to form clean metal for realloying. At the present time, most NiMH cells are recovered in secondary stainless steel operations where much of the value of the battery grade material is lost.

In the case of lead extracted from scrapped lead-acid batteries, the recycled lead neatly enters battery manufacturers in recognizable form because a defined and economic point of transfer exists between recycling and manufacturing.

Recycling options for "advanced" batteries

In the case of lithium-ion and nickel metal hydride, two of the more widely used "advanced" battery chemistries, recycling options are highly complex compared to lead-acid. These options are being researched by industry with support from the U.S. Department of Energy. Here is a brief review of various recycling technologies.

Pyrometallurgical operations utilize high temperature processes which reduces elements to their metallic state for resale as base metals in industry. There are several pros and cons to this approach. On the "pro" side, the pyrometallurgical process is a well-established technology that allows for immediate transfer into running plants. However, on the "con" side, it is a complex and expensive process from an environmental remediation perspective. Emissions to the air and water from the pyrometallurgical process require costly scrubbing. Potential loss of many recyclable components and metals to combustion may require the use of hydrometallurgical operation to fully recover all valuable materials.

Hydrometallurgical operations use aqueous chemicals which solubilizes the material for precipitation or electrowinning in further processes. On the "pro" side, the advantage is a well-established process technology with high recovery of materials which may be implemented after a pyrometallurgical process is used to recover metals lost to the slag or matte. On the "con" side, compliance with environmental, health and safety regulations can be expensive because of the pyrometallurgical operations required for initial processing of material before or after hydrometallurgical processing.

Direct recycling based upon physical methods of separation, e.g. comminution, mineral dressing (screening), elutriation, flotation, gravity separation, magnetic and electrostatic separation, is an area of active development. This process uses specific unit operations to separate the different materials into concentrates which may be directly turned back into battery production. There are some very attractive "pros." Low fugitive emissions and recovery of battery grade materials

without reforming compounds may fit the strict definition of recycling set by the European Union Battery Directive (EUBD). However, there are "cons." Direct recycling is in its developmental stage and needs a track record to demonstrate it is robust enough to be used through multiple cycles. The unconventional metallurgical flow sheet may require some pyrometallurgical and hydrometallurgical operations for initial preparation of material.

In time, sufficient data on these three approaches will be accumulated for a comparative economic analysis.

Roadmap required

Essentially all non-lead-acid battery chemistries have been designed to maximize performance while minimizing first run production costs. Recycling, unfortunately, for the most part remains an afterthought. The level of private investment and government research into the recycling of non-lead-acid batteries pales in comparison to the dollars spent in developing, producing and marketing them. This is in stark contrast to the lead-acid battery recycling industry, which has had more than 100 years to develop and is highly efficient and profitable.

	Lead-acid	Lithium-ion	Nickel Metal Hydride
Standard chemistry design	Yes	No	Yes
Battery design compatible with recycling	Yes	No	No
Recycled materials readily accepted by battery producers	Yes	No	No
Recycling costs rolled into battery price	Yes	No	No
Battery recycling rate*	99%**	<15%***	<60%****

* Source: US EPA, USGS
** Most recycled lead is used in new lead-acid batteries.
*** Some cobalt recycled. Other materials "downcycled," i.e., road slag.
**** Most nickel "downcycled" for use in stainless steel production.

Making recycling work for lithium-ion, nickel metal hydride or other "advanced chemistries" involves many challenges. A specific road map is required, one that takes into account the ever-changing realities of economics and public policies in an increasingly circular economy.

Roadmap for advanced battery recycling

Goal – Advanced batteries must have a "closed-loop" life cycle.
- "End-of-life" management must be rolled into the retail price of batteries.

Objective – Make advanced battery R&D compatible with circular economy.
- Recycling must be included in R&D for battery design.

Strategy – Integrate life-cycle management into advanced battery R&D.
- Public-private partnership must consider entire closed-loop process.
- Lessons learned from batteries with established life-cycle management should be shared with other chemistries.

The regulations governing "end-of-life" processes for lead-acid batteries must be extended to other chemistries if the principles of environmental stewardship are to be observed and upheld.

The consequences of a failure apply comparable regulatory treatment throughout all battery chemistries and technologies are already becoming apparent. Many batteries, including lithium-ion, that lack effective recycling, are simply stockpiled in warehouses, disposed in landfills or even mixed into shipping containers with lead-acid batteries and sent to secondary smelters.

In many instances, the physical appearance of lithium batteries is similar to lead-acid batteries, making it difficult for personnel at lead-acid recycling facilities to sort them before they go into crushing machines. This is happening with increasing frequency. On several recent occasions, undetected lithium-ion batteries have exploded inside lead-acid recycling equipment. At a minimum, governments must mandate that all batteries be properly labeled so they can be sorted at secondary lead smelters.

Also, the manner in which recyclers are regulated should be comparable throughout the world. Regulations governing worker safety and environmental protection must be comparable to prevent a "race to the bottom" in which recyclers looking to cut overhead will flock to countries with weak standards and enforcement.

Finally, there must be a recognition that while processes such as "downcycling," "remanufacturing" or "repurposing" of battery materials may have certain worthwhile attributes, they should not considered "just as good" as recycling in the movement toward a more circular economy.

---

[i] United Nations Environmental Program, 2011, "Recycling Rates of Metals, a Status Report."

[ii] Standridge, et al, "Remanufacturing, Repurposing, and Recycling of Post-Vehicle Application Lithium-Ion Batteries," Mineta National Transit Research Consortium, June 2014.

[iii] Kamath, "Expectations for Lithium-Ion Batteries in Post-Vehicle Second-Life Applications," Electric Power Research Institute, March 7, 2011

[iv] Gaines, "The future of automotive lithium-ion battery recycling: Charting a sustainable course," Argonne National Laboratory, October 6, 2014

[v] Mikolajczak, et. al., "Lithium-Ion Batteries Hazard and Use Assessment," Fire Protection Research Foundation, July, 2011

REWAS 2016: Towards Materials Resource Sustainability
Edited by: Randolph E. Kirchain, Bart Blanpain, Christina Meskers, Elsa Olivetti, Diran Apelian, John Howarter, Anne Kvithyld, Brajendra Mishra, Neale R. Neelameggham, and Jeff Spangenberger
TMS (The Minerals, Metals & Materials Society), 2016

PORTLAND CEMENT WITH BATTERY WASTE CONTENTS

Henry A. Colorado*, Sergio A Colorado

Composites Laboratory, Universidad de Antioquia UdeA, Calle 70 No. 52-21, Medellin, Colombia.

Abstract
Waste from alkaline and carbon batteries is processed in this research and combined with white ordinary Portland cement. In Colombia, battery waste is not used or recycled at all, and those that are collected are put in a landfill facility. After removing the metal, plastic and paper from the battery, the waste is mostly composed of zinc, manganese and iron oxides. This research presents results for the use of these materials, and characterization of the by-products. Scanning electron microscopy (SEM), X-Ray Fluorescence, and compression tests were conducted in this investigation. It was found that samples have good compressive strength, this is over 20MPa for 50wt% of battery waste for a process suitable to improve and increase this value. As expected, results showed that compressive strength decreased as waste content increased.

Keywords: battery waste, recycling

Corresponding author:
Email, *H. A. C: henry.colorado@udea.edu.co; Universidad de Antioquia, Facultad de Ingenieria. Bloque 20, Calle 67 No. 53 - 108, Medellin, Colombia

1. Introduction

Battery waste is a big concern nowadays because of its negative effects on life and environment due to the contents of diverse hazardous materials. In Colombia, about 11000 tons per year of battery waste is disposed in repository, from which about 8000 tons corresponds to zinc-carbon (Zn-C), 2000 tons corresponds to alkalines and 1000 tons to secondary and other batteries 1. An alkaline battery is a type of primary battery based on the reaction between zinc and manganese oxide (IV), see Figure 1a. These batteries have a higher energy density and life with the same voltage than zinc carbon batteries. Upon the reaction, zinc and manganese oxide are consumed in the reaction, see equation 1. Analyzing the components, the main by-products are steel, plastic, zinc oxide (ZnO) and manganese oxide (III).

Zinc-carbon (Zn-C) batteries are composed of similar compounds than alkaline batteries, Figure 1b. Carbon does not participate in the reaction of equation 2. This Zn-C battery reaction uses $ZnCl_2$ as an electrolyte.

$$Zn_{(s)} + 2MnO_{2(s)} \rightleftharpoons ZnO_{(s)} + Mn_2O_{3(s)} \quad (1)$$

$$4Zn(s) + 8MnO_2(s) + ZnCl_2(aq) + 9\ H_2O(l) \rightarrow 8\ MnO(OH)(s) + Zn(OH)Cl(aq) + 5H_2O + 4ZnO \quad (2)$$

Several studies about the recovering and characterization of Zn-C and alkaline batteries have been reported before 3 regarding the effect of oxides in the crystalline structure 1, recovering of manganese oxide, thermal and materials characterization 4, and fabrication of new materials 5. Several technologies for recycling these batteries have been reported in a review article by

Sayilgan et al 6 that includes methods such as physical pyrometallurgical and hydrometallurgical processes. Managing processes and life cycle have been also investigated 7, 8.
The aim of this investigation is to fabricate Portland cement with additions of battery waste (BW) using alkaline and zinc-carbon batteries. This process is conducted in order to decrease the negative impact of this waste on life and environment. In addition, this research aims for the development of new cements for especial applications and reduced cost. The waste microstructure is analyzed with scanning electron microscopy (SEM) and compressive strength was evaluated with a Shimadzu AG-250KNG machine.

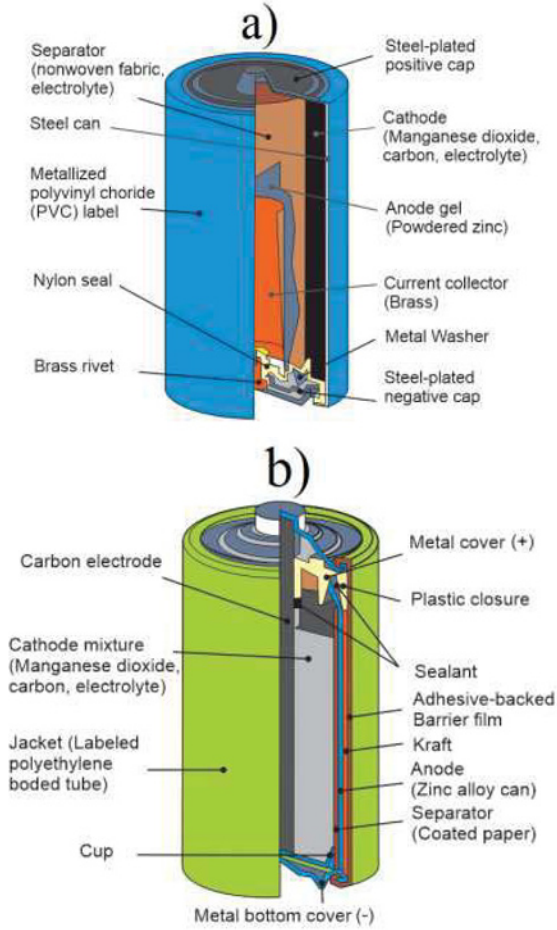

Figure 1 (a) Alkaline and (b) zinc-carbon batteries.

2. Experimental

The Portland cement powder used, corresponds to white cement from Holcim, Colombia (with max. 6.0wt% MgO, and max. 3.5wt% SO_3). Alkaline and zinc carbon batteries were obtained from containers marked for collecting battery waste at the Universidad de Antioquia. Typical batteries are shown in Figure 2a, and an example of the condition of the battery and its parts are shown in Figure 2b. The manufacturing process followed in this research is summarized in Figure 2c: samples were manually fed into a mill. The grinding process gave a black ceramic powder (mainly composed of ZnO and Mn_2O_3), plastic, carbon, paper, and steel. Plastic, paper and steel were initially manually removed. Then, a sieve (U.S. Standard Sieve 30) was used to remove bigger particles.

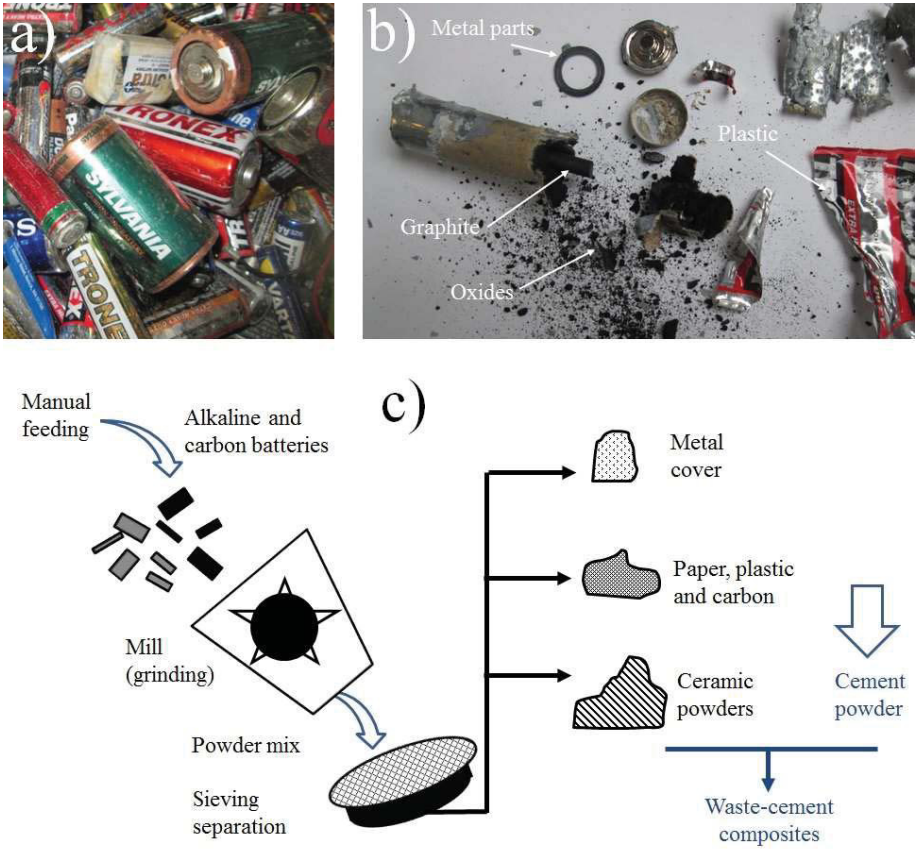

Figure 2 (a) Colombian alkaline and zinc-carbon battery waste, (b) Battery parts, (c) Manufacturing process followed In this research.

Then, the black ceramic powders were mixed with white ordinary Portland cement in the combinations summarized in Table 31. Battery waste was added at 0.0, 0.5, 1.0, 5.0, 10.0, 20.0, 40.0, and 50.0 wt%. All samples kept water to cement ratio (W/C) of 0.4. This liquid formulation was mixed mechanically and released from mold after 28 days. The samples were cut using a diamond saw in samples of 20 mm in diameter by 20mm in length. Samples were slightly prepared with sand paper in order to remove major surface defects and get appropriate flat surfaces for the compression tests. Finally, samples were dried at 30˚C for 2h in a furnace in order to stabilize water into the sample.

Table 1. Sample formulation fabricated in this research.

Samples	**BW(%)**	**Cement (%)**	**Water (%)**	**W/C**
BW-0	0	100	40	0.4
BW-0.5	0.5	99.5	39.8	0.4
BW-1	1	99	39.6	0.4
BW-5	5	95	38	0.4
BW-10	10	90	36	0.4
BW-20	20	80	32	0.4
BW-40	40	60	24	0.4
BW-50	50	50	20	0.4

Compression tests were conducted in a Shimadzu AG-250KNG machine. A set of 5 samples (20mm length and 20mm in diameter) was tested for each composite combination at a crosshead speed of 1 mm/min. The microstructure of samples was analyzed using optical scanning electron (SEM) microscopy and X-ray florescence (XRF). For SEM, the sample preparation required the samples to be dehydrated in a furnace at 30˚C for 24 hours. Next, the samples were cracked to expose the microstructure. Thereafter, samples were mounted on an aluminum stub and gold sputtered with a Hummer 6.2 system, at conditions of 15mA AC for 30 sec, in order to obtain a thin film of Au of around 1nm. The SEM used was a JEOL JSM 7100F in a high vacuum mode.

3. Results

Table 2 summarizes the XRF results for the ordinary Portland cement. This cement is known to have a high degree of whiteness because components such as Cr_2O_3 is below 0.003%, Mn_2O_3 is below 0.03%, and Fe_2O_3 is below 0.35% in the clinker. No Cr_2O_3 has been detected, and the other components are below the maximum limits. Table 3 shows the powder waste composition, which confirms the by-products MnO and ZnO as the main battery waste components.

Table 2. XRF Relative composition of ordinary white Portland cement

Component	SiO_2	Al_2O_3	Fe_2O_3	MgO	1.25	CaO	Na_2O	K_2O	Mn_2O_3	Reactive CaO	LOI	Total
weight %	22.3	4.1	0.21	1.82	1.41	64.78	0.2	0.24	0.02	1.2	3.72	100

Table 3. XRF Relative composition of battery waste

Component	MnO	ZnO	K_2O	SiO_2	Fe_2O_3	SO_3	Al_2O_3	CaO	CuO	Total
weight %	47.63	42.64	3.74	2.82	1.41	0.863	0.652	0.214	0.0309	99.999

Figure 3a shows the battery waste powder after grinding and most of steel, paper and plastic are removed. Figure 3b illustrates our fabricated cylindrical cement paste-battery waste samples. The darkness of samples is related to the waste loading.

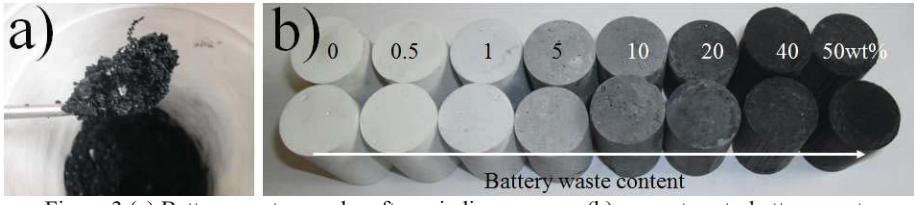

Figure 3 (a) Battery waste powder after grinding process; (b) cement paste-battery waste samples.

Figure 4 shows the compressive tests that increasing the waste contents cause a decrease in the compressive strength. However, even for samples with 50wt% of waste, the compressive strength was over 20MPa, which is a very competitive value for several applications including structural.

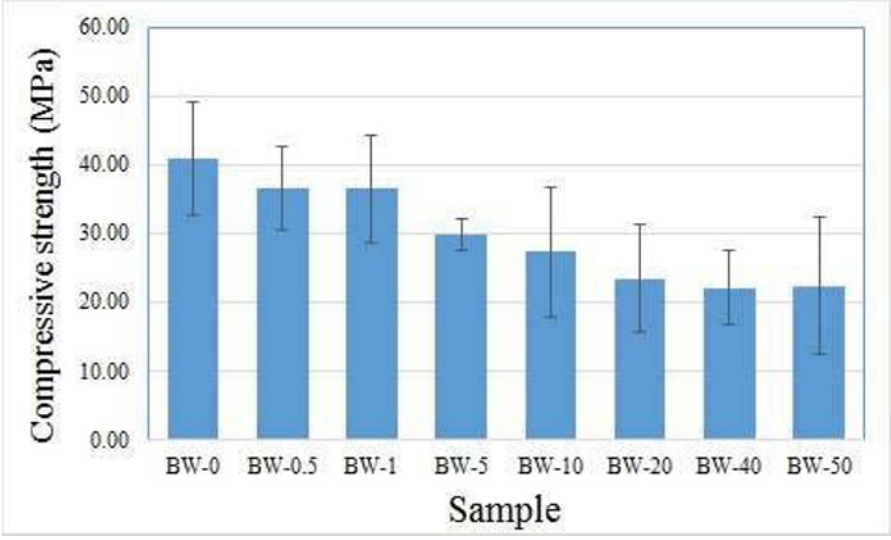

Figure 4 Compressive strength for the composite fabricated.

Scanning electron microscopy images from Figure 5 revealed a complex microstructure powered by the complexity of the raw materials itself because of the amount of components, see Table 2 for cement and Table 3 for waste. Figure 5a is a picture of the battery waste mainly composed by two type of particles, some small porous particles below 20μm, and some denser and bigger particles below 50μm. These particles were related to zinc and manganese oxides respectively.

Figure 5b correspond to cement paste without waste. Microstructures of samples with 0.5, 1.0, 5.0, 10.0, 20.0 and 50.0 wt% of battery waste are showed in Figures 5c, d, e, f, g, and h respectively. Sample with 50wt% of waste shows a lot of waste similar to Figure 5a, also micro pores appear as a result of powder waste agglomeration and a lack of cement binder. In samples of 10wt% of waste and below pores were very rare.

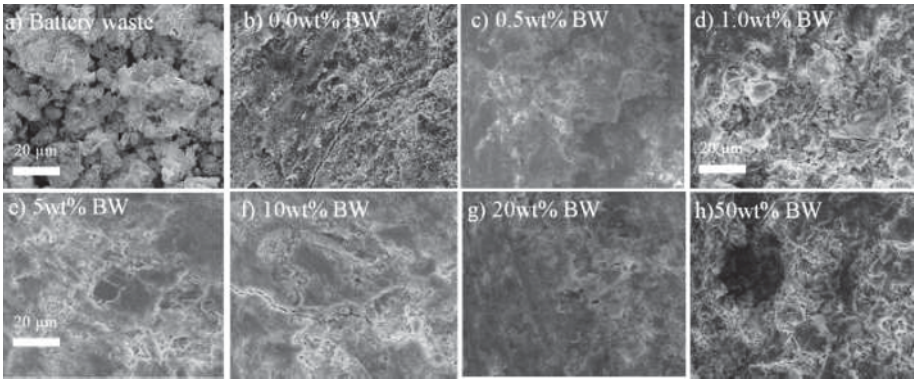

Figure 5 Scanning electron microscopy images for samples fabricated

4. Discussion

Compressive strength results showed the battery waste composed mainly from the ceramic powders obtained from the processsing of spent alkaline and Zn-C batteries is good as a filler material for several applications including structural. This enablesf this material as a filler, which is a green solution since this waste type is a major source of rivers and land contaminats around the world.

As expected, compressive strength decreased with the increasing in waste loading. This is because the effective binder amount decreases in the composite and the waste powder agglomeration increases (due to the lack of binding as well). As a consequence of all this porosity increases reducing the compressive strength. This means that with an optimized processing via powder pre-treatment or cement additives, this high loading has good possibility to create new cement formulations with enhanced electrical or other tailored properties. This is the case if ZnO, a well know piezo-electric material, is optimized in the formulation as piezo-cements.

Further investigation is needed to understand the effect of this complex oxide mix in the setting point of the cement paste. It is know than zinc delay the cement reactions, however, calorimetry is needed to understand the effect of the mix on this important parameter.

5. Conclusion

Cement paste-battery waste composites were fabricated in this research with a competitive compressive strength. Up to 50wt% of waste was added to the cement. For this high waste loading, more than 20MPa in compression was obtained.

Microscopy images showed a good powder impregnation and low porosity for samples of 10wt% of waste and below.

Due to the high amount of this waste around the world and its substantial impact on people and environment, this solution could have a significant influence in many countries.

6. References

1. Informe Convenio de Cooperación Científica y Tecnológica para Desarrollar Actividades Relacionadas con la Gestión de los Residuos Posconsumo de Fuentes de Iluminación, Pilas Primarias Y Secundarias. Ministerio de Medio Ambiente, Universidad Nacional de Colombia. 2008.
2. Li, Po-Chieh, Chi-Chang Hu, Tai-Chou Lee, Wen-Sheng Chang, and Tsin Hai Wang. "Synthesis and characterization of carbon black/manganese oxide air cathodes for zinc-air batteries." *Journal of Power Sources* 269 (2014): 88-97.
3. Gallegos, María V., Lorena R. Falco, Miguel A. Peluso, Jorge E. Sambeth, and Horacio J. Thomas. "Recovery of manganese oxides from spent alkaline and zinc–carbon batteries. An application as catalysts for VOCs elimination."*Waste management* 33, no. 6 (2013): 1483-1490.
4. Belardi, G., P. Ballirano, M. Ferrini, R. Lavecchia, F. Medici, L. Piga, and A. Scoppettuolo. "Characterization of spent zinc–carbon and alkaline batteries by SEM-EDS, TGA/DTA and XRPD analysis." *Thermochimica Acta* 526, no. 1 (2011): 169-177.
5. Ma, Ya, Yan Cui, Xiaoxi Zuo, Shanna Huang, Keshui Hu, Xin Xiao, and Junmin Nan. "Reclaiming the spent alkaline zinc manganese dioxide batteries collected from the manufacturers to prepare valuable electrolytic zinc and LiNi 0.5 Mn 1.5 O 4 materials." *Waste Management* 34, no. 10 (2014): 1793-1799.
6. Sayilgan, E., T. Kukrer, G. Civelekoglu, F. Ferella, A. Akcil, F. Veglio, and M. Kitis. "A review of technologies for the recovery of metals from spent alkaline and zinc–carbon batteries." *Hydrometallurgy* 97, no. 3 (2009): 158-166.
7. Xará, Susana, Manuel Fonseca Almeida, and Carlos Costa. "Life cycle assessment of three different management options for spent alkaline batteries."*Waste Management* 43 (2015): 460-484.
8. Sun, Mingxing, Xuechun Yang, Donald Huisingh, Renqing Wang, and Yutao Wang. "Consumer behavior and perspectives concerning spent household battery collection and recycling in China: a case study." *Journal of Cleaner Production* (2015).

REWAS 2016: Towards Materials Resource Sustainability
Edited by: Randolph E. Kirchain, Bart Blanpain, Christina Meskers, Elsa Olivetti, Diran Apelian, John Howarter, Anne Kvithyld, Brajendra Mishra, Neale R. Neelameggham, and Jeff Spangenberger
TMS (The Minerals, Metals & Materials Society), 2016

AUTOMOTIVE LITHIUM-ION BATTERY RECYCLING: A THEORETICAL EVALUATION

Reza Beheshti[1] and Ragnhild E. Aune[2]

[1]Dept. of Materials Science and Engineering, Royal Institute of Technology (KTH), Stockholm, SE-10044, Sweden
[2]Dept. of Materials Science and Engineering, Norwegian University of Science and Technology (NTNU), Trondheim, NO-7491, Norway

Keywords: Li-ion Battery, Electrical Vehicle, Pyrometalurgy, Aluminum Recycling

Abstract

Lithium-ion Batteries (LiBs) are today used in significant quantities in the automotive industry. As these batteries are expected to last the lifetime of the vehicle, they will not be ending their useful lives in large numbers for another 10-15 years. An opportunity does therefore exist to prepare for some of the roadblocks that might arise during the development of technologies for environmentally sound recycling of LiBs. In view of this, there is a need for reliable thermodynamic and kinetic data so that a secondary product of high enough metal value, as well as quality, can be produced making it possible to find a market for its purpose.
In the present study the equilibrium conditions for obtaining the best conditions possible for recovering the metal content through the aluminum recycling process were studied. All thermodynamic calculations were performed using the FactSage™ software, and the chosen chemical compositions represent the two main families of LiBs, *i.e.* $LiNiCOAlO_2$ and $LiFePO_4$. The possible production of PH_3 and P_4 (white phosphor) during the recycling process is also briefly discussed.

Introduction

It is expected that in the end of 2015 about 1.3 million Electric Vehicle (EV) batteries will have been produced in the world, and about 80% of these will be Li-ion Batteries (LiBs). Based on this it is estimated that more than half a million end-of-life EVs' battery packs will need to be treated by 2022 [1]. On the other hand, due to the continues development and changes in view of (i) the overall design, (2) the use of new materials in the anodes/cathodes, and (3) the assembly techniques used for the production of LiBs batteries, it is very difficult to predict what type of batteries will be available in the future. It is also important to note that LiBs is a collective name for a group of batteries containing lithium ions, but this group of batteries already varies widely in composition, *i.e.* $LiCoO_2$, $LiFePO_4$, $Li_2Mn_2O_4$ and $LiNiCoAlO_2$.

Over the last couple of years there have been many attempts throughout the world to legislate recycling processes for LiBs. There is, however, still no best available technology/practices that offer a consistent and comprehensive solution in view of recycling of metal values, environmental impact and sustainability. Presently the state-of-art in this area is based on hydrometallurgical processes, which includes complex process steps such as manual dismantling, leaching, precipitation and solvent extraction, as well as separate steps to remove less valuable

metals such as iron and aluminum. Presently these processes are mainly focusing on recycling the materials in the cathodes [2-7], and some of the process steps do clearly represent a burden on the environment.

The only full-scale industrial pyrometallurgical process for recycling of metal values from LiBs is developed and operated by Umicore battery recycling (Belgium). In this process the full battery is fed to a high-temperature shaft furnace consisting of three heating zones together with a fluxing agent, *i.e.* a mixture of limestone and silica. In the first heating zone (pre-heating zone) the temperature is below 300ºC and this is where the electrolyte evaporates. The next zone (the plastics pyrolizing zone) is operated at about 700ºC and it is here that the carbon material burns and supply heat to the process. In the last zone (the smelting and reducing zone) the temperature is 1200-1450ºC some of the metallic materials are transformed into a slag containing lithium, aluminum, silicone, calcium, manganese and some iron. In addition, an alloy with copper, cobalt, nickel, and some iron is produced. All gasses leaving the furnace are treated to capture the halogens that evaporate from the electrolyte [8-11]. The process is today mainly focusing on the recovery of cobalt and nickel from LiBs, and the reported metal recycling efficiency is ~ 69 % [12]. Due to the volume involved and the economic value of cobalt, it is today feasible to operate the present process with a positive economic outcome. In view of the new trends in the chemical composition of LiBs the overall recovery efficiency may, however, be significantly lowered for the new cathode formulations containing much lower cobalt, *i.e.* $LiFePO_4$ and $LiNiMnCoO_2$. The process can then be both technologically and economically challenged. In other words, there is a need for processes that allows for the recovery of a wider spectra of materials/elements securing that the recycling of all LiBs chemistries becomes economical [13, 14]. It should also be mentioned that due to the size of the battery modules, as well as the high volume of end of life EV batteries that need to be recycling in the future, presently available dismantling, shredding and physical separation techniques/facilities will represent a bottleneck in regards to recycling LiBs. If a process could be designed, that allowed for the direct feed of the whole battery without any dismantling or separation steps it would be an advantage to consider.
The objective of the present work is to theoretical investigating the possibility of the recovery of aluminum and lithium from LiBs through the conventional aluminum recycling process. A theoretical evaluation of the possible production of PH_3 and P_4 (White phosphor) during the process is also briefly discussed.

New Concept Based on Theoretical Calculations

A schematic view of the proposed process route is presented in Figure 1. As can be seen from the figure, the process consists of several different steps, *i.e.* (1) pyro 1 – the pre-heating zone (max 300ºC), (2) pyro 2 – conventional aluminum recycling (max 750ºC), (3) pyro 3 (max 1250ºC) and hydro 1 – Black Dross (BD) treatment and leaching, and (4) pro 4 – aluminum melt refining (max 800 ºC). The main aim of the proposed combination of process steps is to allow for (1) the recovery of metal values and heat from spent LiBs with limited amount and/or no amount of cobalt present, as well as (2) draw on experiences from the aluminum recycling technology in view of processing BD and aluminum melt refining for the production of value added products.

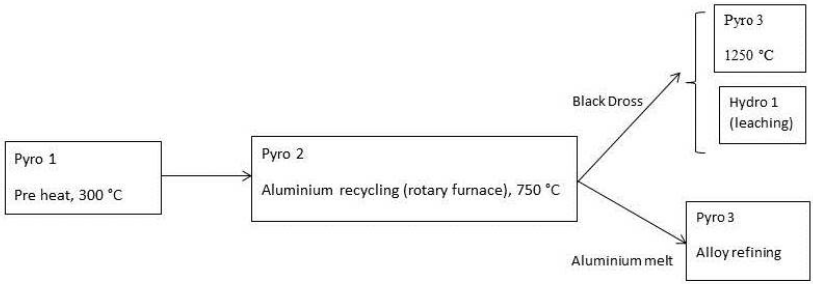

Figure 1. Proposed process route for the recovery of aluminum and lithium from LiBs through the conventional aluminum recycling process

It is a well-known fact that BD is heterogeneous in nature making the recovering of elements from the dross very challenging and costly [2, 15-17]. In view of this, it is of utmost importance to theoretically investigate the possibility of keeping the elements of interest, *i.e.* aluminum and lithium in the melt to maximize the metal recovery. On the other hand, if any of these elements are transferred into the dross phase, or if any other elements of economic value end up in the dross, a theoretical evaluation on how to retrieve the elements in question from the dross should also be conducted. In the present study only the equilibrium conditions most likely to be advantageous for the recovery of aluminum and lithium have been studied.

A thorough literature review on the thermodynamic and thermo-physical properties of different lithium systems, as well as optimum process conditions in terms of (i) the properties of the produced slag/metal phases, (ii) the processing temperature, and (iii) the process atmosphere, were conducted. Very limited information/data proved to have been published, making it clear that there is a need for small-scale thermodynamic and kinetic experiments to be conducted under well-controlled conditions. In view of this, it was decided to try to evaluate possible process conditions for future experiments.

Theoretical Evaluation and Phase Diagram Calculation

Based on a review by Akhtar *et al* published in 2015 [18] lithium proves to have a high reactivity with both air and moisture, making it necessary to conduct any small scale experiments in an inert atmosphere (Ar), or in vacuum. This is then also necessary to be the conditions used for the evaluation of the thermodynamics of different lithium systems. Moreover, since lithium easily reacts with alumina, magnesia, silicon carbide, stainless steel or graphite should be used as refractory material.

In the present work the two main families of LiBs, *i.e.* the $LiFePO_4$ and $LiNiCoAlO_2$ systems were considered, and their thermodynamic properties calculated by the use of the FactSage™ software (Version 6.4). It was decided to use the ternary system Al-Cu-Li as the reference system and starting point of all calculations. The normalized chemical compositions of the LiB systems in question are reported in Table 1.

Table 1. The normalized composition of the $LiFePO_4$ and $LiNiCoAlO_2$ systems [12, 14]

Element (at%) / LiB type	Al	Li	Cu
$AlFePO_4$	69	13	18
$LiNiCoAlO_2$	63	16	21

The isothermal section of the ternary system Al-Li-Cu, as calculated by Zinkevich *et al* [19] at 615ºC, is presented in Figure 2. As can be seen from the figure, two specific compositions, *i.e.* $AlFePO_4$ and $LiNiCoAlO_2$, have been marked out at point 1 and point 2 respectively. It can also be seen that point 1 is located in the liquid-state area of the system, and point 2 in the liquid- and solid state area. Based on this it was concluded that during re-smelting of $LiNiCoAlO_2$ at 615ºC the conditions favors the transfer of lithium from the metal phase to the dross phase.

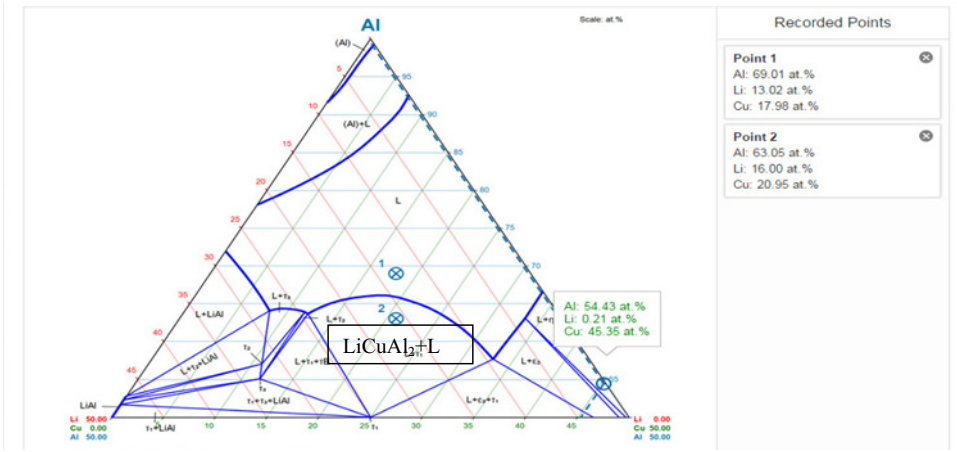

Figure 2. The Al-Cu-Li ternary phase diagram at 615ºC [19]

Results and Discussion

Figure 3 shows the isothermal section of Al-Cu-Li phase diagram at 1000 K that is calculated by FactSage. It can be seen both points are located in liquidus area. Moreover, moving toward copper will stabilize the solid phases. Therefore, addition of extra aluminum to the melt will shift the distribution of Li towards liquid phase.

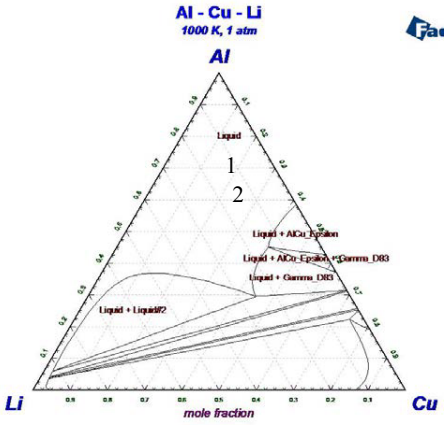

Figure 3. The isothermal section of Al-Cu-Li phase diagram at 1000 K

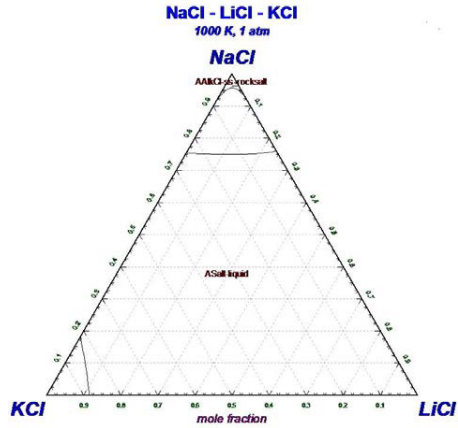

Figure 4.The isothermal ternary phase diagram of KCl-NaCl-LiCl at 1000 K

The common fluxing agent in aluminum industry is equimolar mixture of NaCl - KCl. In presence of lithium, NaCl is not satiable (see Figure 4) and it results in sodium being picked up by melt and lithium transfer to the slag phase (black dross) which is undesirable for enhanced metal recovery.

The stable phases for Al-Cu-Fe-P and Al-Cu-Fe-Ni-Co system calculated and presented in Table 2 and Table 3. Presence of Fe, P and Ni, Co stabilize the solid phases and slag formation.

Table 2. The results of thermodynamic calculation on Al-Cu-Fe-P at 1000 K

Composition (Molar ratio)	liquid	$FeAl_3$ (s)	AlP (s)	Al_5Fe_2
0.69Al+0.18Cu+0.13Li	1			
0.62Al+0.16Cu+0.12Li+0.1Fe	0.64	0.073		
0.56Al+0.15Cu+0.1Li+0.09Fe+0.1P	0.5		0.1	0.04

Table 3. The results of thermodynamic calculation on Al-Cu-Fe-Ni-Co at 1000 K

Composition (Molar ratio)	liquid	Ni_2Al_3 (s)	AlCo (s)
0.63Al+0.16Cu+0.21Li	1		
0.54Al+0.14Cu +0.18Li + 0.14Ni	0.64	0.07	
0.53Al+0.14Cu + 0.18Li + 0.13Ni + 0.03Co	0.61	0.064	0.03

Conclusion

Thermodynamic evaluation performed on the systems that are relevant for the chemical compositions formed during recovery of LiBs. Two different types of batteries have been selected for thermodynamic studies. Overall it may be concluded that:

- The common fluxing agent in aluminum smelting, NaCl-KCl mixture should be modified to avoid lithium being picked up by the black dross.
- Under control conditions, lithium remains in the melt, and Fe, Ni, Co and P form the slag phase.

Future work

To verify the thermodynamic evaluation, experimental under controlled conditions on synthetic materials is planned. The material preparation should be done in a glow box, to avoid contact between lithium and air. Samples will heat to 1073 K and kept for 2 hours under argon atmosphere. After the experiment is finished, sample will lowered to the cold area of the furnace and let the sample to be cool down. After that all the samples will characterize by SEM, EDS, XRD and ICP-MS.

References

[1] H. Wang, D. Friedmann, M. Vest, and B. Friedrich, "Innovative recycling of Li-based electric vehicle batteries," presented at the 7th European Metallurgical Conference, 2013.

[2] E. Gratz, Q. Sa, D. Apelian, and Y. Wang, "A closed loop process for recycling spent lithium ion batteries," *Journal of Power Sources,* vol. 262, pp. 255-262, 2014.

[3] L. Li, L. Zhai, X. Zhang, J. Lu, R. Chen, F. Wu, and K. Amine, "Recovery of valuable metals from spent lithium-ion batteries by ultrasonic-assisted leaching process," *Journal of Power Sources,* vol. 262, pp. 380-385, 2014.

[4] X. Zeng, J. Li, and L. Liu, "Solving spent lithium-ion battery problems in China: Opportunities and challenges," *Renewable and Sustainable Energy Reviews,* vol. 52, pp. 1759-1767, 2015.

[5] T. Georgi-Maschler, B. Friedrich, R. Weyhe, H. Heegn, and M. Rutz, "Development of a recycling process for Li-ion batteries," *Journal of Power Sources,* vol. 207, pp. 173-182, 2012.

[6] X. Zhang, Y. Xie, X. Lin, H. Li, and H. Cao, "An overview on the processes and technologies for recycling cathodic active materials from spent lithium-ion batteries," *Journal of Material Cycles and Waste Management,* vol. 15, pp. 420-430, 2013.

[7] X. Zeng, J. Li, and N. Singh, "Recycling of spent lithium-ion battery: A critical review," *Critical Reviews in Environmental Science and Technology,* vol. 44, pp. 1129-1165, 2013.

[8] J.B. Dunn, L. Gaines, M. Barnes, J. Sullivan, and M. Wang, "Material and energy flows in the materials production, assembly, and end of life stages of the automotive lithium ion battery life cycle," 2012.

[9] J. Tytgat, "EV battery recycling: resource recovery," presented at the Plug-in 2011, Raleigh, NC, US, 2011.

[10] S. Al-Thyabat, T. Nakamura, E. Shibata, and A. Iizuka, "Adaptation of minerals processing operations for lithium-ion (LiBs) and nickel metal hydride (NiMH) batteries recycling: Critical review," *Minerals Engineering,* vol. 45, pp. 4-17, 2013.

[11] K. Verscheure, M. Campforts, and C. M. Van, "Process for the valorization of metals from hev or ev batteries," ed: Google Patents, 2011.

[12] L. Gaines, J. Sullivan, A. Burnham, and I. Belharouak, "Life-cycle analysis for lithium-ion battery production and recycling," in *Transportation Research Board 90th Annual Meeting, Washington, DC*, 2011, pp. 23-27.

[13] L. Gaines, "The future of automotive lithium-ion battery recycling: Charting a sustainable course," *Sustainable Materials and Technologies,* vol. 1–2, pp. 2-7, 2014.

[14] S. Brouwer, J. Heulens, and H. D. Van, "Process for recycling li-ion batteries," ed: Google Patents, 2015.
[15] R. Beheshti, J. Moosberg-Bustnes, S. Akhtar, and R. E. Aune, "Black Dross: Processing Salt Removal from Black Dross by Thermal Treatment," *JOM,* vol. 66, pp. 2243-2252, 2014.
[16] W.J. Bruckard and J.T. Woodcock, "Characterisation and treatment of australian salt cakes by aqueous leaching," *Minerals engineering* vol. 20, pp. 1376-1390, 2007.
[17] M. Davies, P. Smith, W.J. Bruckard, and J.T. Woodcock, "Treatment of salt cakes by aqueous leaching and bayer-type digestion," *Minerals Engineering,* vol. 21, pp. 605-612, 2008.
[18] N. Akhtar, W. Akhtar, and S. J. Wu, "Melting and casting of lithium containing aluminium alloys," *International Journal of Cast Metals Research,* vol. 28, pp. 1-8, 2015.
[19] M. Zinkevich, T. Velikanova, M. Turchanin, and Z. Du. (2006, 01-10-2015). *Partial isothermal section at 615°C*. Available: http://materials.springer.com/msi/phase-diagram/docs/sm_msi_r_10_015854_02_full_LnkDia8

REWAS 2016: Towards Materials Resource Sustainability
Edited by: Randolph E. Kirchain, Bart Blanpain, Christina Meskers, Elsa Olivetti, Diran Apelian, John Howarter, Anne Kvithyld, Brajendra Mishra, Neale R. Neelameggham, and Jeff Spangenberger
TMS (The Minerals, Metals & Materials Society), 2016

LIFE CYCLE ANALYSIS SUMMARY FOR AUTOMOTIVE LITHIUM-ION BATTERY PRODUCTION AND RECYCLING

Jennifer B. Dunn[1], Linda Gaines[1], Jarod C. Kelly[1], Kevin G. Gallagher[2]

1 Energy Systems Division, Argonne National Laboratory; 9700 S Cass Avenue; Argonne, IL 60439
2 Chemical Sciences and Engineering Division, Argonne National Laboratory; 9700 S Cass Avenue; Argonne, IL 60439

Keywords: Lithium-ion battery, life cycle analysis, battery recycling

Abstract

Some have raised concerns regarding the contribution of lithium-ion battery pack production to the total electric vehicle energy and emissions profile versus internal combustion vehicles, and about potential battery end-of-life issues. This detailed life cycle analysis (LCA) examines these issues and identifies potential hot-spots within the battery pack life cycle for five cathode materials and a proposed lithium metal anode. The battery assembly stage, identified by some as an energy concern, is determined to be problematic only for "pioneer" plants (i.e. low-throughput facilities), but not for at-capacity plants, and battery electric vehicles with batteries from either facility type outperform conventional vehicles in terms of lowering GHG emissions. For at-capacity plants, the battery materials dominate energy impacts, with cathode materials representing 10-50% of that energy, depending on cathode type. Recycling can further mitigate battery life-cycle impacts, while also being economically attractive for all cathode materials, even those with low elemental values.

Introduction

Battery electric vehicles (BEV) are expected to contribute to efforts to reduce transportation sector greenhouse gas (GHG) emissions. While they emit no carbon dioxide or air pollutants during operation, their advantage relative to conventional vehicles must be evaluated on a life-cycle basis, which includes the vehicle production and end-of-life stages. One of the most critical elements of this stage for BEVs is the production of the battery pack, which has been flagged as energy- and GHG-intensive with some raising the concern that the impacts of battery production could render BEVs at a disadvantage compared to conventional vehicles [1].

Automotive Lithium-Ion Battery Production from Cradle-to-Gate

Recently, we have undertaken an in-depth analysis of battery pack production from cradle-to-gate, estimating energy consumption, GHG emissions, and emissions of other air pollutants such as sulfur oxides (SO_x) using Argonne National Laboratory's Greenhouse gases, Regulated Emissions and Energy use in Transportation (GREET^{TM}) model [2,3]. We have examined the influence of cathode and anode chemistry variations on these results. The results we have developed rely on estimates of battery compositions developed with Argonne's BatPaC model and estimates of the material and energy intensity of battery materials developed from a

combination of literature data and engineering estimates [4,5]. Table I reports the energy and GHG-intensity of lithium-ion battery cathode and anode materials on a per mass basis (Dunn et al. 2015a, Dunn et al. 2015b).

Cathodes that contain large amounts of cobalt and nickel (i.e., lithium cobalt oxide (LCO) and nickel-manganese-cobalt (NMC)) are the most energy intensive to produce from the mine to the assembly facility gate. When we examined the effect of using either hydrothermal or solid state techniques for preparing cathodes, solid state techniques that did not require solvent heating were less energy- and GHG-intensive. Graphite is the lowest impact anode material we considered, but research and development efforts are also targeting graphite-silica combinations and even pure lithium anodes. These two anode materials are more energy intensive than graphite to produce. An important point to consider, however, is the relative amounts of each of these materials that would be incorporated in a battery given their different properties. This battery composition will influence overall battery mass, which in turn affects cradle-to-gate energy and emissions associated with battery production.

Table I. Energy and GHG Intensity of Cathode and Anode Materials for Lithium-Ion Batteries [5]

Cathode or Anode Material	Cradle-to-Gate Energy Intensity (MJ/kg)	Cradle-to-Gate GHG Intensity (kg CO_2e/kg)
LCO prepared hydrothermally ($LiCoO_2$)	320	23
LCO prepared with a solid state method	180	13
NMC ($LiNi_{0.4}Co_{0.2}Mn_{0.4}O_2$)	140	9.9
LMR-NMC ($0.5Li_2MnO_3 \cdot 0.5LiNi_{0.44}Co_{0.25}Mn_{0.31}O_2$)	140	10
LFP prepared hydrothermally ($LiFePO_4$)	60	4.0
LMO ($LiMn_2O_4$)	40	3.6
LFP prepared with a solid state method	40	2.6
Silicon	1000	50
Lithium	160	12
Graphite	90	5.3

To illustrate this point, Table II contains cradle-to-gate energy consumption and GHG emissions for five different battery chemistries. To estimate the battery compositions that underpin this analysis, we used BatPaC to model a BEV battery pack with a power of 149 kW and an energy of 28 kWh. Two of the entries in Table II reflect relatively conventional battery chemistries that use graphite as the anode and either LFP or NMC as the cathode material. The other entries reflect a cathode material that is under development, LMR-NMC, paired with either a graphite, graphite-silicon blend, or lithium anode. Table II also contains compositional information about these batteries and their total weight.

Table II. Characteristics and Cradle-to-Gate Energy Consumption and GHG Emissions for Battery Packs with Five Different Chemistries

Cathode		Anode		Total Mass (kg)	Cradle-to-Gate per Battery	
Type	% Mass	Type	% Mass		MJ	kg CO_2e
NMC	28%	Gr	18%	170	20,000	1,400
LFP	24%	Gr	15%	230	18,000	1,200
LMR-NMC	20%	Gr	20%	160	17,500	1,200
	24%	Gr/Si	6%/2%	140	18,500	1,300
	40%	Li	3%	114	16,500	850

One result of interest in Table II is that the batteries with NMC and LFP cathode materials, which are commercially available, have roughly equivalent cradle-to-gate energy and GHG intensities. Although the NMC cathode material is over three times as energy intensive to produce as LFP, it has a higher energy density (675 Wh/kg vs Li-metal compared to 515 Wh/kg vs Li-metal). As a result, less cathode material is needed in the battery containing the more energy dense cathode material and the overall battery mass is lower, yielding a lower cradle-to-gate GHG and energy intensity. The battery with an anode-cathode combination that is still under development, LMR-NMC paired with lithium, has the lowest overall energy and GHG intensity despite tapping cathode and anode materials that are more burdensome to produce than conventional materials. Pursuit of high-performing materials that enable lower battery weights is one important way to cut battery cradle-to-gate energy consumption and GHG emissions.

Another important factor in estimating the cradle-to-gate energy and emissions associated with automotive lithium-ion battery production is the burdens that battery assembly incurs. Here, we define battery assembly as the steps taken to put together a battery from its component parts including the electrodes, cells, battery management system, and packaging. We estimate this energy on an intensity basis: the energy consumed to produce a given quantity of batteries. Because battery assembly involves the use of a dry room and other equipment that may operate at the same rate regardless of assembly facility throughput, assembly facilities operating below capacity could exhibit a fairly high assembly energy intensity. As the battery industry matures, however, and throughput approaches capacity – an n^{th} plant scenario – the energy intensity of battery assembly will decline. In our analysis, we assume that the assembly facility is operating near capacity. For at-capacity plants, the battery materials dominate energy impacts, with cathode materials representing 10-50% of that energy, depending on cathode type. In the case of batteries assembled at low-throughput, first-of-a-kind plants, battery assembly tends to dominate cradle-to-gate energy consumption and GHG emissions [3].

Comparison of Electric and Conventional Vehicles Well-to-Wheels GHG Emissions

Figure 1 illustrates the results generated from combining battery cradle-to-gate energy consumption into total per mile GHG emissions for BEV (approximately 110 km range) and plug-in hybrid electric vehicles (PHEV) (we use PHEV50 to denote a PHEV with an all-electric range of 50 km) and comparing impacts to those of internal combustion engine vehicles (ICEV) based on parameters within GREET [3]. In all cases, BEV and PHEV50 GHG emissions are less than those of the conventional ICEV, despite higher vehicle cycle emissions for electric vehicles

stemming from the contribution of the battery. Well-to-pump GHG emissions are lower for the California grid than for the U.S. overall grid, which is more reliant on coal-fired power plants (46% coal) than California's (7.6% coal). Pump-to-wheels GHG emissions are zero for BEVs, while the contribution from PHEV use of gasoline is taken into account. The battery with an NMC cathode contributes more heavily to the total vehicle cycle emissions than the battery with an LMO cathode, as is more evident for the results for the BEV, which has a larger battery. These results are consistent with those in other recent studies that indicate that the GHG emissions of BEVs are lower than those of ICEVs [6,7].

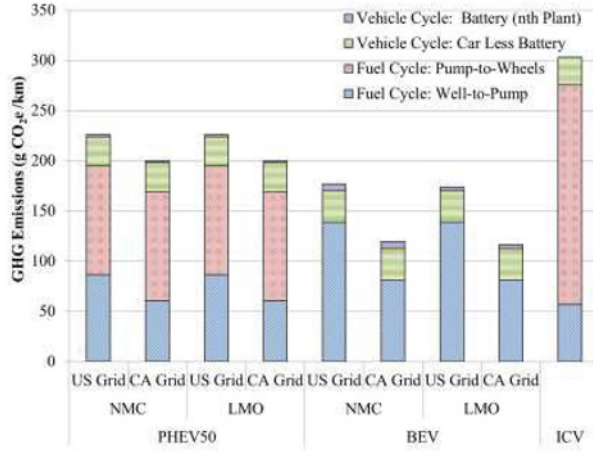

Figure 1. Fuel cycle and vehicle cycle greenhouse gas emissions for BEVs, PHEV50s, and ICEVs. The PHEV50 is modelled as being in charge-depleting (CD) and charge-sustaining (CS) modes during 47.5% and 52.5% of operation, respectfully. The PHEV50 is assumed to have a fuel economy of 3.2 and 8.5 gasoline equivalent L/100 km in CD and CS modes, respectively. The BEV is assumed to have a fuel economy of 2.9 gasoline equivalent L/100 km while the ICEV operates at 10 L per 100 km The liquid fuel used by the ICEV and the PHEV50 during CS mode is conventional gasoline, 4% of which derives from oil sands recovered via in-situ production. The electric vehicles use either the conventional U.S. grid mix or the California grid mix when charging.

Automotive Lithium-Ion Battery Recycling

As discussed previously, pursuit of high-performing anode and cathode materials that reduce battery mass is one route to reducing battery impacts. Another critical route is to recycle batteries with the potential for reusing some or all of the recovered material in new batteries. There are several different processes that show potential, or are currently in operation, for

recycling lithium-ion batteries [8]. These processes tap pyrometallurgical, hydrometallurgical, or physical techniques. Table III compares the attributes of these recycling technologies. In previous analyses [2], we estimated that recovering cathode and structural materials (e.g., aluminum) from battery recycling could reduce cradle-to-gate lithium-ion battery GHG impacts by up to 50%. Furthermore, recovering and reusing spent cathode material could avoid harmful air emissions from smelting at mines that recover Co and Ni (Figure 2).

Table III. Automotive Lithium-Ion Battery Recycling Process Attributes

Attribute	Pyrometallurgical Process	Hydrometallurgical Process	Physical Process
Temperature	High	Low	Low
Materials Recovered	Co, Ni, Cu (Li and Al to slag)	Metals or salts, Li_2CO_3 or LiOH	Cathode, anode, electrolyte, metal
Feed Requirements	None	Separation desirable	Single chemistry required
Comments	New chemistries yield reduced product value	New chemistries yield reduced product value	Recovers potentially high-value materials; Could implement on in-plant scrap

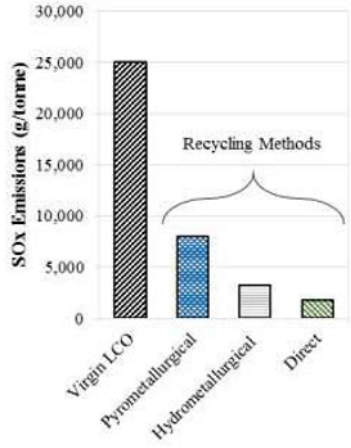

Figure 2. Estimated SO_x emissions from producing virgin LCO as compared to emissions from processes that recover this cathode material from spent automotive lithium-ion batteries

Despite energy and environmental motivations for battery recycling, recycling infrastructure is in very early stages. Without regulations to drive recycling, economics must support its implementation. Figure 3 illustrates that for LCO, NMC, LMO, and LFP cathode materials, recycling process economics could be favorable when the cathode itself is recovered because the

cathode has significantly added value as compared to the component elements. Importantly, recycling processes that enable recovery of cathode materials that have retained some degree of functionality (it is likely recovered cathode materials would need to undergo some upgrading) could offer a significant economic advantage. These processes also consume less energy than high-temperature, pyrometallurgical processes that recover metals in their elemental form. Currently, the influence of process conditions (e.g., pH, temperature, duration) of direct, physical processes on the properties of the recovered cathode is being investigated. Optimizing direct recycling to limit detrimental effects on cathode material morphology and performance is an important technology improvement towards viable automotive lithium-ion battery recycling processes.

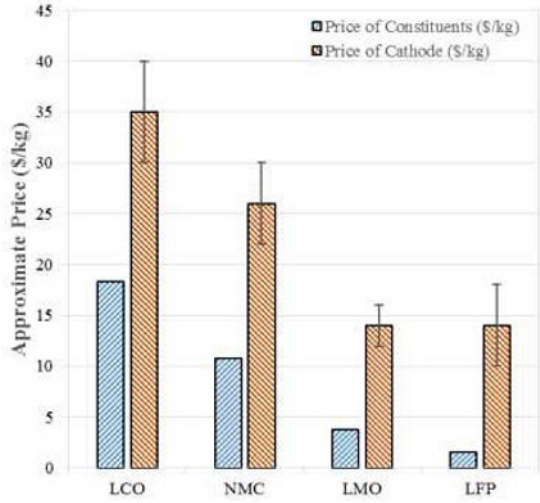

Figure 3. Price of cathode constituents and finished cathode materials ($/kg)

Conclusion

Automotive-lithium ion batteries contribute minimally to well-to-wheel energy consumption and GHG emissions of electric vehicles. Overall, BEVs and PHEVs offer energy and GHG savings on a per km basis as compared to conventional ICEVs. Two options for decreasing the contribution of the battery to EV energy and environmental impacts include developing advanced cathode and anode materials that reduce battery mass and recycling batteries to recover cathode and other battery materials. Importantly, recycling processes that operate at mild conditions and directly recover cathode materials could further enhance the economic and environmental desirability of lithium-ion battery recycling because cathode materials are more valuable than their component parts.

Acknowledgements

The authors are very grateful for the support of David Howell and Jake Ward. This work was supported by the Vehicle Technologies Office of the Office of Energy Efficiency and Renewable Energy of the United States Department of Energy, under contract DE-AC02-06CH11357.

References

1. B. Lomborg. "Green Cars Have a Dirty Little Secret." *Wall St. J.* March 11, 2013.

2. J. B. Dunn, L. Gaines, J. Sullivan, M. Q. Wang, "Impact of Recycling on Cradle-to-Gate Energy Consumption and Greenhouse Gas Emissions of Automotive Lithium-Ion Batteries," *Environmental Science and Technology*, 46 (2012), 12704-12710.

3. J. B. Dunn, L. Gaines, J. C. Kelly, C. James, K. G. Gallagher, "The Significance of Li-Ion Batteries in Electric Vehicle Life-Cycle Energy and Emissions and Recycling's Role in it's Reduction," *Energy and Environmental Science*, 8 (2015), 158-168.

4. J. B. Dunn, L. Gaines, M. Barnes, J. Sullivan, M. Wang, "Material and Energy Flows in the Materials Production, Assembly, and End-of-Life Stages of the Automotive Lithium-Ion Battery Life Cycle" (Report ANL/ESD/12-3 Rev., Argonne National Laboratory, 2014).

5. J. B. Dunn, C. James, L. Gaines, K. Gallagher, "Material and Energy Flows in the Production of Cathode and Anode Materials for Lithium Ion Batteries" (Report ANL/ESD/-14/10 Rev., Argonne National Laboratory, 2015).

6. N. Warburg, A. Forell, L. Guillon, H. Teulon, B. Canaguier, "Elaboration Selon les Principes ses ACV Des Bilans Energetiques, des Emissions de Gas à Effet de Serre et des Autres Impacts Environnement aux Induits par l'Ensemble des Filières de Véhicules lectriques et de Véhicules Thermiques, VP de Segment B (Citadine Polyvalente) et Vue à l'Horizon 2012 et 2020," (Report, Agence de l'Environnement et de la Maitrise de l'Energie, http://www.ademe.fr/sites/default/files/assets/documents/90511_acv-comparative-ve-vt-rapport.pdf, 2014).

7. Renault, "Fluence and Fluence Z.E. Life Cycle Assessment October 2011," (Report, http://group.renault.com/wp-content/uploads/2014/09/fluence-acv-2011.pdf, 2011).

8. L. Gaines "The Future of Automotive Lithium-Ion Battery Recycling: Charting a Sustainable Course." 2014 *Sustainable Materials and Technologies*, 1-2:2-7

Enabling & Understanding Sustainability - Rare Earth Element Applications

REWAS 2016: Towards Materials Resource Sustainability
Edited by: Randolph E. Kirchain, Bart Blanpain, Christina Meskers, Elsa Olivetti, Diran Apelian, John Howarter, Anne Kvithyld, Brajendra Mishra, Neale R. Neelameggham, and Jeff Spangenberger
TMS (The Minerals, Metals & Materials Society), 2016

LIFE CYCLE ASSESSMENT OF RARE EARTH PRODUCTION FROM MONAZITE

Callum Browning, Stephen Northey, Nawshad Haque, Warren Bruckard and Mark Cooksey
CSIRO Mineral Resources
Private Bag 10, Clayton South, VIC 3168, Australia

Corresponding author: Nawshad.Haque@csiro.au

Keywords: LCA, REE, GHG, sustainability, metals

Abstract

The environmental life cycle impacts of conceptual rare earth production processes were assessed. An average greenhouse gas emission of 65.4 kg CO_2e/kg was estimated for the 15 rare earths produced from monazite, ranging from 21.3 kg CO_2e/kg for europium to 197.9 kg CO_2e/kg for yttrium. The average water consumption of rare earth production was 11,170 kg/kg ranging from 3,803 kg/kg for samarium and gadolinium to 29,902 kg/kg for yttrium. The average gross energy requirement for production was 917 MJ/kg, ranging from 311 MJ/kg for samarium and gadolinium to 3,401 MJ/kg for yttrium. Given the low concentration of HREE in monazite, the high impacts across all categories for yttrium and other HREE are not necessarily representative of HREE sourced from all rare earth resources. Further studies into other rare earth mineral resources (e.g. bastnasite and xenotime) are recommended to improve the overall understanding of environmental impacts from rare earth production.

Introduction

The rare earth elements are comprised of the lanthanide series (atomic numbers 57 to 71) along with scandium (atomic number 21) and yttrium (atomic number 39). The rare earths coexist in varying concentrations in deposits where they must be extracted and separated for commercial use. The physical and chemical properties of rare earths are similar, which not only accounts for their coexistence in deposits, but also demands complex processing for separation and purification.

Demand for rare earth elements is growing due to their use in a number of growing industries and products such as colour screen phosphors, high strength magnets, lasers, chemical catalysts and medical equipment. Recent production data has been reported in Haque et al. [1]. One of the major economic sources of rare earths is monazite, a phosphate based mineral ((Ce, La)PO_4). Monazite features rare earths, thorium and uranium along with radioactive decay products and various impurities such as iron and aluminium in a substitution arrangement of phosphates. Thus monazites have a variable content of rare earths from around 42% in North Korean monazite to around 61% in monazite from certain Australian deposits [2]. The concentration of radioactive substances in monazite also varies; 0.18–0.45% for uranium and 4.5–9.5% for thorium [2].

The environmental impacts of rare earth mining, processing and waste management are poorly understood on a quantitative level. This is due to a lack of systematic impact assessment studies, particularly those that include baseline monitoring prior to resource development. The human health and ecosystem impacts associated with illegal mining of rare earths also have not been properly quantified. There is a recognition of the environmental impacts of rare earth production at local scales. For instance, in-situ leaching is replacing heap leaching of ion-adsorbed rare earth

deposits in southern China. However, this is only suitable for specific geochemical and hydrological environments.

Previous analysis of the environmental impacts associated with monazite processing has generally focused on issues relating to the handling of radioactive wastes. Other environmental issues such as the contribution to climate change, water depletion and indirect toxicity issues have received much less attention. Largely, this is due to the relatively small scale of the industry and the importance of addressing and improving local environmental management practices. The environmental impacts resulting from monazite processing has seen some investigation due to the high concentration of radioactive material contained within the mineral (particularly thorium and uranium). The historical disposal of these radioactive wastes has caused long term environmental groundwater pollution in Brazil [3, 4] where wastes from the decomposition of monazite were disposed in (direct contact with) soil. Recently, impacts of the occupational radiation exposure in monazite processing facilities in India have also been investigated [1].

In spite of past environmental studies there is an incomplete understanding of environmental impacts resulting from the processing of monazite for recovery of rare earths. The present study was aimed at improving this knowledge by conducting a LCA of rare earths resulting from this production route. Improving the breadth of the understanding is paramount and a number of impact categories was investigated including gross energy requirement (GER), global warming potential (GWP), water consumption, material resource consumption, toxicity and ionising radiation. Developing improved understanding of these types of environmental impacts associated with rare earth production is critical for downstream evaluations of processes and products containing rare earth minerals.

Methodology

A LCA model was selected as the most suitable environmental tool available to study the environmental effects of rare earth production from monazite. The LCA was conducted based on ISO14040 and ISO14044 [5, 6].

Goal, Scope and Functional Unit

The overall goal of the study was to improve the understanding of environmental impacts resulting from the processing of monazite currently conducted worldwide in the production of rare earth elements. The study, therefore, was specified as a 'cradle-to-gate' LCA, as only the production process was included in the scope. A number of limiting assumptions were made in defining the monazite deposit. These assumptions were necessary to fully specify the processing path followed to produce rare earths and to generate usable results. The boundary and simplified flowsheets are shown in Figure 1. The solvent extraction processes consisted of an organic medium which is mixed with the aqueous rare earth solution in multiple stages (extraction) to selectively extract rare earths into the organic phase. The rare earths are then recovered by further mixing with aqueous solutions of acid (stripping). There were variations in the processing of individual rare earths. The majority of inventory data for the flowsheets were collected from the open literature [7].

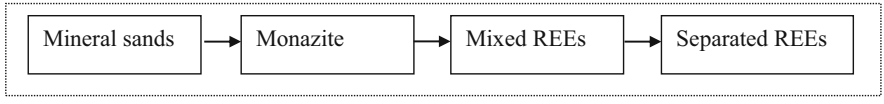

Figure 1: Boundary for life cycle based impact assessment.

Results and Discussion

Grouping and presentation of results

Data relating to global warming potential, gross energy requirement and water consumption have been presented graphically.

In the production stages, mixed REEs were assumed to be formed as oxide or chloride flakes for further separation. Due to the nature of the allocation (by mass), identical results across all impact categories were observed for rare earths sharing flowsheets regardless of individual concentration. For this reason the 15 rare earths will be grouped into nine rare earth groups as listed below under groups:

- Lanthanum (La)
- Cerium (Ce)
- Praseodymium (Pr)
- Neodymium (Nd)
- Samarium (Sm) and gadolinium (Gd)
- Europium (Eu)
- Terbium (Tb) and dysprosium (Dy)
- Holmium (Ho), erbium (Er), thulium (Tm), ytterbium (Yb) and lutetium (Lu)
- Yttrium (Y)

Global warming potential (GWP)

The global warming potential for the production of rare earths from monazite is presented in Figure 2. Tthe production of thermal energy and electricity specified for this study were natural gas and coal, respectively. As the study was aimed at presenting a generalised LCA for worldwide monazite processing, these sources were taken to be the most representative and applicable for the majority of global monazite and rare earth processing facilities. The highest GWP resulting from yttrium production (200 kg CO_2e/kg) is largely due to the large electricity consumption for the production of this rare earth and production of ammonium thiocyanate.

Gross Energy Requirement (GER)

Energy consumption in the production of rare earths is presented in Figure 3. Similarly to GWP, yttrium shows the highest GER (3400 MJ/kg) are due to high electricity consumption and ammonium thiocyanate production. The consumption of coal and natural gas are generally associated with electricity and thermal energy, respectively. However production of chemical reagents also contributes somewhat to the use of these energy resources.

Water consumption

The consumption of water in rare earth production from monazite is shown in Figure 4. One result of interest is the high water consumption associated with production of the inert nitrogen atmosphere for europium production. Nitrogen is required to evacuate oxygen and atmospheric moisture to prevent re-oxidation of europium to elicit good separation of this rare earth. The highest water consumption observed for all rare earths was again yttrium (29,900 kg/kg) due to the high energy and chemical reagent consumption.

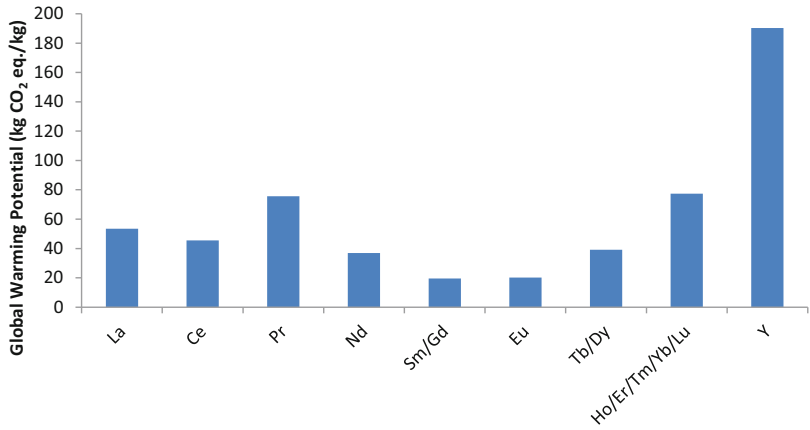

Figure 2: Estimated global warming potential associated with production of individual REEs.

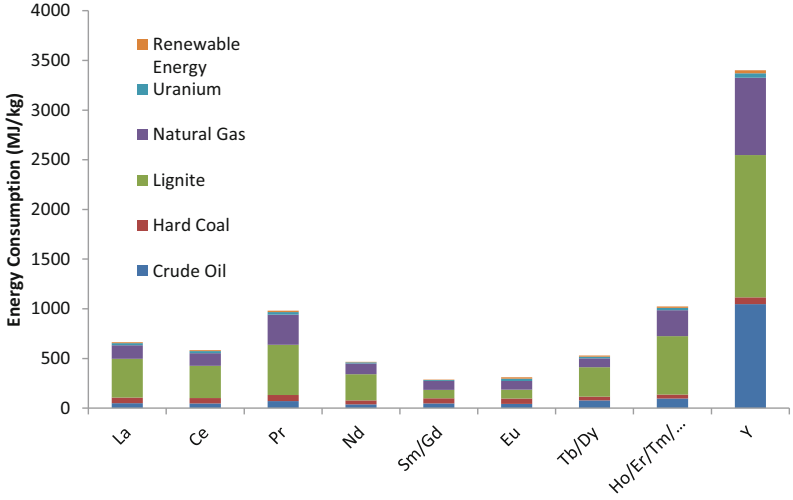

Figure 3: Estimated energy consumption associated with production of individual REEs (in x-axis).

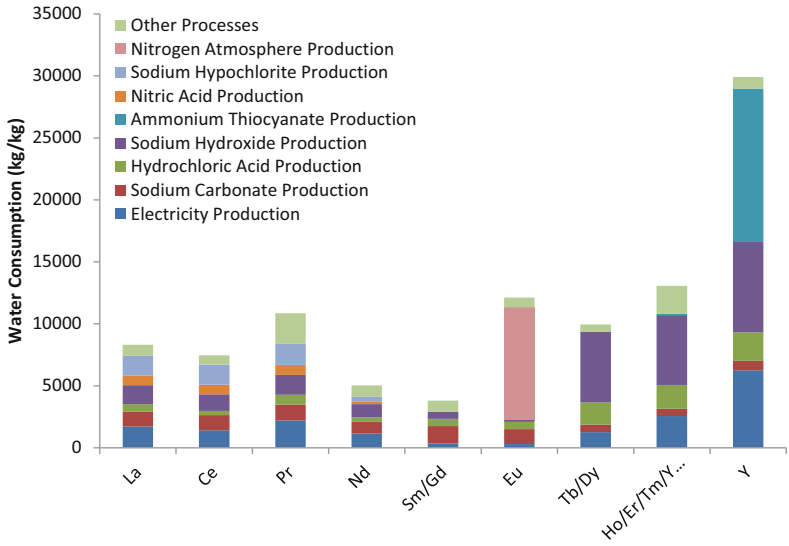

Figure 4: Estimated water consumption associated with production of individual REEs.

Other impacts

Table I contains the LCA results for the remaining impact categories investigated, namely mineral, fossil and renewable resource consumption; solid waste burden (SWB); human, freshwater and marine toxicities; and ionising radiation production.

Table I. Estimated impacts associated with individual REE.

Rare Earth	Resource Consumption	Solid Waste Burden	Human Toxicity	Freshwater Ecotoxicity	Marine Ecotoxicity	Ionising radiation
	kg/kg	kg/kg	kg 1,4 DB_e/kg	kg 1,4 DB_e/kg	kg 1,4 DB_e/kg	GBq/kg
La	960	450	1.31	4.0×10^{-3}	3.4×10^{-3}	7.45
Ce	690	370	1.08	3.7×10^{-3}	3.0×10^{-3}	7.50
Pr	1,360	570	1.67	6.2×10^{-3}	4.5×10^{-3}	7.86
Nd	610	300	0.83	2.7×10^{-3}	2.3×10^{-3}	5.75
Sm-Gd	300	120	0.56	2.7×10^{-3}	1.7×10^{-3}	8.51
Eu	370	120	0.61	2.7×10^{-3}	1.8×10^{-3}	7.43
Tb-Dy	780	330	1.38	3.9×10^{-3}	3.3×10^{-3}	3.62
Er-Ho-Tm-Yb-Lu	2,190	650	2.09	5.5×10^{-3}	5.1×10^{-3}	3.57
Y	3,310	1,560	4.27	1.0×10^{-2}	1.6×10^{-2}	4.63

Resource consumption was taken to be the raw materials used in rare earth production not including water resources. The majority of this impact category was comprised of minerals, soil and rock sourced for production of energy and chemical reagents. Other impact categories were

included to further investigate the influence of the lesser occurring resources with properties leading to large impacts in other categories.

Conclusions

The results indicate that rare earth production from monazite produces impacts far greater in magnitude than any other metals currently investigated with a LCA. This is due to the large and complicated flowsheet with high energy consumption associated primarily with numerous solvent extraction stages and high chemical consumption due to the inherent difficulty in separating the individual rare earth elements. The GWP of titanium from the Becher and Kroll process is 35.7 kg CO_2e/kg [8] while results from this study indicate an average GWP of 65.4 kg CO_2e/kg for monazite processing. Similar results are seen for the GER (361 MJ/kg for titanium, 917 MJ/kg rare earth average) and SWB (351 kg/kg for nickel via hydrometallurgical processing [8], 497 kg/kg REs average). It is a reasonable assumption that all other impact categories investigated also display far higher impacts for rare earths than for other commodity metals. This study represents a starting point for further research into investigation of environmental effects resulting from rare earth production. Building a knowledge base of the rare earth minerals may assist in decision making for further development of the rare earth industry, and result in cleaner production of these industrially important metals.

Acknowledgements

This study has been undertaken with support from CSIRO Mineral Resources.

References

1. N. Haque, A. Hughes, S. Lim, and C. Vernon, C. “Rare Earth Elements: Overview of Mining, Mineralogy, Uses, Sustainability and Environmental Impact”. *Resources*, 3 (2014), 614-635.
2. P.M.B. Pillai, “Naturally occurring radioactive material (NORM) in the extraction and processing of rare earths”, 2007, Seville, Spain, International Atomic Energy Agency, pp. 197-222.
3. C. Briquet, M. Cipriani, and A.C. Ferreira, “Soil contamination in a rural site used for rare earth industry by-product disposal”, 2004, Szczyrk, Poland, International Atomic Energy Agency, pp. 99-103.
4. D. da Costa Lauria, and E.R.R. Rochedo, "The legacy of monazite processing in Brazil. Institute of Radiation Protection and Dosimetry (IRD)”, 2005, pp. 546-550.
5. ISO. “International Standard. In: Environmental Management - Life Cycle Assessment - Principles and Framework” ISO 14040 (2006). Geneva: International Organisation for Standardization.
6. ISO, “International Standard. In: Environmental Management - Life Cycle Assessment - Requirements and Guidelines” ISO 14044 (2006). Geneva: International Organisation for Standardisation.
7. C.K. Gupta and N. Krishnamurthy, “Extractive Metallurgy of Rare Earths”, 2005, Florida, USA: CRC Press.
8. T.E. Norgate, S. Jahanshahi, and W.J. Rankin, “Assessing the environmental impact of metal production processes”. *Journal of Cleaner Production*, 15 (2007), 838-848.

REWAS 2016: Towards Materials Resource Sustainability
Edited by: Randolph E. Kirchain, Bart Blanpain, Christina Meskers, Elsa Olivetti, Diran Apelian, John Howarter, Anne Kvithyld, Brajendra Mishra, Neale R. Neelameggham, and Jeff Spangenberger
TMS (The Minerals, Metals & Materials Society), 2016

RECOVERY OF RARE EARTH ELEMENTS FROM THE FERROUS FRACTION OF ELECTRONIC WASTE

Lars K. Jakobsson, Mark W. Kennedy, Ragnhild E. Aune and Gabriella Tranell

Department of Materials Science and Engineering, NTNU Norwegian University of Science and Technology, N-7491 Trondheim, Norway

Keywords: Recycling, electronic waste, NdFeB magnets, rare earth elements

Abstract

Rare Earth Elements (REEs) have unique properties that have led to a rapid increase of consumption in modern technological products. This has in turn led to a greater awareness of the limited and highly localized nature of mineral reserves, and the dilute nature of the undeveloped resources including those from secondary sources.

Recycling of REEs is seen as one possible way to increase the supply of these elements with less impact on the environment than extraction from ores. In the present recycling processes for electronic waste these elements are, however, largely oxidized and diluted into discarded streams making recycling a challenging task.

Selected industrial ferrous streams of electronic waste that contain significant amounts of NdFeB magnets were investigated in the present work. Highly reducing conditions and high temperature were applied to obtain a slag containing only the most stable oxides, which also proved to include very high concentrations of REEs.

Introduction

The use of Rare Earth Elements (REEs) in electronic equipment is increasing due to their unique properties. Exploitable mineral reserves of REEs are, however, limited and the concentrations are relatively low in most ore deposits rendering them uneconomic to exploit. Extraction of the rare earths from deposits is also known to require many processing steps, which produces large quantities of toxic waste. The increased use of REEs has also led to an increasing concentration of REEs in electronic waste streams.

REEs are presently not recovered using conventional processing methods for recycling of metals from electronic waste, which are mainly targeted at precious and base metals. Only recently have the REEs started to get attention as attractive candidates for recycling, and both the European Commission (2014) and U.S. Department of Energy (2011) has identified the REEs as critical for their respective economies.

Due to the high stability of rare earth oxides, the REEs typically end up dissolved in a slag phase at low concentrations during smelting of electronic waste, e.g. in Electric Arc Furnace slag. Researchers have up till now mainly aimed at recovering the REEs by other methods than deliberate slag formation (Binnemans, 2013).

The present work aims at recovering the REEs as oxides instead of as metals. Using this approach, the stability of the rare earth oxides can be used as an advantage for their recovery. The levels of other metals and metal oxides must, however, be controlled to obtain a

concentrated rare earth oxide slag that can be further processed/purified. With this in mind, industrial ferrous streams of electronic waste with a relatively high content of NdFeB magnets were selected and used to make the rare earth oxide slag. Physical separation methods were used to make these streams, which involved standard industrial WEEE processing methods such as manual sorting, shredding, magnetic separation, electrostatic separation, sizing and/or gravity separation. The results of the pyrometallurgical treatment of one of these selected streams are discussed in the present paper.

Experimental

The selected stream had a measured neodymium content of approximately 6500 mass ppm, while the main constituent was iron. The input material was heated in a graphite crucible under an argon atmosphere using a resistance heated tube furnace. The crucible was filled with 111.3 g of input material and heated from room temperature to 1600 °C in one hour and held at this temperature for another hour. The crucible and contents were then cooled by 10 °C per minute to 1000 °C before the furnace was turned off leaving the material to further cool uncontrolled to room temperature.

The melting step proved to have produced two distinct phases, one oxide (slag) phase and one metal phase. The resulting slag was analyzed by X-Ray Fluorescence (XRF), Electron Probe Micro Analysis (EPMA), X-Ray- Diffraction (XRD) and the sessile drop technique, while the metal was analyzed by Inductively Coupled Plasma – Mass Spectroscopy (ICP-MS).

Results

The produced phases, i.e. the metal and slag phase, were easily separated from each other and the graphite crucible. The separated slag phase had a mass of 2.4 g and the metal phase had a mass of 96.1 g. This is significantly lower than the initial mass but some mass loss was expected due to fuming of volatiles. In addition there was some degree of splashing causing some slag and metal to get outside the crucible. A sample of 0.5 g of the slag was analyzed by XRF. The analysis results are shown in Table I and a very high rare earth oxide content is observed.

EPMA was used to investigate the microstructure of the solidified slag and a micrograph of the slag is shown in Figure 1. The numbers seen in the micrograph indicate the points that were analyzed by Wave Dispersive Spectroscopy (WDS), and the analysis results are shown in Table II. As can be seen from the table, neodymium, praseodymium and dysprosium are concentrated in certain phases of the solidified slag. A total quantified content below 100 percent indicated that boron (part of the magnet composition) also was present in the slag phase. Boron is known to have very low energy peaks in the WDS spectrum and is therefore hard to quantify. In the present work, boron was qualitatively verified to be present by observation peaks in the WDS-spectrum that are characteristic for boron. The content was, however, too low to determine quantitatively.

Table I. Slag composition in mass percent measured by XRF using quantification software provided with the instrument.

Compound	Nd_2O_3	Al_2O_3	SrO	BaO	SiO_2	CaO	Pr_2O_3	MgO	Dy_2O_3	TiO_2
Mass percent	28.2	19.2	17.9	9.7	8.0	5.4	3.9	1.9	1.1	1.1

*Only oxides present in concentrations above one percent are included.

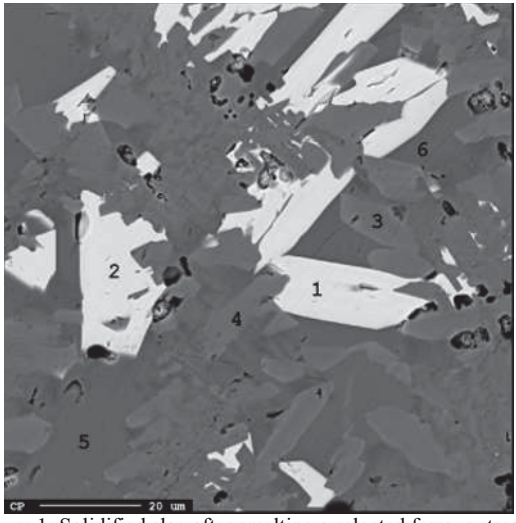

Figure 1: Solidified slag after smelting a selected ferrous stream.

The slag was also investigated by XRD, but even in this case it was challenging to identify the peaks in the spectrum in a way that was in agreement with the findings by WDS. Moreover, a sample of the slag was taken and investigated by the sessile drop technique to determine an approximate melting point. The slag was observed to start deforming at approximately 1320 °C and to be completely molten at 1400 °C, as can be seen in Figure 2.

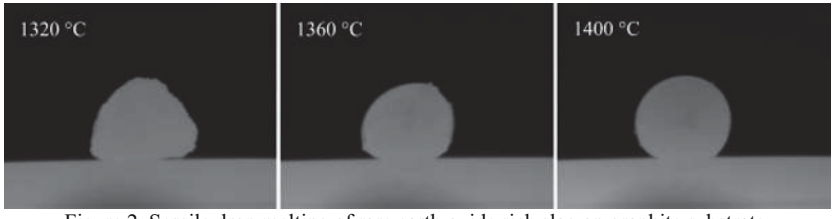

Figure 2. Sessile drop melting of rare earth oxide rich slag on graphite substrate.

Table II. Mass percent of different elements in the solidified slag. Numbers correspond to those phases labelled in Figure 1.

No.	Mg	O	S	Fe	Al	Ca	Nd	Si	Ba	Pr	Sr	Ti	Dy	Total
1	0.1	23.2	0.8	0.0	0.4	3.8	37.9	9.1	1.6	5.3	8.7	0.0	4.0	95.0
2	0.1	20.5	0.8	0.0	0.4	3.6	37.2	9.1	1.7	7.8	9.4	0.1	3.5	94.2
3	0.2	30.2	0.0	0.1	24.0	1.1	0.3	0.5	20.8	0.1	23.6	0.8	0.1	101.8
4	0.3	29.8	0.0	0.0	24.0	0.9	0.3	0.6	22.2	0.1	23.3	0.9	0.1	102.6
5	1.3	31.9	0.8	0.0	8.5	9.9	3.0	6.6	15.1	0.6	17.6	0.8	1.4	97.5
6	1.2	31.3	0.6	0.0	8.6	9.6	3.1	6.7	15.4	0.6	17.5	0.7	1.5	97.0

Table III. Rare earth element content in metal analyzed from three separate samples. Concentration given in mass ppm.

No.	Praseodymium	Neodymium	Dysprosium
1	1.9	13.2	1.4
2	0.6	4.0	0.3
3	0.3	2.1	0.2

Three parallel samples were drilled out of the metal phase, and approximately 100 mg of each was dissolved using 1.5 mL HCl and 0.5 mL HNO_3. The samples were observed not to be completely dissolved in the acid mixture. This was expected due to formation of carbides in the metal, which are known to be hard to dissolve. This issue will be addressed in future analyses. The measured concentration of neodymium, praseodymium and dysprosium in the metal phase is shown in Table III. The concentration of the REEs in the metal proved to be in the low ppm range, and the concentration of other REEs was even lower. A significant variation between the samples was, however, established to exist, which may be caused by traces of slag in the metal samples.

Discussion

The obtained results confirm that REEs are oxidized and collected into a slag phase. Both the XRF and the WDS results are semiquantitative since there are no calibration standards covering the composition of the slag investigated in the present work. A calculated recovery close to 100 percent does however indicate that the values for the main constituents should be reasonable both for the XRF and the WDS analysis. The agreement between elements found by XRF and WDS also indicates that the identified elements are actually present in the slag.

Neodymium, praseodymium and dysprosium were the only REEs identified in the slag, which indicates that NdFeB magnets are the main source of REEs in the selected ferrous stream. A heavy distribution of the REEs towards the slag was expected, and the concentration of REEs in the slag was measured to be in the range between 10 000 and 50 000 times higher than in the metal. The observed REEs were found to be enriched in certain phases in the solidified slag. Therefore it is believed to be possible to further concentrate the REEs by physical separation of certain phases in the slag, e.g. by grinding and heavy media or by electromagnetic separation.

Significant amounts of the alkaline earth metals calcium, strontium and barium also proved to be present in the slag, see Table I and Table II. The origin of these oxides is somewhat uncertain, but the authors believe that they may come from capacitors present in the electronic waste. The alkaline earth metals probably functioned as fluxing agents of the slag lowering the melting point to the observed value between 1320 and 1400 °C. The aluminum and silicon oxides, which were also present, will contribute to lowering the melting point of the rare earth oxide containing slag, but not to such a large degree as the alkaline earth metals.

Conclusion

Rare Earth Elements (REEs) in selected industrial ferrous streams of electronic waste were collected and enriched as oxides in a slag phase with only trace levels remaining in the metal. Elements present in the selected waste stream gave a slag with a low enough melting point to give a liquid slag with good separation from the metal at steelmaking temperatures.

Neodymium, praseodymium and dysprosium were the only REEs found to be dissolved in the slag phase, and they were observed to be even further enriched in certain phases of the solidified slag offering opportunities for even greater separation.

Acnowledgements

The project is funded by research grant EU FP7-603564 – REEcover. Assistance from Morten Peder Raanes with the EPMA-WDS analysis and from Torild Sørløkk with the XRF-analyses is highly appreciated.

References

1. European Commission, “Report on critical raw materials for the EU,” (2014).

2. U.S. Department of Energy, “Critical materials strategy,” (2011).

3. K. Binnemans, P. T. Jones, B. Blanpain, T. V. Gerven, Y. Yang, A. Walton, and M. Buchert. "Recycling of rare earths: a critical review," *Journal of Cleaner Production*, 51 (2013), 1-22.

REWAS 2016: Towards Materials Resource Sustainability
Edited by: Randolph E. Kirchain, Bart Blanpain, Christina Meskers, Elsa Olivetti, Diran Apelian, John Howarter, Anne Kvithyld, Brajendra Mishra, Neale R. Neelameggham, and Jeff Spangenberger
TMS (The Minerals, Metals & Materials Society), 2016

FUNDAMENTAL STUDY OF THE RARE EARTHS RECYCLING THROUGH THE PYROTETALLURGICAL ROUTE - PHASE RELATIONS AND CRYSTALLIZATION BEHAVIOR OF THE $CaO\text{-}SiO_2\text{-}Nd_2O_3$ SYSTEM

Thu Hoai Le, Annelies Malfliet, Bart Blanpain and Muxing Guo

Department of Materials Engineering, KU Leuven,
Kasteelpark Arenberg 44 bus 2450, B-3001 Heverlee (Leuven), Belgium

Keywords: Phase relations, rare earths recycling, solidification

Abstract

This study aims to investigate phase relations of the $CaO\text{-}SiO_2\text{-}Nd_2O_3$ ternary system for high temperature recycling of Neodymium. The slag samples were equilibrated at 1500°C and 1600°C for 24h in Ar, and quenched in water. From the phase analysis of the samples, the isothermal sections were partially constructed and the liquid stability regions were assessed. Based on the identified phase relations, a solidification process with different cooling paths was studied in-situ using a confocal scanning laser microscope within the interesting slag phase regions for recycling. The phases needed for optimizing recycling can be produced accordingly.

Introduction

The increasing demands for rare earth based materials, which are widely used in electronic devices, has raised the needs of the efficient use of rare earths to minimize environmental impacts, solve supply risk of critical raw materials, and moderate the "balance problem"[1..6]. In particular, attention has been drawn on recycling of rare earth elements (REE) from REE enriched waste streams. Hydrometallurgy, which has shown potential in this specific area, suffers from large amounts of chemicals needed and difficulties in dismantling, separation, and processing steps when applied for recycling of rare-earth containing batteries and magnets. A combination with pyrometallurgy, therefore, has been considered as an alternative route with a potentially lower environmental and economic impact. In this process, rare earths containing wastes are melted in furnaces (Electric Arc Furnaces (EAFs)) or other smelters. The resulting product is a slag containing rare earths elements, which is now challenging metallurgists to extract them efficiently. In order to enhance the recycling of rare earths through the pyrometallurgical route, fundamental understandings of the rare earths distribution in the slag and precipitation behavior of the REE containing compounds during slag solidification are of significant importance.
This work focuses on the phase relations of the rare earth containing metallurgical slag and its crystallization behavior during cooling by using the confocal laser scanning microscope (CLSM).

Experimental

The set-up of isothermal equilibration and quenching from high temperature of the selected slag systems has been described in detail in our previous work [7]. Samples were equilibrated at controlled conditions and then cooled rapidly so that the phase assemblage and phase compositions can be preserved at room temperature. This method is suitable to determine silicate slag systems' phase equilibria because of the ability to retain their phases as glass on fast cooling. Selected amorphous slags, which were prepared according to the procedure, have been used for their solidification behavior analysis with a confocal scanning laser microscope (CSLM) [8]. A platium-20%Rhodium crucible containing the prepared slag sample was placed on the sample holder inside the CSLM. Before heating the sample to desired temperature, CSLM chamber was evacuated and flush with argon three times and then the Ar stream was used continuously during the experiments. After maintaining at the desired temperature for 30mins, the sample was cooled to room temperature with the desired cooling rate. The laser scanned images of this cooling process were captured and used for further investigation.

Results and discussion

From the phase analyses of the quenched samples of the equilibrium experiments, the isothermal sections of the ternary CaO-Nd_2O_3-SiO_2 system at 1500 and 1600 °C were determined [7]. These sections are shown in Figure 1. As for the compositions within the CaO-Nd_2O_3-C_3S and Nd_2O_3-SiO_2-$Ca_{2+x}Nd_{8-x}(SiO_4)_6O_{2-0.5x}$ triangles, the samples obtained after quenching were in the form of loosely packed powders, only the Ca_3SiO_5(C3S)-SiO_2-Nd_2O_3 pseudo ternary system is considered in the construction.

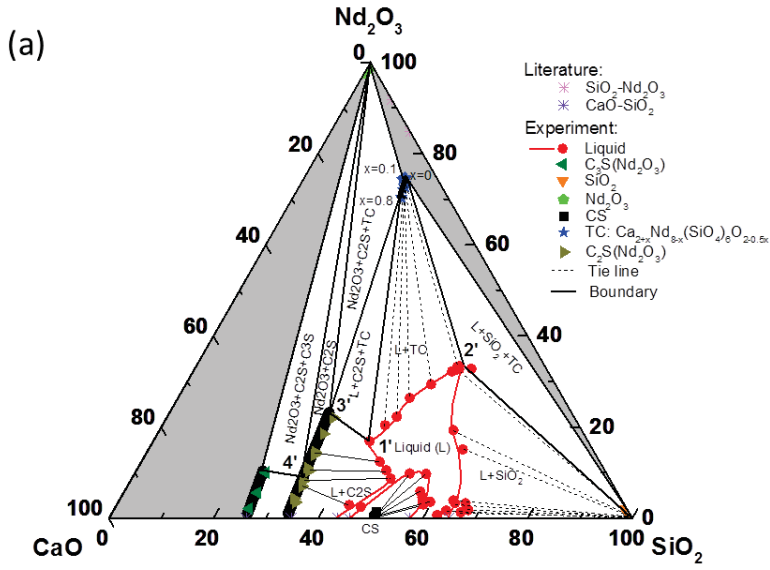

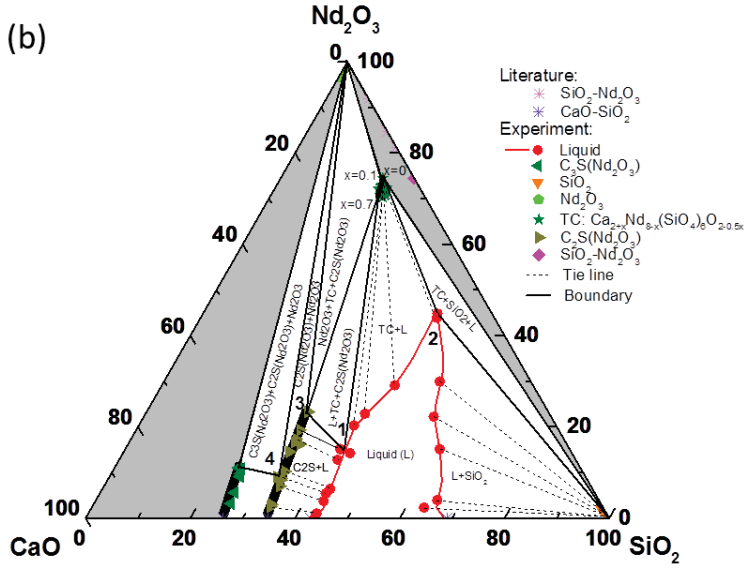

Figure 1. Observed isothermal section of CaO-SiO_2-Nd_2O_3 phase diagram and tie lines at a) 1500 °C and b) 1600 °C. Phase relations of the pseudo system CaO-$C3S$-Nd_2O_3 have been omitted for clarity.

Based on these isothermal sections, a possible REE recycling scheme could be based on the precipitation of the REE-rich solid phase from the Liquid + $Ca_{2+x}Nd_{8-x}(SiO_4)_6O_{2-0.5x}$ region.

By separating these $Ca_{2+x}Nd_{8-x}(SiO_4)_6O_{2-0.5x}$ precipitates from the slag, a REE-enriched product could be obtained, which can serve as a REE-rich input stream in a next step of the REE recycling process. As a first step to evaluate the possibility of recycling the REE by this method, the solidification behavior is investigated with confocal scanning laser microscopy (CSLM) for one composition within the Liquid + $Ca_{2+x}Nd_{8-x}(SiO_4)_6O_{2-0.5x}$ region. The composition has been selected as 5%CaO-45%SiO_2-20%Nd_2O_3 for which the ternary compound $Ca_{2+x}Nd_{8-x}(SiO_4)_6O_{2-0.5x}$ should be the primary phase to precipitate during slag cooling. Three CSLM experiments have been performed in which the cooling rate was increased from 5 and 20 to 100 °C/min. The results are shown in Figures 2-4. In these figures, the first image represents the system in a complete liquid state at a given temperature. The network that is visible in these images, is the microstructure (i.e. grain boundaries) of the platinum-rhodium crucible bottom which can be seen through the transparent liquid slag. For all investigated cooling rates, the nucleation and growth of precipitates have then been continuously recorded, by which the precipitates are in-situ identified by seeing a different structure appearing, moving and growing in the liquid. Only the main images of this process are given in Figures 2-4. The circles indicate the precipitates that are clearly visible, which appear depending on their position as either a whiter or darker color. The precipitates grow with a dendritic shape, as can be most clearly seen in Figures 2-4 (c). The

temperature at which the first precipitate has appeared and at which solidification has been completed is given for the different cooling rates in Table I.

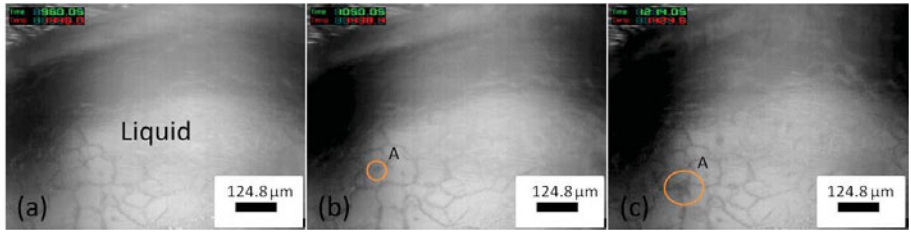

Figure 2. Cooling rate at 5 °C/min (a) transparent liquid slag (b) precipitate appearing (c) precipitate growing and moving.

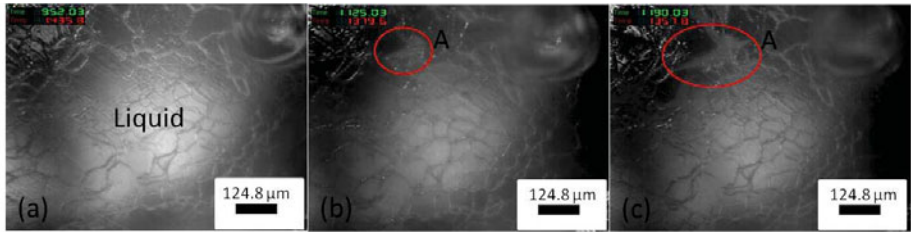

Figure 3. Cooling rate at 20 °C/min (a) transparent liquid slag (b) precipitate appearing (c) precipitate growing and moving.

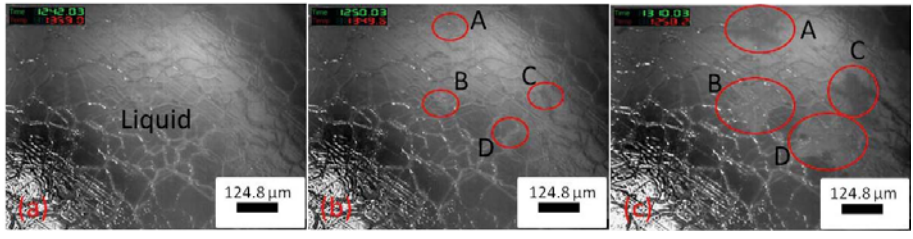

Figure 4. Cooling rate at 100 °C/min (a) transparent liquid slag (b) precipitate appearing (c) precipitate growing and moving.

Table I. Precipitation and complete solidification temperatures at different cooling rates of the slag with composition 5%CaO-45%SiO_2-20%Nd_2O_3.

Cooling rate, °C/min	$T_{precipitatation}$, °C	$T_{solidification}$, °C
5	1448	1365
20	1445	1230
100	1404	1175

As a follow-up of this preliminary study to evaluate the potential of recycling REE from the waste through the precipitation of the REE-rich ternary compound from the Liquid + $Ca_{2+x}Nd_{8-x}(SiO_4)_6O_{2-0.5x}$ region, the composition of the precipitates and the microstructure of the samples will be characterized by Electron Probe Micro-Analyzer (EPMA). Further experiments should include completing the data for more slag compositions and a broader range of cooling rates. These data are necessary to construct the Continuous Cooling Transformation (CCT) diagrams which are a practical tool for the REE recyclers to select appropriate slag compositions and cooling rates and to optimize the process. Furthermore, the influence of additives, such as P_2O_5, on the crystallization behavior will be investigated.

Conclusion

The behavior of REE in the CaO-SiO_2-Nd_2O_3 slag system is clearly interpreted from the isothermal sections determined in the present work. It provides information regarding the selection of suitable flux materials for rare earth containing wastes recycling processes from which their slags are considered as the starting secondary raw materials, as an alternative to rare earth ores. The solidification behavior with subsequent variations in the cooling paths shows that the phases of interest for optimizing the recycling process are produced. The efficiency of REEs recovery and slag recycling can thus be enhanced by a properly engineered hot stage slag treatment process.

Acknowledgement

The authors acknowledge the support from the Hercules Foundation (project no. ZW09-09) in the use of the FEG-EPMA and FEI-Nova Nanosem system.

References

1. K. Binnemans, P. T. Jones, B. Blanpain, T. Van Gerven, Y. Yang, A. Walton, and M. Buchert, *Recycling of rare earths: a critical review*, J. Clean. Prod., 51, 1-22 (15 July 2013).

2. K. Binnemans, P. T. Jones, B. Blanpain, T. Van Gerven, and Y. Pontikes, *Towards zero-waste valorisation of rare-earth-containing industrial process residues: a critical review*, J. Clean. Prod., 99, 17-38 (15 July 2015).

3. S. Chu, *Critical materials strategy*, U.S. Department of Energy, December 2011; http://energy.gov/sites/prod/files/DOE_CMS2011_FINAL_Full.pdf

4. R. J. Weber, and D. J. Reisman, *Rare earth element: A review of production, processing, recycling, and associated environmental issues*, U.S. Environmental Protection Agency, August 2012;
http://www.epa.gov/superfund/remedytech/tsp/download/2012_spring_meeting/fff_wed/4_weber-rare_earth_minerals.pdf.

5. L. T. Peiro, G. V. Mendez, and R. U. Ayres, *Rare and Critical Metals as By-products and the Implications for Future Supply*, INSEAD Social Innovation Centre, 2011; http://www.insead.edu/facultyresearch/research/doc.cfm?did=48916

6. T.G. Goonan, 2011, *Rare earth elements—End use and recyclability*, U.S. Geological Survey Scientific Investigations Report 5094, 2011; http://pubs.usgs.gov/sir/2011/5094/

7. T. H. Le, A. Malfliet, B. Blanpain, M. Guo, *Phase relations of the CaO-SiO2-Nd2O3 system and the implication for the rare earths recycling*, to be submitted.

8. P. T. Jones et al., "Using confocal scanning laser microscopy for the in situ study of hig-temperature behavior of complex ceramic materials", Journal of the European Ceramic Society, 27, 3497-3507, (2007).

REWAS 2016: Towards Materials Resource Sustainability
Edited by: Randolph E. Kirchain, Bart Blanpain, Christina Meskers, Elsa Olivetti, Diran Apelian, John Howarter, Anne Kvithyld, Brajendra Mishra, Neale R. Neelameggham, and Jeff Spangenberger
TMS (The Minerals, Metals & Materials Society), 2016

MITIGATING SUPPLY RISK OF CRITICAL AND STRATEGIC MATERIALS: THE ROLE OF TRADE POLICIES

Vasken Xhaxhollari[1], Michele Bustamante[1], Gabrielle Gaustad[1]

[1]Golisano Institute for Sustainability, Rochester Institute of Technology
111 Lomb Memorial Drive, Rochester, NY, 14623-5608, USA

Keywords: criticality, sustainability, tariffs, supply chain

Abstract
Critical materials are minerals with potential supply chain risks that cannot be easily substituted in many of their applications, including, but not limited to, clean energy technologies, LEDs, smartphones, lasers, and microwave circuits. With increasing demand for these products, supply chain disruptions pose an ever-growing risk to the economic wellbeing of many nations, including the United States. One under-examined potential source of risk arises from sociopolitical instabilities and direct or indirect market manipulations, referred to generally as trade risks. To illustrate the potential challenges posed by some of these trade risks, US tariff policies for nine critical materials were examined for potential to inform future material-related trade policies. Two of these case study materials, gallium and tantalum, were examined in depth to estimate relevant economic impacts. Findings from these case studies suggest that a reduction or abolishment of tariffs in general may foster trade, economic growth, and a lowering of supply risk. Further work will be required to cement a cause and effect link between trade barriers and criticality risk.

Introduction

Critical materials are highly-demanded substances with potentially limited and volatile supplies, often lacking direct substitutes. They are particularly relevant to clean energy technologies and defense applications, but their use is pervasive across a variety of industries. Examples in the clean energy sector include gallium in thin film solar cells, dysprosium in wind turbine magnets, lithium in lightweight rechargeable batteries, and germanium in fiber-optics[1, 2]. Lack of adequate substitutes render many widely-used products completely dependent upon the supply dynamics of a particular critical material input. This can potentially leave the broader economy at risk of instability in the case of supply disruption events[3]. However, a robust and fluid supply chain has the potential to mitigate such risks by enabling international markets to better meet the needs of individuals, industry, and governments.

Recent research suggests that open trade policies allow for greater country growth [4, 5]; the use of tariffs and other restrictions typically have negative effects[6]. Although there are many different factors that can lead to short-term unavailability of critical materials (e.g. coproduction, price volatility, environmental and human health disasters), in the present work, supply risk stemming from economic disruption of commodity trade caused by tariff policies will be examined. A number of reasons are given by governments when they decide to enact tariffs, or economic penalties on trade of a particular material. For instance, import tariffs are

commonly used as economic disincentives to reduce foreign competitors. A tariff makes it more costly for outside producers to bring their products into the United States, for example, so local producers gain a cost advantage in the process. This approach can be employed as a means of fostering growth in new industries as well as protecting failing domestic industries.

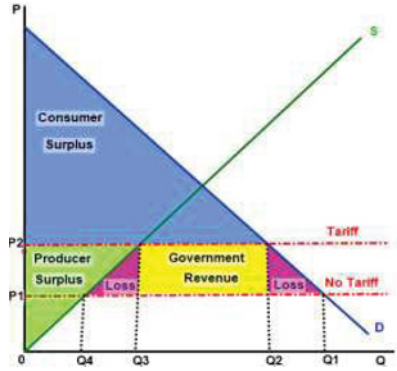

Figure 1. Generalized impact of tariffs on trade.

The economic impacts of a generalized tariff policy are illustrated in Figure 1. Quantity is plotted on the horizontal axis and price is plotted on the vertical axis. The green "S" curve is representative of the domestic supply of a particular good. The blue "D" curve is likewise representative of the domestic demand. If the only producers in the world were domestic producers and the market was open and free from disruptions, then an equilibrium quantity and price would be reached where the supply and demand curves meet. However, in a globalized system of trade, foreign producers who can produce the same good as domestic ones have the opportunity to import their products. They choose to do this because they can produce at lower costs than domestic producers and therefore charge less for their product. This process of international trade bids down the price of the good until a new equilibrium is reached at P1 and Q1. At this equilibrium, domestic producers sell a quantity of Q4. So, without a tariff, trade allows a market clearing price where domestic supply plus imported supply meets demand with an optimal quantity of Q1 and optimal price of P1. With the tariff, the price increases to P2 and quantity decreases to Q2. Domestic producers now sell more of their product at Q3 and the rest of supply is again filled by imports.

In this general case, consumer surplus, the benefit consumers enjoy by paying less for a product than their maximum willingness to pay actually decreases because consumers now face a higher price for the product. Producer surplus, the benefit that producers enjoy by selling above their least willingness to sell price also increases. The government also gets a portion of the revenue because the tariff acts as a tax. However, the total benefits from trade actually decrease because the tariff creates market inefficiencies. The purple areas on the graph represent the losses from forgone trades that would otherwise have occurred without the tariff. For example, some consumers cannot purchase the product anymore because of the increase in price.

Therefore, although it may be seen as a beneficial strategy for the importing country, on the whole, tariffs can be problematic because they generate a net economic loss to society.

Methods

To understand the frequency of tariff use in critical material markets, tariff values for a variety of materials identified as critical by the Department of Energy[7] and the European Union Commission on Critical Materials[8] were collected from the US Geological Survey[9] and the UN Comtrade[10] over the period 2002 to the most recent available report for each commodity. Market share was examined by calculating the Hirschman-Herfindahl Index (HHI) [11]. The HHI is calculated by taking the market share of each producer as a decimal out of one hundred, squaring it, and then adding it with the other squared market shares from every other producer. More formally: $HHI = [a_1]^2 + [a_2]^2 + \ldots + [a_n]^2$ where each "a" variable is a producer up to "n" number of producers. Similarly, this data was used to also compute the US import reliance for several of these critical materials. Together, the import reliance and HHI can indicate areas where supply vulnerabilities may exist for these important materials. Two specific case studies were chosen to examine in further depth: gallium and tantalum. These materials were chosen for their broad utilization across industries and their interesting trade circumstances. Gallium is used in many devices such as LED's, integrated circuits, military technology, and emerging thin film solar technologies[1, 12]. The United States does not domestically mine gallium metals and gallium arsenide wafers are imported[13]. Important end uses for tantalum include automotive electronics, computers, and mobile phones. Tantalum is not significantly mined in the United States with a considerable amount being imported from conflict zones in socio-political turmoil[14]. Customs valuations were also compiled from the USGS in order to project revenues from tariffs as compared to the ad.valorem values.

Results

Figure 2 shows selected critical materials with their ad.val. tariff values ranging from "free" or 0% up to a high of 14% for wrought manganese metal. The table also shows specific tariffs and their values for gallium and tantalum materials. One can see that many materials with key criticality issues still have significant tariffs levied on them.

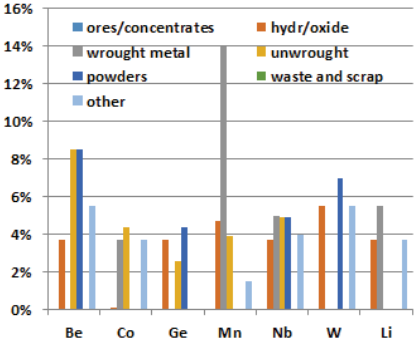

Ga and Ta Materials	Tariff #	Tariff
Gallium arsenide wafers, undoped	2853.00.0010	2.8% ad val.
Gallium arsenide wafers, doped	3818.00.0010	Free
Gallium metal	8112.92.1000	3.0% ad val.
Synthetic tantalum-niobium concen	2615.90.3000	Free
Tantalum ores and concentrates	2615.90.6060	Free
Tantalum oxide	2825.90.9000	3.7% ad val.
Potassium fluorotantalate	2826.90.9000	3.1% ad val.
Tantalum Powders	8103.20.0030	2.5% ad val.
Tantalum Alloys and metal	8103.20.0090	2.5% ad val.
Tantalum, waste and scrap	8103.30.0000	Free
Tantalum, other	8103.90.0000	4.4% ad val.

Figure 2. Selected Critical Materials and their Ad.Val Tariffs[15]

Analysis of global production and import data suggests the United States relies heavily on imports to supply many raw materials critical to clean energy, high technology, and national defense applications as shown in Table 1. Indium, niobium, and the two case study materials gallium and tantalum meet all of their demand from foreign sources of production. Many times, this circumstance is unavoidable; global mineral supply chains are largely dictated by the natural geographic distribution of mineral resources, which know no geopolitical boundaries. However, when a small number of foreign nations supply the majority of US material needs, any external disruption or restriction of supply has the potential to negatively impact the US economy.

Table 1. US 2014 Import Reliance and Top Producers of Select Minerals[15]

Materials	Percentage	Top Producers
Indium	100	China, Canada, Belgium, Japan
Niobium	100	Brazil, Canada
Tantalum	100	Russia, Germany, Kazakhstan, China
Gallium	99	Germany, United Kingdom, China, Japan
Germanium	95	China, Belgium, Russia, Canada
Platinum	85	Germany, South Africa, United Kingdom, Canada
Zinc	81	Canada, Mexico, Peru
Cobalt	76	China, Norway, Russia, Finland
Rare Earths	59	China, France, Japan, Estonia

In highly concentrated markets, economies are open to higher exposure of supply risk because of a lack of producers. If a disruption in supply affects one producer it is likely to significantly impact the domestic economy. According to the United States Department of Justice and the Federal Trade Commission, a market with an HHI value at or above 25% can be considered to be highly concentrated. Gallium market concentration (HHI) was determined to be about 25%, putting it right on the cusp of this threshold. One of the largest contributors to gallium imports, China, supplies about twenty three percent of the US imports. Given the sometimes tenuous relationship between these two countries, it is conceivable that some supply might be reduced in times of political distress by unilateral action. Recently, the World Trade Organization found that China had inappropriately applied export restrictions, duties, and other limitations on the export of tungsten, molybdenum, and other rare earths [16]. The effect was that supply of these materials was less than what it would have otherwise been in the open market, increasing the cost of these materials. Similarly, tantalum market concentration was also determined to be high, with an HHI of about 32%. The tariff on the imports below adds additional risk. It lowers the quantity that would have been imported and increases the price of tantalum.

As shown in Figure 2, there is currently a 3.0% ad valorem tax on importation of unwrought, waste, and scrap gallium into the US and a 2.5% tariff on unwrought powder, ore, and concentrates of tantalum. Since ad valorem taxes are rendered on the price of the material, it is important to understand trends in average pricing as well. Figure 3 (lines) shows the average yearly price for both materials over the period 2003-2013; prices have generally followed an

upward trend with some downward pressure seen in recent years for gallium. Despite this upward trend, tariff revenue (dots in Figure 3) demonstrates a large degree of variability indicating aspects beyond price are driving imports.

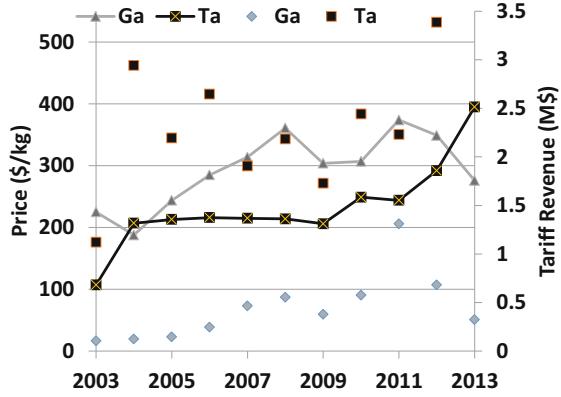

Figure 3. Average price of gallium and tantalum (lines); Revenue generated from tariff applied to customs value of gallium and tantalum (dots)

The tariffs imposed on gallium and tantalum imports do several things: (1) they lower the supply that is available to United States consumers because of the increase in costs to outside producers, (2) they provide revenue for the federal government, and (3) they increase supply risk by acting as a market disruption due to an increase in overall costs to outside producers. Generally speaking, governments always benefit from tariff revenue and regardless of the reason for the implementation of these tariffs, an incentive exists to levy tariffs on imported goods. In fact, historically, tariffs have been important government revenue sources. However, as was suggested from Figure 1, this economic benefit to the importing government will result in a net loss of economic welfare due to a loss of trades.

Conclusion

Critical materials are in high demand with highly concentrated supply and few substitutes. Many of the materials also come from a small number of top producers as exemplified through case study analyses of gallium and tantalum. A highly concentrated market will be affected much more by supply risk. The United States mines or produces very little to none of these materials. Import reliance and especially concentration of import supply from a small number of countries may create vulnerability in the event of a trade restriction or other supply disruptions.

Supply disruptions could potentially cause damage to economic output. As such, disruptions in supply due to tariffs enacted in the United States, especially the tariffs against many of these materials, may act to increase supply risk. These tariffs have the possibility to make it more costly to import these materials by lowering the supply of imports. Because of the lack of production in many critical materials, the United States may wish to consider the removal of many of these tariffs in order to lower general supply risk and the cost that it would take to

import key critical materials. Future work analyzing supply and demand trends in the context of tariffs and other trade policies will help to better assess this potential threat.

Also, the potential might exist for a country to unilaterally disrupt supply to the United States (as long as it is a top producer). While a global economy exists and trade allows for a reduction of this risk, the perception that the United States might not be able to import what it needs would be disastrous for the domestic economy as well the world economy as a whole. Given some of the risks associated with a small supply source, the United States should be encouraged to seek ways to keep trade open and reduce the possibility of supply risk.

References

1. Moss, R., et al., *Critical Metals in Strategic Energy Technologies. Assessing Rare Metals as Supply-Chain Bottlenecks in Low-Carbon Energy Technologies*. 2011, Institute for Energy and Transport IET, Petten (Netherlands).
2. Yoshio, M., R.J. Brodd, and A. Kozawa, *Lithium-Ion Batteries*. 2009: Springer.
3. Alonso, E., et al., *Material Availability and the Supply Chain: Risks, Effects, and Responses.* Environmental Science & Technology, 2007. **41**(19): p. 6649-6656.
4. Wacziarg, R., *Measuring the dynamic gains from trade.* The world bank economic review, 2001. **15**(3): p. 393-429.
5. Wacziarg, R. and K.H. Welch, *Trade liberalization and growth: New evidence.* The World Bank Economic Review, 2008. **22**(2): p. 187-231.
6. Schularick, M. and S. Solomou, *Tariffs and economic growth in the first era of globalization.* Journal of Economic Growth, 2011. **16**(1): p. 33-70.
7. Bauer, D., et al., *Critical Materials Strategy*. 2010, U.S. Department of Energy: Washington, D.C.
8. E.C., *Critical raw materials for the EU*. 2010. p. 84.
9. Kelly, T.D. and G.R. Matos. *Historical statistics for mineral and material commodities in the United States*. Aluminum 2010 [cited 2010 7-12-10]; Available from: http://pubs.usgs.gov/ds/2005/140/.
10. Comtrade, U., *United Nations Statistics Division.* Commodity Trade Statistics Database, 2011.
11. DOJ, F. *Horizontal Merger Guidelines*. 2010 6/25/15 [cited 2015 7/22]; Available from: http://www.justice.gov/atr/horizontal-merger-guidelines-08192010#foot9.
12. Romans, S.F., *The Role of the National Defense Stockpile in the Supply of Strategic and Critical Materials*. 2008, DTIC Document.
13. *Energy Critical Elements: Securing Materials for Emerging Technologies*. 2011, American Physical Society, Materials Research Society.
14. Young, S.B. and G. Dias, *LCM of Metals Supply to Electronics: Tracking and Tracing'Conflict Minerals'.* Available at SSRN 1875976, 2011.
15. Gambogi, J., *Mineral Commodity Summaries 2014.* USGS, Washington DC, 2014: p. 17.
16. Morrison, W.M. and R. Tang, *China's Rare Earth Industry and Export Regime: Economic and Trade Implications for the United States*, C.R. Service, Editor. 2012, Library of Congress.

REWAS 2016: Towards Materials Resource Sustainability
Edited by: Randolph E. Kirchain, Bart Blanpain, Christina Meskers, Elsa Olivetti, Diran Apelian, John Howarter, Anne Kvithyld, Brajendra Mishra, Neale R. Neelameggham, and Jeff Spangenberger
TMS (The Minerals, Metals & Materials Society), 2016

SUSTAINABLE PROCESSING OF PHOSPHOGYPSUM WASTE STREAM FOR THE RECOVERY OF VALUABLE RARE EARTH ELEMENTS

Mugdha Walawalkar[1], Connie K. Nichol[2], Gisele Azimi[1,3]

[1]University of Toronto,
Laboratory for Strategic Materials, Chemical Engineering and Applied Chemistry Department
200 College St., Toronto, ON, M5S3E5, Canada
[2]Agrium Inc., 11751 River Road, Fort Saskatchewan, AB, T8L4J1, Canada
[3]University of Toronto,
Laboratory for Strategic Materials, Materials Science and Engineering Department
184 College St., Toronto, ON, M5S3E5, Canada

Keywords: Rare earth elements, Recovery, Phosphogypsum, Waste valorization

Abstract

Rare earth elements (REEs) are among the strategic materials that have revolutionized modern industry. These materials have unique properties, so they are essential to the production of many technologically advanced products that are dominating the world; thus the REEs demand is continuously rising. To address this challenge, finding new sources for them is highly of interest. Here, we identified a waste stream from phosphoric acid production plants, called phosphogypsum, which contains some amounts of REEs. We developed a novel hydrometallurgical process to recover REEs from phosphogypsum. We investigated several leaching agents at various conditions and identified the optimum leaching parameters. Not only can the developed process decrease the size and associated environmental risks with the existing phosphogypsum stacks, but also can slow down the need for additional stacks. In addition to waste valorization, this novel process provides a new source for REEs production, addressing the sustainability challenges associated with them.

Introduction

REEs constitute a group of 17 elements, which include 15 lanthanides, scandium and yttrium. Despite their name, REEs are not rare, as most of them occur abundantly in the earths crust [1]. The problem with REEs is that they do not occur in minerals as individual rare earth compounds and are scattered within other minerals. Furthermore, they are primarily concentrated in a few minable resources across the world (mainly in China, Brazil, India, and the United States). Also, they co-occur and their similar physicochemical properties make their individual separation and purification challenging [2].

REEs have unique magnetic, spectroscopic, catalytic, and hydrophobic properties and because of that they are critical to the production of many high-tech products, such as wind turbines, electric and hybrid cars, automotive catalytic convertors, petroleum cracking catalysts, fluorescent lams, and hand held electronic devices. Their current annual demand is about 136,000 tonnes worldwide [3], and it is predicted that their demand will increase to around 200,000 tonnes per year by 2016 (47% increase) [4]. The reduction in availability of primary sources for these

elements coupled with increasing demand has led to increased prices for REEs over the past few years. Although, recently there was a slight decrease in their price due to the slow economy, it is expected that the price will start to rise again when the economy picks up. For those reasons, REEs have become a strategically important class of materials, and the importing countries, including Canada, United States, and European Union members have accelerated efforts to find secondary sources for these elements to satisfy their demands [5,6].

Apatite is one of the minerals that contain REEs; however its main use is in the production of phosphate fertilizer. In this process, apatite is leached by sulfuric acid to produce phosphoric acid. The by-product of this process is called phosphogypsum (PG), which is mainly calcium sulfate dihydrate ($CaSO_4.2H_2O$). In most cases, PG is wet stacked adjacent to fertilizer production facilities, spanning hundreds of hectares in area and a few meters in height occupying vast amounts of land [7-9]. The REEs content in apatite is about 0.04 – 1.57 wt.% depending on the source and composition of apatite concentrate [10,11]. It has been reported that 65-85% of REEs in apatite are precipitated with PG [11]. Therefore, PG can be used as a source of REEs.

In this study, we investigated the recovery of REEs from phosphogypsum that was the by-product of phosphoric acid production from Kapuskasing phosphate rock in Canada. We obtained the PG sample from the Agrium's fertilizer production plant in Redwater, Alberta. Figure 1 (a) presents a bird eye view of the PG stacks next to the Redwater plant, indicating that the size of PG stacks is more than 2 times of the plant. Figure 1 (b) presents a closer look of one of the stacks near the plant.

In this work, first, we performed a thorough characterization of the PG sample using acid digestion, ICP-OES, SEM-EDS, and TEM/STEM-EDS. Then, we performed a systematic study to investigate REEs recovery using three leaching agents: nitric acid, hydrochloric acid and sulfuric acid. We studied the effect of acid concentrations, solid-to-liquid (S/L) ratio, temperature, and residence time. The final aim of the present research work was to identify the most efficient leaching agent and the optimum operating conditions to acquire knowledge that will enable the development of novel leaching processes, as the first step for commercial production of REEs from PG stacks located in Canada, mainly in Alberta that has the largest PG stacks. A similar approach to what was taken in this study can be taken to develop leaching processes for various types of PG around the world. Not only can these processes provide a secondary source for the production of increasingly important REEs, but also they can have significant environmental benefits.

Figure 1. Phosphogypsum Stack in Redwater, Alberta, Canada (courtesy: Agrium Inc.)

Results and Discussions

Phosphogypsum Characterization

Agua Regia Digestion and Inductively-Coupled Plasma (ICP-OES). The PG sample was obtained from Agrium Inc. located in Alberta, Canada. To determine the amount of REEs present in the PG, we performed aqua regia digestion (Ethos EZ Microwave Digestion System) followed by Inductively-Coupled Plasma (Agilent 720-ES ICP-OES). Table 1 presents the concentration of REEs in the sample (in ppm). The total content of REEs in the feed is 202 ppm. As can be seen, Y, La, Ce, Nd, and Sm have higher concentration than the rest of the REEs, so for extraction purposes, we only focused on these 5 elements.

Table 1. The concentration of REEs in the PG sample (in ppm)

Element	ppm	Element	ppm	Element	ppm
Y	53	Sm	22	Er	3
La	36	Eu	1	Tm	1
Ce	26	Gd	17	Yb	3
Pr	6	Dy	5	Lu	1
Nd	27	Ho	1		

Scanning Electron Microscopy (SEM) and Energy Dispersive Spectroscopy (EDS) characterization. SEM analysis of as-received PG sample was performed to observe the overall morphology of the powders. We also looked at the cross-section of the powder particles to gain information on the distribution of REEs in the sample. EDS analysis of the cross-section images identified Ca, S, and O as the main components of the particle. In addition, we were able to identify regions of REEs (La and Y picks) within the particles. Figure 2 represents the cross-section of the polished particles. Regions with REEs present are the brighter spots, indicated in the red boxes.

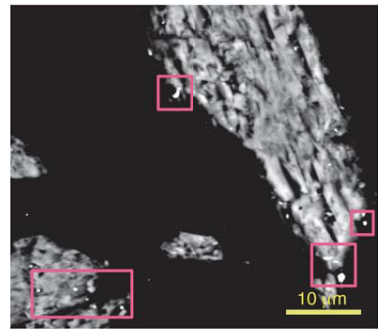

Figure 2. Cross-section of polished particles: the bright spots show REEs picks in EDS analysis

Transmission Electron Microscopy (TEM), Scanning Transmission Electron Microscopy-energy-Dispersive X-ray Spectroscopy (STEM-EDS) characterization. TEM/STEM-EDS characterization of the PG sample was performed on the as-received powder to observe the structure and elemental mapping of its constituents, particularly REEs. Fig. 3 (a) presents the TEM image of a PG particle and Fig. 3 (b) presents the elemental maps of the particle. We can clearly observe a lump of ~ 1 μm in size within the PG particle, containing Ce and La, respectively.

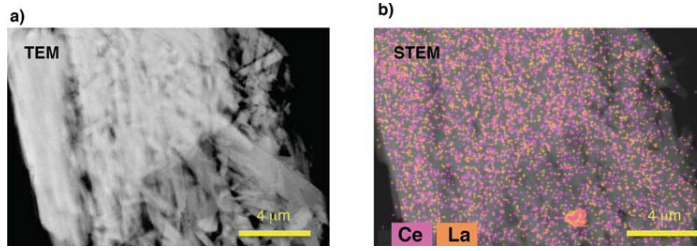

Figure 3. a) TEM image of a PG particle. b) STEM/EDS elemental map of Ce and La

Leaching Experiments

In the present research work, we performed leaching of REEs from PG using three acids: HNO_3, HCl, and H_2SO_4. To identify the most effective leaching agent and the optimum conditions for the leaching process, we investigated several acid concentrations, solid/liquid (S/L) ratios, temperatures, and residence times. First, we investigated the leaching kinetics and found that it was very fast in all cases (which we attribute to the very small size of particles, 50-100 μm), with about 5-10 minutes to reach maximum extraction values. Therefore, we chose 20 min as the optimum residence time for the process.

To study the effect of temperature, we investigated two temperatures: 50°C and 80°C at constant acid concentration and S/L ratio. We found that overall REEs extraction decreases with temperature. The reason behind this observation is that gypsum solubility in the presence of acids increases with temperature up to 80°C [12,13], and then decreases due to the transformation of gypsum to anhydrite [14]. Hence, we chose 80 °C as the optimum temperature for the REEs leaching process.

To study the effect of S/L ratio, we investigated three ratios that are the typical operating conditions in industrial applications: 1/6, 1/8, and 1/12 and we found that the extraction levels increase with decreasing S/L ratio. However, we observed that calcium extraction from PG also increases with decreasing S/L. Considering that we are interested in maximum REEs extraction levels and low calcium extraction level (since it has to be rejected downstream) and the fact that larger ratios are more economical, we decided to choose S/L ratio of 1/8 for further experiments.

To study the effect of acid concentration, we performed leaching tests at 1.5 M and 3 M concentrations, since solubility of gypsum is optimum at these concentrations [12,13]. We found

that increasing acid concentration slightly increases the REEs extraction level; however, it also increases calcium extraction, which is not desirable in this process. Thus, we concluded 1.5 M concentration at 80°C and S/L of 1/8 are the optimum conditions for REEs extraction from PG.

Comparison of the three acids indicated that H_2SO_4 is not an effective acid for REEs leaching and the extraction level of REEs was significantly lower than that when HCl and HNO_3 were used. The reason behind this observation is that at 80°C, the solubility of gypsum in H_2SO_4 is about 40 times lower than that in HCl (0.075 M vs. 0.3 M, respectively) [12,13]. For the case of HNO_3 and HCl, the average % extraction after 20 minutes was 57% and 51%, respectively. Considering that HCl is a more economical agent than HNO_3, we concluded that it is a better leaching agent for the proposed process. However, in special cases, HNO_3 is produced at the site (for example in Agrium plant), and therefore that is a better choice for the extraction process. Figure 4 presents the % extraction of Ce, La, Nd, Sm, and Y for all three acids at 1.5 M concentration, 80 °C and S/L ratio of 1/8 (after 20 min residence time).

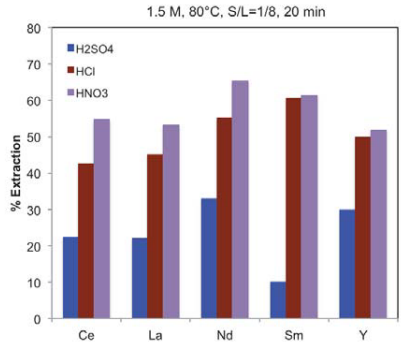

Figure 4. Comparison of extraction levels of Ce, La, Nd, Sm, and Y after 20 minutes residence time using H_2SO_4, HCl, and HNO_3 as the leaching agent at 1.5 M concentration, 80°C and S/L ratio of 1/8.

Conclusions

In this research work, we investigated the extraction of REEs (mainly Ce, La, Nd, Sm, and Y) from phosphogypsum (PG), which is the by-product of phosphoric acid production that is used for fertilizer applications. We obtained the PG sample from Agrium Inc. located in Alberta, Canada. We first conducted a comprehensive characterization study of the PG sample to determine the concentration of REEs and their morphology within the solid phase. Then, we studied the extraction process using three acids (HCl, HNO_3, and H_2SO_4) under various operating conditions, including temperature, concentration, residence time, and solid-to-liquid (S/L) ratio. The results showed that 1.5 M acid concentration, S/L of 1/8, T = 80°C and residence time of 20 minutes were the ideal operating conditions that can be replicated in industrial settings as well. Among the three acids, HCl and HNO_3 resulted in the highest extraction levels for Ce, La, Nd, Sm, and Y. Since HCl is a more economical acid, we propose that as the leaching agent

for the extraction of REEs from PG. The knowledge acquired in this study enables development of novel routes for production of REEs from existing PG stacks. If implemented, the new route would also decrease the size and associated environmental risks of the PG stacks.

Acknowledgments

The authors would like to acknowledge the financial support provided by Natural Sciences and Engineering Research Council of Canada (NSERC) for this project. Also, Agrium Inc. is gratefully acknowledged for providing us with phosphogypsum samples and for reviewing of the manuscripts.

References

[1] N.E. Topp, The Chemistry of The Rare Earth Elements, Elsevier, Amsterdam, 1965.
[2] D.J. Fray, Separating rare earth elements, Science 289 (2000) 2295–2296.
[3] M. Humphries, Rare earth elements: the global supply chain, Congressional Research Service Report, R41347, 2013, pp. 3.
[4] B. Mishra, A. Anderson, Extraction and recovery of rare-earth metals: challenges in processing, in: ERES 2014, 1st European Rare Earth Resources Conference, Greece, 2014, pp. 19–25.
[5] U.S. Department of Energy, Critical Materials Strategy, 2011, pp. 113–120.
[6] Report on critical raw materials for the EU, (Report of the Working Group on defining critical raw materials), 2014.
[7] P.M. Rutherford, M.J. Dudas, J.M. Arocena, Radioactivity and elemental composition of phosphogypsum from three phosphate rock sources, Waste Manage. Res. 13 (1995) 407–423.
[8] S.M. Luther, M.J. Dudas, P.M. Rutherford, Radioactivity and chemical characteristics of Alberta phosphogypsum, Water Air Soil Pollut. 69 (1993) 277–290.
[9] M.E. Jackson, Assessment of Soil capping for phosphogypsum stack reclamation at Fort Saskatchewan, Alberta, University of Alberta, Edmonton, 2009.
[10] B.I. Pålsson, O. Martinsson, C. Wanhainen, A. Fredriksson, Unlocking rare earth elements from European apatite-iron ores, in: ERES2014, 1st European Rare Earth Resources Conference, Milos Island, Greece, 2014, pp. 211–220.
[11] F. Habashi, The recovery of the lanthanides from phosphate rock, J. Chem. Tech. Biothechnol. 35A (1985) 5–14.
[12] G. Azimi, V.G. Papangelakis, J.E. Dutrizac, Modeling of calcium sulfate solubility in concentrated multi-component sulfate solutions, Fluid Phase Equilib. 260 (2007) 300–315.
[13] G. Azimi, V.G. Papangelakis, J.E. Dutrizac, Development of an MSE-based chemical model for the solubility of calcium sulfate in mixed chloride–sulfate solutions, Fluid Phase Equilib. 266 (2008) 172–186.
[14] G. Azimi, V.G. Papangelakis, Mechanism and kinetics of gypsum-anhydrite transformation in aqueous electrolyte solutions, Hydrometallurgy 108 (2011) 122–129.

REWAS 2016: Towards Materials Resource Sustainability
Edited by: Randolph E. Kirchain, Bart Blanpain, Christina Meskers, Elsa Olivetti, Diran Apelian, John Howarter, Anne Kvithyld, Brajendra Mishra, Neale R. Neelameggham, and Jeff Spangenberger
TMS (The Minerals, Metals & Materials Society), 2016

LIFE CYCLE ANALYSIS FOR SOLVENT EXTRACTION OF RARE EARTH ELEMENTS FROM AQUEOUS SOLUTIONS

Ehsan Vahidi [a], Fu Zhao [a, b]

[a] Division of Environmental and Ecological Engineering, Purdue University, West Lafayette, Indiana 47907, United States
[b] School of Mechanical Engineering, Purdue University, West Lafayette, Indiana 47907, United States

Keywords: Life-cycle analysis, rare earth element, solvent extraction

Abstract

Recently Rare Earth Elements (REEs) have received increased attention due to their importance in many high-tech and clean energy applications. Although production of REEs is known to be heavy polluting, very limited environmental Life Cycle Assessment (LCA) studies have been conducted. This is particularly true for the solvent extraction of REEs from aqueous solutions, a key step in the REE production pathway. In this study, an LCA is carried out on a typical REE solvent extraction process using P204/kerosene. The material and energy flow data were based on production information collected from several solvent extraction facilities in Inner Mongolia, China. The life cycle inventory was developed using Simapro 7.1 and Ecoinvent 3, in combination with mass/energy balance and stoichiometry. Eco-indicator 99H was used for impact assessment and LCA results were used to evaluate and identify environmental hotspots of solvent extraction process. Moreover, challenges and opportunities for improved environmental performance of solvent extraction process were discussed.

Introduction

Rare earth metals are defined as elements which are scarce in the earth crust and their extraction processes from ores are laborious. They are included of 15 elements from the lanthanide series in the periodic table starting from lanthanum (La) to lutetium (Lu). Since scandium (Sc) and yttrium (Y) have similar chemical and physical properties, they are also considered as rare earth metals (Castor and Hedrick, 2006; Golev et al., 2014; Haque et al., 2014). Due to their unique structures (e.g., 4f orbitals) and distinctive mechanical characteristics, rare earth metals have been employed in various advanced industries and high-tech products such as fluorescent lightning, rechargeable batteries, cellphones, ceramics, catalysts, wind turbines, hybrid vehicles, optics, lasers, and military systems (Eggert et al., 2008; Grasso, 2013; Fouquet and Martel-Jantin, 2014).

As the largest producer of Rare Earth Elements (REEs) in the world, China supplies more than 90% of the total world's demand although; China has begun to process and utilize its REE production in various industries, concurrently. Since the remainder of the world has not actively solicited to explore new REE supplies, the global REE market will become extremely fragile in the near future. Furthermore, due to the very low concentration (e.g., less than 1%) of REEs in various wastes and crucial challenges in terms of collection and processing, recycling and reuse

cannot accommodate satisfying the growing demand for REEs (Korinek and Kim, 2010; Chu and Majumdar, 2012).

The U.S. Department of Energy (DOE) established the Critical Materials Energy Innovation Hub in 2013 in order to reduce reliance on critical materials and address three different challenges as follows: i) diversifying REE resources, ii) exploring REE alternatives, and iii) recycling REE wastes (Grasso, 2013). Depending on the mineralogy of the REE-containing concentrate which is produced by physical beneficiation, the extraction of REEs may include acid or alkaline leaching methods however; 90% of the REE production is achieved using acidic route. In order to enhance REE dissolution rates in the aqueous media, hydrometallurgical processes generally comprise of various steps of pretreatment. Although, this method requires rather high chemical usage and due to the co-extraction of non-REEs, the process offers low selectivity.

The next step is separation and recovery of different REEs from the leach solution which is mostly implemented by solvent extraction as the commonly used hydrometallurgical process. During solvent extraction which has recently attained industrial significance in various REE recovery and separation methods (Wang et al., 2010; Navarro & Zhao, 2014), concentrate metal ions solution produced after leaching process is mixed with organic solvents as extractant. The REE ions in the aqueous solution react with the extractant and form compounds which are more soluble in the organic phase compared to the aqueous phase and accordingly REEs are transferred into the organic solvent. Then in the stripping process, the REEs are eventually re-extracted and transferred from the organic solvent to a new aqueous solution in which the REEs are more soluble. The concentration of REEs in final solution is often 10-100 times that of the leaching solution before solvent extraction process (Preez & Preston, 1992; Vander Hoogerstraete et al., 2013). The conventional organic solvent utilized for REE separation and refining is P204 (Di [2-ethylhexyl] phosphoric acid). To separate REEs from complex compounds, P204 as an acidic extractant may be used either in sulfate, phosphate, or chloride media. Furthermore, P204 as an effective organic solvent in REEs separation gives an average separation factor, the ratio of distribution coefficients when both solutes are present in a system, around 2.0 between neighboring REEs which reflects the efficacy of P204 in REEs separation (Siekierski & Fedelis, 1978).

As the major method to recover and separate REEs, solvent extraction has several advantages such as simplicity and ready adjustability to process scale-up. Although, cost of chemicals are high and large volume of organic extractants and strong acids are required especially when processing dilute aqueous solutions which is not environmentally friendly and by far, this process is considered as the most challenging stage in REE processing. In recent years, environmental destruction caused by the production of REEs has received significant attention. The Mountain Pass mine in California managed by Moly-Corp which produced almost 70% of the world REE demand in the 1970s and 1980s closed in 2002 due to environmental damages incurred during the production process (Chakhmouradian and Wall, 2012; Zhang, 2013; Fuerstenau, 2013). The first step toward decreasing the environmental destruction during REE production processes is a comprehensive sustainability analysis of the environmental impacts and the most common methodology is Life Cycle Analysis (LCA) as the main method in sustainable product development (Ness et al., 2007; Evans et al., 2009; Golev et al., 2014)

This investigation is innovative because, to the best of our knowledge, there is limited information on LCA of solvent extraction process and the main goal of this study was to assess and quantify environmental impacts of solvent extraction process of rare earth elements from aqueous solutions. Moreover, previous LCA studies have simply considered “unspecified organic solvent” as a general inventory for all solvent extraction processes and ignored different

environmental impacts incurred by utilizing various organic solvents (extractants). The specific objectives to achieve this goal are as follows: i) compose an inventory of the material and energy inputs in the life cycle of a solvent extraction system using P204 as organic solvent; ii) compare environmental impacts of the composed inventory for P204 and standard inventory in the SimaPro software, "organic solvent", which has been previously used by other researchers; iii) quantify the environmental impacts of raw and auxiliary materials used in solvent extraction of REEs in solvent extraction facilities in Inner Mongolia, China.

Taken together, these three contributions greatly improve our knowledge about environmental impacts of REEs solvent extraction process and this, in turn, enables us to analyze current solvent extraction technologies for various REEs separation and helps us design new sustainable treatment processes for answering the growing demand for rare earth metals and improving environmental performance of solvent extraction processes more effectively.

Life cycle assessment methodology

U.S. Environmental Protection Agency (U.S. EPA) has described Life Cycle Assessment (LCA) as a methodology to analyze potential environmental impacts associated with a product or process through their entire life cycle for product improvement and sustainability (SAIC, 2006). According to their materials and energy inputs and outputs, LCA examines environmental impacts to improve sustainability. Since this study only focuses on solvent extraction process to recover and separate REEs, a cradle-to-gate LCA methodology was used to properly address restriction of the scope. The cradle to gate approach defines the boundaries as "from raw material to factory gate". Excluding other processing stages, in cradle to gate approach, environmental impacts of solvent extraction process were analyzed. Based on ISO 14040 (2006), LCA methodology is included the following steps: 1) goal and scope definition to determine the targets and system boundaries of the assessment; 2) assessment of the life cycle inventory for the quantification of the LCA inputs and corresponding outputs of materials or energy which are required for various processes; 3) analysis of the LCA results and their impacts on different environmental parameters to obtain a quantitative approximate of environmental impacts; 4) interpretation to assess and summarize the results obtained from the three first steps to reach a significant conclusion as well as determine the gaps in the study.

Table 1. Consumption of raw and auxiliary materials and energy in Baotou, China.

Materials	Specification	Comsumption
P204 Extraction Agent (D2EHPA)	3M	120 (ton/year)
Kerosene	Sulfonated Kerosene	272.96 (ton/year)
Hydrochloric Acid	31%	34000 (ton/year)
Ammonium Bicarbonate	17%	11250 (ton/year)
Caustic Soda Flakes	>93%	7500 (ton/year)
Sodium Carbonate	>98%	7500 (ton/year)
Naphthenic Acid	Industry Grade	3.41 (ton/year)
Iso-octyl Alcohol	Industry Grade	3.41 (ton/year)
Alamine336	Industry Grade	4.78 (ton/year)
Barium Chloride	Industry Grade	614.16 (ton/year)
Water	underground water from deep-well	227000 (m^3/year)
Coal	washed coal form Shen Mu Mine	26136 (ton/year)
Electricity	local power grid	6924360 (kWh/year)

The functional unit in this investigation was defined as the materials/energy needed for processing of 18000 ton/year aqueous solution containing REOs at a facility in Baotou in China. Table 1 shows the consumption of raw and auxiliary materials and energy as input data used in

the LCA. In this study, the environmental impacts of separation of individual REOs from 220 g/L of rare earth chloride solution were quantified. In addition, a comparative LCA as a systematic way was used to quantify and compare the environmental impacts of the composed inventory for P204 and standard inventory in the SimaPro software, "organic solvent", which has previously been studied in the literature. In combination with mass/energy balance and stoichiometry, the life cycle inventory was developed using SimaPro 7.1. In addition, the Eco-indicator methodology as a problem-oriented approach was developed for product design to aggregate LCA results into easily understandable and user-friendly numbers or units. Eco-indicator 99 (H) in SimaPro was used to assess various environmental impacts including eco-toxicity, photochemical smog formation, global warming, human health cancer, acidification, eutrophication, ozone depletion, human health particulate effects, human health non-cancer, and fossil fuel depletion effects.

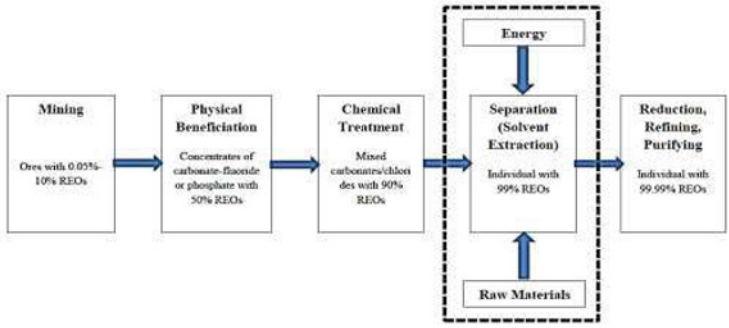

Figure 1. Simplified system boundary of REO processing

Setting the system boundary which is directly related to the data inventory and results is a substantial stage of the LCA study. The brief system boundary of this study is shown in Figure 1. Since most recent publications focused on the production of rare earth elements are well explained in Chinese language, data availability is one of the most important difficulties encountered in life cycle analysis. To perform LCA, users may use their own data to build new inventories, or to update and supplement the SimaPro® software's libraries. It includes both European and U.S. databases, including Ecoinvent, USA Input Output Database 98, ETH-ESU 96, BUWAL 250, Industry Data 2.0, DK Input Output Database 99, IDEMAT 2001, and Franklin Database. The input data (materials and processes) required to conduct a product LCI came from several different supporting databases including both European and US inventories to cover all steps.

Results and Interpretation

Comparison between unspecified organic solvent and P204

A comparative study of the LCA of unspecified organic solvent and P204 was carried out and the characterization results obtained are shown in Figure 2a. As mentioned, previous investigations have focused on unspecified organic solvent and therefore, various environmental impacts were ignored by utilizing different organic extractants. The figure brings to light the impact of the life cycle of the two mentioned organic solvents on different environmental categories and is represented on a percentage scale. P204 production is considered more

impactful on all environmental categories compared to the production of unspecified organic solvent.

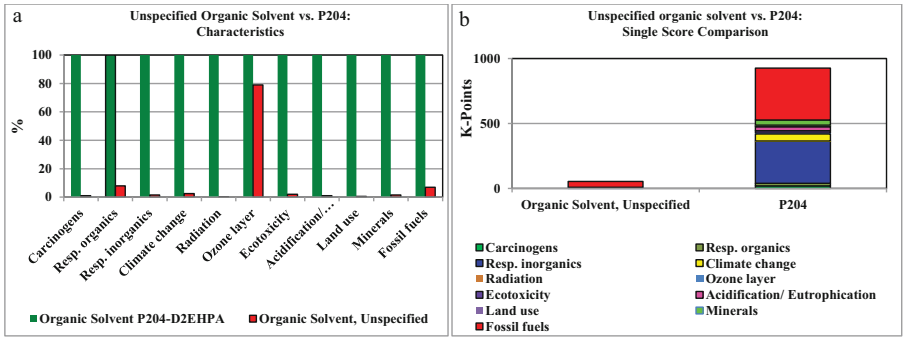

Figure 2. a) Characterization Graph for Life Cycle Comparison of unspecified organic solvent and P204; b) Single Score Graph for for Life Cycle Comparison of unspecified organic solvent and P204.

Considering the amount of toxic release inventory such as acetone, toluene, xylene, and methanol used in the production of unspecified organic solvent, the single important impact of the production of unspecified organic solvent was on ozone layer with a substantial percentage of about 80%. The results confirm previous findings about the contribution of unspecified organic solvent production to the depletion of the protective ozone layer in the stratosphere (Sivasakthivel and Reddy, 2011; Sultana et al., 2015). Figure 2b represents the single scores comparison between unspecified organic solvent and P204. The single score is calculated as the weighted average of each environmental category over all the other categories. The build-up of the P204 production comprised environmental categories such as respiratory inorganics and fossil fuels. The production of unspecified organic solvent had no significant effect on different environmental impacts but fossil fuel can be reported as the single important category influenced by the production of unspecified organic solvent.

LCA results for REE solvent extraction process using P204

The characterization results of solvent extraction to process rare earth elements are shown in Figure 3. The figure represents the impact of all different input materials/energy in solvent extraction process on various environmental categories and they are relatively expressed with regard to the highest value. The hydrochloric acid and coal have the maximum impact on most categories as is evident from the graph. One potential reason for this could be the fact that both hydrochloric acid and coal require large amount of energy and material input during their production stages and significant environmental emission is generated after utilizing the mentioned materials in solvent extraction. To conclude, the results in figure 3 reveal the significant contribution of hydrochloric acid, coal, P204, and ammonium carbonate on most environmental categories. For instance, coal (42%), and hydrochloric acid (20%) were followed by the P204 (18%) and ammonium carbonate (15%) were found to have significant impact on climate change. Since the amount of Alamine 336, 2-Ethylhexanol and naphthenic acid utilized in the solvent extraction process were very low compared to other materials, their environmental impact were almost negligible. In addition, according to Table 1 and figure 3, although the rate

of sulfonated kerosene consumption is as twice as P204 in the process, the impact of P204 as organic extractant is much higher than sulfonated kerosene.

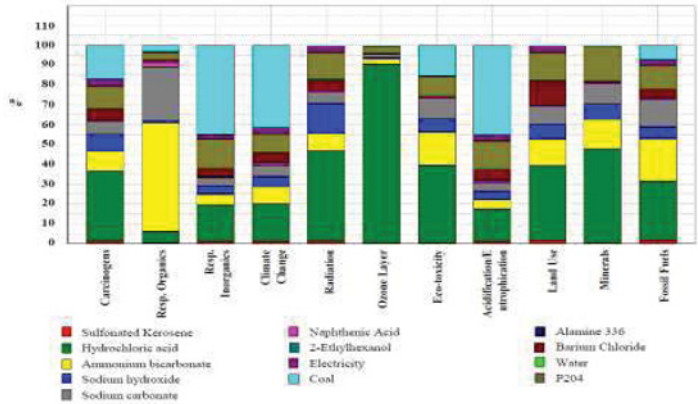

Figure 3. Characterization Graph for Life Cycle analysis REE solvent extraction using P204 in Baotou, China.

Conclusion

The life cycle analysis of solvent extraction of rare earth elements has not thoroughly been described in the previous studies and findings in this investigation greatly improve our knowledge about environmental impacts of REEs solvent extraction process and enables us to design new sustainable treatment processes to answer the growing demand for rare earth metals and environmental performance of solvent extraction processes will be improved more effectively. According to the results, compared to the production of unspecified organic solvent which has been used in the software by previous investigators, P204 production is considered more impactful on all environmental categories. However, the single important impact of the production of unspecified organic solvent was on ozone layer with a substantial percentage of about 80%.

Since the production of unspecified organic solvent had no significant effect on different environmental impacts, the build-up of the P204 production comprised environmental categories such as respiratory inorganics and fossil fuels. Based on the results from LCA study on the solvent extraction process, hydrochloric acid, coal, P204, and ammonium carbonate have significant impacts on most environmental categories. For instance, coal (42%), and hydrochloric acid (20%) were followed by the P204 (18%) and ammonium carbonate (15%) were found to have significant impact on climate change. Moreover, the amount of Alamine 336, 2-Ethylhexanol and naphthenic acid were very low in the solvent extraction process compared to other materials and therefore, their environmental impacts were almost negligible as regards impact on the environment was concerned. Also, in spite of higher rate of sulfonated kerosene consumption compared to P204 in the solvent extraction process, the impact of P204 as organic extractant is much higher than sulfonated kerosene. The large amounts of high-purity solvents which are highly expensive is the most important disadvantage of solvent extraction processes and since organic extractants are usually toxic, the solvent extraction process results in the production of hazardous waste. Thus, the major challenge in solvent extraction process development is finding a more sustainable and affordable solvent.

References

Castor, S.B., & Hedrick, J.B. (2006). Rare earth elements. Industrial minerals volume, 7th edition: Society for mining, metallurgy, and exploration, Littleton, Colorado, 769-792.

Chakhmouradian, A. R., & Wall, F. (2012). Rare earth elements: minerals, mines, magnets (and more). Elements, 8(5), 333-340.

Chu, S., & Majumdar, A. (2012). Opportunities and challenges for a sustainable energy future. nature, 488(7411), 294-303.

Eggert, R.G., Carpenter, A.S., Freiman, S.W., Graedel, T.E., Meyer, D.A., McNulty, T.P., Moudgil, B.M., Poulton, M.M., & Surges, L.J. (2008). Minerals, critical minerals and the US economy. National Research Council (US).

Evans, A., Strezov, V., & Evans, T. J. (2009). Assessment of sustainability indicators for renewable energy technologies. Renewable and sustainable energy reviews, 13(5), 1082-1088.

Fouquet, Y., & Martel-Jantin, B. (2014). Rare and strategic metals. In Deep Marine Mineral Resources (pp. 55-64). Springer Netherlands.

Fuerstenau, D. W. (2013). Design and development of novel flotation reagents for the beneficiation of Mountain Pass rare-earth ore. Minerals & Metallurgical Processing Journal, 30(1), 1-9.

Golev, A., Scott, M., Erskine, P.D., Ali, S.H., & Ballantyne, G.R. (2014). Rare earths supply chains: Current status, constraints and opportunities. Resources Policy, 41, 52-59.

Grasso, V. B. (2013, September). Rare earth elements in national defense: background, oversight issues, and options for Congress. LIBRARY OF CONGRESS WASHINGTON DC CONGRESSIONAL RESEARCH SERVICE.

Haque, N., Hughes, A., Lim, S., & Vernon, C. (2014). Rare earth elements: Overview of mining, mineralogy, uses, sustainability and environmental impact. Resources, 3(4), 614-635.

Humphries, M. (2012). Rare earth elements: the global supply chain. Congressional Research Service, 7-5700.

Navarro, J., & Zhao, F. (2014). Life-Cycle Assessment of the Production of Rare-Earth Elements for Energy Applications: A Review. Frontiers in Energy Research, 2, 45.

Ness, B., Urbel-Piirsalu, E., Anderberg, S., & Olsson, L. (2007). Categorising tools for sustainability assessment. Ecological economics, 60(3), 498-508.

Pothen, F. (2013). Dynamic Market Power in an Exhaustible Resource Industry. The Case of Rare Earth Elements. The Case of Rare Earth Elements (December 19, 2013). ZEW-Centre for European Economic Research Discussion Paper, (14-005).

Preez, A. D., & S Preston, J. (1992). The solvent extraction of rare-earth metals by carboxylic acids. Solvent Extraction and Ion Exchange, 10(2), 207-230.

Siekierski, S., & Fedelis, I. (1978). Extraction chromatography of lanthanides. In Extraction chromatography.

Sivasakthivel, T., & Reddy, K. S. K. (2011). Ozone layer depletion and its effects: a review. International Journal of Environmental Science and Development, 2(1), 30.

Sultana, S., Vandenbroucke, A. M., Leys, C., De Geyter, N., & Morent, R. (2015). Abatement of VOCs with Alternate Adsorption and Plasma-Assisted Regeneration: A Review. Catalysts, 5(2), 718-746.

Vander Hoogerstraete, T., Wellens, S., Verachtert, K., & Binnemans, K. (2013). Removal of transition metals from rare earths by solvent extraction with an undiluted phosphonium ionic liquid: separations relevant to rare-earth magnet recycling. Green Chemistry, 15(4), 919-927.

Wang, L., Long, Z., Huang, X., Yu, Y., Cui, D., & Zhang, G. (2010). Recovery of rare earths from wet-process phosphoric acid. Hydrometallurgy, 101(1), 41-47.
Yang, D., Kang, X., Dai, Y., Hou, Z., Cheng, Z., Li, C., & Lin, J. (2013). Hollow structured upconversion luminescent NaYF 4: Yb 3+, Er 3+ nanospheres for cell imaging and targeted anti-cancer drug delivery. Biomaterials, 34(5), 1601-1612.
Zhang, S. (2013). Problems and countermeasures of rare earth industry in China. Canadian Social Science, 9(3), 9-14.

REWAS 2016: Towards Materials Resource Sustainability
Edited by: Randolph E. Kirchain, Bart Blanpain, Christina Meskers, Elsa Olivetti, Diran Apelian, John Howarter, Anne Kvithyld, Brajendra Mishra, Neale R. Neelameggham, and Jeff Spangenberger
TMS (The Minerals, Metals & Materials Society), 2016

CHARACTERISTICS OF LIGHT RARE EARTHS FROM KOREAN COAL POWER PLANTS ASH

T. Thriveni[1], Ahn Ji Whan[2]*

[1,2]Mineral Resources Research Division, Korea Institute of Geosciences and Mineral Resources, 124Gwahagno, Gajeong-dong, Yuseong-gu, Daejeon 305-350, Republic of Korea.

Keywords: Light rare earth elements (Nd), recovery, Characteristics, CO_2 sequestration, CO2 utilization

Abstract

We reported the possibilities of controlling the critical rare metals crisis existed for several years. Currently, critical rare metals are highly demanded and growing fast in green technologies. Recycling of mineral waste sources for the recovery of critical rare metals are one of the alternative resources for this critical rare metals crisis. Various mineral waste sources such as mine residues and coal ash are rich sources of rare earth elements. This study sought to identify the information needed to determine whether there might be a potential for commercial extraction of the rare earth elements (Nd, Dy) from coal power plants ash. The aim of this study was to recovery and characterize the light rare earth metals from Korean coal power plants ash and simultaneous utilization of CO_2. Accelerated carbonation was a more suitable process for CO_2 capture and simultaneous utilization of this CO_2 for the manufacturing of "green cement" (Calcium Sulfo Aluminate) from coal power plants ash.

Introduction

Basically, rare earth elements are divided into two categories i) light rare earths and, ii) heavy rare earths [1](Fig. 1]. Among these rare earths, light rare earths have seen wide applications in several industries and are considered to be the most critical strategic elements. Over the past decade, the demand for rare earth elements has significantly increased and they are essential for emerging technologies such as clean tech industry, green energy, military, defense, navy and aerospace[2]. China currently produces 95% of world rare earth elements. As a result of Chinese government restrictions and cost of rare earth imports major countries have been finding alternative sources of rare earth elements [3, 4]. Currently, the global rare earths supply and demand is presented in the figure 2 and particularly light rare earths supply and demand reached 30 ~ 35,000 tons per anum in 2015(Table 1)[5].

Coal is an important resource that accounts for 29.9% of global primary energy. Coal produces 41% of all electricity around the world and is used in 70% of steel production globally [6]. Since the Fukushima Daiichi nuclear power plant disaster in Japan, the global trend has been shifting away from the construction of new nuclear power plants [7]. Combined with increased electricity demand and advancements in electrical generation technology, the abundant supply of coal reserves and its low cost have led to a rise in coal demand [8]. Looking at total global coal production by year, coal consumption rose from 4677Mt in 1990 to 7608 Mt in 2011, and to 7830Mt in 2012[9].

Along with this trend, coal ash dumping is becoming a serious problem in countries around the world. The U.S. produces over 92 Mt of coal ash annually, 40% of which is recycled in various applications while the other 60% goes into storage or to disposal sites, leading to environmental issues[10].

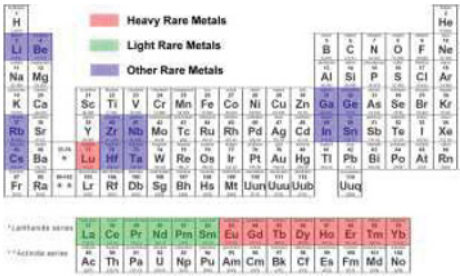

Figure 1. light rare earths in the periodic table

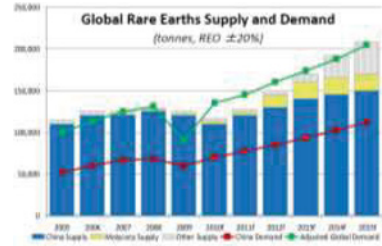

Fig.2. Global rare earths supply and demand from 2005-2015.

Rare Earth Oxide	Demand	Supply
Cerium	60-65,000t REO	75-80,000t REO
Neodymium	30-35,000t REO	30-35,000t REO
Europium	700-800t REO	500-600t REO
Terbium	450-550t REO	350-400t REO

Table 1. Light rare earths demand and supply

Raw coal used in coal-fired power plants, which largely determine the composition and properties of coal combustion products, contains about 120 different minerals. Typical materials found in coal ash include arsenic (As), lead (Pb), mercury (Hg), cadmium (Cd), chrome (Cr), selenium (Se), aluminum (Al), antimony (Sb), barium (Ba), beryllium (Be), boron (B), chlorine (Cl), cobalt (Co), manganese (Mn), molybdenum (Mo), nickel (Ni), thallium (Tl), vanadium (V), and zinc (Zn)[11].

Overview of the coal fired power plants Situation and Coash Production in South Korea

South Korea total primary energy consumption by fuel type, 2014 and coal imports from overseas presented in Figure 3[12]. As coal-fired power plants offer advantages in terms of lower investment costs and fuel costs as well as shorter construction periods, more Korean corporations are entering the business of coal-fired power generation. Since the restructuring of the electricity market in 2001, power companies have been working to combat increased competition by reducing the cost of raw materials, which takes up the largest proportion of costs involved in coal-fired power generation [13]. Following fuel price fluctuations in 2007 and 2008, power

companies greatly increased the proportion of low rank coal in fuel imports in order to lower costs and this has since been a continuing trend.

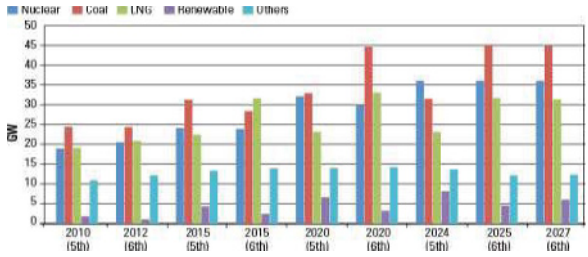

Figure 3. Coal energy consumption

In Korea, coal ash production is increasing due to increasing numbers of coal-fired power plants to meet the rapidly growing electricity demand. The rise was most pronounced in 2011. Although recycling rates are increasing steadily (Figure 4), they remain at a lower rate than other developed nations and areas of application are still limited. Thus, there is a growing trend of transition to circulating fluidized bed boilers, which are environmentally friendly boilers that produce electricity at high efficiency and low cost.

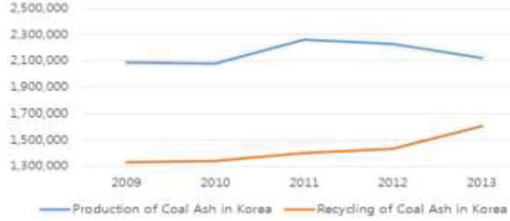

Figure 4. Production (Blue) and Recycling (Red) of Coal combustion product (Coal ash) from South-East Power Plant South Korea (unit: ton).

Experimental Methods

In order to study the heavy metal content and behavior of coal and coal ash, samples of coal (Hadong Coal), bottom ash, and fly ash from a fluidized boiler (Yeosu ash-B/A and Yeosu ash-F/A), and bottom ash from a pulverized coal boiler (Taean ash-B/A) were analyzed. Hadong coal, provided by Hadong Thermal Power Site Division of Korea Southern Power Co., Ltd., was imported from Long Daliq, Long Iram, West Kutai, East Kalimantan. Yeosu ash-B/A and Yeosu ash-F/A were provided by the Yeosu Thermal Power Site Division of Korea South-East Power Co., Ltd., which uses a fluidized bed boiler system. Taean as-B/A was supplied by the Taean Thermal Power Complex Division of Korea Western Power Co., Ltd.

An XRF analysis was conducted to determine the chemical content of each sample. The XRF analysis was commissioned to the Geoanalysis Center of the Korea Institute of Geoscience and Mineral Resources, R&D Tech-Biz Division. Test conditions were set at 24 ± 3 ℃ temperature, and 25 ± 5% R.H. humidity. The heavy metal content analysis was commissioned to the Center for Chemical Analysis at the Korea Research Institute of Chemical Technology and conducted using the ICP-AES test method. The experimental apparatus showed in Figure 5.

Figure 5. Experimental apparatus of Heavy metals leaching by carbonation method

Results and Discussion

Major and Minor Component of Coal and Coal Ash

Coal contains about 120 types of different elements, of which 33 are common, and 8 types make up the majority [11]. Results of the XRF content analysis to identify the basic components of coal are compiled in the table below.

Table 2. Major and minor chemical composition of samples by XRF (unit: wt.%)

	SiO_2	Al_2O_3	Fe_2O_3	CaO	MgO	K_2O	Na_2O	TiO_2	MnO	P_2O_5	Igloss
Hadong Coal	2.4	16.85	47.93	1067	2.44	0.11	0.23	0.6	0.77	0.04	12.42
Yeosu ash-B/A	42.51	4.55	8.51	29.62	2.84	0.4	0.72	0.22	0.11	0.1	1.85
Yeosu ash-F/A	35.05	14.04	10.52	25.65	5	0.86	0.35	0.9	0.15	0.11	3
Taean ash-B/A	57.84	20.77	9.11	4.29	1.32	1.08	0.92	1.13	0.1	0.31	3.44

The major mineral components of coal consist of quartz (SiO_2), aluminosilicates, calcite, siderite with iron content, and pyrite with sulfur content. The XRF analysis showed that Hadong coal had higher Fe_2O_3, unlike ordinary coal which has high Si and Al content. This appears to be due to the orogeny of the Central Kalimantan Range and operations of Muller Mts in Kalimantan, Indonesia[14]. Yeosu ash B/A, Yeosu ash-F/A and Taean ash-B/A are products of coal combustion in the respective power plants. Yeosu ash B/A and Yeosu ash-F/A from a fluidized bed boiler had CaO values of 29.62 wt.% and 25.65 wt.%, respectively, while Taean ash-B/A from the PC boiler had a CaO value of 4.29 wt.%, showing a much lower value than that from the fluidized bed boiler.

Rare Earths in Coal ash

Quality and Critical Elements in Coal Ash

Coal ash is rich sources of rare earth elements and extracted from coal ash by several conventional methods such as acidic extraction process, basic extraction process and Super critical CO2 system(Neumann Systems group)[15-17].

Coal ash samples were provided by Korea Southern Power. Measurement of rare earth elements in coal ash samples at Geoanalysis Center of Korea Institute of Geoscience and Mineral Resources. Rare earth elements were evaluated with alkali fusion, acid digestion, and ICP-MS.

Table 3. Rare Earth Elements concentrations in Coal Ash

Light Rare Earth Elements(μg/g)						Heavy Rare Earth Elements(μg/g)								
Y	La	Ce	Pr	Nd	Sm	Eu	Gd	Tb	Dy	Ho	Er	Tm	Yb	Lu
45	42.8	103	12.3	48.5	10.6	2.98	11.4	1.58	7.94	1.46	3.58	0.46	2.76	0.42

The results for rare earth elements in Table 3 show a high LREE concentration in coal ash. Light rare earths (LREs) namely yttrium, lanthanum, cerium, praceodymium and neodymium are primarily separated each other. The hydrometallurgical technique solvent extraction applied for the present study. Primarily the general flow sheets of this rare earths presented in the Figure 6, the effect of pH on light rare earths with the extractant Di(2-ethylhexyl)phosphoric acid(D2EHPA) presented in Figure 7 and extraction efficiency of Nd is presented in Figure 8.

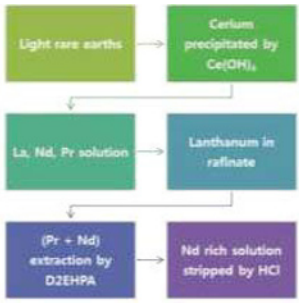

Figure 6. Flow sheet of rare earths separation

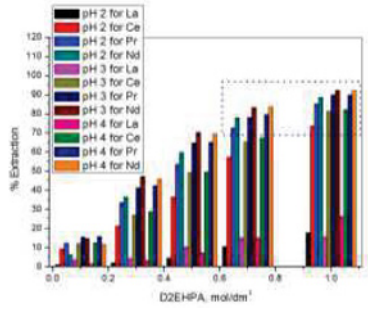

Figure 7. pH effect on light rare earths

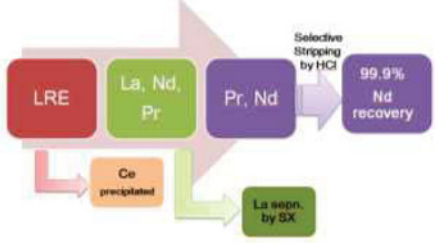

Figure 8. Extraction efficiency of Nd from coal ash

CONCLUSIONS

Globally, coal combustion waste produced from coal-fired power plants causes serious problems on the environment and human due to toxic materials. Countries all over the world endeavor to find the solution by recycling the waste or utilization of coal ash waste. In this research, we investigated chemical composition of coal and coal ash samples. We investigated the possibilities of rare earths recovery from coal ash by applying solvent extraction methods and

heavy metals were stabilized by accelerated carbonation method. We tried to extract the light rare earths and significant strategic element Nd from different coal-fired power plants ash samples in South Korea. Nd is extracted from coal ash by solvent extraction used D2EHPA extractant with select stripping by HCl with 99.9%.

Acknowledgments

This research was conducted in 2014 with support from the Energy Technology Development Project [20141010101880] of the Korea Institute of Energy Technology Evaluation and Planning, financed by the Ministry of Trade, Industry and Energy.

References

1. Ian Chalmers, " Focus on Rare Earths Projects Around the World", (Rare Earths, Speaciality and Minor Metals investment Summit, March 2010, The London Chamber of Commerce and Industry), 2010, 1-37.
2.DavidB.Mayfield, and Ari S. Lewis, "Environmental Review of Coal Ash as a Resource for Rare Earth and Strategic Elements" (paper presented at the 2013 World Coal Ash(WOCA) Conference, April 22-25, 2013 in Lexington, KY), 1-11.
3. Nabeel Mancheri, Lalitha Sundaresan, and S. Chandrasekhar, " Dominating the World China and the Rare Earth Industry", *National Institute of Advanced Studies"*, R10-2013(2013), 1-74.
4. Cindy Hurst, "China's Rare Earth Elements Industry: What Can the West Learn?", *Institute for the Analysis of Global Security(IAGS),* March 2010, 1-42.
5. Dudly J. Kingsnorth, "Rare Earth opportunities: Real or imaginary, Metal Pages rare earth Conferences, 2011, Beijing, China.
6. Coal Facts 2013, *World Coal Association*, 9 (2013), 1-4.
7. Fukushima Accident-updated by 2014', World Nuclear Association,http://www.world-nuclear.org/info/Safety-and-Security/Safety-of-Plants/Fukushima-Accident.
8. Gukjin Bae, Outlook of Coal-fired power plant market - Necessity enlargement of High efficiency and low pollution technology of coal, " KISTI Market Report", 3(6)(2014), 15- 19.
9. The 6th Basic Plan for Electricity Supply and Demand, The Ministry of Knowledge Economy (2013~2027), 2(2013), 22-23.
10. Coal Ash: Characteristics, Management and Environmental Issues, Technical Update-Coal Combustion Products-Environmental Issues, Electric Power Research Institute, 9(2009), 1-12.
11. Barbara Gottlieb, Steven G. Gilbert, PhD, DABT and Lisa Gollin Evans, "Coal Ash: The toxic threat to our health and environment" *A Report from Physicians for Social Responsibility and Earthjustice*, (2010), 1-27.
12. South Korea International Energy Data and Analysis, U.S. Energy Information Administration, 2015.
13. Sehyun Baek, Hoyoung Park and SungHo Ko, "Economic Evaluation of Coals Imported in Last 3 Years for Power Plant Based on Thermal Performance Analysis", *J. Korean Soc. Combust.*, 18(3)(2013),44-53.
14. Sri Widodo et al., "Distribution of sulfur and pyrite in coal seams from Kutai Basin (East Kalimantan, Indonesia): Implications for Paleoenvironmental conditions", *International Journal of Coal Geology*, 81(2010),151-162.
15. J.C.Hower, S.Dai, V.V.Seredin, L.Zhao, I.Kostova, Luis F.O.Silva, S.M.Mardon, G.Gurdal, " A Note on Occurrence of Yttrium and Rare Eearth Elements in Coal Combustion Products",

Coal Combustion and Gasification Products, 5(2013), 39-47.
16. Prakash B. Joshi, "Recovery of Rare Earth Elements and Compounds from Coal Ash", US 20130287653A1, October 31, 2013.
17. Vladimir V. Seredin, Shifeng Dai, Yuzhuang Sun, Igor Yu. Chekryzhov, " Coal Deposits as Promising Sources of Rare Earth Metals for Alternative Power and Energy Efficient Technologies", *Applied Geochemistry,*31(2013),1-11.

Enabling & Understanding Sustainability - Building Materials & Slag Valorization

REWAS 2016: Towards Materials Resource Sustainability
Edited by: Randolph E. Kirchain, Bart Blanpain, Christina Meskers, Elsa Olivetti, Diran Apelian, John Howarter, Anne Kvithyld, Brajendra Mishra, Neale R. Neelameggham, and Jeff Spangenberger
TMS (The Minerals, Metals & Materials Society), 2016

ENERGY GENERATION FROM WASTE SLAGS: BEYOND HEAT RECOVERY

Jinichiro Nakano[1,2], James Bennett[1], Anna Nakano[1]

[1] U.S. Department of Energy National Energy Technology Laboratory; 1450 Queen Ave.; Albany, OR 97321, USA
[2] AECOM; P.O. Box 1959; Albany, OR 97321, USA

Keywords: slag utilization, iron and steelmaking, gasification, CO_2, CO, H_2O, H_2

Abstract

In this study, metallurgical and gasification slags mixed at a specific composition were heated to a slag discharge temperature range (*i.e.*, tap out temperatures in iron & steelmaking) in the presence of CO_2, resulting in a reaction generating energy – enough to convert CO_2 to CO which can be used in other processes such as ore reduction, gas turbine power generation, and synthetic liquid/gaseous fuel production. Computational simulations suggested that the generation of H_2 from H_2O would also be possible using the same mixed slag approach at no additional heat supply. Energy generated from the reaction remains largely in excess after conversion (CO_2 to CO), which can be utilized independently for or support other processes. Furthermore, a final slag volume is expected to decrease to about 30%, dramatically decreasing landfill burden.

Introduction

Iron & steelmaking and slagging gasification processes utilize carbon feedstock such as coal and petroleum coke (petcoke) in production of metal, power, and/or chemicals; but also generate large quantities of gas (high in CO_2) and slag as waste byproducts. In the course of processing, slag forms as molten agglomerates from non-volatile components in feedstock, additives, and/or metal ores' impurities. For every ton of hot metal (iron) production, 1.5 tons of CO_2 is emitted while additional 0.9 tons of CO_2 per ton of steel produced is generated from subsequent steelmaking processes [1]. Reportedly, approximately 523 million tons of slag is annually generated from the iron & steelmaking industry worldwide [2] and less than 65 wt.% is utilized for recovering valuable elements [3]. In the gasification industry, for example, a 500 megawatts (thermal) slagging gasifier used for power/chemical generation operating at a 35% efficiency would need 3,800 tons petcoke carbon feedstock per day, producing approximately 38 tons/day of slag. Currently in the world, gasifiers worth 174 gigawatts (thermal) are being built for 2016 and planned for 2019 [4], including Jamnagar Gasification Plant in India with 9.8 gigawatts (thermal) syngas output [5]. With the existing plants worldwide, gasifiers worth a total of 310 gigawatts (thermal) would be in operation by 2019 [4], generating up to 23,560 tons petcoke slag every day worldwide, depending on the petcoke usage.

Typical iron & steelmaking slags are rich in calcium oxide while petcoke slags from gasification are rich in vanadium oxide as shown in Figure 1 where literature data [2, 6-10] were graphically summarized. Up to 60 wt.% CaO in steelmaking slag and up to 74.5 wt.% V_2O_5 in petcoke ash were reported. Due to strong chemical affinity of calcium oxide to vanadium oxide when reacted

under certain conditions, the presence of calcium influences valence of vanadium and changes it from 3+ to 5+, forming calcium orthovanadate ($3CaO{\cdot}V_2O_5$). The vanadate formation occurs by removing oxygen from the surrounding in the system, following the fundamental reaction:

$$3CaO + V_2O_3 + 2[(CO_2)_x + (H_2O)_{1-x}] \rightarrow (CaO)_3(V_2O_5) + 2[(CO)_x + (H_2)_{1-x}] + \text{heat} \qquad (1)$$

Excess heat generated from the reaction ranges from 104 kJ to 163 kJ per mole of calcium vanadate at 1573 K [11], depending on x (x = 0 – 1). The transformation is, thus, highly exothermic and expected to be capable of breaking down carbon dioxide and/or water molecules into carbon monoxide and/or hydrogen, respectively. In this work, in-situ experiments were conducted on a synthetic slag mixture based on calcium rich metallurgical slag and vanadium rich petcoke slag to investigate potential fuel production from waste gas stream containing CO_2.

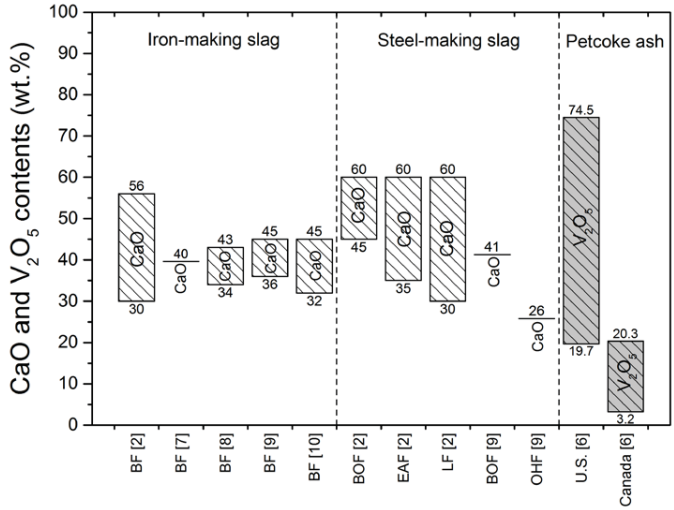

Figure 1: Availability of calcium oxide in metallurgical slags and vanadium oxide in petcoke ash. Shaded bars indicate ranges found while horizontal lines indicate single data points. Note vanadium content is typically reported as V_2O_5 but exists as V_2O_3 in gasification slag. (BF = blast furnace, BOF = basic oxygen furnace, EAF = electric arc furnace, LF = ladle furnace, OHF = open hearth furnace)

Experimental

10 g of synthetic slag of $8.2Al_2O_3$-$24.7CaO$-$8.2Fe_2O_3$-$1.6SiO_2$-$57.3V_2O_3$ (by weight) in a high density alumina boat was heated from room temperature to 1773 K at 150 K/hr in a closed alumina tube. The slag composition was determined based on mixing of a metallurgical slag (Ca-rich) and gasification petcoke ash (V-rich) to maximize the CO_2-to-CO (or H_2O-to-H_2) gas conversion and to promote the slag to melt. The atmosphere in the furnace tube was designed to be saturated with CO_2 by using 0.07 g of carbon powder to react with oxygen present in the sealed air during the heating stage. The carbon quantity was determined so that no elemental

carbon would remain from the reaction. The electromotive force (EMF) inside an yttria-stabilized zirconia oxygen sensor ($SIRO_2$® - Ceramic Oxide Fabricators, Australia) was continuously measured, which was converted to oxygen partial pressure. An experimental error of the oxygen sensor was reported to be < ± 0.2 log units between 1273 and 1773 K for 10^{-5} – 10^5 Pa [12]. Concentrations of CO and CO_2 in the atmosphere in the tube were determined by thermodynamic computational software, FactSage 6.4 with FactPS and FToxid databases [13] based on the empirical oxygen potentials. Note that due to a lack of a slag database containing vanadium oxide in FactSage, V_2O_3 solubility in the slag was assumed to be negligible. Creation of a database for slag containing vanadium is currently underway [6, 14]. The test was performed a second time for reproducibility, and was conducted with and without the slag to ensure no effect of carbon on oxygen potentials during CO_2 conversion.

Results and Discussion

EMF measurements for the CO_2 saturated atmosphere sealed inside the reaction tube during the tests are presented in Figure 2. Time in the figure was adjusted for simplification purposes (*i.e.*, 1500 K starts at 0 min). The EMF without the slag (test 0) remained relatively constant between 1373 and 1773 K, with an average oxygen partial pressure of 5×10^3 Pa. This agrees with a theoretical value of 2×10^3 Pa determined by FastSage. Rapid increases in the EMF at approximately 55 min in Figure 2 c) correspond to sudden drops in the oxygen partial pressure caused by the slag interacting with CO_2 being converted to CO. First derivatives of the EMF with respect to time ($dEMF/dt$) for tests 1 and 2 are shown in Figure 2 d). The CO_2-to-CO conversion was rapidly initiated at 1695 – 1703 K, and the majority of the reaction was completed within 5 min. A minimal decrease in the oxygen partial pressure (*i.e.*, increase in EMF) was noted after the rapid conversions. The oxygen partial pressure determined from the EMF reached near-asymptotes of 2×10^{-5} – 5×10^{-5} Pa as heating continued. The result indicated a CO_2 conversion rate of 97% (to CO). The formation of $(CaO)_3V_2O_5$ was confirmed by X-ray diffraction analysis (Rigaku Ultima IV) on the quenched slag, implying the CO_2-to-CO conversion was triggered by the vanadate formation (involving a valence change from V^{3+} to V^{5+}).

Computational thermodynamic simulations by FactSage suggested that if the same slag methodology is applied to water instead of carbon dioxide, H_2 would be produced following reaction (1). An oxygen atom is stripped off from a H_2O molecule when CaO and V_2O_3 react to form $(CaO)_3(V_2O_5)$, leaving H_2 as a byproduct. Theoretically, up to 1 ton of H_2 gas would be generated from the reaction with slag containing 4.2 tons of V_2O_3. Because H_2 is generated from the highly exothermic reaction, the H_2 conversion rate would be significantly greater than that from the traditional thermal dissociation routes where heat is supplied by recovering from the discharged slag in iron and steelmaking.

When the calcium vanadate forms in the molten slag, the density of the bulk slag increases from 1.12 g/cm^3 [15] to 3.96 g/cm^3 [16], which in turn decreases the slag volume to approximately 30 % of the original volume per unit mass. The volume reduction of the final slag would help conserve landfill sites as required for the current slag disposal in industries.

A larger scale test to examine the practicality of the process is underway. The effect of preparation and chemistry modification of slags, as well as timing of mixing the two slags will be investigated to maximize the generation of heat and syngas (H_2 and CO).

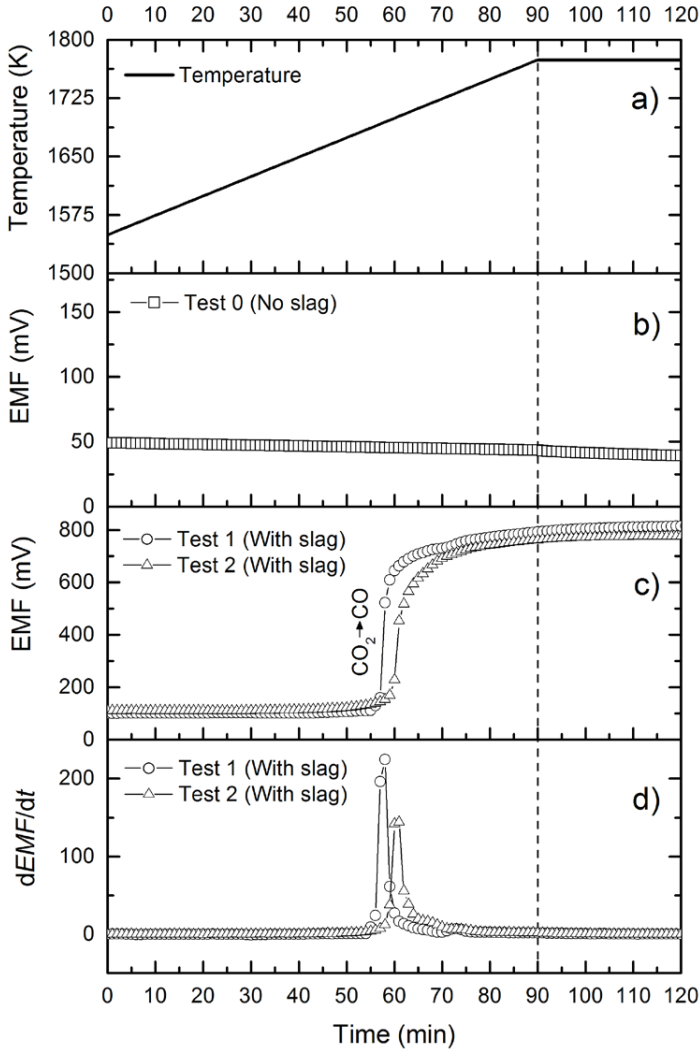

Figure 2: In-situ measurements of a) temperature inside the tube and EMF of b) without the present slag, c) first and second tests with the present slag mixture, and d) the first derivative of the EMF (d*EMF*/d*t*) of first and second tests.

Conclusion

Synthetic iron & steelmaking and gasification slags mixed at a specific composition were heated at a slag discharge temperature range in the presence of CO_2, resulting in production of CO due to the formation of calcium orthovanadate. Computational simulations suggested that H_2 would be generated from H_2O using same mixed slag approach. The final slag volume would decrease to about 30% of the original volume, lightening burden imposed on landfill sites. The present research result would suggest a potential approach to reduce current environmental loads while commercially benefitting metallurgical and gasification industries.

Acknowledgement

This research was supported in part by an appointment to the National Energy Technology Laboratory Research Participation Program, sponsored by the U.S. Department of Energy and administered by the Oak Ridge Institute for Science and Education.

References

[1] Fruehan RJ. Research on Sustainable Steelmaking. Metall Mater Trans B. 2009;40:123-33.
[2] Barati M, Esfahani S, Utigard TA. Energy recovery from high temperature slags. Energy. 2011;36:5440-9.
[3] Semykina A, Shatokha V, Iwase M, Seetharaman S. Kinetics of Oxidation of Divalent Iron to Trivalent State in Liquid FeO-CaO-SiO_2 Slags. Metall Mater Trans B. 2010;41:1230-9.
[4] U.S. Department of Energy National Energy Technology Laboratory. Gasifipedia. http://www.netl.doe.gov/File%20Library/Research/Coal/energy%20systems/gasification/gasifipedia/index.html.
[5] Gasification Technology Council. World Gasification Database. http://www.gasification.org/.
[6] Nakano J, Duchesne M, Bennett J, Kwong K-S, Nakano A, Hughes R. Thermodynamic effects of calcium and iron oxides on crystal phase formation in synthetic gasifier slags containing from 0 to 27 wt.% V_2O_3. Fuel (doi:101016/jfuel201411008). 2014.
[7] Gan L, Zhang C, Shangguan F, Li X. A Differential Scanning Calorimetry Method for Construction of Continuous Cooling Transformation Diagram of Blast Furnace Slag. Metall Mater Trans B. 2012;43:460-7.
[8] Mineral Aggregate Conservation Reuse and Recycling. Report for Aggregate and Petroleum Resources Section, Ontario Ministry of Natural Resources prepared by John Emery Geotechnical Engineering Limited1992.
[9] Emery J. Steel slag utilization in asphalt mixes. National Slag Association MF186-1. 1984:1-11.
[10] Lewis DW. Properties and uses of iron and steel slags. National Slag Association MF182-6. 1992:1-11.
[11] Nakano J, Bennett J. CO_2 and H_2O gas conversion into CO and H_2 using highly exothermic reactions induced by mixed industrial slags. Int J Hydrogen Energ. 2014;39:4954-8.
[12] Mendybaev RA, Beckett JR, Stolper E, Grossman L. Measurement of oxygen fugacities under reducing conditions: Non-Nernstian behavior of Y_2O_3-doped zirconia oxygen sensors. Geochim Cosmochim Ac. 1998;62:3131-9.

[13] Bale CW, Belisle E, Chartrand P, Decterov SA, Eriksson G, Hack K, et al. FactSage thermochemical software and databases - recent developments. Calphad. 2009;33:295-311.
[14] Nakano J, Kwong KS, Bennett J, Lam T, Fernandez L, Komolwit P, et al. Phase Equilibria in Synthetic Coal-Petcoke Slags (SiO_2-Al_2O_3-FeO-CaO-V_2O_3) under Simulated Gasification Conditions. Energ Fuel. 2011;25:3298-306.
[15] Officials AAoSHaT. Standard Specification for Materials, "Blended Hydraulic Cements". 14th ed1986.
[16] Tashtoush N, Qudah AM, El-Desoky MM. Compositional dependence of the electrical conductivity of calcium vanadate glassy semiconductors. J Phys Chem Solids. 2007;68:1926-32.

Disclaimer

REWAS 2016: Towards Materials Resource Sustainability
Edited by: Randolph E. Kirchain, Bart Blanpain, Christina Meskers, Elsa Olivetti, Diran Apelian, John Howarter, Anne Kvithyld, Brajendra Mishra, Neale R. Neelameggham, and Jeff Spangenberger
TMS (The Minerals, Metals & Materials Society), 2016

PRODUCTION OF LIGHTWEIGHT AGGREGATE AND CERAMIC BALLS USING GOLD TAILINGS, RED MUD AND LIMESTONE

Hyunsik Park, Soo-kyung Kim, Doyun Shin, Jeong-soo Sohn

Urban Mine Department, Mineral Resources Research Division,
Korea Institute of Geoscience and Mineral Resources (KIGAM),
124, Gwahak-ro Yuseong-gu, Daejeon, 34132, South Korea

Keywords: Lightweight aggregate, gold tailing, red mud, limestone, sinter, atomizing

Abstract

Lightweight aggregate and ceramic balls were produced from a mixture of gold tailings, red mud and limestone by using a high temperature process. Raw materials were quantitatively analyzed and hazardous materials content was checked by chemical analysis. Oxide systems for the lightweight aggregate and ceramic balls were chosen based on the CaO-FeO_t-Al_2O_3-SiO_2 quaternary system. Sintering, softening and melting behavior of the samples were investigated to optimize the sintering conditions. Phase change during sintering was observed by X-ray diffraction. Microscopic analysis by SEM / EDS was carried out to check the morphological changes of the samples.

Introduction

Mining waste consisting of waste rock and tailings accounts for a hundred times more weight than the corresponding ore concentrates. Most of mine waste management is in fact a method of preservation and minimization of chemical spills from the impoundments.[1] A large quantity of gold tailings produced by floatation is usually landfilled and may cause environmental problems. Tailing heaps, ponds and dams are typical storage facilities that are vulnerable to acid drainage and release of toxic metals. Meanwhile, a huge quantity of waste limestone is generated from limestone mines as by-product. This low quality material does not have any practical value for the cement industry because of its low calcite content. Bauxite residue (red mud) is produced by the alumina / aluminum industry. Current bauxite residue reached an estimated 2.7 billion tons in 2007 and is increasing by 120 million tons per annum.[2, 3] Environmental concerns always remain because of the heavy metals and radioactive elements concentrated in the red mud. However, it is difficult to use mining wastes and mineral process residues as construction materials, owing to the physicochemical requirements of the end products. In the present study, the authors investigated a method for lightweight aggregate and ceramic ball production from gold tailings, using red mud and waste limestone as fluxes. Raw materials were quantitatively analyzed, then the composition of the mixture was decided by thermodynamic calculation. The quaternary oxide system CaO-FeO_t-Al_2O_3-SiO_2 was used as basis. The mixing ratio between gold tailings, red mud and limestone was determined anticipating the composition of the end product. High temperature treatment was conducted at temperatures between 1050°C (1323K) and 1250°C (1523K). Specimens were analyzed after the experiments to investigate the effect of temperature. Morphological study using SEM / EDX supported the verification of the sintering mechanism.

Experimental Procedures

X-Ray Fluorescence Spectrometers (XRF-1800, Shimadzu) was used for the quantitative analysis of raw materials. The compositions of gold tailing, red mud and limestone are shown in **Table I**.

Table I. Quantitative analysis of raw materials by X-ray fluorescence analyzer

Composition (wt%)	Gold tailing (GT)	Red mud (RM)	Limestone (LS)
SiO_2	**87.9**	12.9	12.8
Al_2O_3	6.0	**25.4**	2.5
Fe_2O_3	1.1	**31.6**	1.4
CaO	0.1	4.7	**43.3**
MgO	0.2	-	2.9
Na_2O	-	8.9	-
K_2O	1.3	-	1.3
TiO_2	0.2	7.0	0.4
Ig. loss	3.2	9.5	35.4

Phase analysis of the raw materials was carried out by powder X-ray diffractometer (D/Max 2200, Rigaku). It is observed that quartz is the main phase in gold tailings. The hematite phase was dominant in the red mud. Limestone was mostly comprised of calcite. Chemical analysis by ICP-OES (ICAP 6500, Thermo Fisher Scientific) was carried out to evaluate the heavy metals which are possibly contained in the raw materials. The potential hazardous elements were far below the regulations for construction materials. Thus, the risks of heavy metals were not considered in the present study. In **Figure 1**, a schematic of a pyrometallurgical process for gold tailings is described. There are two different concepts in manufacturing of ceramic products depending on process temperature. Below 1200^{o}C (1473K), lightweight aggregate is obtained by sintering. This low temperature treatment is advantageous in terms of energy efficiency and easiness of process control. In contrast, melting and atomizing process to make fine ceramic ball needs to be done above 1200^{o}C (1473K).

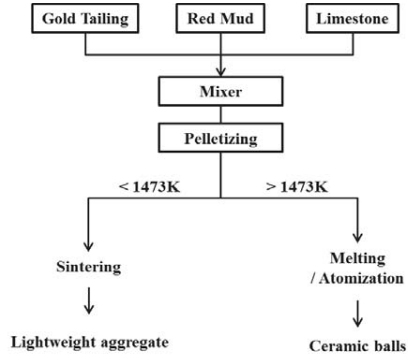

Fig.1. A schematic of pyrometallurgical gold tailing's treatment process

Figure 2 shows the liquid line of 1573K in CaO-10FeO_t-Al_2O_3-SiO_2 ternary phase diagram.[6] In conventional brick or aggregate production, sintering takes place below 1573K. Thus, the area colored with grey is available for the process of the current raw materials combination. The composition pointed by black dot was selected to take advantage of the eutectic triple point that has the lowest melting temperature.

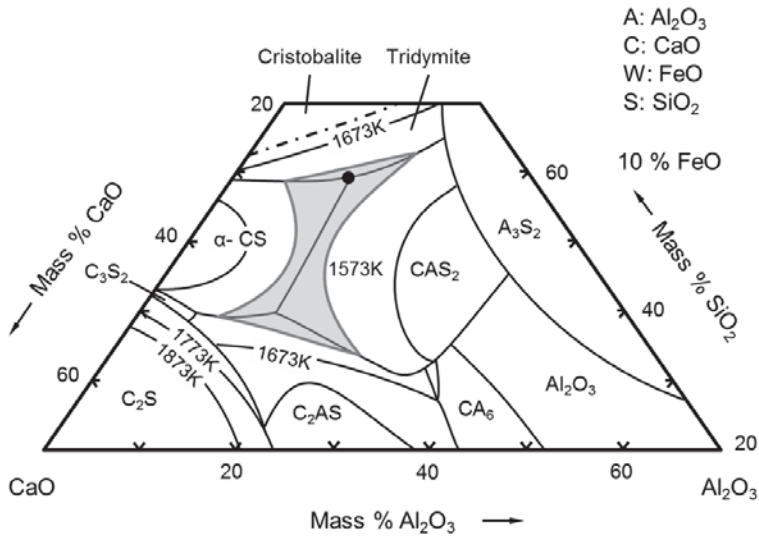

Fig.2. Selected composition for lightweight aggregate (●) and liquidus line of 1573K shown at CaO–10FeO_t–Al_2O_3–SiO_2 ternary oxide system

The ratio of gold tailing 2 / red mud 1 / limestone 1 was selected that showed the best match with the composition in **Figure 2**. The composition in **Table I** was used as weight percentage. The moisture contents and ignition loss by calcination was excluded in calculations. In **Table II**, the composition of mixture pellets prepared for lightweight aggregate production is shown. Silica content is slightly lower than the composition in **Figure 2,** but other components show similar values. For sample preparation, gold tailing, red mud and limestone in powder type sized under 100μm were mixed and pelletized. Spherical pellets sized at 10mm diameter were prepared by hand rolling with drops of purified water. Samples were dried at 200°C (473K) for 48 hours to eliminate residual moistures.

Prepared pellets were arranged in alumina crucibles and the crucibles were inserted into a box furnace with SiC heating elements. Sintering temperature was varied from 1050°C (1323K) to 1250°C (1523K) to optimize the high temperature process. The experiment was conducted in air for 30 minutes to prevent excess heat treatment.

Table II. Composition of pellets for lightweight aggregate production
(Mixing ratio of GT 2 : RM 1 : LS 1)

Composition (wt%)	SiO_2	Al_2O_3	Fe_2O_3	CaO	MgO	Na_2O	K_2O	TiO_2
Lightweight aggregate	**54.3**	**11.1**	**9.7**	**18.4**	1.1	2.4	1.1	2.0

A powder X-ray diffractometer (D/Max 2200, Rigaku) was used to investigate phase changes of the samples. X-Ray patterns were recorded. Specimens treated at different temperatures show different peak arrangements indicating significant phase transformations. The measurement procedure was identical to the case of the raw materials. A scanning electron microscope (JSM-6380LA, JEOL) equipped with energy dispersive X-ray analysis (EDX) was used to analyze the microstructure of the specimen. In each sample, oxide phases at several spots were analyzed by EDX at 1,000 times magnification, with particular focus on the variation of phase change of silica, hematite and lime.

Results and Discussion

Sintering, softening and melting behavior of the pellet were investigated to find the optimum sintering temperature. A temperature ranging from 1050°C (1323K) to 1250°C (1523K) was selected to simulate the conventional lightweight aggregate firing process. In **Figure 3**, pellets quenched after high temperature treatment are shown. The color gets dark and particles adhere tightly as the temperature increases until 1100°C (1373K). Sold state sintering occurs below 1100°C (1373K) producing more physical contacts. The pellet softened and half melted at 1150°C (1423K). The surface became lustrous at this temperature due to glassy phase. The pellet melts further at 1200°C (1473K) and becomes complete molten at 1250°C (1523K). It is considered that keeping the temperature at 1150°C (1423K) is imperative to make intact lightweight aggregates.

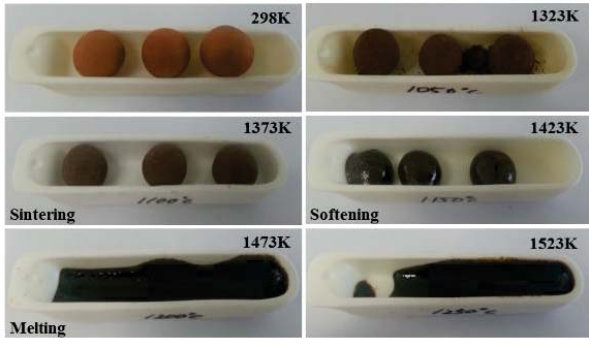

Fig.3. Shape change of samples depending on temperature

From the X-ray diffraction patterns, dominant phases could be determined at each temperature. Changes in the major peaks as a function of temperature are seen in **Figure 4**. The green pellet at 25°C (298K) has quartz, hematite and calcite as it is a simple mixture of three raw materials. Calcite decomposes at 897°C (1170K) and it is not observed above 1050°C (1323K).[4] At 1050°C (1323K) and 1100°C (1373K), quartz and hematite are the main components. Raw materials are physically agglomerated at 1100°C (1373K) and no compounds of the simple oxides are seen up to that temperature. However, a new compound confirmed to be fayalite (Fe_2SiO_4) is observed at 1150°C (1423K). Fayalite is a well-known phase which has an olivine structure, and is a common mineral in nature. It is widely used as a slag component in copper smelting because of its low melting temperature, ranging from 1177°C (1450K) to 1205°C (1478K), dependent on Fe/SiO_2 ratio.[5]

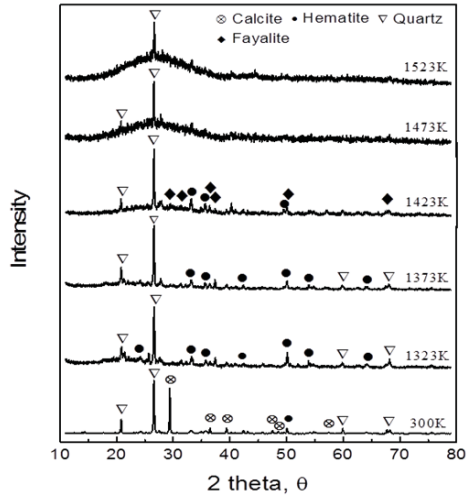

Fig.4. XRD patterns of pellet samples at different temperatures

The formation of fayalite in the pellet changes the sintering mechanism thoroughly and it enables lower temperature processing. Meanwhile, when the specimen melts at temperatures higher than 1200°C (1473K), the XRD patterns show a typical amorphous state. Quartz peaks remain at 1250°C (1523K) due to slow cooling condition, but the intensity reduces as the silicate structure forms at higher temperature.

The sintering mechanism of the pellet is clarified by investigating its microstructural behavior. Morphological change of the pellet was seen by SEM / EDX analysis. In **Figure 5**, SEM images and point analysis by EDX are shown. At 1100°C (1373K), solid particles are agglomerated and exist as dense phases as seen in **Figure 5(a)**. Quartz and hematite adhere and formulate an intermediate phase mainly composed of SiO_2 and FeO_t at this temperature. White parts are distinguished from surrounding parts. These bulk phases were analyzed to be calcium oxide that did not chemically react with quartz and hematite. This is due to the low reaction temperature and short reaction time of 30 minutes. Therefore,

higher sintering temperature than 1100°C (1373K) is necessary for lightweight aggregate to prevent the expansion by unreacted free limes. On the other hand, new phases appear at 1150°C (1423K). As seen in SEM image of **Figure 5(b)**, spherical droplets are observed in the pellet. The widely distributed droplets were confirmed as fayalite phase from EDX analysis. FeO_t (53.83wt%) and SiO_2 (30.59wt%) contents shown in **Figure 5(b)** correspond to fayalite in FeO_t - SiO_2 binary phase diagram.[6] Fayalite phase is easier to form at 1150°C (1423K) due to low gibbs free energy.

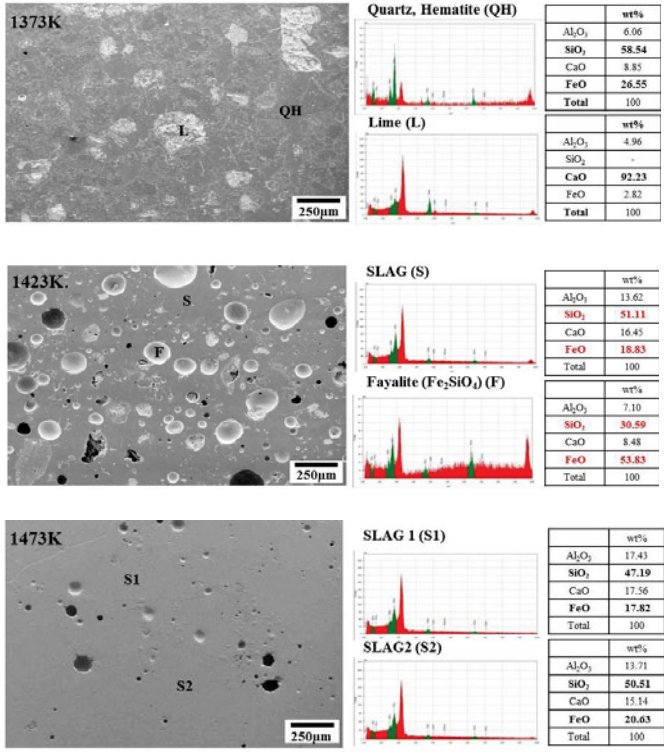

Fig.5. SEM image and EDX results of sample after treated at (a) 1373K, (b) 1423K and (c) 1473K

From microscopic analysis, it is obvious that liquid phase sintering takes places in the pellets. Isolated liquid droplets and remainder phases in **Figure 5(b)** can be applied to the liquid / solid system. Wetting and spreading of the liquid is an important factor for the liquid phase sintering mechanism.[7] In addition, the solubility of solid in the liquid and the dihedral angle (ψ) for a liquid at a grain boundary control the shape of the liquid between solid phases.[7] As the fayalite has very low viscosity and high wettability, dihedral angle is certainly higher than 120° and the ratio of the interfacial energies (γ_{ss}/

γ_{sl}) must be lower than unity. Furthermore, fayalite and the surrounding oxides have a high mutual solubility since fayalite easily diffuses to the surroundings. This was seen from the experiment as the specimens were melted and spread when heated over 30 minutes. The formation of fayalite in the pellet enables liquid phase sintering that lowers operation temperature. Meanwhile, at higher temperature above 1200^{o}C (1473K), completely molten phases are observed as shown in **Figure 5(c)**. Every point analyzed by EDX shows the similar oxide composition.

Conclusions

Lightweight aggregate production using gold tailings, red mud and waste limestone was investigated from the pyrometallurgical viewpoint. Raw materials were quantitatively analyzed and the composition obtained was used for the oxide system design. Environmental risks of heavy metals and radioactive elements were checked by chemical analysis and confirmed as negligible. The following conclusions can be made from this study.

1. A thermodynamic study focusing on the CaO-FeO_t-Al_2O_3-SiO_2 quaternary oxide system was carried out. The lowest melting point (eutectic triple point) was found to be the ideal composition for current raw materials combinations.

2. An optimum ratio of three raw materials was identified: the ratio of gold tailings 2 / red mud 1 / limestone 1 was suitable for lightweight aggregate production. Through high temperature experiments, 1150^{o}C (1423K) was confirmed to be the optimum temperature for the sintering process.

3. The sintering reaction mechanism was clarified from the microstructural analysis of the specimen. The sample showed a typical liquid phase sintering process due to the formation of a fayalite phase. Fayalite which has low viscosity and low interfacial tension is formed below 1205^{o}C (1478K). This facilitates the low temperature sintering.

References

1. G. M. Ritcey, "Tailings management in gold plants," *Hydrometallurgy,* 78[1–2] 3-20 (2005).

2. G. Power, M. Gräfe, and C. Klauber, "Bauxite residue issues: I. Current management, disposal and storage practices," *Hydrometallurgy,* 108[1–2] 33-45 (2011).

3. C. Klauber, M. Gräfe, and G. Power, "Bauxite residue issues: II. options for residue utilization," *Hydrometallurgy,* 108[1–2] 11-32 (2011).

4. D. R. Gaskell, "Introduction to the Thermodynamics of Materials, Fifth Edition.″ Taylor & Francis, (2003).

5. H. Park and V. Sahajwalla, "Influence of CaO-SiO2-Al2O3 Ternary Oxide System on the Reduction Behavior of Carbon Composite Pellet: Part II. Morphological Properties," *Metallurgical and Materials Transactions B,* 44[6] 1390-97 (2013).

6. V. Stahleisen and V. D. Eisenhüttenleute, "Slag Atlas.″ Verlag Stahleisen, (1995).

7. N. Rahaman, *Sintering of ceramics*; pp. 182-187. CRC Press, (2007).

REWAS 2016: Towards Materials Resource Sustainability
Edited by: Randolph E. Kirchain, Bart Blanpain, Christina Meskers, Elsa Olivetti, Diran Apelian, John Howarter, Anne Kvithyld, Brajendra Mishra, Neale R. Neelameggham, and Jeff Spangenberger
TMS (The Minerals, Metals & Materials Society), 2016

ACCOUNTING FOR VARIATION IN LIFE CYCLE INVENTORIES: THE CASE OF PORTLAND CEMENT PRODUCTION IN THE U.S.

Xin Xu, [a,b] Maggie Wildnauer, [a,b] Jeremy Gregory, [a,b] Randolph Kirchain[b]

[a] Department of Civil & Environmental Engineering, Massachusetts Institute of Technology, Cambridge, MA 02139; [b] Material Systems Laboratory, Massachusetts Institute of Technology, Building E38-432, Cambridge, MA 02139

Keywords: life cycle inventory (LCI); uncertainty; variation; portland cement production

Abstract

Variation in life cycle inventories (LCI) for a materials industry are significant but rarely reported, in spite of the fact that inventories are often created by aggregating data from several locations. In this study, two approaches for aggregating LCI data, inventory-level (horizontal) and plant-level (vertical), were compared in the context of a specific materials industry: portland cement production in North America. We present a derivation of the methodologies to highlight the similarities and differences. Finally, we show results from a life cycle impact assessment of cradle-to-gate portland cement production using a Monte Carlo simulation approach to explore the quantitative differences. For the case study, we observe that the mean values of GWP using both approaches are similar, but the standard deviations can be significantly different. The reasons for this difference – the handling of correlation across exchange magnitudes within a facility and zero-inflated data – are discussed.

Introduction

Variation and uncertainty is pervasive in life cycle assessment (LCA). Evaluating that uncertainty can improve the credibility of LCA results. One specific issue that has received little attention in the LCA literature is the aggregation of data and the characterization of uncertainty in life-cycle inventory (LCI) data. As will be shown, the manner in which inventory data are aggregated can change the measure of dispersion for LCI flows. This will be demonstrated in the context of a specific industrial case: portland cement production in North America.

Concrete is the most extensively used construction material in the world. Because of this scale and the carbon emissions released during cement production, many LCA studies have examined the environmental impacts of various concrete structures and products [1-4].

Literature Review

In current practice, the inventory associated with an activity is represented by summary statistics and a distributional form for each flow. These summary statistics are computed by aggregating (i.e. analyzing) the observations from a sample of that activity.

Common practices for data aggregation are horizontal averaging and vertical aggregation. Horizontal aggregation is commonly performed when multiple unit processes, or aggregated datasets, are combined to represent a more general process [5]. Vertical aggregation appears to be common in studies of individual industries [6-9]. Despite the importance of data aggregation,

little formal discussion about the methodological choices or their implications is found in the literature.

Life Cycle Methodology

Scope

Functional unit. In this report, the functional unit is defined as one metric ton of portland cement manufactured in the United States from domestically produced clinker.

System boundary. For this LCI study, cement production as a whole is treated as a unit process and primary data were collected within the manufacturing process as shown in

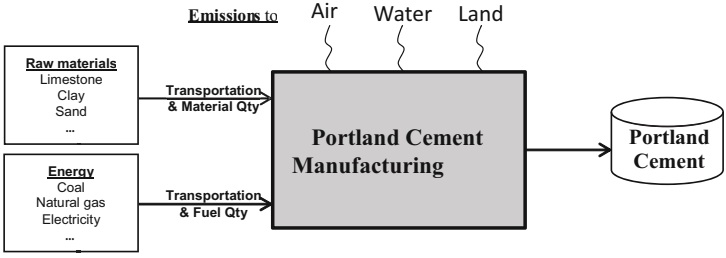

Figure 1.

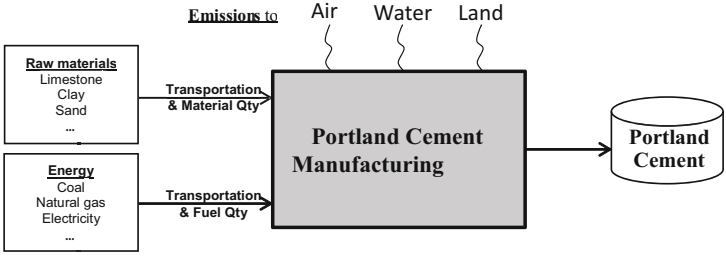

Figure 1. The system boundary for the LCI

Data Source

The LCI data used here are primarily based on the Portland Cement Association (PCA) 2010 U.S. and Canadian Labor-Energy Input Survey and the associated supplemental survey, 2010 Production Information Summary (PIS), which were conducted across approximately 95% of U.S. cement production plants, and relevant energy data have also been collected by PCA annually for many years [10]. Secondary data sets from ecoinvent [11], the USLCI database, as well as US Environmental Protection Agency (EPA) reported emission factors [12] are used to calculate the burdens of upstream processes, the transportation and the combustion emissions on site.

Cement Life Cycle Impact Assessment

A single-attribute life cycle impact assessment, using Global Warming Potential (GWP) is performed as a means of exploring the implications of the data aggregation methods.

Monte Carlo simulations are conducted using Microsoft Excel with a Crystal Ball add-in to estimate the statistical characteristics of the LCIA when aggregated horizontally and vertically for producing 1 metric ton (mt) of portland cement.

Methodology for Averaging LCI Data and Environmental Impacts

There are at least two ways of aggregating raw data when constructing an LCI: horizontal aggregation and vertical aggregation.

Horizontal aggregation

In horizontal aggregation, the statistical moments of each exchange in the inventory are first computed and then these are summed to compute the inventory for the activity. This means that information about inventory exchanges are first aggregated horizontally, across plants, before being combined vertically (across exchanges). Current LCA practice implicitly aggregates these exchange-level inventories assuming that they are independent or at least uncorrelated.

Vertical aggregation

By contrast, vertical aggregation first estimates the total inventory associated with a particular facility (plant) before then assessing the statistical characteristics of the inventories across those estimates. This means that first LCI data are calculated within a plant vertically, and then the resulting vertical values are aggregated across the plants.

For either approach, the inventory of exchanges can be mapped to the associated inventory of elementary flows (e.g., CO_2) by multiplying them by appropriate emissions factors (*e;* for example, kg CO_2/MJ of coal combustion).

Differences in horizontal and vertical estimates of inventory

At face value, these two approaches appear to differ only in the order of operations. However, these two approaches can lead to differences in the estimate of dispersion for the inventory, because of a) correlation among flow magnitudes within a plant and b) the zero-inflated nature of many LCI datasets.

The implications of correlation are easy to describe. Assuming that observations are uncorrelated can either over or under estimate dispersion depending on whether the covariance is predominantly positive or negative.

Zero inflation is a statistical term which implies that a dataset contains more zeroes than would be predicted by typical distributions. In LCI data, zero inflation can occur when two or more exchanges are substitutable (e.g., oil and natural gas) across facilities. An analytical treatment of LCI math has shown that: *conventional horizontal aggregation will always overstate the actual dispersion in a zero-inflated inventory.*

Results: LCIA of Portland Cement Production

Statistics of the LCIA simulations for GWP of portland cement are summarized for the whole population and for one subtype of kiln process a precalciner (which represents more than 60% of facilities) in Table 1. The results are all weighted by plant production. The two aggregation approaches produce nearly identical mean values for the entire population and for each process type. Interestingly, the standard deviations estimated through more conventional horizontal

aggregation is 50% higher than those estimated through vertical aggregation for the Precalciner population.

Table 1. Statistics on GWP of portland cement manufacturing by process type

	Horizontal		Vertical	
	Mean	Standard Deviation	Mean	Standard Deviation
Precalciner	0.95	**0.21**	0.94	**0.14**
Average	0.99	**0.23**	0.99	**0.18**

It is not possible to know the generalizability of these magnitudes. Future studies should consider the relative magnitude of these effects.

H*orizontal aggregation* is required for LCA because it is the only way to create transparent, unit-process inventories. Nevertheless, the current implementation of horizontal aggregation overstates uncertainty in the inventory. To begin to address this, future studies should assess inventory data for the presence of correlation and zero-inflation. Hopefully, future software will allow for horizontal aggregation while accounting for these statistical characteristics.

Acknowledgements

This research was conducted as part of the Concrete Sustainability Hub at the Massachusetts Institute of Technology, which is supported by the Portland Cement Association and the Ready Mixed Concrete Research and Education Foundation.

References

1. Lemay, L., *Life Cycle Assessment of Concrete Buildings.* Natl. Ready Mix. Concr. Assoc., 2011. **1-12**.
2. Loijos, A., *A. Life Cycle Assessment of Concrete Pavements : Impacts and Opportunities*. 2011, Massachusetts Institute of Technology.
3. Santero, N.J. and A. Horvath, *Global warming potential of pavements.* Environmental Research Letters, 2009. **4**(3): p. 034011.
4. Zhang, J., J.C. Cheng, and I.M. Lo, *Life cycle carbon footprint measurement of Portland cement and ready mix concrete for a city with local scarcity of resources like Hong Kong.* The international journal of life cycle assessment, 2014. **19**(4): p. 745-757.
5. *Global guidance principles for life cycle assessment databases—a basis for greener processes and products*. 2011, UNEP/SETAC.
6. *Life Cycle Inventory (LCI) of Primary Zinc Production*. 2009, The International Zinc Association.
7. *The Environmental Footprint of Semi-Finished Aluminum Products in North America: A Life Cycle Assessment Report*. 2013, The Aluminum Association.
8. Association, W.S., *Life cycle inventory study for steel products.* Life Cycle Assessment Methodology Report, 2011.
9. ECOBILAN, *Eco-profile of high volume commodity phthalate esters (DEHP/DINP/DIDP)*. 2001, The European Council for Plasticisers and Intermediates (ECPI).

10. Marceau, M., Nisbet, MA, VanGeem, MG, *Life Cycle Inventory of Portland Cement Manufacture.* 2006. **No. 2095b**.
11. Weidema, B.P., et al., *Overview and methodology: Data quality guideline for the ecoinvent database version 3*. 2013, Swiss Centre for Life Cycle Inventories.
12. *U.S. Life Cycle Inventory Database https://www.lcacommons.gov/nrel/search (accessed Apr 4, 2015).* National Renewable Energy Laboratory.

REWAS 2016: Towards Materials Resource Sustainability
Edited by: Randolph E. Kirchain, Bart Blanpain, Christina Meskers, Elsa Olivetti, Diran Apelian, John Howarter, Anne Kvithyld, Brajendra Mishra, Neale R. Neelameggham, and Jeff Spangenberger
TMS (The Minerals, Metals & Materials Society), 2016

KINETICS OF DEPHOSPHORIZATION FROM STEELMAKING SLAG BY LEACHING WITH $C_6H_8O_7$-NaOH-HCl SOLUTION

Yong Qiao[a], Jiang Diao [a,*], Xuan Liu[a], Xiaosa Li[a], Tao Zhang[b], Bing Xie[a]

[a] College of Materials Science and Engineering, Chongqing University, Chongqing 400044, P. R. China.
[b] Department of Scientific Research, Chongqing University of Education, Chongqing 400065, P. R. China.
Corresponding author: Jiang Diao, E-mail:diaojiang@163.com; Tel: +86 23 65102469

Abstract

It is well-known that the recycling of steelmaking slag in iron and steel industry would bring out a problem of phosphorus enrichment in hot metal, which will do harm to steelmaking process. In the present paper, dephosphorization from steelmaking slag by leaching with solution composed of citric acid, sodium hydroxide and hydrochloric acid was studied. Kinetic parameters including temperature, slag particle size and solution pH were optimized. The results showed that temperature has no obvious effect on dissolution of phosphorus. The dephosphorization rate increase with the decrease of slag particle size and pH value of solution. 90.0% of phosphorus can be dissolved in the solution while the corresponding leaching ratio of iron was only 30.0% in the optimal condition. Leaching kinetics of dephosphorization follows the unreacted shrinking core model with a rate controlling step by the solid diffusion layer and the corresponding apparent activation energy is 1.233 kJ mol^{-1}.

Keywords: Steelmaking slag, Dephosphorization, Leaching, Kinetic

Introduction

Great amounts of steelmaking slags from iron and steel industry are produced through basic oxygen furnace and electric arc furnace. The amount of steelmaking slags from different steel plants are 100~150 kgs/t of steel output[1,2]. The increasing accumulation of steelmaking slags not only occupies plenty of land, but also pollutes the environment and water. It becomes a seriously problem of both the society and the iron and steel industry itself[3]. Various studies have been made on the utilization of steelmaking slags. Recycling of steelmaking slag into iron and steel industry always plays a fairly important role as it could both recover valuable metal Fe and fluxing agent CaO, FeO, SiO_2, MgO, MnO and so on. Especially, recycled steelmaking slag make better utilization of CaO. At present, recycled steelmaking slag is mainly used as sintered flux, blast furnace flux and steelmaking additive. However, most steelmaking slags contain a notable amount of phosphorus (1~3%) [4], the recycling of steelmaking slag in iron and steel industry was limited due to the enrichment of phosphorus in hot metal or steel. Therefore, it is necessary to remove the phosphorus before recycle steelmaking slag into the iron and steel industry.

It is well known that most of the phosphorus forms the $n$$C_2S$-$C_3P$ solid solution in steelmaking slags[5]. Therefore, dephosphorization from the steelmaking slag also means removal of the $n$$C_2S$-$C_3P$ solid solution from the matrix phase of steelmaking slag. Therefore, some researchers studied the removal of solid solution from steelmaking slag according to the density differences for different mineral phases in the slag[6]. The density of the $n$$C_2S$-$C_3P$ solid solution is about 2.75 g/cm^3, which is lower than that of the residual matrix phase (3.14 g/cm^3). Therefore, the

solid solution can be separated during slow cooling of molten slag. The authors have concluded that more than 70% of the phosphorus can be separated in the optimal condition. Some researchers studied the removal of $n$$C_2S$-$C_3P$ solid solution from steelmaking slag according to the differences in the magnetic property for different mineral phases in the slag[7-9]. The $n$$C_2S$-$C_3P$solid solution has a diamagnetic property with weak magnetization, but the matrix phase shows a strong magnetization. It was found that more than 62% of the solid solution can be separated in the optimal condition. Although some of these processes are effective for removing $n$$C_2S$-$C_3P$ solid solution from the steelmaking slag. But some strict conditions such as good slag fluidity, slow cooling rate, high energy consumption and low separation rate limit their industrial application. In addition, some researchers tried to explore that selective extraction of phosphorus and iron in aqueous solution by leaching [10,11].They concluded that the dissolution ratio of Ca is close to 1.0 while the dissolution ratio of P was about 0.1 and did not change by the C_3P content and the CaO/SiO_2 ratio in the residue was similar and the P_2O_5/Fe_2O_3 ratio was slightly larger after leaching by aqueous solution.

Based on the above backgrounds, if the dissolution ratio of the $n$$C_2S$-$C_3P$ solid solution in an aqueous solution is higher than that of the matrix phase, the separation of P and Fe in steelmaking by using a leaching treatment becomes possible. To obtain the optimal condition of dephosphorization from industrial steelmaking slag and clarify the mechanism of the selective extraction of P and Fe, the leaching experiments were conducted in the present work.

Experimental

Steelmaking slag was ground into small particles and used as the raw material in the experiments. Three type of particle sizes of >187 μm, 125–187 μm and 75–125 μm were selected in present work. The mass fraction of phosphorus and iron in slag is shown in Table I. To keep the pH at a nearly constant value in the experiments, a buffer solution containing a mixture of $C_6H_8O_7$, NaOH, HCl and ion-exchanged water was adopted as the aqueous solution. The pH values of 2.2, 3.1, 4.3 and 5.8 were investigated.

Table I. The mass fraction of phosphorus and iron in slag

Elements	P_2O_5	Fe_2O_3
Mass fraction (%)	3.136	22.010

One gram of the slag sample was placed in 400 mL of $C_6H_8O_7$-NaOH-HCl solution. A three-necked bottle was used as the experimental vessel. The reaction mixture was stirred with a magnetic stirrer and heated in a thermostat bath at designed temperatures. Leaching temperature was varied in the range of 25 °C to 80 °C. The rotate speed was fixed at 600 rpm. About 5 mL of solution was sampled at adequate intervals and filtrated using a syringe filter (< 0.45 μm). After the experiment, all the solution was filtered and the residue on the filter was rinsed several times by ion-exchanged water. After filtering, the filtered solutions were analyzed using inductively coupled plasma optical emission spectrometry (ICP-OES).

Results and discussion

Influencing factors of phosphorus dissolution ratio

Fig 1 illustrates the effect of the pH values on dissolution ratio of phosphorus. It can be seen that the dissolution ratio of phosphorus decreased significantly with increasing the pH from 2.2 to 5.8. It is worth noting that over 90.0% of the phosphorus can be dissolved in the $C_6H_8O_7$-NaOH-

HCl solution when at pH 2.2. As shown in Fig 2, although the leaching ratio of phosphorus increases with the increase of leaching temperature, however, the magnitude of the increase was not much. The increase of the dissolution ratio of phosphorus is less than 10% with leaching temperature increases from 25 °C to 80 °C. Fig 3 shows the effect of slag particle size on dissolution ratio of phosphorus. It can be seen that with the increase of particle size, the dissolution ratio of phosphorus increased significantly. The effect of pH on dissolution of iron was consistent with that on dissolution of phosphorus. In contrast to phosphorus, the dissolution ratio of iron increases significantly with increasing the leaching temperature from 25 °C to 80 °C As well as phosphorus, the dissolution ratio of iron increases with the decrease of particle size. As shown in Fig 4, 90.0% of phosphorus can be dissolved in the solution while the corresponding leaching ratio of iron was only 30.0% in the optimal condition.

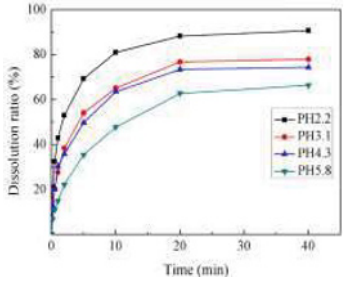

Fig 1. Effect of pH on dissolution ratio of phosphorus (25 °C,75-125 μm)

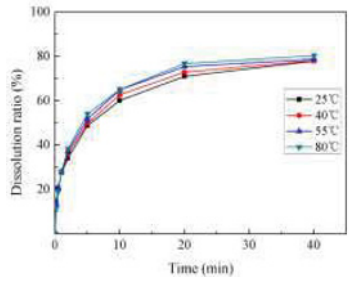

Fig 2. Effect of leaching temperature on dissolution ratio of phosphorus (pH 3.1,75-125μm)

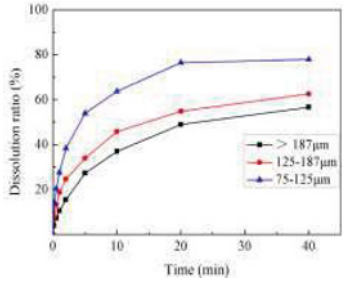

Fig 3. Effect of particle size on dissolution ratio of phosphorus (pH 3.1, 25 °C).

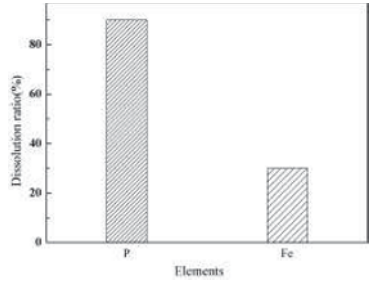

Fig 4. Comparison of dissolution ratio between phosphorus and iron(pH2.2, 25 °C, 75-125 μm).

Kinetic analysis

The experimental results were fitted with a variety of models, such as pseudo second order model and unreacted shrinking core model. After repeated siftings, the unreacted shrinking core model was adopted in the present study. The leaching reaction of phosphorus can be expressed by reaction (1).

$$A_{(aq)} + bB_{(s)} \rightarrow Product_{(aq)} \quad (1)$$

where, A, B and b represent $C_6H_8O_7$-NaOH-HCl solution, steelmaking slag and stoichiometric coefficients. Each step could be the rate-controlling step during leaching process and relative integral rate equations derived from SCM were given in the following：

1）If the rate of leaching process was controlled by the step of diffusion through solid layer around the unreacted core, the integral rate equation was expressed as

$$1-3\left(1-x\right)^{2/3}+2\left(1-x\right)=\mathrm{k_d}t \tag{2}$$

2）If the leaching rate was controlled by the surface chemical reaction, the integral rate equation was

$$1-\left(1-x\right)^{1/3}=\mathrm{k_r}t \tag{3}$$

3）If the leaching rate was controlled by the liquid film diffusion, the integral rate equation was

$$1-\left(1-x\right)^{2/3}=\mathrm{k_l}t \tag{4}$$

where x is the leaching ratio of phosphorus; k_d is the pore diffusion rate constant; k_r is the apparent rate constant for the surface chemical reaction; k_l is the apparent rate constant for diffusion through the fluid film and t is the leaching time. In present study, the experimental data were fitted with the rate equations of each control step. the results showed that the largest regression coefficients of determination (R^2) were obtained for the type of product layer diffusion control. The plots of Eq (2) versus time for the tests at different temperatures are shown in Fig 5(a), and the rate constants are expressed by the slope. The regression coefficients of determination are close to 1 and all the lines are passed through the original point. With the increase of the temperature, the rate of leaching process increased slightly. As shown in Fig 5(b), the activation energy of the reaction using an Arrhenius relationship (5) was calculated to be about 1.233 kJ/mol.

$$\ln k = \text{-Ea/R}T+\ln\mathrm{A} \tag{5}$$

The activation energy of diffusion controlled process is typically below 12 kJ/mol while for chemical reaction controlled process this value is usually higher than 40 kJ/mol, when activation energy is between 12 and 40 kJ/mol, the process is controlled by both diffusion and chemical reaction[12]. Therefore, it was confirmed that the rate of leaching process is controlled by diffusion and dependent on temperature slightly. Fig 6(a) and Fig 7(a) show the plots of Eq (2) versus time for tests at different pH values and particle sizes. Seen from these Fig 6 (a) and Fig 7 (a), with the decrease of the pH and particle size, the rate of leaching process increased significantly. In order to specifically express the effect of various factors on the dissolution ratio of phosphorus, the following semiempirical equations were established [13]:

$$1-3(1-x)^{2/3}+2(1-x)=\mathrm{k_0}(pH)^{\mathrm{c}}(d_{\mathrm{p}})^{\mathrm{p}}\exp(-\mathrm{E_a}/\mathrm{R}T)t \tag{6}$$

According to Fig 5(b), Fig 6(b) and Fig 7(b), the values of k_0, c, and p can be calculated. Therefore, the kinetics equation in present study can be expressed by

$$1-3(1-x)^{2/3}+2(1-x)=3951.29(pH)^{-1.386}(d_{\mathrm{p}})^{-1.98}\exp(-148/T)\,\mathrm{t} \tag{7}$$

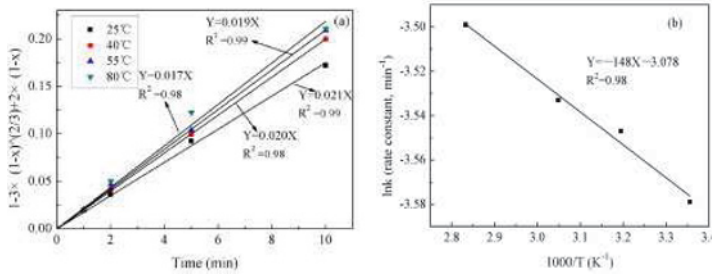

Fig 5. (a) Plot of $(1-3\times(1-x)^{2/3}+2\times(1-x))$ versus time for tests at different temperatures; (b) Arrhenius plot for activation energy calculation (pH 3.1, 75-125 μm,).

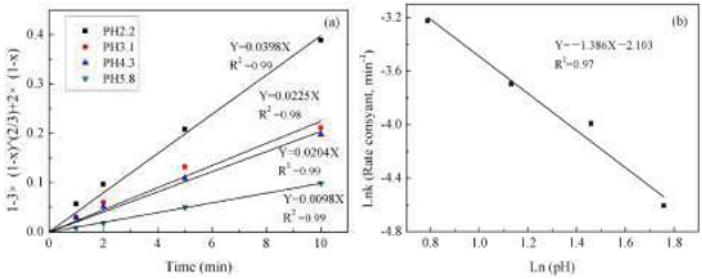

Fig 6. (a) Plot of $(1-3\times(1-x)^{2/3}+2\times(1-x))$ versus time for tests at different pH values; (b) Effect of pH on the rate of dissolution of phosphorus (25°C, 75-125 μm).

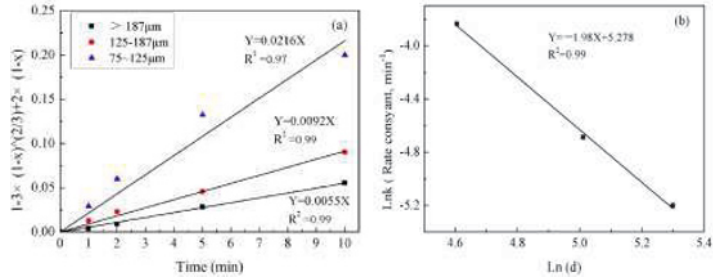

Fig 7. (a) Plot of $(1-3\times(1-x)^{2/3}+2\times(1-x))$ versus time for tests at different particle sizes; (b) Effect of particle size on the rate of dissolution of phosphorus (25°C, pH 3.1).

Conclusions

In this work, dephosphorization from steelmaking slag by leaching with acidic aqueous solution composed of citric acid, sodium hydroxide, hydrochloric acid and ion-exchanged water was studied. Based on results obtained in this paper, it was concluded that:

(1) Kinetic parameters including leaching temperature, slag particle size and pH value of solution were optimized. Over 90.0% of the phosphorus can be dissolved in the solution while the corresponding leaching ratio of iron was only 30.0% after 40 min at pH 2.2, 25 °C and 75-125 μm particle sizes.

(2) Leaching kinetics of dephosphorization follows the unreacted shrinking core model with a rate controlling step by the solid diffusion layer and the corresponding apparent activation energy is 1.233 kJ mol^{-1}.

(3) In order to specifically express the effect of various factors on the dissolution ratio of phosphorus ,the semiempirical equation was established:

$$1-3(1-x)^{2/3}+2(1-x)=3951.29(pH)^{-1.386}(d_p)^{-1.98}\exp(-148/T)\,t$$

Acknowledgment: This work was partially supported by the Fundamental Research Funds for the Central Universities (Project CDJZR 14130001) and National Basic Research Program of China (No. 2013CB632604). We express our gratitude to all those who helped us during the writing of this paper.

References

1. Gao. X., Okubo, M., Maruoka, N., Shibata, H., Ito, T., Kitamura, S. Y. "Production and utilisation of iron and steelmaking slag in Japan and the application of steelmaking slag for the recovery of paddy fields damaged by Tsunami." *Trans. Insti. Min. Metall. C.* 124 (2)(2005), 116-124.
2. Proctor, D. M., Fehling, K. A., Shay, E. C., Wittenborn, J. L., Greem, J. J., Avent, C., Bigham, R. D., Connolly, M., Lee, B., Shepker, T. O., Zak, M. A., "Physical andchemical characteristics of blast furnace, basic oxygen furnace, andelectric arc furnace steel industry slags." *Environ. Sci.Technol*. 34 (8)(2000), 1576-1582.
3. Dippenaar, R., "Industrial uses of slag (the use and re-use ofiron and steelmaking slags)". *Ironmak. Steelmak.* 32 (1)(2005), 35-46.
4. Shen, H., Forssberg, E., "An overview of recovery of metals from slags". *Waste Manage.* 23(2003), 933-949.
5. Pahlevani F, Kitamura S, Shibata H, et al., "Distribution of P_2O_5 between Solid Solution of $2CaO{\cdot}SiO_2$-$3CaO{\cdot}P_2O_5$ and Liquid Phase". ISIJ international, 50(6)(2010): 822-829.
6. Ono H., "Removal of phosphorus from LD converter slag by floating of dicalcium silicate during solidification." *Tetsu-to-Hagane(Journal of the Iron and Steel Institute of Japan)*, 66(9)(1980),1317-1326.
7. Fujita T, Iwasaki I., "Phosphorus Removal From Steelmaking Slags Slow-Cooled in a Non-Oxidizing Atmosphere by Magnetic Separation/Flotation." *Iron Steelmaker*,16(1)(1989), 47-55.
8. Kubo H, Matsubae-Yokoyama K, Nagasaka T., "Magnetic separation of phosphorus enriched phase from multiphase dephosphorization slag." *ISIJ international*, 50(1)(2010), 59-64.
9. Diao, J., Xie, B., Wang, Y. H., Guo, Xu., "Recovery of phosphorus fromdephosphorization slag producedby duplex high phosphorus hot metal refining." *ISIJ Int.* 52 (6)(2012), 955-959.
10. Teratoko T, Maruoka N, Shibata H, et al., "Dissolution behavior of dicalcium silicate and tricalcium phosphate solid solution and other phases of steelmaking slag in an aqueous solution." *High Temp. Mater. Proc.,* 31(2012), 329–338.
11. Numata M, Maruoka N, Kim S J, et al., "Fundamental Experiment to Extract Phosphorous Selectively from Steelmaking Slag by Leaching." *ISIJ International,*54(8)(2014), 1983-1990.
12. Ashraf M, Zafar Z I, Ansari T M., "Selective leaching kinetics and upgrading of low-grade calcareous phosphate rock in succinic acid." *Hydrometallurgy,* 80(4)(2005), 286-292.
13. Ekmekyapar A, Aktaş E, Künkül A, et al., "Investigation of leaching kinetics of copper from malachite ore in ammonium nitrate solutions." *Metallurgical and Materials Transactions B,* 43(4)(2012), 764-772.

REWAS 2016: Towards Materials Resource Sustainability
Edited by: Randolph E. Kirchain, Bart Blanpain, Christina Meskers, Elsa Olivetti, Diran Apelian, John Howarter, Anne Kvithyld, Brajendra Mishra, Neale R. Neelameggham, and Jeff Spangenberger
TMS (The Minerals, Metals & Materials Society), 2016

TREATMENT OF MOLTEN STEEL SLAG FOR CEMENT APPLICATION

João B. Ferreira Neto[1], Catia Fredericci[1], João O. G. Faria[1], Fabiano F. Chotoli[1], Tiago R. Ribeiro[1], Antônio Malynowskyj[1], Andre N. L. Silva[1], Valdecir A. Quarcioni[1], Andre A. Lotto[1]

[1]Institute for Technological Research (IPT), 532 Av. Prof. Almeida Prado, São Paulo – SP, 05508-901, Brazil

Keywords: Steel Slag, Cement Slag, Pyrometallurgy

Abstract

Steel slag can be an alternative in cement mineral admixture, partially as a substitute for blast furnace slag. A pyrometallugical process has been investigated to promote the chemical composition modification of molten steelmaking slag in a metallurgical reactor. Experiments were conducted by remelting 300 kg of steel slag followed by chemical modification of liquid slag. The modified slags were naturally cooled in the metallurgical reactor or cooled by steel balls. XRD and SEM analysis of slag samples revealed the relationship among chemical composition, cooling conditions and amorphous and crystalline phases. Cement samples were produced by mixing 25% of treated steelmaking slag with 75% of Portland cement, resulting in more than 280 J/g of accumulated hydration heat in 72 h, expansion lower than 0,1% in the autoclave tests and compressive strength higher than 42 MPa after 28 days. The process indicates potential to be applied as a steelmaking slag treatment.

Introduction

The construction industry in Brazil has grown more than 5%/y, whereas the crude steel production has been steady at approximately 32 millions of tons in the last 10 years, and there is no expectation of growth. Therefore, a shortage of blast furnace slag for the cement industry will likely develop in the future. Steelmaking slag could be an alternative in cement mineral admixture, as a substitute for blast furnace slag[1-4]. However, the use of steelmaking slag directly in cement admixture is not allowed because of expansion during hydration, caused by free CaO and MgO and Mg-rich wustite (RO phase)[5,6]. A pyrometallurgical process to promote the modification of the chemical composition of molten steel slag to make it more appropriate for cement manufacturing was investigated. The hydraulic activity of slags is affected by the chemical composition, glass content and their combination [7]. Highly basic slags ($CaO+MgO/SiO_2+Al_2O_3 = 1.5$) are mainly crystalline[7] and a glassy structure forms in acidic slags containing sufficient Al_2O_3. In addition, the development of glassy phase or crystalline, and crystal size, depends on the cooling conditions[8].

Methodology

The purpose of the experiments conducted in the present work was to study the effect of cooling rate and chemical composition on slag crystallization. Modified slags were produced in a metallurgical reactor[9] by adding modifying agents to 300 kg of BOF molten Steel Slag (SS)

supplied by an Iron and Steelmaking Company in Brazil. Two by-products were used, one rich in Al_2O_3 and one rich in SiO_2.
Table I shows the chemical composition of BOF steel slag (SS) and the chemical compositions of eight modified steel slags (SS-MX) determined by X-ray fluorescence (XRF).
These modified slags were produced by adding by-products of the metallurgical and civil construction industries in Brazil. Two by-products were used, one rich in Al_2O_3 and one rich in SiO_2.
Modified slags were divided in two groups. The experiments of group 1 (Slags SM-4, SS-M6, SS-M7 and SS-M8) aimed amorphous slags, whereas the experiments of group 2 (Slags SM-09, SM-10, SM-11 and SM-12) aimed crystalline slags, especially C_2S formation.

Table I. Chemical compositions and basicity (%CaO/%SiO_2) of Steel Slag (SS) and modified slags (wt%).

		Group 1				Group 2			
FRX	**SS**	**SS-M4**	**SS-M6**	**SS-M7**	**SS-M8**	**SS-M9**	**SS-M10**	**SS-M11**	**SS-M12**
Fe_2O_3 (%)* **	13,6	2,0	1,22	0,53	3,86	1,43	5,18	2,5	6,92
FeO (%)*	18,3	7,6	7,5	3,8	6,3	20,6	18,8	21,8	21,3
Fe^0 (%)**	0,2	0,3	0,4	0,25	0,54	0,45	0,49	0,32	0,15
CaO (%)	38,1	37,3	34,28	37,15	33,6	36,43	35,59	36,2	36,4
S (%)	0,1	<0,1	0,05	0,06	0,04	0,05	0,04	0,05	0,04
SiO_2 (%)	9,9	32,2	30,68	30,82	31,8	22,01	21,64	19,9	18,5
Al_2O_3 (%)	1,7	4,8	11,66	11,61	10,66	3,31	2,94	2,8	1,59
MgO (%)	8,6	9,8	9,13	9,53	9,8	10,49	10,05	11,2	10,3
TiO_2 (%)	0,3	0,2	0,32	0,3	0,3	0,25	0,25	0,26	0,26
MnO (%)	4,4	3,1	3,7	3,32	3,83	4,33	4,39	4,35	4,42
P_2O_5 (%)	1,3	0,8	0,95	0,77	0,94	1,36	1,45	1,39	1,39
CaO F (%)	5,7	N.D	0,21	0,23	0,16	0,25	0,25	0,33	0,22
B (%CaO/%SiO_2)	3,85	1,16	1,12	1,21	1,06	1,66	1,64	1,82	1,97
FeO + Fe_2O_3	31,9	9,6	8,7	4,3	10,2	22,0	24,0	24,3	28,2

(*) FeO: ASTM E 246-10 - Determination of Iron by Dichromate Titrimetry. (**) Fe^0: XU, Z et al[10] (***) Fe^{3+} (%) = Fe_t FRX (%) – Fe^{2+} (%) - Fe^0.

After chemical modification, most of modified slags were cooled by steel balls, using the technique developed and patented by the company Paul Wurth, which has authorized the Institute for Technological Research (IPT), based on a cooperation agreement, to perform tests using such cooling conditions. The principle of cooling by steel balls is described in the patent[11] and in the literature[12]. However, some modified slags (SS-M9 and SS-M11) were naturally cooled in the same reactor in which the modification occurred, to evaluate the effect of cooling conditions on the slag crystallization.
After cooling, steel balls were separated from the slag by magnetic separation. The slags were milled and homogenized to obtain samples suitable for chemical and mineralogical characterization.
Thermodynamic simulations were performed using FactSage 6.4 software to predict phases formed during slags solidification.
Chemically modified steel slags were ground to a particle size less than 0.075 mm, and mixed with Ordinary Portland Cement (OPC) resulting in Portland Slag Cements samples (PSC) in a proportion of 25 wt%/75 wt% (modified slag/Portland cement), named PSC-MX. Cement manufactured with steelmaking (PSC-SS) was also prepared using the same ratio (25% slag/75% Portland cement), for comparison.

Compressive strength, according to Brazilian Standard NBR 11578 (analogous to European Standards EN 197-1, ISO EN 196-1 and ISO EN 196-3) and volume soundness (slag expansion), according to autoclave expansion test (standard ASTM C), were performed in PSC samples.
PSC hydraulic activities were determined by measuring the heat generated during hydration for 72h.

Results and Discussion

Table II presents the mineralogical phases of slag samples, determined by X-ray diffraction (XRD), adopting the Rietveld methodology for quantification.

Table II. Mineralogical phases (%) of Steel Slag and modified slags determined by XRD (Rietveld).

Phases		SS	SS-M4	SS-M6	SS-M7	SS-M8	SS-M9	SS-M10	SS-M11	SS-M12
Larnite	C2S	35,6					26	23	58,6	56,3
Brownmillerite	$Ca_2(Al,Fe)_2O_5$	38,7								
RO	FeO, MgO, MnO,CaO	21,5		0,6			22	30	29,4	31,3
Lime	CaO	4,2								
Merwinite	$3CaO,MgO,SiO_2$		34,9	29,5	30,4	27,4	39,7	25	4,5	
Monticellite	CaO,MgO,SiO_2		42,8							
Melilite	Aker + Geh			9,4		2,2				3,1
Akermanite	$2CaO,MgO,SiO_2$		10,9		15,6			8,5		
Srebrodolskite	$Ca_2Fe_2O_5$						2,6	10,2		
Magnetite	$Fe^{2+}Fe^{3+}{}_2O_4$							3,3		
Diopside	CaO,MgO,2SiO2									5,1
Enstat. Ferroan	$(Mg,Fe)SiO_3$			2,6						2,4
Gehlenite	$2CaO,Al_2O_3,SiO_2$			1,1			9,8		4,2	
Spinel(%)	$MgAl_2O_3$								1,3	1,8
Amorphous		-	11,5	56,8	54	68,1	0	0	0	0

As shown in Table II, the steel slag (SS) is mostly crystalline, because this type of slag has high basicity (CaO/SiO_2 = 3.8) and a high content of iron oxides, which can act as nuclei for crystallization[13]. The crystalline phases are those typically observed in steelmaking slags [14,4,8]: brownmillerite ($Ca_2(Fe,Al)_2O_5$), larnite (Ca_2SiO_4), RO phase (solid solution among FeO, MnO, MgO and CaO) and lime. The lime content, as determined by XRD (4.2 wt%), is too high to prevent volume soundness. The chemical composition of the RO phase determined through EDS analysis at different points of microstructure of Steel Slag, revealed a high MgO/FeO molar ratio (0,81), which is, together with free MgO and CaO, a limitation for the utilization of steelmaking slag in cement. The MgO/FeO ratio calculated with the mineralogical phases presented in Table II was similar (0,84), showing agreement between both methodologies. Qian et al. [6] reported that a higher MgO/FeO ratio in the RO phase increases potential reactivity with water, affecting the expansion of the material. According to the results, the RO phase is a Mg-rich wustite that has the potential to react with water to produce brucite ($Mg(OH)_2$).

Group 1

As shown in Table I, all modified slags of this group present low basicity, between 1,1 and 1,2, and alumina content of approximately 11%, excepting SS-M4, which presents 4,8% Al_2O_3. Slag SS-M7 was further reduced by modifying agents, resulting in lower FeO + Fe_2O_3 (4,2%)

compared to modified slags SS-M4, SS-M6 and SS-M8, which presented, respectively, 9,6; 8,7 and 10,8% $FeO+Fe_2O_3$.

As presented in Table II, crystalline phases are constituted mainly by calcium and magnesium silicates, such as Merwinite, Monticellite, Akermanite and Melilite (solid solution between Akermanite and Gehlenite). Furthermore, a significant reduction of RO phase was observed, that was caused in part by a decrease in iron oxides, due to the presence of modifying agents, and in part by transfer of MgO from RO phase to calcium and magnesium silicates. In addition to MgO stabilization as calcium and magnesium silicates, the elimination of free lime from steel slag was observed, preventing volume soundness.

Despite the low basicity of slag SS-M4, only 11,5% of amorphous phase was detected. Two main reasons explain such result, lower alumina content compared to other slags of the same group, which can reduce the possibility of glass formation and a lower Steel balls/slag mass ratio adopted in this experiment (1,8), promoting inappropriate cooling rate for amorphous phase stabilization.

In order to increase the amount of glassy phase, the Slag SS-M6 was produced containing higher alumina (11,6%) and adopting higher cooling rate (weight of steel balls/weight of slag ratio = 2,1) than adopted during the modification process of slag SS-M4. As shown in Table II, an increasing of amorphous phase to 56% was observed.

The simulation of solidification of slag SS-M6 under thermodynamic equilibrium exhibited in Figure 1 is relatively consistent with the experimental results. The slag cooled by steel balls corresponds to temperature of 1280°C with approximately 57 wt% glassy phase, and reveals the presence of Melilite (Akermanite + Gehlenite) and Merwinite, both phases observed in slag SS-M6 (table II).

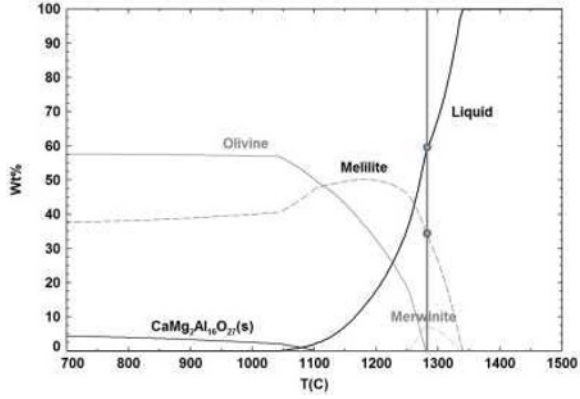

Figure 1. Simulation of SS-M6 slag solidification under thermodynamic equilibrium performed in FactSage™ software**.**

Based on a previous work[15], a modified slag, not only containing higher alumina, but also containing lower iron oxide and appropriate low basicity, presented the same behavior of a blast furnace slag, in terms of amount of glassy phase produced under fast cooling, because high iron oxide content acts as nuclei for crystallization[13].

Therefore, the slag SS-M7 was produced containing the same alumina content (11,6%) and cooling conditions (weight of steel balls/weight of slag ratio = 2,1) of SS-M6, but containing lower iron oxide ($FeO+Fe_2O_3$ = 4,3%).
As shown in Table II, the amount of amorphous phase was almost the same observed in SS-M6, indicating that the decreasing of $FeO+Fe_2O_3$ from 8,7% to 4,3% was insufficient to affect the amount of glassy phase, which it is lower than the glassy phase present in blast furnace slags cooled by water quenching.
The slag SS-M8 was produced in the same condition of slag SS-M6, excepting by the Steel balls/slag ratio, which was increased from 2,1 to 2,9. As shown in Table II, 68% of amorphous phase was observed in slag SS-M8, indicating a significant effect of the cooling conditions on the amorphous phase stabilization. In fact, Figure 1 shows a sloped *liquidus* cooling line, indicating that any modification in the cooling conditions can result in an abrupt changing in the amorphous phase. A heat transfer model has shown an average cooling rate, up 1200°C, of approximately 8 °C/s for SS-M8 slag, higher than the average cooling rate calculated for SS-M6 (4,7 °C/s).

Group 2

As shown in Table I, a significant fraction of Fe^{3+} content in the slags of this group was reduced, causing an increasing of Fe^{2+}. The increasing of Fe^{2+} caused a decreasing of MgO/FeO ratio of the RO phase, preventing volume soundness. The chemical composition of the RO phase, determined by EDS analysis in several points of RO phase of the microstructures of slags SS-M11 and SS-M12, revealed lower MgO/FeO ratios than Steel Slag (SS), respectively 0,41 and 0,42; indicating the formation of Mg-poor wustite, which presents less potential to react with water and consequent expansion, according to Qian et al[6].
Slags SS-M9 and SS-M10 were produced with lower basicity than slags SS-M11 and SS-12, to evaluate the effect of this parameter on the slag crystallization. In addition, slags SS-M9 and SS-M11 were naturally cooled in the metallurgical reactor where the modification process occurred, whereas slags SS-M10 and SS-M12 were cooled by steel balls. As observed in Table II and, as expected, an increase of basicity caused an increase of C_2S in the crystallized slags. In addition, an increase of cooling rate, by the presence of steel balls, caused a decrease of the size of C_2S crystals, as shown in Figure 2.

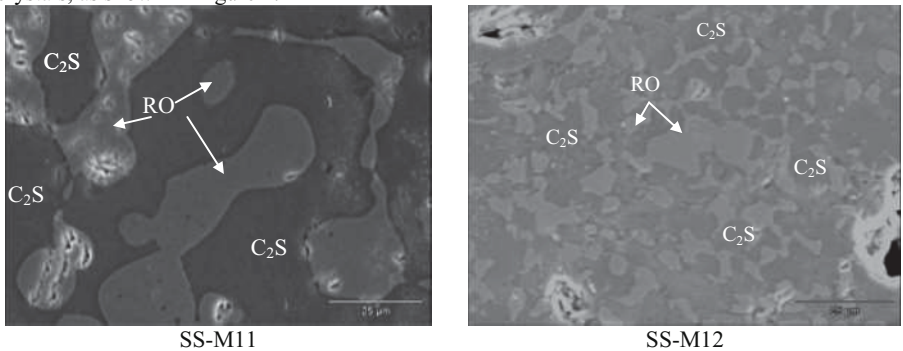

SS-M11 SS-M12

Figure 2. Microstructures of modified slag SS-M11 (naturally cooled) and SS-M12 (cooled by steel balls).

Figure 3 presents the simulation of the solidification of slags SS-M10 (B = 1,64) and SS-M12 (B = 1,97) under thermodynamic equilibrium, showing the effect of the basicity on the C_2S fraction of crystalized slag. In the same figure the prediction of RO formation is presented, phase observed in crystallized slags of this group. The simulation predicts relatively well the phases obtained during slag crystallization.

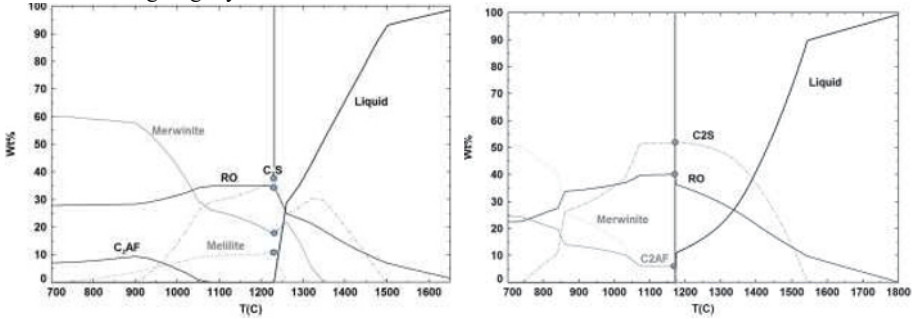

SM-10 SM-12

Figure 3. Simulation of solidification of slags SS-M10 and SS-M12 under thermodynamic equilibrium performed in FactSage™ software**.**

Table III shows the heat generated in 72 h, expansion determined according to autoclave test and compressive strength in ages of 3, 7 and 28 days for cement samples produced with 75% of ordinary Cement and 25% of Steel Slag (PCS-SS) and with 75% of ordinary Cement and 25% modified slags of groups 1 and 2 (PCS-MX).

Table III. Heat generated in 72 h, expansion in autoclave and compressive strength in 3, 7 and 28 days of cements samples produced with 25% of slag and 75% of ordinary cement.

		Group 1				Group 2			
	PCS-SS	PCS-M4	PSC-M6	PSC-M7	PSC-M8	PSC-M9	PSC-M10	PSC-M11	PSC-M12
Heat (72 h) (J/g)	280,5	278,2	303,9	307,3	284,3	297,4	299,3	N.D	N.D
Expansion Autoclave (%)	0,44	0,07	0,04	0,04	ND	0,07	0,08	0,07	0,08
R 3d (MPa)	27	28,3	26,6	28	30,2	27,8	27,1	29,4	29,8
R 7d (MPa)	34,1	31,2	34,7	32,9	37,1	33,9	34,1	34	35,4
R 28d (MPa)	41,1	36,9	41,3	43,8	45,3	35,5	39,5	40,7	42,4

As shown in Table III, the heat generated in most samples is higher than the heat generated in cement sample manufactured with 25% of Steel Slag (PCS-SS). Furthermore, cement samples produced by adding modified slags presented expansions much lower than that determined for cement sample produced by adding steel slag without any modification.

Regarding group 1, cement samples produced by adding slags SS-M6 and SS-M7 presented higher compressive strengths than cement produced by adding Slag SS-M4, especially for 28 days, since those slags have higher contents of amorphous phase. Moreover, cement produced with slag SS-M7 shows better results, in terms of compressive strength, than cement sample produced with slag SS-M6, especially for 28 days, indicating that an amorphous phase with lower iron oxide can be more reactive than an amorphous phase containing high iron oxide content.

In addition, an improvement of cooling conditions of slag SS-M8, increasing the amount of amorphous phase to 68%, resulted in an increasing of compressive strength in 28 days of cement produced with such slag, compared with cement sample produced with slag SS-M6, which contained nearly the same iron oxide. Therefore, is possible to expect an additional increase of compressive strength of cement produced with slag SS-M8, if it would have lower iron oxide content. This possibility will be investigated in the future.
Concerning group 2, an increase of C_2S in slags SS-M11 and SS-M12 compared to slags SS-M9 and SS-M10, caused an increase of compressive strength of cements samples produced by adding such slags. Moreover, comparing the pair of cements samples PSC-M10 x PSC-M9 and PSC-M12 x PSC-M11, an increase of compressive strength in cement samples produced by adding slags cooled faster (SS-M12 and SS-M10) was observed, probably caused by a higher reactivity of slags containing smaller C_2S crystals.
It is noticed a few differences of compressive strengths comparing cement sample PCS-SS and cement samples produced by adding modified slags. Probably, the presence of C_2S and free CaO in Steel Slag is contributing for the strength of cement sample. However, despite this compressive strength, Steel Slag caused significant volume soundness in cement sample PCS-SS, whereas PCS-MX samples, produced by adding modified slags, presented much lower expansions.

Conclusions

The main conclusions can be summarized as follows:

Lower basicity, higher alumina and lower iron oxide content in modified slags contributed to the glassy phase formation under fast cooling. MgO was stabilized in calcium and magnesium silicates and free lime was eliminated by the molten slag treatment.
The partial reduction of Fe^{3+} to Fe^{2+} for a basicity of approximately 1,8, stabilized C_2S and RO, with low MgO/FeO ratio, as the main crystalline phases of modified slags. An increase of basicity from 1,6 to 1,8, caused an increase of C_2S in the crystallized slag, whereas an increase of cooling rate caused a decrease of the size of C_2S crystals.
Cement samples produced by adding 25% of modified slags, containing higher fraction of amorphous phase or containing smaller C_2S crystals, to ordinary cement, resulted in an increasing of compressive strengths compared with cement sample produced by adding Steel Slag. In addition, Steel Slag caused significant expansion in cement sample, whereas PCS-MX samples, produced by adding modified slags, presented much lower expansions.

Acknowledgements

The authors acknowledge the financial support from InterCement and Embrapii.

References

1. Belhadj E, Diliberto C, Lecomte A (2012) Characterization and activation of Basic Oxygen Furnace slag. Cement and Concrete 34, 34-40.
2. Faraone N, Tonello G, Furlani E, Maschio S (2009) Steelmaking slag as aggregate for mortars: Effects of particle dimension on compression strength. Chemosphere 77, 1152-1156.

3. Li JX, Yu QJ, Wei JX, Zhang TS (2011) Structural characteristics and hydration kinetics of modified steel slag. Cement and Concrete 41, 324-329.
4. Tossavainen M, Engstrom F, Yang Q, Menad N, Larsson ML, Bjorkman B (2007) Characteristic of steel slag under different cooling conditions. Waste Management 27, 1335-1344.
5. Kriskova L, Pontikes Y, Pandelaers L, Cizer O, Jones PT, van Balen K, Blanpain B (2013) Effect of High Cooling Rates on the Mineralogy and Hydraulic Properties of Stainless Steel Slags. Metallurgical and Materials Transaction B 44, 1173-1184.
6. Qian GR; Sun DD; Tay JH; Lai ZY (2002) Hydrothermal reaction and autoclave stability of Mg bearing RO phase in steel slag – British Ceramic Transactions 101, 4, 159-164.
7. Mostafa NY, El-Hemaly SAS, Al-Wakeel EI, El-Korashy SA, Brown PW (2001) Characterization and evaluation of hydraulic activity of water-cooled slag and air-cooled slag. Cement and Concrete Research 31, 899-904.
8. Gautier M, Poirier J, Bodenan F, Franceschini G, Véron E (2013) Basic oxygen furnace (BOF) slag cooling: Laboratory characteristics and prediction calculations. International Journal of Mineral Processing 123, 94–101.
9. Ferreira Neto JB, Ribeiro TR, Lotto AA, Quarcioni VA, Chotoli FF (2014) Sistema de Modificação de Escória, Patent application BR 10 2014 023505 1.
10. Xu Z, Hwang J, Greenlund R, Huang X, Luo L, Anschuetz S (2003) Quantitative Determination of Metallic Iron Content in Steel-Making Slag". Journal of Minerals and Materials Characterization and Engineering 2, 65-70.
11. Solvi M, Greiveldinger B, Hoffmann M, Friederici C, Michels D (2012) Granulation of metallurgical slag. WO2012/0836 A1, pp 1–15.
12. Kappes H, Michels D (2015) Dry slag granulation and energy recovery. In: Proceedings of the fourth international slag valorization symposium. Leuven, pp 39–52.
13. Jung SS, Sohn II (2013) Effect of FeO Concentration on the Crystallization of High-Temperature CaO-Al2O3-MgO-FeO Melts. Journal American Ceramic Society 96, 4, 1309-1316.
14. Shi CJ (2004) Steel Slag – Its Production, Processing, Characteristics and Cementitious Properties. Journal of Materials in Civil Engineering 16, 230-236.
15. Ferreira Neto, J. B.; Faria, J. O. G. ; Fredericci, C.; Chotoli, F. F.; Silva, A. L. N.; Ferraro, B. B.; Ribeiro, T. R. ; Malynowskyj, A.; Quarcioni, V. A. ; Lotto, A. A. . Modification of molten steelmaking slag for cement application. International Slag Valorisation Symposium Zero Waste, 4, 2015, Leuven. Proceedings, 2015. p. 1-7.

REWAS 2016: Towards Materials Resource Sustainability
Edited by: Randolph E. Kirchain, Bart Blanpain, Christina Meskers, Elsa Olivetti, Diran Apelian, John Howarter, Anne Kvithyld, Brajendra Mishra, Neale R. Neelameggham, and Jeff Spangenberger
TMS (The Minerals, Metals & Materials Society), 2016

INCORPORATION OF SEWAGE SLUDGE INTO HEAVY CLAY CERAMIC BODY

Carlos Mauricio Fontes Vieira[1,a], Isabela Oliveira Rangel Areias [1,b], Sergio Neves Monteiro[2,c]

[1] State University of the North Fluminense Darcy Ribeiro – UENF
Av. Alberto Lamego 2000, CEP 28013-602, Campos dos Goytacazes, RJ, Brazil
[2]Military Institute of Engineering, IME, Materials Science Department
Praça General Tibúrcio, 80, Praia Vermelha, Urca, CEP 22290-270, Rio de Janeiro, RJ, Brazil
[a]vieira@uenf.br; [b]oraisabela@gmail.com; [c]snevesmonteiro@gmail.com.br

Keywords: Clay, Ceramic, Incorporation, Sewage sludge, Waste.

Abstract

This work has as its objective to evaluate the use of sewage sludge from wastewater treatment plant into heavy clay ceramic body. Compositions were prepared with amounts of 0, 2.5, 10 and 15 wt.% of sludge incorporated into the clay body. Rectangular specimens were obtained by 20 MPa pressure molding and then fired at 850ºC in a laboratory furnace. Characterization of the waste was done by X-ray-fluorescence, differential scanning calorimetry and thermogravimetric analysis. Ceramic properties related to the water absorption and compression strength were determined. The results indicated that the incorporation of the sludge into clay bricks must be done in low amounts. In higher amounts the sludge increases the water absorption and reduces the mechanical strength of the ceramic. This is a consequence of the changes caused in the porosity by the relatively elevated weight loss of the waste during the firing stage.

Introduction

Disposal of sewage sludge waste (**SSW**) is a worldwide problem for any municipality. Landfilling, incineration, dumping at sea and agricultural uses are the most common disposal methods [1-3]. Therefore, alternatives to reuse this type of waste by incorporation into building materials has been also investigated [4-7]. In particular to the brick-making industry, the high temperature firing stage, normally ranging from 700 to 1000ºC, is not only fundamental to the clay particles consolidation but can also permit the complete disintegration of organic compounds as well as the immobilization of inorganic contaminants, specially the chemical products, within the silicate phases eventually present in the waste.

In the county of Campos dos Goytacazes, located in the north region of the state of Rio de Janeiro, Brazil, the population is of approximately 480,000 people. In Campos, six wastewater treatment plants are response by the treatment of around 70% of the generated sewage, producing 160 ton/month of dry sludge.

Campos dos Goytacazes also has an important heavy clay ceramic production, with a production about 60 million pieces/month by 120 industries, basically bricks and minor amounts of roof tiles, rustic tiles and others.

Since the addition of sludge may affect the characteristics and properties of the final heavy clay ceramic products, this work has as its objective to characterize and to evaluate the influence of the incorporation of sewage sludge waste (**SSW**) in the technological properties of clayey ceramic.

Materials and Methods

The raw materials used in this investigation were a typical kaolinitic clay body, from the region of Campos dos Goytacazes, State of Rio de Janeiro, Brazil, usually applied in the fabrication of bricks, and sewage sludge waste (**SSW**) obtained in the Chatuba wastewater treatment plant also from Campos dos Goytacazes. The type of treatment of this plant involves anaerobic reactor ascendant Flow, anoxic filter, Biodrum filter, secondary and tertiary decanters.

The **SSW** was submitted to an inertization process to eliminate microorganisms and pathogens with calcium hydroxide. It was added 15 wt.% of calcium hydroxide to the **SSW**. After the application, the pH remains close to 12 for 2 hours and 11.5 for 48 hours, as recommended by the National Environmental Council [8].

Both raw materials were then dried at 110ºC before representative samples were separated by quartering. The chemical composition of the waste was obtained by fluorescence spectrometry in a Philips, PW 2400 equipment. The **SSW** was also submitted to differential scanning calorimetry and thermogravimetric analyses. These analyses were simultaneously conducted in a TA model SDT 2960 instrument operating under a flow of argon (100 $mL.min^{-1}$) and heating rate of 10ºC/min up to a maximum temperature of 1200ºC using a 25 mg powder sample, screened at 200 meshes (75 μm).

Different mixtures were prepared with amounts of 0, 2.5, 10 and 15 wt.% of **SSW** incorporated into the clay. Rectangular (11.5x2.5x1.0 cm) specimens, with 8% of humidity, were molded by 20 MPa uniaxial pressure. These specimens were then dried at 110ºC for 24 h in a stove. The firing of the specimens was performed at 850ºC in an electric laboratory furnace. This range of temperatures is normally used in the fabrication of clayey bricks and roofing tiles. The heating rate of the electric furnace used for firing was 2ºC/minutes with two hours soaking at the maximum temperature. Cooling occurred by natural convection inside the furnace after it was turned off.

Five specimens for each composition were tested to obtain the technological properties related to linear shrinkage, water absorption and compression strength. The water absorption was determined according to standard procedure [9]. The compressive strength, samples with 25x10 mm of square section by 25 mm of height, was determined in an Instron 5582 Universal Testing Machine.

Results and Discussion

The chemical composition of the **SSW**, Table I, shows that SiO_2, CaO, Al_2O_3 and Fe_2O_3 are the most predominant oxides present in the waste. The **SSW** also displays a

relatively large amount of LoI that is associated mainly to the presence of organic matter, as will be shown in Fig. 1. High LoI can be a disadvantage during the firing stage of the ceramic process owing to the possibility of increasing the porosity as well as causing excessive shrinkage of the pieces. The significant amount of Fe_2O_3 may contribute for the reddish color of the ceramic after firing stage. It is important to mention that the amount of Al_2O_3 and Fe_2O_3 in the **SSW** can also be caused, to a certain extent, by the aluminum sulphate and iron chloride used as floculant agents. The CaO content is due to the use of calcium hydroxide to stabilize the waste.

Table I. Chemical composition of **SSW** (wt.%).

Al_2O_3	SiO_2	Fe_2O_3	K_2O	MgO	MnO	Na_2O	CaO	P_2O_5
8.83	14.26	7.78	0.71	0.76	< 0.05	0.19	12.78	2.04
TiO_2	BaO	Co_2O_3	Cr_2O_3	PbO	SrO	ZnO	ZrO_2+HfO_2	LoI
0.63	< 0.1	< 0.1	< 0.1	< 0.1	< 0.1	0.11	< 0.1	43.57

Figure 1 shows the DSC/TG/DTG curves for the **SSW**. In these curves two endothermic and one exothermic peak were identified. The first endothermic peak, which occurs at 132.52ºC associated with a weight loss of 5.1%, is characteristic of released physically adsorbed water. The first exothermic peak at 302.02ºC, can be related to the oxidation of organic matter. The weight loss associated with this reaction is 23.92%. The second endothermic peak, at 685.85ºC, is associated with calcium carbonate, calcite, decomposition and corresponds to a weight loss of 7.39%. As discussed previously, if organic matter promotes the appearance of porosity, on the other hand, energy economy can be an important advantage to reduce the fuel consumption during the firing stage of the ceramic. It can be observed in Fig. 1 that the heat flow due to the combustion of organic matter is of 2973 J/g or 710 kcal/kg. Considering that are necessary 265 kcal to sintering 1 kg of clay [9], the energy economy with the use of 1 wt.% of **SSW** incorporated into the clay is of approximately 2.7%.

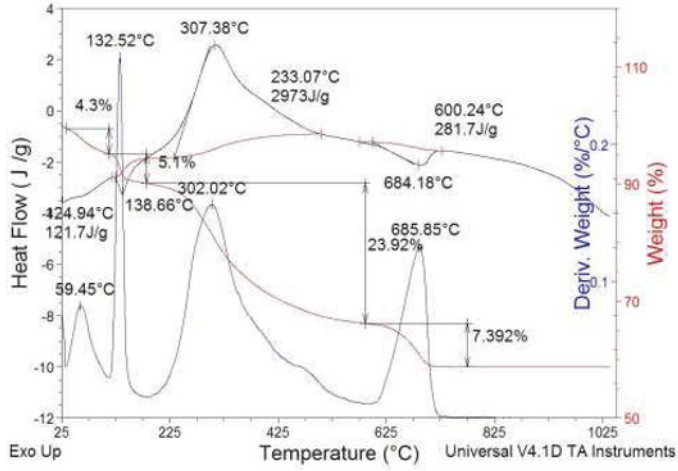

Figure 1. DSC/TG/DTG curves of the **SSW**.

Figures 2 and 3 show, respectively, the water absorption and compression strength of the fired compositions as a function of **SSW** addition.

One should observe in Fig. 2 that the **SSW** addition abruptly increases the water absorption of the pure clay body with 10 and 15 wt.% addition. This result can be explained by the increment in weight loss, mainly due to the organic matter combustion. It is also observed that the compositions with 0 and 2.5 wt.% **SSW** attend the specification for bricks [ref], i.e., 22%. Compositions with higher amounts of **SSW** do not attend the Brazilian norm. Finally, none composition attend the water absorption for roof tiles, i.e., 20%, at the investigated temperature.

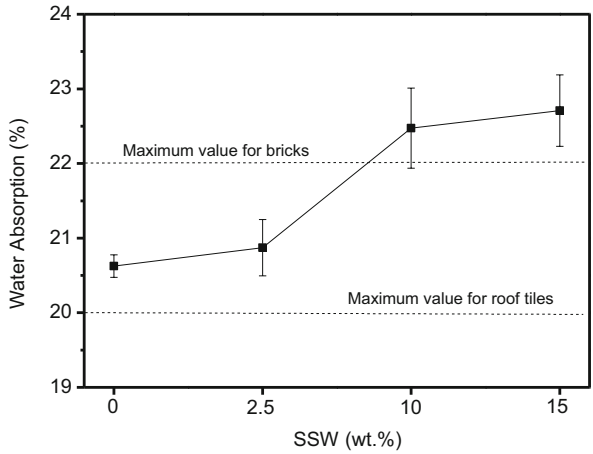

Figure 2. Water absorption of the clay as a function the amount of **SSW** addition fired at 850ºC.

It could be seen in Fig. 3 that the compression strength of the pure clayey body is decreased with **SSW** additions. This is consequence of the increase in porosity, mainly due to the organic matter combustion presents in the waste. It is well-known that the porosity has a marked influence on the mechanical strength of the ceramic [11]. The reduction of the compression strength of the clay with 2.5, 10 and 15 wt.% of **SSW** was 22.9, 34.1 and 57%, respectively.

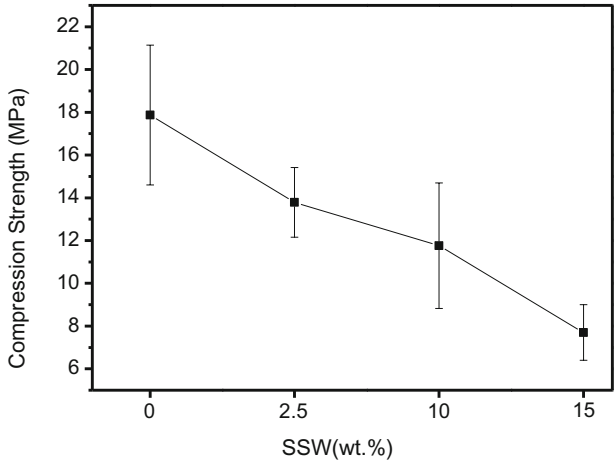

Figure 3. Flexural rupture strength of the clay as a function the amount of **SSW** addition fired at 850ºC.

As a final remark, it can notice that the sludge from wastewater treatment plant is nowadays a worldwide environmental problem. The recycling/reuse of wastes is preferred, rather than its simple disposal. This work showed that the brick-making industry may be receptor of this type of waste. However, the incorporations must be done in low amount to avoid the damaging of the technical performance of the product. Another important aspect to its recycling into heavy clay ceramic fabrication is the necessity to submitted the **SSW** to an inertization process to eliminate microorganisms and pathogens.

Conclusions

The characterization of a sludge waste obtained from wastewater treatment plant and its incorporation into clay used for building ceramics, led to the following conclusions:

- The waste has an elevated loss on ignition mainly due to the relatively high amount of organic matter that causes porosity in the fired ceramic. However, the heat flow of 710 kcal/kg, due to the combustion of organic matter, can possibility an energy economy of 2.7% with 1 wt.% of waste incorporated in the clay during the firing stage of the ceramic. The predominant chemical constituents are associated with SiO_2, CaO, Al_2O_3 and Fe_2O_3.
- The incorporation of the waste of up to 2.5 wt.% do not change the water absorption of the clayey body. However, in higher amounts, the waste abruptly increases the water absorption of the ceramic. With respect to the mechanical strength, any investigated amount of waste is deleterious to the mechanical strength of the ceramic.
- Finally, the incorporation of this type of waste in heavy clay can be advantageous for energy savings but must be done in low percentage to avoid increase in water absorption as well as significant decrease in mechanical strength of the ceramic.

Acknowledgement

The authors thank the Brazilian agencies CNPq, proc. n. 302930/2014-0 and FAPERJ, proc. n. E-26/201.192/2014 for supporting this research work. The authors are also thankful to the facilities provided by Águas do Paraíba Company.

References

1. U. Song and E.J. Lee, "Environmental and economical assessment of sewage sludge compost application on soil and plants in a landfill," *Resour. Conserv. Recycl*., 54 (2010), 1109–1116.
2. A.B. Hernandez, J.H. Ferrasse, P. Chaurand, H. Saveyn, D. Borschneck and N. Roche, "Mineralogy and leachability of gasified sewage sludge solid residues", *J. Hazard. Mater*., 191 (2011), 219–227.
3. J.A. Cusidó, A. Lázaro and V. Cremades, "Environmental effects of using clay bricks produced with sewage sludge: Leachability and toxicity studies", *Waste Management,* 32 (2012), 1202–1208.
4. Y. Lina, S. Zhoua,F. Li and Y. Lina, "Utilization of municipal sewage sludge as additives for the production of eco-cement", *Journal of Hazardous Materials,* 213– 214 (2012), 457– 465.
5. M.I.A. Almeida, M.R.Amaral, A.M. Sousa Correia, na M. Fonseca Almeida, "Ceramic building materials: an alternative in disposal of sewage sludge", *Key Eng. Materials,* 132–136 (1997), 2280–2284.
6. M. Devant, J.A. Cusidó, and C. Soriano, "Custom formulation of red ceramics with clay, sewage sludge and forest waste", *Applied Clay Science,* 53 (2011), 669–675.
7. A.G. Liew, A. Idris, A.A. Samad, H.K. Wong, M.S. Jaafar and A.M Baki "Reusability of sewage sludge in clay bricks", *Journal of Material Cycles and Waste Management,* 6 (1) (2004), 41–47.
8. CONSELHO NACIONAL DO MEIO AMBIENTE – CONAMA, Resolução n° 375/06, "Define os critérios e procedimentos, para o uso agrícola de lodos de esgoto gerados em estações de tratamento de esgoto sanitário e seus produtos derivados, e dá outras providências", (2006).
9. American Society for Testing and Materials. "Water Absorption, Bulk Density, Apparent Porosity, and Apparent Specific Gravity of Fired Whiteware Products", C 373-72, 1972.
10. Más, E. "Quality and Technology in Heavy Clay Ceramic" (in Portuguese), Ed. Pólo Produções Ltda, São Paulo, 20102.
11. W.M. Carty and U. Senapati, "Porcelain-Raw Materials, Processing, Phase Evolution, and Mechanical Behavior," *J Am Ceram Soc.* 81 (1) (1998), 1-18.

Designing Materials and Systems for Sustainability

REWAS 2016: Towards Materials Resource Sustainability
Edited by: Randolph E. Kirchain, Bart Blanpain, Christina Meskers, Elsa Olivetti, Diran Apelian, John Howarter, Anne Kvithyld, Brajendra Mishra, Neale R. Neelameggham, and Jeff Spangenberger
TMS (The Minerals, Metals & Materials Society), 2016

INDUSTRIAL SYMBIOSIS AMONG SMALL AND MEDIUM SCALE ENTERPRISES: CASE OF MUZAFFARNAGAR, INDIA

Shourjomoy Chattopadhyay[a], Nandini Kumar[a], Charlie Fine[b], Elsa Olivetti[c]

[a]TERI University Institute for Industrial Productivity, [b]Sloan Management School [c] Department of Materials Science and Engineering, Institute of Technology, 77 Massachusetts Avenue, Cambridge, MA 02139, USA

Keywords: Industrial symbiosis, small and medium enterprises

Abstract

Developing countries like India, characterized by large working populations and significantly lower cost of capital, have become hotbeds for manufacturing activities. A distinctive feature in regions of India is that majority of the industrial material flows are through unorganized micro, small and medium scale enterprises (MSMEs). These highly constrained MSMEs have limited resources to comply with environmental regulations because of significant investments required in pollution control measures. An important way to improve the environmental performance of these industrial clusters is to quantify, treat, and reduce industrial byproducts. This objective could be achieved through industrial symbiosis or byproduct synergy, terms used for beneficial reuse of materials or energy streams from one facility by another. In the present study an attempt has been made to identify and understand existing and potential industrial symbiosis connections in Muzaffarnagar, an industrial town in north India home to several dozen paper mills, another dozen sugar mills, and a large range of other MSME manufacturing entities. In addition to the presence of small and medium enterprises there is also a strong bond between industry owners in the region.

Introduction

Industrial activity all over the world has increased over the last six or seven decades [1, 2]. Due to heavy concentration of population and inexpensive cost of capital in developing countries, including India, there has been a significant rise in manufacturing activities [3]. As of 2010, the manufacturing sector accounted for 15% of India's GDP. Increased industrial activity is synonymous with human development and improved life style conditions. Advancement in extraction, use and disposal of natural resources has been an integral part of this human development, but not without compromising resource availability [4]. This rapid unplanned development has led to depleting natural resources, waste management and increasing pollution becoming important concerns in the world today.

In the present study an attempt has been made to identify and understand industrial symbiosis activities in an industrialized region northwest of Delhi, India in a region called Muzaffarnagar. Industrial symbiosis represents a collective engagement of traditionally separate industries through exchange of materials [5]. Very few studies have been done in India on implementation of industrial symbiosis [3, 6]. In India, material flow through the informal sector is much larger than that through the organized industrial sector [7]. Hence, for a greater impact, any strategy for symbiosis has to factor in the informal sector [8].

The Muzaffarnagar region has a number of diverse industries (brick, paper, steel and sugar). The following summarizes the key findings of the industrial flows including collection of input and output data pertaining to the selected industries. This helped forming a material flow for the region. With the help of this flow, the existing symbiosis network was identified.

Results

The Muzaffarnagar region is home to 29 paper mills producing eight different types of paper. In addition there are 500 brick and three ceramic brick kilns, 43 steel mills and seven sugar mills. By mass percentage the share of annual production in the industry is 22% brick, 27% sugar, 29% paper and 22% sugar. The paper, steel and sugar industries are organized in nature. The brick industry is highly unorganized. The location of the paper and steel mills is in the old (within Muzaffarnagar city) and new (outside Muzaffarnagar city, along the national highway) industrial areas of the region. The brick kilns and the sugar mills are located in different parts of the district with no certain pattern to their locations.

The overall inflows outflows and exchanges found in the region are shown in Figure 1 below. shows the flow of materials through selected industries in the study area. The thick black line represents the system boundary for the study. The horizontal black arrows represent the inputs and outputs in the industries. The inputs and outputs specific to a particular industry have been placed near the box representing the industry. The direction of the arrow with respect to the system boundary signifies input or output. The vertical brown arrows represent the wastes being disposed into landfills, drains, etc. The red arrows represent flows within the system boundary. Distilleries have been kept at the system boundary to signify that only the symbiotic input into the system has been quantified.

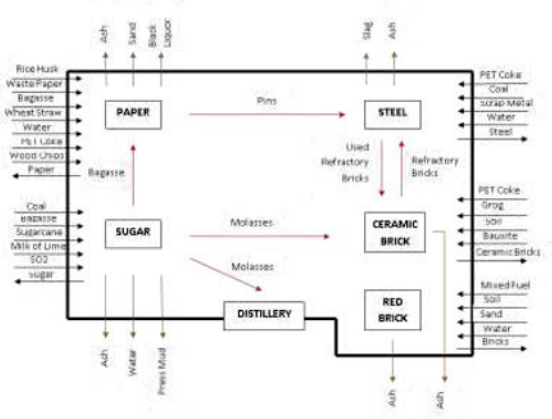

Figure. 1 Flow of materials through selected industries in Muzaffarnagar.

Figure 2a shows the inputs in the selected industries in terms of solids and liquids. Inputs include both raw material as well as energy sources. A few specifics are mentioned here by industry. For the brick facilities soil is the major solid input and a small volume of liquid is used. A major point of concern is that the soil used for making bricks is the fertile top soil. Even though there

are government regulations on the depth to which soil can be excavated for brick making, these are flouted all over the region. For paper the major input is the waste paper and bagasse used for pulping. The paper industry is quite water intensive because the industry is dependent on waste paper as one of the raw materials used in pulping. For steel the major input is scrap metal with coal and pet coke used as energy sources. Finally the solid input for the sugar industry is the highest because the volume of sugarcane needed for sugar extraction is very high. The liquid input (water) for this industry is also considerably higher than that for the brick industry but less than that of the paper industry.

Most of the industries in the area have a high dependence on fossil fuels as a power source. Coal and PET coke are extensively used in the steel and sugar (during off-season) mills. Even though the paper and brick industry use bio fuels, but many times these do not meet the fuel demands completely. It was concluded through stakeholder interviews that years of unchecked groundwater extraction has caused the groundwater table to fall drastically. Even though the industry hasn't yet faced any shortage of water, it is possible that water availability would become an issue in the future.

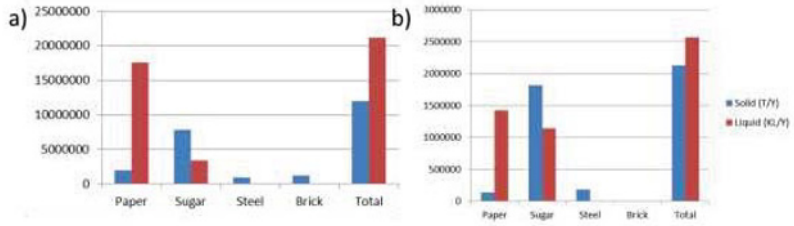

Figure 2. a) Inputs to selected industry in terms of solid and liquid. Inputs include raw material and fuel used. b) Waste output from selected industry in terms of solid and liquid. Solid flows are presented in tons per year and liquid flows in liters per year. *Input data for steel and waste data for steel and brick could not be completed.

Figure 2b shows the waste output from industries in terms of solid and liquid. Most of the wastes are disposed of in an unorganized manner. There are no official industrial landfills in the region for disposing of industrial wastes. Solid wastes are generally dumped in low lying land or on the side of roads. These have been referred to as 'unofficial landfills'. Liquid waste is put in drains which ultimately reach the major rivers flowing in the district.

Solid waste generated from the brick industry includes ash from the different fuels used such as rice husk, mustard seeds and wood chips as well as waste bricks from the production process. Solid waste outputs from the paper industry include boiler ash from the different fuel combinations used, pins, plastic and sand. Most of the boiler ash is rice husk. The liquid waste from the paper industry is black liquor. These are sent into drains which ultimately reach the major rivers in the region. These drains flow through the agriculture fields in the region. Crop productivity in these fields has been affected due to the black liquor. Thus there is soil contamination caused by this. Soil contamination may lead to groundwater contamination in the long run. Thus, black liquor is a big environmental burden for the region. More than 180000 T/Y of solid wastes is generated from the steel industry. This includes slag and used molds. Slag is

disposed of in unofficial landfills. Most of the used molds are sent back to the ceramic units where they were produced to be reused in the production processes. Large quantities of solid waste are generated in the manufacture of sugar. Liquid waste from sugar includes molasses and waste water. Molasses is sent to distilleries for production of alcohol while the waste water is discharged to drains.

Finally, the existing symbiosis and reuse information was synthesized from the input and output flows cataloged above. Figure 3 shows a comparison of final disposal of all wastes (solid &liquid) generated by selected industries in Muzaffarnagar, including and excluding the sugar industry. The key findings of this study relate to the areas to develop symbiotic activity, in the future. The key output flows that could be reused more beneficially are ash, black liquor, and plastic waste from the paper industry as well as press mud from the sugar industry.

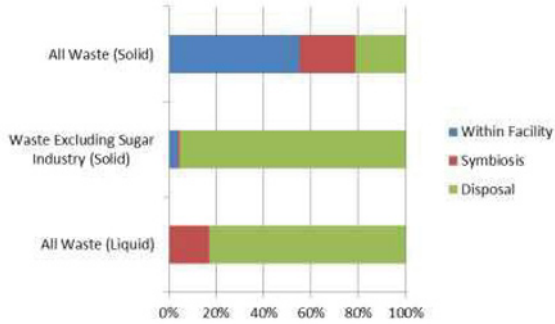

Figure 3. Waste by mass or volume broken down by fate including within facility reuse, symbiotic exchanges and disposal

References

1. Geng, Y., Q. Zhu, and M. Haight, *Planning for integrated solid waste management at the industrial Park level: A case of Tianjin, China.* Waste management, 2007. **27**(1): p. 141-150.
2. Vigneswaran, S., V. Jegatheesan, and C. Visvanathan, *Industrial waste minimization initiatives in Thailand: concepts, examples and pilot scale trials.* Journal of Cleaner Production, 1999. **7**(1): p. 43-47.
3. Bain, A., et al., *Industrial symbiosis and waste recovery in an Indian industrial area.* Resources, Conservation and Recycling, 2010. **54**(12): p. 1278-1287.
4. Ehrenfeld, J.R., *Industrial Ecology Paradigm Shift or Normal Science?* American Behavioral Scientist, 2000. **44**(2): p. 229-244.
5. Chertow, M.R., *Industrial symbiosis: literature and taxonomy.* Annual review of energy and the environment, 2000. **25**(1): p. 313-337.
6. Singhal, S. and A. Kapur, *Industrial estate planning and management in India—an integrated approach towards industrial ecology.* Journal of Environmental management, 2002. **66**(1): p. 19-29.
7. Erkman, S. and R. Ramaswamy. *Cleaner production at the system level: industrial ecology as a tool for development planning (case studies in India)*. in *United Nations Environmental*

Programme (UNEP): Plenary Lecture presented at UNEP's 6th High Level Seminar on Cleaner Produciton, Montreal, October. 2000.
8. Chertow, M.R., W. Ashton, and R. Kuppalli, *The industrial symbiosis research symposium at Yale: advancing the study of industry and environment*. 2004: Yale School of Forestry & Environmental Studies New Haven, CT.

REWAS 2016: Towards Materials Resource Sustainability
Edited by: Randolph E. Kirchain, Bart Blanpain, Christina Meskers, Elsa Olivetti, Diran Apelian, John Howarter, Anne Kvithyld, Brajendra Mishra, Neale R. Neelameggham, and Jeff Spangenberger
TMS (The Minerals, Metals & Materials Society), 2016

LIFE CYCLE ASSESSMENT OF METALLURGICAL PROCESSES BASED ON PHYSICAL FLOWSHEET MODELS

Madeleine Scheidema[1], Markus Reuter[2], and Antti Roine[1]

[1]Outotec (Finland) Oy, Kuparitie 10, FI-28101 Pori, Finland
[2]Helmholtz Institute Freiberg for Resource Technology
Halsbrücker Straße 34, 09599 Freiberg, Germany

Keywords: "Process Modeling, Environmental Footprints, LCA, Recycling"

Abstract

Simulation combined with Life Cycle Assessment (LCA) can be used to quantify the environmental impact of metals production processes. The results for different processing options, as well as the effect of having the same plant at different locations can be evaluated and compared. HSC SIM 8, which is linked with GaBi, or other LCA software can be used to carry out this work. The material flows are calculated using HSC SIM, and they are then converted to environmental indicators. The refining of silver using the High Current Density (HCD) electrorefining process is used as an example in this paper in order to show the link between simulation software and LCA.

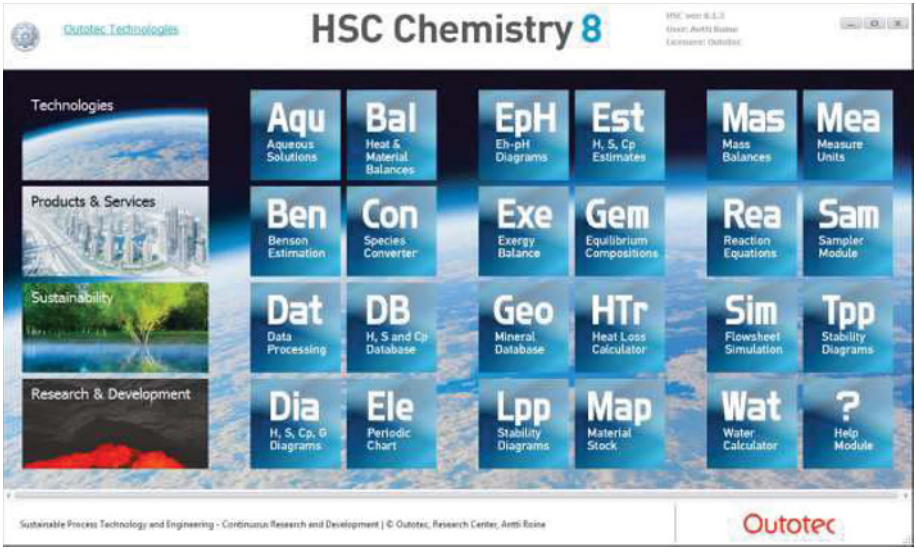

Figure 1: HSC Main Menu with links to modules.

Introduction

HSC Chemistry 8 modeling and simulation platform is a tool for process R&D, design, and digitalization, Figure 1 [1]. It may be used to estimate variables such as process efficiencies, yields, and environmental footprints. The software makes it possible to carry out thermodynamic and mineral processing calculations on a standard computer.

HSC development started at 1960s in Outokumpu Oy. More than 20000 licenses have been sold since 1987. The HSC contains 24 modules for process development and 12 databases which HSC modules utilize automatically.

HSC contains several modules for different type of applications, such as equilibrium, EpH, heat balances, heat transfer, etc. The HSC SIM module is a main platform for process flowsheet models, the process calculation results may be connected to environmental footprint calculations.

In order to minimize the environmental impact of metals production processes, in-depth knowledge of the process in terms of techno-economic understanding as well as simulation of the system is required [2]. For simulation, tools such as HSC SIM 8 [1] can be used, in which process design data, thermodynamic data, and/or process data are used. Life Cycle Assessment tools can then be used to quantify the environmental performance, based on the results obtained from simulation. This will reveal the strengths and weaknesses of the processes and enable the improvement of resource efficiency through innovation [2].

Copper is a key enabler of resource efficiency [2, 3], since primary copper minerals as well as secondary copper materials carry numerous technology elements [4]. Technology elements are valuable minor elements, such as silver and gold. It is possible to concentrate technology elements during the processing of copper and also other base metals such as zinc, lead and nickel to some extent and extract them during the refining stage [3]. A detailed overview of the technology elements that can be recovered through different process routes, visualized as the Metal Wheel, can be found in [5, 6].

Because copper is such an important element, its environmental impact through different processing routes has already been evaluated [3, 4, 5]. In addition to the copper production process, the impact of recycling applications has also been evaluated for small household appliances [2], LED lamps [5, 7], E-waste and copper scrap smelting using TSL technology [5], as well as nickel pig iron production [8] and lead smelting [7]. The environmental impact of a copper concentrator plant has also been evaluated [9]. In this article, the environmental impact of the refining step of silver – a technology element – will be shown as an example.

Methodology

Linking HSC SIM or similar types of simulation software with Life Cycle Assessment (LCA) software, such as GaBi [9], enables the evaluation and quantification of the environmental performance of a specific process or plant at a specific location. The use of simulation software will also ensure the use of closed mass and energy balances. The link between HSC SIM and GaBi will make it possible to create GaBi processes from the HSC SIM process simulation

models for plants or reactors. The information extracted from HSC SIM is a blackbox, which only shows the major in- and outflows. [4]

A Life Cycle Assessment includes the obtaining of raw materials, production, use, and disposal [10]. Thus not only the direct impact from the plant is taken into account, but also indirect impacts. The different types of emissions are defined in the Greenhouse Gas (GHG) Protocol [11] as Scopes 1–3. Scope 1 emissions are direct GHG emissions from the plant. Scope 2 emissions are indirect GHG emissions from the production of purchased electricity. Scope 3 includes other indirect GHG emissions from both upstream and downstream activities, for example, the production of fuels and materials, and from waste handling.

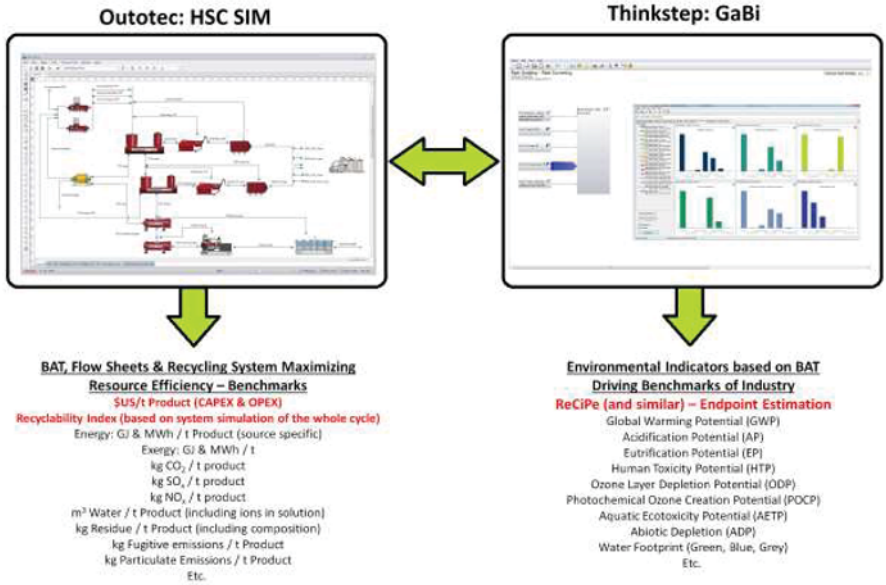

Figure 2. HSC SIM 8 [2] linked with GaBi [9].

Figure 2 shows the link between HSC SIM software and GaBi. In HSC SIM the material flows are calculated, which are then converted in GaBi to environmental indicators such as Global Warming Potential, Acidification Potential, Eutrophication Potential, and Photochemical Ozone Creation Potential (summer smog).

Example: Silver refinery

In the High Current Density (HCD) silver electrorefining process, silver anodes from Doré casting are dissolved in electrorefining cells and continuously deposited on cathodes. Silver is removed from the cathode using an automated scraper system and it is collected at the bottom of the cell. Impurities such as gold and PGMs are collected in anode bags and can be refined

further. The cell contents are discharged into a sieve tank; the electrolyte is returned to the circulation tank and the silver is washed and dried. The emission of NOx gases from the electrolysis cells is avoided by automatic control of the pH and temperature of the electrolyte. The operators' manual work is reduced to a minimum due to a high degree of automation. [12, 13] Please note that this process is only a small step in the entire metals production chain. An LCA of only part of the process can, however, be useful when considering different processing options for the refining step, or when considering a change in the materials flow through the system.

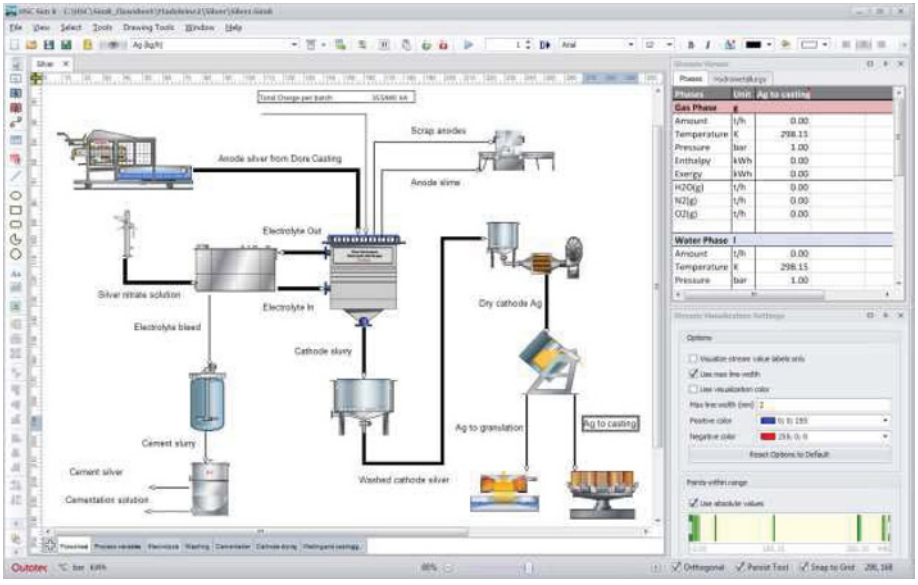

Figure 3. Flowsheet of silver refinery model created using HSC SIM 8 [2].

The evaluation comprises the following steps: A simulation model is created based on design data, experimental data, plant data, or on their combination thereof, in HSC SIM, as shown in Figure 3.

The streams of the flowsheet are collected and mapped, using the 'LCA Evaluation' tool in SIM. The mapping is used so that the SIM stream names are linked to their equivalents in the GaBi database. It is also specified whether the stream is released to the nature or remains in the technosphere, which has an influence on the impact. The main product is selected (in this case cathode silver) and the other streams are normalized at around one kilogram of main product. Additional information, which is not in the simulation model, can be added as manual inputs and outputs. The data can then be exported directly to GaBi as a process or as an Excel file that can be used in other LCA software.

Figure 4. Sim LCA Evaluation dialog is used to map the Sim streams to LCA database streams.

The process is now ready for use in GaBi and the origin (country) of the input streams can be specified. In this case, European mixes were used when possible and German mixes were used when no European equivalent was available. A comparison of the footprint between different geographical locations can be made by changing the country of origin of the input streams. This may have a large effect on the results because local conditions vary a lot. Cathode silver was selected as main product of the Output streams, Figure 4.

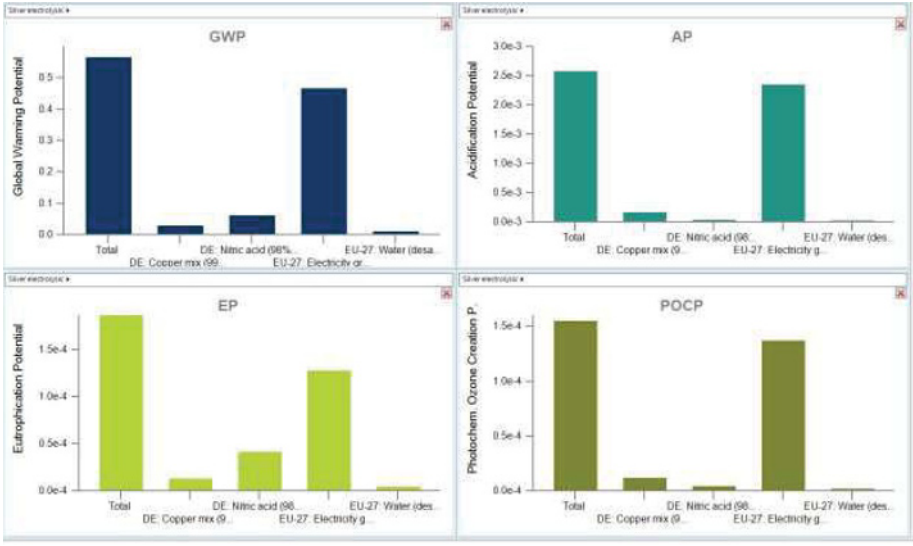

Figure 5. The impact of the silver refining process, given using four main indicators: Global Warming Potential (GWP), Acidification Potential (AP), Eutrophication Potential (EP), and Photochemical Ozone Creation Potential (POCP).

The impact of the process can be calculated using different indicators; in this case four main indicators were used: Global Warming Potential (GWP), Acidification Potential (AP), Eutrophication Potential (EP), and Photochemical Ozone Creation Potential (POCP). The results of the impact assessment are shown in Figure 5. The results of the LCA analysis show that the main environmental impact for each of the four indicators comes from the production of electricity. Electricity is not only used for electrolysis, but also for pumps and other auxiliary equipment. The GWP is strongly dependent on the electricity grid mix that is used, as the production method will determine the footprint. This is illustrated in Figure 6 by showing the global warming potential for the production of one kilogram of cathode silver in different countries, thus using different electricity mixes.

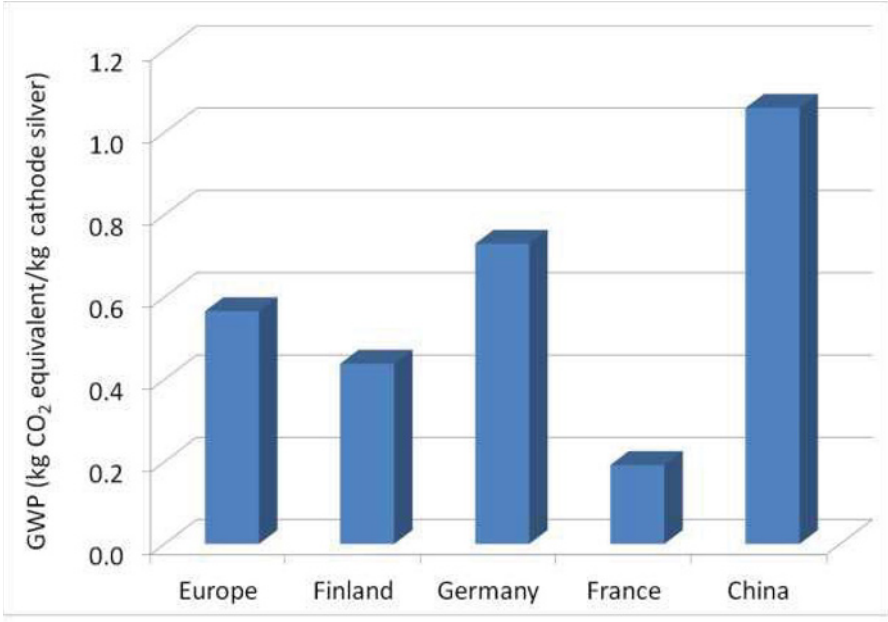

Figure 6. The effect of the choice of electricity grid mix on the Global Warming Potential.

Conclusions

The link between simulation and Life Cycle Assessment (LCA) was illustrated using the High Current Density (HCD) electrolytic refining of silver as an example. The process calculations were carried out using HSC SIM8, after which the input and output flows were mapped and exported to GaBi. The environmental impact of the silver refining process was evaluated using the following indicators: Global Warming Potential (GWP), Acidification Potential (AP), Eutrophication Potential (EP), and Photochemical Ozone Creation Potential (POCP).

References

[1] Roine, A. HSC Chemistry 8.0 User's Guide. Report 14024-ORC-J. Outotec Research Center. Finland 2014. www.outotec.com

[2] Reuter, M. A. Plenary Lecture: Copper – A Key Enabler of Resource Efficiency. In: Proceedings of Copper/Cobre 2013, Santiago, Chile, December 1–4, 2013. Instituto de Ingenieros de Minas de Chile, Vol. 1, pp. 23-37.

[3] Reuter, M. A.; Kojo, I. V. Copper: A Key Enabler of Resource Efficiency. World of Metallurgy - ERZMETALL, 2014. Vol. 67, No. 1, pp. 46-53.

[4] Reuter, M. A.; Kojo, I.; Roine, A.; Jåfs, M.; Gediga, J.; Florin, H. Environmental Footprinting of Metallurgical Copper Processing Technology – Linking GaBi to HSC SIM. In: Proceedings of Copper/Cobre 2013, Santiago, Chile, December 1–4, 2013. Instituto de Ingenieros de Minas de Chile, Vol. 1 pp. 181-194.

[5] Reuter, M. A.; van Schaik, A. Product-Centric Simulation-Based Design for Recycling: Case of LED Lamp Recycling. Journal of Sustainable Metallurgy, 2015. Vol. 1, Issue 1, pp. 4–28.

[6] Reuter et al. UNEP Metal Recycling: Opportunities, Limits, Infrastructure. A Report of the Working Group on the Global Metal Flows to the International Resource Panel of the United Nations Environmental Programme, 316 p. Link: http://www.unep.org/ resourcepanel/Portals/24102/PDFs/Metal_Recycling_Full_Report.pdf

[7] Reuter, M.A.; Matusewicz, R. van Schaik, A. Plenary Lecture: Lead, Zinc and their Minor Elements: Enablers of a Circular Economy. World of Metallurgy - ERZMETALL, 2015, Vol. 68, No. 3, pp. 132–146.

[8] Reuter, M. A.; van Schaik, A.; Gediga, J. Simulation-Based Design for Resource Efficiency of Metal Production and Recycling Systems: Cases – Copper Production and Recycling, E-Waste (LED lamps) and Nickel Pig Iron. The International Journal of Life Cycle Assessment, 2015. Vol. 20, Issue 5, pp. 671–693.

[9] Kotiranta, T.; Horn, S.; Jansson, K.; Reuter, M. Towards a 'Minimum Impact' Copper Concentrator: A Sustainability Assessment. To be presented at Procemin 2015, 11th International Mineral Processing Conference, October 21–23, 2015, Santiago, Chile.

[10] GaBi ts (1992-2015) "Software and System Databases for Life Cycle Engineering", Stuttgart-Ecahterdingen, http://www.gabi-software.com/software/

[11] International Standard ISO 14040 Environmental Management– Life Cycle Assessment – Principles and Framework, 1997. 12 p.

[12] The Greenhouse Gas Protocol, link: http://www.ghgprotocol. org/files/ghgp/public/ghg-protocol-revised.pdf

[13] Outotec Silver Refining Plant brochure, http://www.outotec.com/en/Search-material/

[14] Maliarik. M. et al. High Current Density Silver Electrorefining Process: Technology, Equipment, Automation and Outotec's Silver Refinery Plants. In: Proceedings of the 7th International Symposium on Hydrometallurgy, June 22–25, 2014. Volume 2, pp. 91–100.

REWAS 2016: Towards Materials Resource Sustainability
Edited by: Randolph E. Kirchain, Bart Blanpain, Christina Meskers, Elsa Olivetti, Diran Apelian, John Howarter, Anne Kvithyld, Brajendra Mishra, Neale R. Neelameggham, and Jeff Spangenberger
TMS (The Minerals, Metals & Materials Society), 2016

TOTAL-CORROSION EFFECTS OF *ANTHOCLEISTA DJALONENSIS* AND $Na_2Cr_2O_7$ ON STEEL-REBAR IN H_2SO_4: SUSTAINABLE CORROSION-PROTECTION PROSPECTS IN MICROBIAL/INDUSTRIAL ENVIRONMENT

Joshua Olusegun OKENIYI[1], Cleophas Akintoye LOTO[1,2], Abimbola Patricia Idowu POPOOLA[2]

[1]Mechanical Engineering Department, Covenant University, Ota 112001, Nigeria
[2]Chemical, Metallurgical and Materials Engineering Department, Tshwane University of Technology, Pretoria 0001, South Africa

Keywords: sustainable/eco-friendly corrosion inhibitor; macrocell corrosion measurement; total-corrosion analysis; concrete steel-reinforcement embedment; microbial/industrial simulating-environment; inhibition efficiency.

Abstract

This paper studies total-corrosion effects of *Anthocleista djalonensis* (green natural-plant) and $Na_2Cr_2O_7$ (well-known inhibitor, but environmentally-hazardous chemical) on steel-reinforcement in concrete immersed in 0.5 M H_2SO_4, simulating microbial/industrial environment. Equal-mass models of the plant leaf-extract and of $Na_2Cr_2O_7$ were employed as admixtures in steel-reinforced concrete samples immersed in the test-system, from which macrocell corrosion measurements were obtained and analysed as per ASTM G109-99a. Results showed that only the 3.33 g/L *Anthocleista djalonensis*, among the equal-mass models of leaf-extract and the chemical admixtures, was outperformed by the 3.33 g/L $Na_2Cr_2O_7$ in total corrosion reduction effects. In the study, 5.00 g/L *Anthocleista djalonensis* exhibited optimal effectiveness, η = 93.77%, on the total-corrosion effect of concrete steel-reinforcement. The many *Anthocleista djalonensis* admixtures that exhibited better inhibition than $Na_2Cr_2O_7$ admixtures indicates positive prospects of the plant as an eco-friendly and sustainable corrosion-protection alternative for the toxic chemical in microbial/industrial environment.

Introduction

Use of admixtures in concrete is identified in many studies with the capability to improve resistance of concrete and of the steel-rebar to corrosion attacks in acidic sulphate environments [1-3]. While many of these studies have employed chemical admixtures as corrosion inhibitors, due to their effectiveness and ease of applications, research focus is shifting towards use of green inhibitors due to inherent toxicity either of the chemicals or of the means of their syntheses. Usually, compounds of chromates have exhibited very good effectiveness at inhibiting steel-rebar corrosion in concrete immersed in sulphuric acid environments [1,3]. However, deleterious effects of the chromate compounds on living organs makes their usage unsustainable but is rather making restrictions on their use widespread in many regions of the world [4]. The issue with this compound is that its high effectiveness performance on the inhibition of metallic corrosion in aggressive media is making search for its replacement difficult.

Extracts from plants constitute rich biochemical sources [5], which are safe, non-toxic, and readily available with attendant potency of affordability even as many of them have been successfully employed for mitigating metallic corrosion in acidic medium. For example, extract obtained from the bark of *Anthocleista djalonensis* (*A. djalonensis*) A. Chev Loganiaceae have exhibited anticorrosive effect on aluminium metal in sulphuric acid medium [6]. Also, leaf-extract of *A. djalonensis* has been shown to exhibit negligible toxicity on experimental mice [7], a prospect of sustainability, even as it had been employed for concrete steel-reinforcement

corrosion in saline/marine simulating-environment in reported work submitted elsewhere [8]. However, there is dearth of study on the use of *A. djalonensis* leaf-extract for improving concrete steel-reinforcement resistance to sulphuric acid corrosion. No study has deliberated on comparison of the performance of *A. djalonensis* leaf-extract with that of $Na_2Cr_2O_7$ admixture in steel-reinforced concrete immersed in sulphuric acid medium.

Therefore, the objective of this study is to investigate effects *A. djalonensis* leaf-extract on the total corrosion of steel-rebar in concrete immersed in 0.5 M H_2SO_4, for simulating microbial/industrial environment. For this, comparison of the anticorrosion effectiveness of the green natural plant extract will be studied versus that of sodium dichromate, $Na_2Cr_2O_7$, a well-known, although toxic, chemical inhibitor. While this form of comparison finds conformity with practice from other similar studies [9,10], this study is also of the intent that the use of the natural plant for replacement of the toxic chromate chemical exhibit potency of sustainable steel-rebar corrosion-protection in the acidic medium.

Experimental Methods

Experimental Materials

The procedure for collection and authentication (with FHI. No. 109496 at the Forestry Herbarium Institute, Ibadan, Nigeria) of fresh leaves of *A. djalonensis* and the preparation of methanolic extract, as prescribed in [11], from the leaf were as detailed in reported study [8]. Concentrations of the leaf-extract ranging from 0.00 g/L (for the control) in increments of 1.67 g/L up to 8.33 g/L, per volume of concrete mixing water, were admixed in 100 mm × 100 mm × 200 mm steel reinforced concrete samples. For the comparison of the plant extract performance on steel-rebar corrosion, equal mass model of $Na_2Cr_2O_7$ also in increments of 1.67 g/L up to 8.33 g/L were admixed in another set of steel-reinforced concrete samples. These constitute eleven steel-reinforced concrete samples for the study. The concrete mixing formulation employed for the study followed that from previous studies [12-13], which includes 300.0 kg/m^3 cement, 890.6 kg/m^3 river sand, 1106.3 kg/m^3 granite stones passing 19 mm sieve and 149.7 kg/m^3 water. These imply water/cement ratio = 0.499 [12,14].

Composition of the 12 mm diameter deformed steel rods that were cut into 190 mm samples for use in the present study is the same as that detailed in [12]. Each rod for which surface preparation was as per ASTM G109-99a [15] has 150 mm of its length centrally placed in their requisite sample of concrete casting such that the protruding 40 mm, which was painted with glossy paint after casting, could be used for electrochemical connection.

Experimental Setup and Test-Data Measurements

Each sample of steel-reinforced concrete was immersed longitudinally in bowls containing 0.5 M H_2SO_4, for simulating microbial/industrial environment [2,16]. In each bowl, the H_2SO_4 test-medium was made up to just below the rebar protrusion from the concrete but without touching the rebar. Electrochemical measurements of macrocell corrosion current were taken versus $Cu/CuSO_4$ electrode (CSE) [5,17,12,18-20] through use of zero-resistance ammeter (ZRA), from each sample in 5 days interval for the first 40 days then in 7 days interval for the following 5 weeks. These constitute data-point measurements that totalled 14 in the 75-day experimental period [8,12].

Experimental Data Analyses

As had been exemplified in studies [12,17], the macrocell current measurements from each steel-reinforced concrete sample find usefulness for the analysis of total corrosion, *TC* in Coulomb (C), through subjection of the measured current to the standard formula from ASTM G109-99a [15]:

$$TC_j = TC_{k-1} + \left[\left(t_k - t_{k-1} \right) \times \left(i_k + i_{k-1} \right) / 2 \right]; \;\; k = 2,\ 3,\ \ldots,\ n \tag{1}$$

Where: n = 14 is the number of data-points of electrochemical test-measurements of the macrocell current in the experimental period, t is the time (s) elapsed between the previous, (k–1), macrocell current measurement i_{k-1} (A), at time t_{k-1}, and the present, (kth), macrocell current measurement i_k (A) at time t_k [12,15,17]. As specified in [15], the total corrosion modelled from Equation (1) was used for estimating corrosion inhibition efficiency, η(%), for each inhibitor admixed steel-reinforced concrete sample, relative to the control sample, using the formula [13,16,21-22]:

$$\eta(\%) = \frac{TC_{control\ sample} - TC_{admixed\ sample}}{TC_{control\ sample}} \times 100 \tag{2}$$

Results and Discussion

Trends of macrocell current measurements obtained from the steel-reinforced concrete samples in the 75-day experimental period of concrete test-immersion in 0.5 M H_2SO_4 medium are plotted in Figure 1. This figure shows that, with just few exceptions, the macrocell current measurements of the steel-rebar in the control sample, with 0.00 g/L admixture, overshot the current measurements from the steel-rebar in inhibitor admixed samples through the experimental period. The exceptions to this include macrocell current measurements from the 3.33 g/L $Na_2Cr_2O_7$ admixed sample on the 0th day and the 5th day of concrete immersion as well as the measurements from the 3.33 g/L *A. djalonensis* admixed sample on the 61st day.

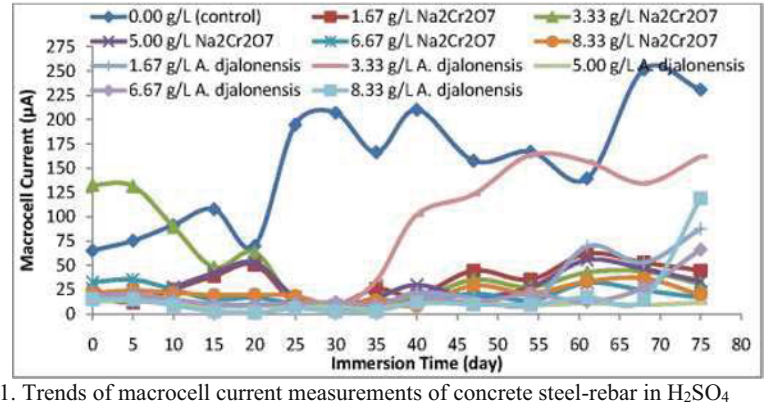

Figure 1. Trends of macrocell current measurements of concrete steel-rebar in H_2SO_4

The total corrosion models, analysed for each steel-reinforced concrete samples from the macrocell current measurements using Equation (1), are presented in Figure 2. It is first observable from the figure that the total corrosion test-results linearised the stochastic macrocell current measurements plotted in Figure 1 and that this linearization portends possibility of better interpretation than what obtains from Figure 1. The total corrosion of the control steel-reinforced concrete sample (with 0.00 g/L admixture) still overshot the total corrosion models of the admixed samples through the experimental period. The only exception to this being the modelled total corrosion for the 3.33 g/L $Na_2Cr_2O_7$ admixed sample from the 0th day through the 20th day. However, the total corrosion of this sample reduced relative to that from the control after the 20th day, thus, indicating the inhibition action of the $Na_2Cr_2O_7$ chemical at that concentration.

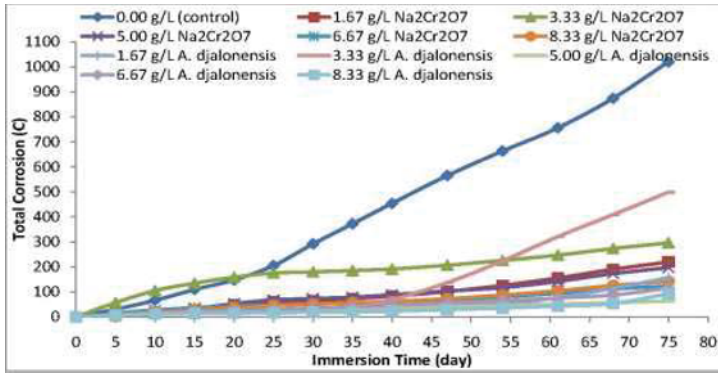

Figure 2. Plots of total corrosion modelling from the steel-reinforced concrete samples

The results of rendering the total corrosion models, from the steel-reinforced concrete samples, to the inhibition efficiency, η(%) analyses, Equation (2), are presented for each sample in Figure 3, in ranking order of corrosion inhibition performance of the admixtures employed in the study.

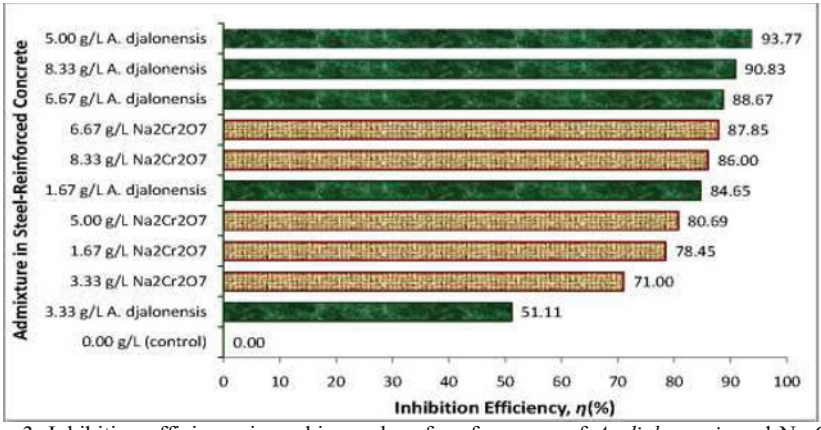

Figure 3. Inhibition efficiency in ranking order of performance of *A. djalonensis* and $Na_2Cr_2O_7$ admixtures on steel-rebar corrosion in H_2SO_4-immersed concrete

Figure 3 show that three concentrations of *A. djalonensis* leaf-extract admixture surpassed the also highly effective $Na_2Cr_2O_7$ concentrations at inhibiting concrete steel-rebar corrosion in the study. Except for the 3.33 g/L *A. djalonensis* admixed concrete, the remaining equal mass models of *A. djalonensis* leaf-extract concentrations outperformed their $Na_2Cr_2O_7$ counterpart admixtures at inhibiting steel-rebar corrosion in the H_2SO_4-immersed concretes. Only the 3.33 g/L $Na_2Cr_2O_7$ exhibited higher inhibition efficiency, η = 71.00%, than the equal mass model 3.33 g/L *A. djalonensis* admixture having η = 51.11% efficiency performance. Optimal inhibition efficiency in the study was exhibited by 5.00 g/L *A. djalonensis* admixture, at η =93.77%, followed in respective effectiveness by the 8.33 g/L *A. djalonensis* (η = 90.93%) and the 6.67 g/L *A. djalonensis* (η = 88.67%). The performance of many *A. djalonensis* leaf-extract concentrations that surpasses that of $Na_2Cr_2O_7$ admixtures on steel-rebar corrosion in H_2SO_4 bare supports for the suitability of the plant extract as an effective alternative for replacing the toxic

$Na_2Cr_2O_7$ chemical inhibitor. This suitability indicates positive prospects of sustainable corrosion-protection for concrete steel-reinforcement in microbial/industrial environments that is green, non-toxic, non-hazardous but eco-friendly and biocompatible extract of natural plant.

Conclusions

In this study, total corrosion effects showed that many concentrations of *A. djalonensis* leaf-extract outperformed equal mass models of also highly effective $Na_2Cr_2O_7$, a well-known but toxic chemical inhibitor, on the corrosion inhibition of steel-rebar in H_2SO_4 medium. It is therefore concluded that such performance of inhibition effect by the leaf-extract bare indication of positive prospects on the suitability of the extract as sustainable alternative for replacing the toxic $Na_2Cr_2O_7$ inhibitor of steel-rebar corrosion. Such applicable natural plant extract exhibit green, non-toxic, non-hazardous but eco-friendly/biocompatible corrosion-protection system for steel-reinforcement embedment in concrete designed for the microbial/industrial environments.

References

1. J.O. Okeniyi, C.A. Loto, and A.P.I. Popoola, "Inhibition of steel-rebar corrosion in industrial/microbial simulating-environment by *Morinda lucida*," *Solid State Phenomena*, 227 (2015), 281–285.

2. H. Gerengi, Y. Kocak, A. Jazdzewska, M. Kurtay, and H. Durgun, "Electrochemical investigations on the corrosion behaviour of reinforcing steel in diatomite- and zeolite-containing concrete exposed to sulphuric acid," *Construction and Building Materials* 49 (2013), 471–477.

3. J.O. Okeniyi, I.O. Oladele, I.J. Ambrose, S.O. Okpala, O.M. Omoniyi, C.A. Loto, and A.P.I. Popoola, "Analysis of inhibition of concrete steel-rebar corrosion by $Na_2Cr_2O_7$ concentrations: Implications for conflicting reports on inhibitor effectiveness," *Journal of Central South University*, 20 (12) (2013), 3697–3714.

4. J.O. Okeniyi, I.O. Oladele, O.M. Omoniyi, C.A. Loto, and A.P.I. Popoola, "Inhibition and compressive-strength performance of $Na_2Cr_2O_7$ and $C_{10}H_{14}N_2Na_2O_8{\cdot}2H_2O$ in steel-reinforced concrete in corrosive environments," *Canadian Journal of Civil Engineering*, 42 (2015), 408–416.

5. M. Ismail, P.B. Raja, and A.A. Salawu, "Deeper understanding of green inhibitors for corrosion of reinforcing steel in concrete," *Handbook of Research on Recent Developments in Materials Science and Corrosion Engineering Education,* ed. H. Lim, (Hershey, PA: IGI Global, 2015), 118–146.

6. O.O. Adeyemi and O.O. Olubomehin, "Investigation of *Anthocleista djalonensis* stem bark extract as corrosion inhibitor for Aluminum," *The Pacific Journal Science Technology,* 11 (2010), 455–462.

7. A.S. Bassey, J.E. Okokon, E.I. Etim, F.U. Umoh, and E. Bassey, "Evaluation of the *in vivo* antimalarial activity of ethanolic leaf and stembark extracts of *Anthocleista djalonensis*," *Indian Journal of Pharmacology,* 41 (2009), 258–261.

8. J.O. Okeniyi, C.A. Loto, and A.P.I. Popoola, "Electrochemical performance of *Anthocleista djalonensis* on steel-reinforcement corrosion in concrete immersed in saline/marine simulating-environment," *Transactions of the Indian Institute of Metals*, 67 (2014), 959–969.

9. Y. Tang, G. Zhang, and Y. Zuo, "The inhibition effects of several inhibitors on rebar in acidified concrete pore solution," *Construction and Building Materials*, 28 (2012), 327–332.

10. M. Ormellese, L. Lazzari, S. Goidanich, G. Fumagalli, and A. Brenna, “A study of organic substances as inhibitors for chloride-induced corrosion in concrete,” *Corrosion Science*, 51 (2009), 2959–2968.

11. S. Hameurlaine, N. Gherraf, A. Benmnine, and A. Zellagui, “Inhibition effect of methanolic extract of *Atractylis serratuloides* on the corrosion of mild steel in H_2SO_4 medium,” J*ournal of Chemical and Pharmaceutical Research*, 2 (2010), 819–825.

12. J.O. Okeniyi, C.A. Loto, and A.P.I. Popoola, “Modelling *Rhizophora mangle* L bark-extract effects on concrete steel-rebar in 0.5 M H_2SO_4: Implications on concentration for effective corrosion-inhibition,” *TMS2015 Supplemental Proceedings* (Hoboken, NJ, USA: John Wiley & Sons, Inc., 2015), 751–758.

13. J.O. Okeniyi, I.J. Ambrose, I.O. Oladele, C.A. Loto, and P.A.I. Popoola “Electrochemical performance of sodium dichromate partial replacement models by triethanolamine admixtures on steel-rebar corrosion in concretes,” *International Journal of Electrochemical Science*, 8 (8) (2013), 10758–10771.

14. M. Ormellese, M. Berra, F. Bolzoni, and T. Pastore, Corrosion inhibitors for chlorides induced corrosion in reinforced concrete structures,” Cement and Concrete Research 36 (2006) 536 – 547.

15. ASTM G109-99a, *Standard Test Method for Determining the Effects of Chemical Admixtures on the Corrosion of Embedded Steel Reinforcement in Concrete Exposed to Chloride Environments* (West Conshohocken, PA: ASTM International, 2005).

16. J.O. Okeniyi, C.A. Loto, and A.P.I. Popoola, “Electrochemical performance of *Phyllanthus muellerianus* on the corrosion of concrete steel-reinforcement in industrial/microbial simulating-environment,” *Portugaliae Electrochimica Acta* 32 (2014), 199–211.

17. J.O. Okeniyi, O.A. Omotosho, O.O. Ogunlana, E.T. Okeniyi, T.F. Owoeye, A.S. Ogbiye, and E.O. Ogunlana, “Investigating prospects of *Phyllanthus muellerianus* as eco-friendly/sustainable material for reducing concrete steel-reinforcement corrosion in industrial/microbial environment,” *Energy Procedia*, 74 (2015), 1274–1281.

18. J.O. Okeniyi, O.O. Ogunlana, O.E. Ogunlana, T.F. Owoeye, and E.T. Okeniyi, “Biochemical characterisation of the leaf of *Morinda lucida*: Prospects for environmentally-friendly steel-rebar corrosion-protection in aggressive medium,” *TMS2015 Supplemental Proceedings* (Hoboken, NJ, USA: John Wiley & Sons, Inc., 2015), 635–644.

19. G.E. Abdelaziz, A.M.K. Abdelalim, and Y.A. Fawzy, “Evaluation of the short and long-term efficiencies of electro-chemical chloride extraction,” *Cement and Concrete Research*, 39 (2009), 727–732.

20. W.J. McCarter and Ø. Vennesland, “Sensor systems for use in reinforced concrete structures,” *Construction and Building Materials*, 18 (2004), 351–358.

21. J.O. Okeniyi, C.A. Loto, A.P.I. Popoola, “*Morinda lucida* effects on steel-reinforced concrete in 3.5% NaCl: implications for corrosion-protection of wind-energy structures in saline/marine environments,” *Energy Procedia,* 50 (2014), 421–428.

22. J.O. Okeniyi, O.M. Omoniyi, S.O. Okpala, C.A. Loto, and A.P.I. Popoola, “Effect of ethylenediaminetetraacetic disodium dihydrate and sodium nitrite admixtures on steel-rebar corrosion in concrete,” *European Journal of Environmental and Civil Engineering*, 17 (2013), 398–416.

REWAS 2016: Towards Materials Resource Sustainability
Edited by: Randolph E. Kirchain, Bart Blanpain, Christina Meskers, Elsa Olivetti, Diran Apelian, John Howarter, Anne Kvithyld, Brajendra Mishra, Neale R. Neelameggham, and Jeff Spangenberger
TMS (The Minerals, Metals & Materials Society), 2016

MATERIALS RESEARCH TO ENABLE CLEAN ENERGY: LEVERAGE POINTS FOR RISK REDUCTION IN CRITICAL BYPRODUCT MATERIAL SUPPLY CHAINS

Michele L. Bustamante, Gabrielle Gaustad

Golisano Institute for Sustainability, Rochester Institute of Technology
190 Lomb Memorial Drive; Rochester, NY, 14623, USA

Keywords: Critical materials, byproduct mining, clean energy, recycling, REWAS

Abstract

Each year, the TMS Annual Meeting brings together materials experts from across the field and across the globe, creating unique opportunities for multidisciplinary discussions of grand challenges. Enabling a clean energy transition without creating new chronic energy material shortages is one such challenge. The present work aims to inspire materials researchers from across the disciplinary spectrum to consider their skills in the context of need for risk mitigation research; particularly for the vulnerable subclass of critical materials mined as byproducts. Key leverage points are identified and assessed using existing case study data for tellurium. Results show that rapid demand growth, driven by solar PV, rendered supply-side mitigation strategies (byproduct yield improvement and recycling) much less effective than demand-side solutions, like dematerialization and substitution. Overall, the results serve as a reminder that there is no universal mitigation strategy; instead, optimal results can be obtained by targeted and temporally-relevant strategic development.

Introduction

Transitioning to a cleaner energy future is one of today's grand science and engineering challenges. Such a shift introduces a concomitant transition in material demand needed to support the new technologies. This places the materials community at the forefront of emerging clean energy research needs. Although there is still ample room for improvement, significant progress has been made toward advancing performance of clean energy materials. For example, research into solar photovoltaics (PV) has driven crystalline silicon cell efficiency up by 80% in the last 40 years, propelled the recent achievement of a 46% efficient multi-junction solar cell, and led organic PV to quadruple in efficiency (Table I) [1].

However, in many cases, such improvements (higher efficiency, lower cost, or other objective, i.e. flexibility) have come at a price of increased materials scarcity risks. Thin film PV offers reduced material footprint and cost but employ potentially scarce materials such as cadmium, tellurium, indium, gallium, and selenium. Similarly, multi-junction cells can boost efficiency by utilizing more of the solar spectrum, but they employ multiple layers of compounds containing indium, gallium, arsenic, and germanium, among others (Table I) [2]. With the exception of oxygen, present in various organic solar compounds, and amorphous silicon, all other solar elements highlighted in table I require less abundant input materials than traditional

crystalline silicon; several million times less so for some of the rarest: tellurium, selenium, and gallium [3].

Table I. Clean energy materials, progress, and performance. Example: solar photovoltaics.

PV Class	*Technologies*	*Elements in Active Layer*	*Record Cell Efficiency [1]*
Generation I	Crystalline Silicon (c-Si) (multi-, mono-)	Si	20.8% (multi) 25.0% (mono)
Generation II *(thin films)*	Amorphous Silicon (a-Si)	Si, H	12.4%
	CdTe	Cd, Te, S	21.5%
	CIS/CIGS	Cu, In, Se, Ga	21.7%
Generation III	Multi-junction (MJPV) (two-, three-, four+-junction) (concentrator, non-concentrator)	In, Ga, As, P, Ge	31.1% (2J, non) 34.1% (2J, conc) 37.9% (3J, non) 44.4% (3J, conc) 38.8% (4+J, non) 46.0% (4+J, conc)
	Dye-Sensitized (DSSC)	In, Sn, Ti, Zn, O	11.9%
	Perovskite	Pb, I, Br, Cl, C, H, N, O	20.1%
	Organic/Polymer	C, H, N, O	11.5%
	Quantum Dot (QD)	Cd, Se, Ti, O	9.9%
	CZTS/Se	Cu, Zn, Sn, S, Se	11.1%

Such potentially scarce materials are often referred to as critical materials; they are critical in the sense that they are functionally vital to important end-use applications and they are critical in the sense that their supply is vulnerable to crisis (e.g. in critical condition). Generally, critical materials possess high demand, poor substitutability, and multifaceted risk of supply disruption (including economic, social, and environmental factors). However, criticality can be a somewhat ambiguous characteristic because it is highly dependent upon a stakeholder perspective, i.e. to whom is the material important? The same material can be deemed critical to a particular economic sector, e.g. clean energy [4, 5] or defense [6-8] but not to a specific company, like GE [9-11], or perhaps what is critical to a nation or international group, like the EU [12-14] is not necessarily critical to the broader global economy [15-22]. For example, indium, tellurium, selenium, gallium, and germanium are examples of solar-critical materials, whereas rare earth elements (REE), such as dysprosium and neodymium, are critical to wind energy [4].

Criticality research, aimed at characterizing supply risks and impacts of restriction, has received significant attention, particularly in the past decade; however, many studies focus primarily on overall abundance and neglect how the material is actually produced [23]. However, all the clean-energy critical materials referenced in the previous paragraph share a common source of supply risk: reliance on byproduct mining. By definition, byproduct materials are only minor outputs of shared extraction processes, by mass and by value. As such, byproduct materials contribute only marginally to the profit-driven joint extraction operation and have very little influence over how much ore gets extracted as a result. This hampers the ability of byproduct supply chains to react to changes in price and/or demand, leaving it more vulnerable to supply gap conditions, where short-term demand outpaces supply [24].

With so many clean energy technologies subject to strong byproduct mining supply risk [25-29], enabling broader use will require forward thinking and planning. There are numerous mitigation strategies capable of reducing supply risk, but it is not always clear which strategy will provide the greatest specific benefit. This study aims to explore some of the ways in which the diverse TMS materials research community is uniquely prepared to address many different

aspects of the byproduct supply risk challenge, central to clean energy deployment. Additionally, this work will highlight a potential conditions under which different branches of this community can be more effective at reducing risk. The goal is to guide meaningful action toward solving the multidisciplinary sustainability challenge of enabling clean energy in a way that best leverages the unique skillsets of different of material scientists.

Identifying Mitigation Strategies and Leverage Points

Some strategies for supply risk mitigation – like recycling, dematerialization, and substitution – are generally applicable to all kinds of critical materials. Others, such as primary mining development and byproduct yield improvement, are specifically aimed at byproduct critical materials in this text. Naturally, different strategies offer different benefits, and since supply risk is dynamic, effectiveness can vary with time, i.e. when the strategy was employed and whether benefits are delayed. This complexity can be conceptualized by broadly categorizing strategies into lifecycle phases and their ability to reduce supply risk therein. This section will briefly detail each strategy, considered them in the context of demanded technical skills and the different branches of broad materials research potentially offering such skills. Table II summarizes this discussion, allowing it to serve as a general tool to guide materials experts looking to contribute to the challenging task of enabling clean energy.

Table II. Key intervention opportunities for different branches of materials science.

		Branch of Materials Research						
Life Cycle Phase	**Example Mitigation Strategies**	Geology	Extractive Metallurgy	Degradation Analysis	Opto-electronic Properties	Synthesis/ Processing	Recycling	Thin Films
Extraction	Primary Mining	X	X					
	Other Byproduct Mining		X					
Processing	Yield Improvement		X			X		
	Scrap/Waste Recovery		X			X	X	
Manufacturing	Dematerialization				X	X		X
	Substitution				X	X		
Use	Lifetime Modification			X		X		
End-of-Life	Recycling		X				X	
	Remanufacturing					X		

Extraction is the initial phase of a product's lifecycle, during which raw materials are obtained from the natural environment. In the case of metals and minerals, this extraction is typically accomplished via a physical mining process. Two extraction phase intervention strategies are deployment of novel primary mining and exploitation of alternate byproduct mining. Developing primary resources can be a particularly effective strategy in the face of rapidly growing demand because primary production reduces supply risk by creating more flexibility in the supply-chain. Whereas byproduct flows are constrained by the needs of another material, primary mining supply is unattached and optimized to respond to market forces. Developing primary mining as a mitigation strategy requires specialized materials expertise. First, geological and mineralogical research may be required to discover new resources using advanced imaging and exploration techniques. Next, once a suitable primary resource have been identified, knowledge of extractive metallurgy will be required to plan the optimal mining approach, e.g. surface or underground, mining as concentrates or in situ leaching. Alternatively, supply can be expanded through the use of other byproduct mining pathways. This would not change the total amount of ore extracted but rather the decision to recover a material as a

byproduct or not. Just as increased prices can drive development of resources previously deemed unfit for primary mining, increased prices can motivate recovery of byproduct resource from outputs previous deemed as wastes due to lower concentration, i.e. slags, residues, exhaust gases. Alternate byproduct mining can reduce supply risk by diminishing the influence of any single byproduction system or process. Developing these pathways also requires extractive metallurgy to characterize potential waste resources, plan the extraction approach (method, reagents, conditions, etc.), and ensure optimal extraction efficiency.

The next lifecycle stage, *processing*, elevates raw materials to a usable form. For byproduct materials, this involves separation of the main product from the byproduct(s). Two potential processing phase intervention strategies are improvement of byproduct yield and recovery of losses from scrap or wastes. Yield is the overall ratio of byproduct ultimately in usable form as compared to the initial pre-extraction availability, which incorporates individual process efficiencies and losses. Byproduct extraction efficiency is just one component of a larger indicator known as byproduct yield. Recovery of losses from scrap or waste streams is similar to byproduct mining and requires similar skills.

The *manufacturing* phase, which is when all the processed raw materials get incorporated into product form, is another powerful area for materials researchers to intervene because so many of the fundamental processes involve material science, e.g. forming, joining, casting, heat treatment, coating, deposition, and crystal growth. Two common mitigation strategies tied to the manufacturing phase are dematerialization, or reduction of material intensity, and substitution. Dematerialization and substitution both offer supply risk reduction by reducing demand for the critical material per unit of the product, allowing supply growth to catch up to that of demand. However, whereas dematerialization necessarily uses less material overall, substitution may require use of a greater amount of the substitute material to achieve the same performance. Alternately, development of new and better substitutes for non-energy-critical applications can have a beneficial effect on supply risk reduction overall by reducing competition for the material with the rapidly growing critical applications. Both strategies may require advances in synthesis and processing techniques, such as chemical vapor deposition or wafer design. Additionally, thin films expertise is very valuable in consideration of dematerialization processes. Finally, at least for solar materials, it will ultimately be important to research fundamental optoelectronic properties to ensure they will not unacceptably diminish or breakdown with dematerialization and to design perhaps new materials for substitution.

The *use* phase is the period in which the product itself is being utilized by a consumer. This makes it the hardest phase to intervene during as a materials scientist. However, certain approaches taken during manufacturing may actually see most change in impact during the use phase by modifying the product's lifetime. Lifetime modification is an interesting example, however, because the direction of modification can have counterintuitive effects. On the one hand, extending the lifetime of a good should theoretically reduce demand by preventing the consumer from needing to replace it, e.g. disposable versus durable plastic grocery bags. However, while a material is sequestered in a product for a longer time, it cannot be made available for reuse or recycling until after a long delay. From a materials perspective, various processing techniques can be applied to extend the product lifetime, e.g. coating for corrosion and/or degradation resistance. Additionally, research into degradation and failure mechanisms would be helpful to design more robust solar cells and modules. Further, use of low quality material or poor manufacturing can reduce useful life for these kinds of technologies. Finally, substitutions and dematerialization carried out during manufacturing may indirectly affect

product lifetime. For example, frameless glass thin film PV, although lighter in weight, is considered to be more fragile [30].

End-of-life refers to the final stage in a linear model of a product's lifecycle when it ceases to be useful to the current owner in the current form. In reality, end-of-life can often mean new beginnings for many materials and products via recycling and remanufacturing. Recycling and remanufacturing both work to mitigate supply risk by displacing demand for virgin raw materials with recovery of individual substances or product components from end-of-life products. Additionally, providing a secondary supply of material or parts helps to diversify the supply-chain making it potentially more resilient and less vulnerable to disruption. Recycling is a very popular research topic among TMS members as a topic of interest for extractive metallurgy audiences as well as dedicated recycling audiences (i.e. REWAS symposia throughout the years). However, in terms of reducing supply risk, recycling can be challenging to predict because it is so highly dependent upon the product lifetime.

Case Study: Evaluating Leverage Points for Tellurium

To further illustrate the potential usefulness of these mitigation strategies, quantitative supply risk analysis is performed using case study data from a critical byproduct material production system. Tellurium was selected to be the case study material due to its relevance to clean energy and availability of existing data on byproduct supply, solar demand, and modeling techniques are detailed in one of the authors' previous works (see Bustamante & Gaustad 2014 for details) [24]. A few key changes were made to parameter values in the present analysis. They are summarized in Table III.

Table III. Modeling improvements from initial tellurium supply risk study [24].

Previous Study	This Study	Calculation	Notes
Tellurium supply from copper only: S	Total tellurium supply approximated: S' Fraction of tellurium supply from copper: f	S'=S/f	f value from USGS; This study: Baseline f = 90%; Range f = none; Previous study (equivalent): f = 100%.
Tellurium demand from solar only: M	Total tellurium demand approximated: M' Fraction of tellurium demand from solar: n	M' = M/n	n value from SDTA, reported in Candelise et al. 2012.; This study: Baseline n = 40% Range n = 40% and 90% Previous study (equivalent): n = 100% in previous study
Tellurium supply from recycled PV *(assumes perfect collection & recovery):* R	Tellurium supply from recycled PV: R' Tellurium recovery rate from PV recycling: r	R' = R*r S' = S/f + R'	This study: Baseline r = 0% Range r = 0% and 80% Previous study (equivalent): Baseline r = 0% Range r = 0% and 100%

In lieu of simulating every identified mitigation strategy, two illustrative examples are selected: byproduct yield improvement and dematerialization via film thickness reduction. In each instance, the associated parameter values, yield and film thickness, were varied through a range dictated by the previous literature to create multiple scenarios. Then, prospective conditions were selected to test the relative effectiveness of alternate scenarios. Effectiveness is measured by the year in which supply gap conditions are observed for the first time; the sooner the year, the greater the risk. Recycling efficiency improvement and substitution in non-energy

critical applications were also used as alternate conditions for the yield and dematerialization analyses, respectively.

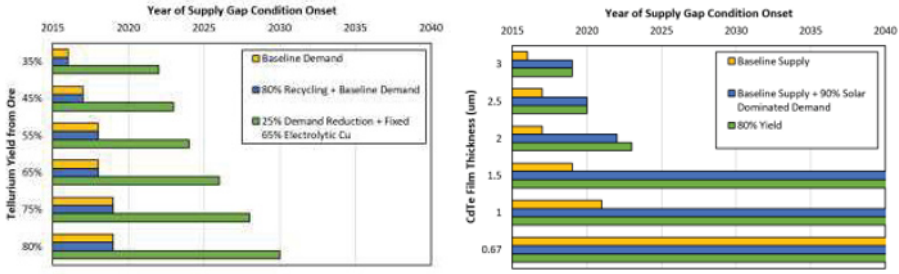

Figure 1. Supply risk as a function of (left) byproduct yield and (right) material intensity, under baseline assumptions (upper series) and improved conditions (lower series).

The first scenarios assessed were calculated by modifying total tellurium supply as a function of byproduct tellurium yield (Fig. 1 (left)). These yield supply scenarios were then compared to a baseline value of projected demand (based on observed historical growth) to obtain the year when (or if) supply gap conditions were expected to emerge. Under the baseline assumptions for supply, yield was 35%, meaning the top bar in figure 1 (left) is thought to represents the current track of observed trends; if this is true, gap conditions could emerge as soon as 2016. This is not to say tellurium supply will definitely experience a disruption event next year, especially if any government or smaller scale industrial stockpiling of the material has been occuring. Rather, it illuminates conditions in which risk is present since the short term supply can no longer match the new demand.

As byproduct yield is increased from the low-end baseline value of 35% up to 80%, the onset of supply gap conditions in the face of baseline rapid solar-driven demand growth is delayed by a maximum of 3 years. Next non-baseline conditions were tested to alert researchers of trends that may be more or less beneficial to their leverage area. For example, even with over 80% recycling rate, the baseline demand growth is too fast for meaningful amounts of tellurium to reach end of life before gap conditions set in. After testing several more conditions to no avail, demand was reduced to 25% of its baseline level. Simultaneously, electrolytic copper production (the only route by which tellurium byproduct is generated), as a fraction of total, was set to 2015 level of 65% rather than following historic declining trends, as in the base case. Interestingly, modifying the latter condition alone did not affect the year of gap onset for each yield value, however, when combined with the demand reduction, it created greater risk reducing effects than the demand reduction alone; particularly for the higher yield values. Supply gap conditions in this compound circumstance were successfully delayed by 6 to 11 years.

For a demand-side perspective, active layer film thickness reduction was explored as a proxy for dematerialization (Fig. 1 (right)). Again, the upper bar represents the baseline condition, except this time for supply with demand changing as a function of solar film thickness. The baseline assumption for film thickness was 3 microns so the top bar represents the same scenario as the top bar in the left chart. However, even without modification, the tipping point for gap conditions is much more responsive to changes in the film thickness range than to the yield range. Below a film thickness of 1 micron, gap conditions can be avoided

altogether. However, this reduction would have be commercialized and deloyed immediately to accurately represent these results, and technological progress takes time and may introduce performance tradeoffs not currently captured by the model. Additionally, a substitution condition was considered where nearly all non-PV tellurium demand was replaced. This led all film thickness scenarios to delay gap conditions by at least 3 years, and even permanently for film reduction to 1.5 microns rather than all the way down to one. Last, demand reduction is also considered under a condition where byproduct yield is high, capturing 80% of the available materiall. This was able to accomplish nearly the same trend as the substitution conditon considered. If materials research reveals that one solution is much simpler and/or less expensive than the other, this finding will speed along its development.

Although these two examples did not address all of the mitigation strategies discussed previously, they should provide readers an idea of the types of analysis that can be done to answer the same questions for different specific strategies and materials. At least two potential heuristics appear to have emerged from this analysis. First, comparing the growth rates of supply and demand growth may be helpful to indicate relative effectiveness of supply-side reduction strategies (such as yield and recycling) versus demand-side strategies (such as dematerialization and substitution). When supply grows slowly compared to demand, it is more difficult to avoid being overtaken by changing small aspects of the supply than changing small aspects of demand. Second, by calculating one scenario - the maximum achievable gap delay from primary and secondary supply – and comparing it with the lifetime of the product, it can be quickly determined whether recycling will be able to meaningfully contribute to supply before gap conditions emerge. In the present analysis, recycling all tellurium atop 80% supply yield would only result in a 4 years of gap delay and current CdTe PV lifetime is about 25 years. Therefore, recycling was never able to prevent gap conditions from emerging.

Conclusions

There is no magic bullet when it comes to mitigating supply risk for critical materials; what worked in this case study for tellurium may not work for a different material with different supply and demand trends. However, the kinds of parameters that were used to assess risk reduction potential can also likely be applied to other similar material systems, which in this case, were byproducts. Further research is needed to explore the responsiveness of some of the other remaining mitigation strategies not presented here, including strategies beyond technical materials-related approaches such as local and international policies or production, trade, and waste management. Additionally, a more dynamic approach to strategy introduction and development over time would provide a much clearer picture, better capable of informing a nuanced response. Last, although recycling did not emerge as a useful option for mitigating supply risks for tellurium in the short term, it does not mean that recycling will not be useful for other materials, perhaps with shorter use phases, and further that it will not be useful for reducing risk in other ways. Recycling offers environmental benefits as well as potential for longterm stabilizing effects. These and other questions remain; however, it is clear that the materials community has many powerful tools and insights to contribute to addressing challenges of risk mitigation, especially for byproduct materials. The research that is pursued now and in the near future in these spaces may very well determine the kinds of energy technologies used to the power TMS Annual Meetings of tomorrow.

Acknowledgements

This work is supported by a National Science Foundation (NSF) CAREER Award (CBET #1454166) granted to Dr. Gaustad. The NSF has not formally reviewed this research. Additional thanks to the Golisano Institute for Sustainability and RIT for use of research facilities and access to scholarly resources.

References

[1] NREL, "Best Research-Cell Efficiencies," ed: National Renewable Energy Laboratory, 2015.
[2] IEA, "Technology Roadmap: Solar photovoltaic energy," I. E. Agency, Ed., ed, 2010.
[3] G. B. Haxel, J. B. Hedrick, and G. J. Orris, "Rare Earth Elements: Critical Resources for High Technology," in *Fact Sheet 087-02*, USGS, Ed., ed, 2002.
[4] D. Bauer, D. Diamond, J. Li, M. McKittrick, D. Sandalow, and P. Telleen, "Critical Materials Strategy," ed: US Department of Energy, 2011.
[5] D. Bauer, D. Diamond, J. Li, D. Sandalow, P. Telleen, and B. Wanner, "Critical Materials Strategy," U.S. Department of Energy, Washington, D.C.2010.
[6] DoD, "Strategic and critical materials 2015 report on stockpile requirements," US Department of Defense, Office of the Under Secretary of Defense, Ed., ed, 2015, p. 189.
[7] DoD, "Strategic and Critical Materials 2013 Report on Stockpile Requirements," Department of Defense, Ed., ed, 2013.
[8] DoD, "Report of Meeting Department of Defense Stategic Materials Protection Board," Department of Defense, Ed., ed, 2008.
[9] A. Ku*, et al.*, "Addressing Rare-Earth Element Criticality: An Example from the Aviation Industry," *JOM,* vol. 66, pp. 2355-2359, 2014/11/01 2014.
[10] A. Y. Ku and S. Hung, "Manage Raw Material Supply Risks," *Chemical Engineering Progress,* vol. 110, pp. 28-35, Sep 2014.
[11] D. Konitzer, S. Duclos, and T. Rockstroh, "Materials for sustainable turbine engine development," *MRS Bulletin,* vol. 37, pp. 383-387, 2012.
[12] European Commission, "Report on Critical Raw Materials for the EU: Report of the Ad hoc Working Group on Defining Critical Raw Materials," ed: European Commission Brussels, 2014.
[13] R. Moss, E. Tzimas, H. Kara, P. Willis, and J. Kooroshy, "Critical Metals in Strategic Energy Technologies: Assessing Rare Metals as Supply-Chain Bottlenecks in Low-Carbon Energy Technologies," European Commission Joint Research Centre Institute for Energy and Transport, 2011.
[14] European Commission, "Critical raw materials for the EU," ed, 2010, p. 84.
[15] E. M. Harper, Z. Diao, S. Panousi, P. Nuss, M. J. Eckelman, and T. E. Graedel, "The criticality of four nuclear energy metals," *Resources, Conservation and Recycling,* vol. 95, pp. 193-201, 2015.
[16] P. Nuss, E. M. Harper, N. T. Nassar, B. K. Reck, and T. E. Graedel, "Criticality of Iron and Its Principal Alloying Elements," *Environmental Science & Technology,* vol. 48, pp. 4171-4177, 2014/04/01 2014.

[17] T. E. Graedel, E. M. Harper, N. T. Nassar, P. Nuss, and B. K. Reck, "Criticality of metals and metalloids," *Proceedings of the National Academy of Sciences,* vol. 112, pp. 4257-4262, 2015.
[18] L. Erdmann and T. E. Graedel, "Criticality of Non-Fuel Minerals: A Review of Major Approaches and Analyses," *Environmental Science & Technology,* vol. 45, pp. 7620-7630, 2011/09/15, 2011.
[19] S. Panousi, E. Harper, P. Nuss, M. Eckelman, A. Hakimian, and T. Graedel, "Criticality of seven specialty metals," *Journal of Industrial Ecology*, 2015.
[20] E. M. Harper*, et al.*, "Criticality of the Geological Zinc, Tin, and Lead Family," *Journal of Industrial Ecology,* 2014.
[21] N. T. Nassar, X. Du, and T. E. Graedel, "Criticality of the Rare Earth Elements," *Journal of Industrial Ecology,* p. 11, 2015.
[22] T. Graedel*, et al.*, "Methodology of metal criticality determination," *Environmental science & technology,* vol. 46, pp. 1063-1070, 2012.
[23] M. L. Bustamante, G. Gaustad, and M. Goe, "Criticality Research in the Materials Community," *JOM,* vol. 66, pp. 2340-2342, 2014.
[24] M. L. Bustamante and G. Gaustad, "Challenges in assessment of clean energy supply-chains based on byproduct minerals: A case study of tellurium use in thin film photovoltaics," *Applied Energy,* vol. 123, pp. 397-414, 6/15/ 2014.
[25] D. I. Bleiwas, "Byproduct mineral commodities used for the production of photovoltaic cells," US Department of the Interior, US Geological Survey2010.
[26] N. T. Nassar, T. E. Graedel, and E. M. Harper, *By-product metals are technologically essential but have problematic supply*, vol. 1, 2015.
[27] L. Talens Peiro, G. Villalba Mendez, and R. U. Ayres, "Rare and critical metals as by-products and the implications for future supply," INSEAD Social Innovation Centre, Working Paper, 2011.
[28] T. Graedel, "On the future availability of the energy metals," *Annual Review of Materials Research,* vol. 41, pp. 323-335, 2011.
[29] A. Elshkaki and T. E. Graedel, "Solar cell metals and their hosts: A tale of oversupply and undersupply," *Applied Energy,* vol. 158, pp. 167-177, 11/15/ 2015.
[30] F. Collins, "Field Performance of Thin-Film," in *Photon International 2nd Thin Film Conference*, 2009.

REWAS 2016: Towards Materials Resource Sustainability
Edited by: Randolph E. Kirchain, Bart Blanpain, Christina Meskers, Elsa Olivetti, Diran Apelian, John Howarter, Anne Kvithyld, Brajendra Mishra, Neale R. Neelameggham, and Jeff Spangenberger
TMS (The Minerals, Metals & Materials Society), 2016

HETEROGENEOUS MATERIALS DESIGN FOR SUSTAINABLE NUCLEAR WASTE STORAGE USING LIFE PREDICTION BY CONFORMAL FINITE ELEMENT ANALYSIS

F. Rabbi,[1] K. Brinkman,[2] and K. Reifsnider[3]
[1] University of South Carolina, [2]Clemson University, [3]University of Texas Arlington

Keywords: Diffusion, COMSOL, Nernst-Planck, Waste form

Abstract

The durability of heterogeneous nuclear waste forms depends on the individual constituent properties as well as their internal morphology and boundary conditions. The end of life is defined by mechanical and chemical failure modes. Chemical failure occurs when increasing porosity reaches a threshold value, creating continuous pathways for the internal material to come in contact with the outside environment. Mechanical failure occurs when the waste form loses its structural strength due to porosity. In this work we employ conformal finite element analysis of heterogeneous waste forms set on the actual microstructure determined by tomography. The model calculates species flux in the constituents and the composite waste form subjected to various storage environments to estimate the development of porosity with time and the subsequent life. The analytical approach with preliminary results is discussed. The method is postulated to be a foundation for design of heterogeneous waste form materials.

Introduction

Radioactive waste produced from a wide range of nuclear application presents researchers with the challenge of managing the waste in an efficient and safe method. As a viable option, ceramic waste form incorporating various radionuclides provides flexibility in processing and operation. It has the potential to be an effective medium, offering an economical alternative for the associated cost in storage and disposal.[1.] Durability and life of the waste form is largely dependent on the variations of size, shape, connectivity, interface/interphase characteristics, and physical properties of the constituent which are all functions of the processing and storage condition. All these parameters in a heterogeneous waste form can change the global transport properties greatly, and greatly affect the durability of the waste form materials. Design of such material systems can be an expensive and time consuming process of anecdotal trial and error unless comprehensive modeling approaches based on the controlling physics and chemistry are available. In this work, to predict failure through degradation of Cesium doped Hollandite, a degradation mechanism has been identified. Degradation prediction will be associated with the formation and development of porosity. Formation of porosity will originate from the removal of cesium ion from the waste form. Initial isolated porosity will not contribute to the failure. Over a long period of time the gradual increase of the isolated pores will form continuous interconnected network. Failure of the waste form occurs when the porous network reaches the surface layer thus connecting the interior region with atmosphere. Porosity will be quantified by calculating the total cesium mass loss by using flux measurement of Nernst-Planck model. For conformal modeling of the waste form, 3D X-ray baseline imaging provided was used to generate real domain representation of the microstructure. The domain was used in COMSOL to

generate finite element meshing and conduct Flux analysis. The COMSOL Nernst-Planck model was able to resolve the conformal domain in static condition. This effort demonstrates the ability of the calculate flux transport by using conformal finite element analysis which can be used as a useful design tool to predict degradation of the heterogeneous material.

Theory

The degradation of the Cesium doped hollandite waste form in its life time can occur in two stages. First release of Cesium occurs due to the oxidation of Ti^{3+} to form rutile/brookite.[2-3] The titanium ion is oxidized by a diffused oxygen ion releasing a Cesium ion from the hollandite structure to maintain charge neutrality. The Cesium ion then diffuses out of the structure creating voids over a longer period of time. The accumulation of the voids over time can be an indicator of degradation of material towards failure as described by Shaw et. al.[4] Figure 1 shows the relation between the open porosity vs total porosity in a ceramic waste form (Shaw, 1998).[4] Shaw showed that there is a very distinct "tipping point total porosity" at which connected paths to the surface of the specimen form as total porosity increases. This is fundamentally a geometric effect and is found to be essentially independent of the materials involved. In our situation, those open paths will greatly increase the flow of nuclear waste products out of the waste form constituents to the storage surface and into the environment, and at the same time greatly increase the flow of corrosive elements into the containment materials to accelerate chemical "failure" of the storage volume.

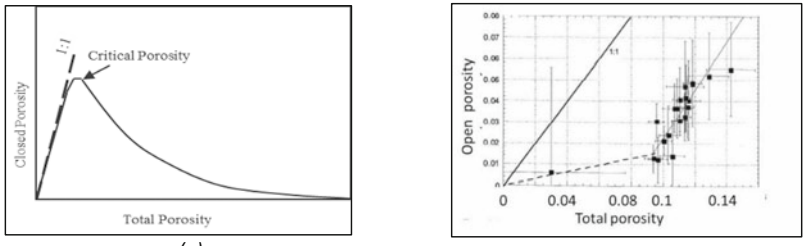

Figure: 1 Relationship of closed vs. total porosity which identifies a "critical porosity" (a) and the corresponding accelerated growth rate of open porosity (b) in ceramic waste forms.[4]

A very large body of historical data define the general dependence of ceramic strength on porosity.[5-6] For structural ceramics, often a porosity of less than 2 percent is required; a drop of strength by 25 percent for porosity of 5 percent is common. Therefore, our model of mechanical "failure" is rational. Estimation of the time for that porosity increase is based directly on constituent material corrosion data that can be obtained from ASTM standard corrosion methods, as a baseline calculation. To calculate the total removal of Cesium from the waste form structure that helps us quantify the total amount of porosity, we used Nernst-Planck flux equation. This equation describes transport of chemical species by convection, migration and diffusion through electrolyte membrane. Nernst-Planck equation has been used to model different charge transport phenomenon.[7-8]. Equation 1 shows Nernst-Planck equation

$$N_i = -D_i \nabla c_i - z_i u_{m,i} F c_i \nabla \phi + c_i u \qquad (1)$$

N_i = *Flux of species, i(mol/m^2.s)*
D_i = *Diffusion co-efficient (m^2/s)*
c_i = *Concentration of ion, i (mol/m^3)*
z_i = *Valance of species*
$u_{m,i}$ = *mobility (s/mol/kg)*
F = *Faraday constant*
ϕ_i = *Electrolyte Potential*
$\boldsymbol{u}$ = *velocity vector (m/s)*

In the case of a solid structure velocity term u_i is ignored. As no potential is applied across any of the boundaries the migration term is ignored. So in the case of solid waste form Cesium release will be controlled by the diffusion coefficient of the species through the waste form medium and the concentration gradient of the species. The amount of Cesium released can be obtained by calculating the total flux using equation 1. The amount of release Cesium will be proportional to the void created due to the diffusion of Cesium out of the waste form structure.

Domain diffusion co-efficient was obtained from reported ionic conductivity of Cesium in hollandite structure.[10] Nernst-Einstein relation is used to calculate the diffusion co-efficient described by Equation 2.[11]

$$\sigma = \frac{z_i^2 e^2 c_i}{k_B T} D_i \qquad (2)$$

Where, D_i = *Diffusion co-efficient (m^2/s)*
σ = *Ionic Conductivity*
z_i = *Valance of species*
c_i = *Concentration of ion, i (mol/m^3)*
k_B = *Boltzmann's constant*

Model description

The Nernst-Planck equation is solved using Nernst-Planck Equation Module of COMSOL Multi-Physics. For conformal finite element analysis we used 3D representation of the actual microstructure provided by Chiu et. al.[9] The sample used here has a chemical composition $Ba_{1.04}Cs_{0.24}Ga_{2.32}Ti_{5.68}O_{16.}$ They use X-ray nano tomography to generate a 3D structural representation of the waste form by using X-ray absorption behavior of the constituents. To generate the 3D computational domain from nano tomographic data, Simpleware commercial code was used. The code uses Tiff image slices containing each point in the microstructure represented based on their grayscale intensity. The code also generates a finite element mesh from the 3D domain which can be directly used for finite element analysis. Figure 2 shows 3D finite element mesh generated using Simpleware. Figure 3 shows 3 phases, Hollandite, a Cesium rich emergent phase and void. We calculate the initial concentration of Cesium in the crystal structure from equation 2 and set all the outside boundaries at a very low Cesium concentration. The concentration gradient between initial internal Cesium and outside surface initiates the outward diffusion of Cesium. The model simulates static solution to measure the diffusion of the

Cesium inside the structure. In this initial study we assume the bulk hollandite have a high Cesium diffusion co-efficient compared to the other two phases and control the flux in the waste form. Diffusion properties of the other phases will be considered in our later works.

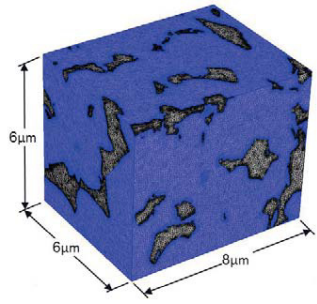

Figure 2: 3D finite element mesh

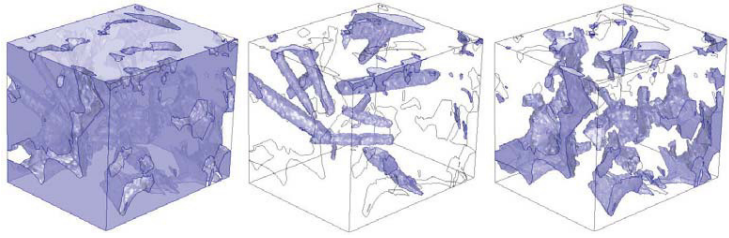

Figure 3: a) Hollandite, b) Cesium rich emergent phase and 3) void in the waste form

Results & Discussion

This model uses an iterative solver to find the static solution of the problem. Figure 4(a) shows concentration gradients of Cesium inside the Hollandite structure. In this calculation we assumed a higher initial concentration of Cesium inside the material with low Cesium concentration outside. The gradient plot shows that after the static solution at equilibrium gradual decrease of concentration is observed from center to the boundary of the structure. The blue regions with lowest or zero Cesium concentration indicates the void regions where we assumed very low Cesium initial concentration.

Figure 4(b) shows a representation of the Cesium flow path through the structure. We can see that as we have set higher concentration of Cesium inside the material with lower concentration boundary condition, the flux path indicating flow of Cesium form the interior to the outside. This can be a useful tool to predict the regions of Cesium removal from the waste form. It is possible to predict flow path of other ions that are involved in this process separately to account for their effect on the degradation on different zones.

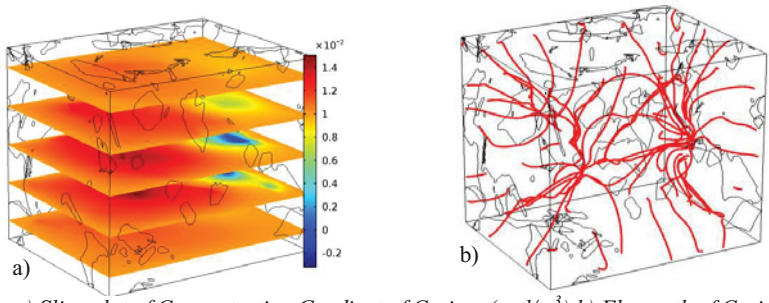

Figure 4: a) Slice plot of Concentration Gradient of Cesium (mol/m^3) b) Flux path of Cesium ion through waste form structure

Figure 5 shows diffusion co-efficient dependent flux of Cesium flowing out from the waste form through the outside boundaries. In this figure, we can see that the flux of Cesium is dependent on diffusion co-efficient of Cesium.

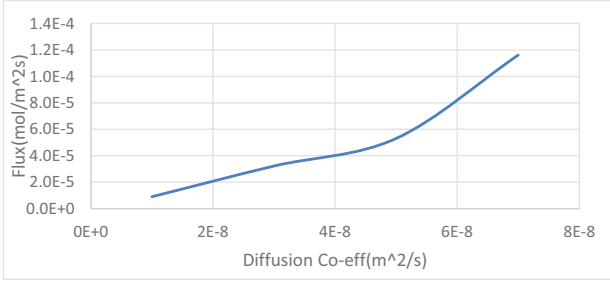

Figure 5: Flux vs Diffusion Coefficient of Cesium in Hollandite

Similarly it is possible to identify the contribution of different parameters i.e. size, shape, connectivity, interface/interphase characteristics, and physical properties of the constituent on the overall flux by systematic variation of the parameters. This will enable us to relate the degradation of the waste form originating from the ionic flux to the above parameters and help in the process of finding and efficient design of the waste form.

Conclusion

The goal of his effort was to demonstrate the capability of the conformal finite element model that can be used as a tool to predict life of a waste form based on its degradation behavior. Conformal finite element was performed by using X-ray nano tomography data to recreate real microstructure of the waste form to apply to the model as a domain. The model was capable of solving the complex micro structure with varying diffusion coefficient of Cesium in Hollandite. The model can be used to understand the concentration gradient of Cesium in Hollandite.

Cesium transport path inside the Hollandite was also predicted which can be used to identify porous network formation path dependent on the micro structure of the material.

Future Work

In the future, this model will be validated with experimental data obtained from leaching of a waste form specifically designed to degrade quickly compared with transient solution of the problem simulating time dependent degradation. Although initial calculations were based on ion diffusion values obtained from literature values, in the future, single phase diffusion values will be obtained experimentally for given operating conditions to include in the degradation model.

Acknowledgement

The authors are grateful for the support of Nuclear Energy University Program of the US Department of Energy (Award ID: DE-NE0008260).

References

1. Waste Forms Technology and Performance Final Report by National Research Council of the National Academies ISBN-10: 0-309-18733-8. *Waste Forms Technology and Performance Final Report by National Research Council of the National Academies ISBN-10: 0-309-18733-8* **2011**.
2. Bursill, L. A. "Structural relationships between β-gallia, rutile, hollandite, psilomelane, ramsdellite and gallium titanate type structures." Acta Crystallographica Section B: Structural Crystallography and Crystal Chemistry 35.3 (1979): 530-538.
3. Angeli, Frédéric, Peter McGlinn, and Pierre Frugier. "Chemical durability of hollandite ceramic for conditioning cesium." Journal of Nuclear Materials 380.1 (2008): 59-69.
4. Shaw, H.F., "Determination of the Open and Closed Porosity in an Immobilized Pu Ceramic Waste Form," UCRL-ID-132605, September 1998
5. C. Hong, X. Zhang, J. Han, S. Meng and S. Du, "Synthesis, Microstructure and Properties of High-Strength Porous Ceramics," Ceramic Materials - Progress in Modern Ceramics, Prof. Feng Shi (Ed.), ISBN: 978-953-51-0476-6, 2012
6. Aleksyuk, M.M., "A Method For The Strength Prediction Of Porous Ceramics," *Strength of Materials, Vol. 33, No. 2, 2001*
7. Gjelstad, Astrid, Knut Einar Rasmussen, and Stig Pedersen-Bjergaard. "Simulation of flux during electro-membrane extraction based on the Nernst–Planck equation." Journal of Chromatography A 1174.1 (2007): 104-111.
8. Rabbi, F., Reifsnider, K. L., "Multiphysics charge transport behavior study of heterogeneous functional material systems using finite element analysis of real microstructural domain ," International Conference on Computational and Experimental Engineering and Sciences, Reno, NV July, 2015
9. W. M. Harris, K. S. Brinkman, Y. Lin, D. Su, A. P. Cocco, A. Nakajo, M. B. DeGostin, Y. K. Chen-Wiegart, J. Wang, F. Chen, Y. S. Chu, and W. K. S. Chiu, "Characterization of 3D interconnected microstructural network in mixed ionic and electronic conducting ceramic composites," Nanoscale, vol. 6, no. 9, p. 4480, 2014.
10. Leinekugel-le-Cocq, A. Y., et al. "Synthesis and characterization of hollandite-type material intended for the specific containment of radioactive cesium." Journal of Solid State Chemistry 179.10 (2006): 3196-3208.
11. P. J. Gellings and H. J. Bouwmeester, Handbook of Solid State Electrochemistry. CRC Press, 1997.

REWAS 2016: Towards Materials Resource Sustainability
Edited by: Randolph E. Kirchain, Bart Blanpain, Christina Meskers, Elsa Olivetti, Diran Apelian, John Howarter, Anne Kvithyld, Brajendra Mishra, Neale R. Neelameggham, and Jeff Spangenberger
TMS (The Minerals, Metals & Materials Society), 2016

LIFE-CYCLE COSTING PROMOTES USE OF CORROSION-RESISTANT ALLOYS

John Grubb[1], James Rakowski[1]

[1]ATI Flat Rolled Products, 1300 Pacific Avenue, Natrona Heights, PA 15065

Keywords: Life-Cycle Costing, Stainless Steel, Recycling

Abstract

The use of "life-cycle costing" makes it more likely that durable and maintenance-free corrosion resistant alloys will be chosen. The cost of corrosion failure is examined and compared with raw material costs, and the excess cost of using lower initial cost, but inadequate material is explored. The desirability of using suitable corrosion-resistant alloys is highlighted. The use of life-cycle costing (LCC) to justify the use of materials with higher initial cost is illustrated.

Introduction

Sustainable options and methods place greater demands upon materials and often drive the use of corrosion-resistant alloys. These demands include:

- Minimization of process discharges causes a decrease in blowdowns and a build-up of in-process contaminants, many of which are corrosive.
- Alternative sourcing of raw materials and increased recycling may increase the concentration of unwanted contaminants in the process environment.
- The desire to reduce plant footprints places constraints on equipment size. For example, space limitations may dictate the use of plate-frame heat exchangers (PFHE) instead of traditional shell and tube heat exchangers. PFHE contain multiple gasketed joints and present a significantly increased risk of corrosion.
- Reduced equipment size, coupled with the need to maintain or increase production, leads to the use of higher pressures and temperatures. This leads to greater corrosion. In some cases, standard materials are no longer adequate for service under the new conditions.
- Use of new processes with different inputs and catalysts may minimize the generation of unwanted byproducts and avoid environmentally hazardous substances, but may inherently increase the risk of corrosion.
- Regulatory changes have removed certain coating products from the marketplace (e.g. chromates, cadmium plating and lead-containing rust inhibitors), and concerns about volatile organic compound (VOC) emissions have restricted the use of solvent-borne coatings. Coating for enhanced environmental resistance has thus become more challenging.

Stainless Steel

Stainless steel is the term used to describe the broad family of corrosion-resistant iron-base alloys that contain a minimum of 10.5% chromium. Chromium is essential to achieve the metal's "stainless" properties. Other alloying elements (such as nickel, molybdenum and copper) provide

a wide range of mechanical and physical properties, and confer greater corrosion resistance in specific environments. Stainless steel's resistance to corrosion, coupled with its low maintenance requirements, make it an inherently green material. It is 100% recyclable, without any degradation or deterioration of quality, Thus it is an ideal material of construction for many applications.

Stainless steel scrap has a high intrinsic value, with the availability of scrap limited by the inherent durability of the product and its subsequent applications. For example, when stainless steel is used in buildings, it remains there for many years and cannot be reused before the building is dismantled. Disposable items are generally not manufactured from stainless steel. The ease of stainless steel recycling and the high value of the scrap ensure that most process scrap is recycled, leading to one of the highest recycling rates of any material. It is estimated that at least 70% of stainless steel is recycled at the end of life [1]. The recycling system for stainless steel is very efficient and requires no subsidies to make it economical. Table I details the significant markets for stainless steel and the recycling percentages for each.

Table I. Life Cycle of Stainless Steel in Main Application Sectors [2]

Application	Percentage of Sales	Average Life (years)	Sent to Landfill	Collected for Recycling	Total as Stainless Steel
Building	16%	50	8%	92%	95%
Transportation	21%	14	13%	87%	85%
Industrial machinery	31%	25	8%	92%	95%
Household appliances	6%	15	18%	82%	95%
Electronics	6%	-	40%	60%	95%
Metal goods	20%	15	40%	60%	80%
Total	100%	22	18%	82%	90%

The electric arc furnace (EAF) is the initial method used in the production of most stainless steel. The primary inputs are scrap metals and electricity, which converts the charge mix into liquid, unrefined stainless steel. This starting metal is then generally fed into a decarburizing or refining process such as argon-oxygen decarburization (AOD), which lowers the carbon content to the desired level and allows for precise adjustment of the final steel chemistry. The ability of the EAF to consolidate a wide variety of input feedstocks and the subsequent refinement via AOD processing are key enabling technologies allowing for efficient recycling of stainless steels. Corrosion-resistant nickel and titanium alloys share many of these attributes. They too exhibit long lives and are readily recycled.

Life Cycle Assessment (LCA)

LCA is a technique to assess the environmental aspects and potential impacts associated with a product, process, or service, by:

- Compiling an inventory of relevant energy and material inputs and environmental releases (life cycle inventory).
- Evaluating the potential environmental impacts associated with identified inputs and releases.
- Interpreting the results to help make a more informed decision [3].

Life Cycle Inventory (LCI)

A life cycle inventory (LCI) is one of the phases of a life cycle assessment. LCI data quantifies the material, energy and emissions associated with a given functional system [4].
As recycled content of stainless steel goes up, the primary energy used in the stainless steel production falls. Stainless steel is one of the most recycled materials. Recycled scrap constitutes a large portion of the materials used to make new stainless steel. The global average rate for the scrap charge ratio in stainless steel is 60%. [5] The North American average is even higher with the average recycled content of 300 series stainless steel grades reaching 75 to 85% [6].

Life Cycle Costing (LCC)

Life cycle costing (LCC) is a tool to determine the most cost-effective option among different competing alternatives to complete a project. LCC takes into account both first cost and all the estimated costs related to future activities, including periodic maintenance and rehabilitation. Costs are usually discounted and totaled to a present day value known as net present value (NPV) [7]. LCC includes projections of future interest and inflation rates, maintenance intervals and costs, and the desired service life. Materials costs are assessed taking into consideration such long- and short-term factors as initial outlay, maintenance and its frequency, downtime effects, production losses, repair, replacement, and other operationally related costs such as manpower and energy consumption.
Experience has shown that the costs of both future maintenance and associated downtime can far outweigh the initial material costs. A full life cycle cost analysis enables the materials specifier to consider the full implications of future costs over the life of the project both in terms of actual monetary value and inconvenience of future maintenance and replacements. The schematic in Figure 1 illustrates that the cost of using less-durable materials A and B substantially increases over time, while the cost of stainless steel usually remains constant due to little or no maintenance requirements [8].

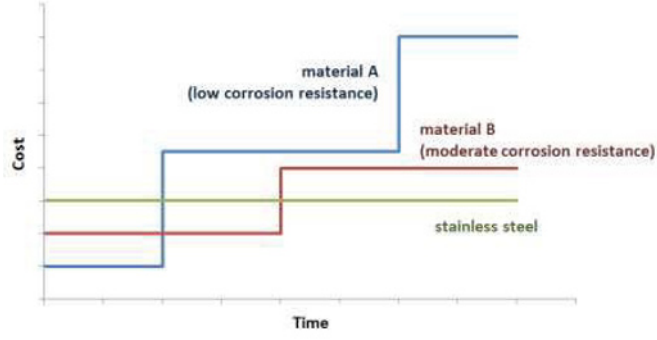

Figure 1. Life cycle cost schematic for stainless steel and less durable materials A and B.

By providing quantitative evidence of potential long-term savings, LCC counters the tendency of many to make decisions based largely on acquisition cost, and this promotes the use of corrosion resistant materials. One weakness of LCC is its sensitivity to the discount (interest) rate used. Often it is beneficial to perform the analysis using several discount rates to provide guidance on the benefits of different options if interest rates change.

Ideally, LCC would account for all costs borne by society associated with the use of any given product. In reality, LCC fails to account for costs associated with pollution, etc. These have been called "external costs." The failure of classic LCC to consider such external costs is one of the drivers behind the development of LCA, LCI and the concept of sustainability. The lack of a consistent yardstick makes these concepts somewhat difficult to apply. New regulations are likely to convert some of these external costs to internal costs. If that happens, LCC comes closer to the goal of LCA.

Cost of Corrosion and Selection of Corrosion-Resistant Materials

Corrosion of metals costs the United States economy over $300 billion annually. It is estimated that about one-third of this cost ($100 billion) is avoidable by use of best known technology. This begins with design, selection of anti-corrosion materials like stainless steel, and quantifying initial and future costs including maintenance by LCC techniques [8].

Pitting Resistance of Stainless Steels

A useful way of ranking the resistance of a material to chlorides is through the Pitting Resistance Equivalent (PREN). Equation 1 gives a common formula for calculating the PREN for austenitic stainless steels [9].

$$\text{PREN} = \%\text{Cr} + 3.3\times\%\text{Mo} + 16\times\%\text{N} \quad (1)$$

The PREN approximates the critical crevice temperature in seawater, or its laboratory stand-in, ferric chloride. The higher the PREN, the more resistant the alloy is to pitting and crevice corrosion in the presence of chlorides. The PREN is not a direct measurement of pitting resistance – it provides a quick predictive comparison among various alloys. The elements Cr, Mo, and N provide resistance to pitting, especially when present together [10-12]. Nitrogen is particularly effective in the superaustenitic alloys combined with high Mo content [13-15]. The formula above is not the only PREN. The reader is referred to the survey of Bauernfeind and Mori for a review of various formulae [16].

Two things about PREN are worthy of special notice:

- Molybdenum is highly effective in increasing PREN, but is one of the most expensive alloying elements commonly added in large quantity to stainless steels.
- Nickel is not shown in the PREN formula, but is a necessary co-solvent to keep molybdenum in solid solution in the alloy. Nickel is the other expensive alloying element commonly added in large quantity to stainless steels.

Thus, alloys with greater pitting (or crevice) corrosion resistance are typically more expensive. Indeed, alloy corrosion resistance and alloy cost are so highly correlated that they might be considered as stand-ins for one another.

Cost of Corrosion Failure

In assessing the materials selection process, it is first necessary to understand that both our knowledge of corrosion and our knowledge of future operating environments are imperfect. Thus, in many cases we cannot predict absolute success or failure, but rather a probability of success. With this in mind, the relationship between the costs of over- and under-design will be examined. The following assumptions have been used:

- Fixed construction costs are about ten times the cost of mid-range material.
- Variable construction costs are material cost plus 100% to reflect the variation in fabrication costs (welding, forming, grinding, pickling, etc.) that may be material cost dependent.
- Failure probability follows a Weibull-like curve and is lower for higher-alloy (higher cost) materials.
- Failure cost is probability of failure multiplied by ten times the fixed construction cost (this includes loss of production and the costs of purchased product). Therefore, cost of failure decreases with increasing cost of material.
- Total cost is the sum of construction cost plus failure cost.

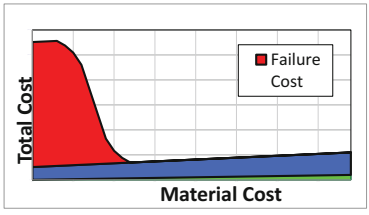

Figure 2. Schematic diagram of total installation costs if failure is considered.

The resultant total cost curve is asymmetric – the risk of under-specifying material quality and experiencing an early failure is far greater than the risk of over-specifying the material.

Conclusions

- The use of life cycle cost (LCC) analysis promotes the use of durable materials such as stainless steels.
- Stainless steel is an inherently green material in that it is 100% recyclable without any degradation or deterioration of quality.
- Stainless steel is one of the most recycled material in the world
- Modern installations may be subjected to more severe corrosion conditions than has historically been the case. Future developments in sustainability may increase the severity of this environment even more. These developments are likely to affect both new and existing units.
- Therefore, prudence suggests that selection of a material with somewhat more than the minimum necessary corrosion resistance reflects sound engineering judgment.

References

1. " Stainless steel and CO_2: Facts and scientific observations", International Stainless Steel Forum, Rue Colonel Bourg 120 B-1140 Brussels Belgium, 2010, www.worldstainless.org
2. B. Reck and T.E. Graedel, *Comprehensive Multilevel Cycles for Stainless Steel for 2000 and 2005*. Preliminary Final Report for Yale University/ISSF Stainless Steel Project, 2009.
3. *Life Cycle Assessment (LCA)* http://www.epa.gov/nrmrl/std/lca/lca.html
4. *Stainless Steel, Architecture and the Environment*, Rimex Metals, 2009
5. *How to quantify the environmental profile of stainless steel*, H. Fujii, T. Nagaiwa, H. Kusuno, and S. Malm, Paper presented at the SETAC North America 26th Annual Meeting, 15-17 November 2005.
6. SSINA *LEED™ Fact Sheet*, http://www.ssina.com/leed.htm
7. B. Dhillon, *Life Cycle Costing: Techniques, Models and Applications* (New York, NY: Gordon and Breach Science Publishers, 1989).
8. *Introduction to Life Cycle Costing for Stainless Steel*, SSINA, March 2000,
9. G. Herbsleb, "Der Einfluss von Schwefeldioxid, Schwefelwasserstoff und Kohlenmonoxid auf die Lochkorrosion von austenitischen Chrom-NickelStählen mit bis zu 4 Massen-% Molybdän in 1 M NaCl-Lösung", Werkstoffe und Korrosion 33 (1982), p. 334.
10. R. J. Brigham, Corrosion, 28 (5), (1972), p. 177.
11. R. J. Brigham, E. W. Tozer, Corrosion, 29 (1), (1973), p. 33.
12. R. J. Brigham, E. W. Tozer, Corrosion, 30 (5), (1974), p. 161.
13. J. R. Kearns, J. Mater. Energy Sys., 7 (1), (1985) p. 16.
14. R. Bandy, Y. C. Lu, R. C. Newman, C. R. Clayton, Proc. Equilibrium Diagrams and Localized Corrosion Symposium, P. Frankenthal and J. Kruger, Eds., (Electrochem. Soc., Pennington, NJ, 1984) p. 471
15. J. E. Truman, M . J. Coleman, K. R. Pirt, Brit. Corrosion J., 12 (4), 1977, p. 236.
16. D. Bauernfeind and G. Mori, " Corrosion of Superaustenitic Stainless Steels in Chloride-and Sulfate-Containing Media - Influence of Alloying Elements Cr, Mo, N and Cu", NACE Corrosion 2003 paper 03257, NACE International, 2003.
17. J. F. Grubb and C. P. Stinner, "Considerations for Material Selection and Fabrication of Corrosion Resistant Alloys for FGD Service," Welding and Fabrication Technology for New Power Plants and Components: 2nd International Conference, EPRI, Orlando, FL, June 2011.

REWAS 2016: Towards Materials Resource Sustainability
Edited by: Randolph E. Kirchain, Bart Blanpain, Christina Meskers, Elsa Olivetti, Diran Apelian, John Howarter, Anne Kvithyld, Brajendra Mishra, Neale R. Neelameggham, and Jeff Spangenberger
TMS (The Minerals, Metals & Materials Society), 2016

SYSTEM OF STATE REGULATION OF SUSTAINABLE ORE PROCESSING AND PRODUCTION WASTE TREATMENT IN THE RUSSIAN ARCTIC

Vyacheslav Tsukerman, Ludmila Ivanova, Vladimir Selin

Institute for Economic Studies, Kola Science Centre, Russian Academy of Sciences;
Fersman Str., 24a; Apatity, Murmansk region, 184209, Russia

Keywords: economic growth, processing of minerals, wastes, innovation technologies.

Abstract

Dynamics of general economic growth is to a considerable extent determined by results of research, technical and innovation policies in the Arctic zone of Russia. According to scholars' evaluations contribution of innovation-technological development of the economy in growth of the country's GDP accounts for 70-80%. Mineral formations, accumulated during the industrial epoch, affect significantly economic and ecological situation in the Arctic region. On the one hand, production wastes destroy the region's environment. On the other hand, man-made mineral formations contain a lot of valuable scarce components. Volumes of solid wastes increase annually. Transition to innovation economy provides re-comprehension of mining in the society. Measures should be directed to radical renovation of production technologies. It will ensure rapid growth of competitiveness, increased demand and stronger position at the international market. Development of innovation technologies can be provided at the expense of active state and private innovation activities.

Introduction

In northern regions it is necessary to fulfill the basic organizational-economic conditions for implementation of industrial innovative policy:

- Aiming at support to innovations, making the basis for the modern technological way;
- Combining the state regulation of innovative activities with market mechanism;
- Promoting development of innovative activities in regions, international transfer of technologies and investment cooperation, protection of interests of national innovative businesses.

The strategy of industrial development in connection with transition from the conceptual export-oriented model to resource-innovative model and to innovative-technological model is considered. The real condition of industrial production, implementation of domestic and foreign technologies, and their subsequent development are taken into account. The article presents some results of the authors' research work on models of industrial development applicable in the North.

Resource export-oriented model

The essence of the conceptual model consists of all-round encouragement of the manufactures focused on exports of products. This model is characteristic for regions of the North and is a special case export-oriented model. The basic incentive measures of the state are directed to development and support of competitive export branches. The priority problem considers manufacture of competitive production and entering the international market.

There is a number of features, which due to geographical, social and economic conditions force to consider the initial "export-oriented model" for the given regions in a new way. Owing to export orientation of mining companies of the North, the majority of them managed to adapt to the market relations, and increased competition. A number of powerful vertically integrated companies, diversified holdings was established (Petukhov, 2007).

Under the modern conditions the high tech mining industry of the Arctic is the most perspective basis for accelerated technological development of the country. Specific features of the economy of northern regions demand prompt solutions of problems connected with development and implementation of regional strategic priorities of the industrial policy. Use of mineral resources of the North in many respects is connected with so-called "economic availability" involving new resources in many respects defined by development of economy and an infrastructure.

In the Arctic zone under the conditions of production fluctuation, decrease in investment activities and lack of an efficient state industrial policy in innovative sphere, measures on re-structuring of the economy have not led to modernization of manufacture on the basis of high tech providing competitiveness of all components of production at all technological stages of its output.

Now the main reasons of low efficiency of minerals processing are:

- lack of modern domestic technologies for deep processing of resources;
- high risks of reduction of production volumes at the final stages of processing caused by imperfection of technologies and production organization, backwardness of industrial and transport infrastructure, lack of qualified personnel, etc.;
- inefficient tax and customs mechanisms, basically encouraging exports of the primary, raw resources. The listed reasons are quite surmountable. So, lack of modern technologies can be filled in by their import. The risks of “long” technological chains, which are inherent in the industry of the North, can be essentially lowered by the purposeful consecutive industrial policy.

Resource export-oriented models have the same shortcomings as export-oriented, including:

- capital-intensive goods are imported for manufacture of exported natural resources;
- more primitive structures of the domestic industry;
- outflow of both human and financial resources from the manufacturing industry and decreasing of its competitiveness;
- reduction of knowledge accumulation, stagnation in the manufacturing industries (the "Dutch" disease) and its backlog from the global level;
- the need to import innovative technologies.

So, despite the general positive results of development of the oil and gas industry, the problematic situations and negative tendencies were generated (Konovalova, 2007).

One of them is the low degree of oil extraction, which in the North is one of the lowest in the world. The scientific and technical potential of modern methods of increase in feedback accumulated in the domestic and world practice is not demanded anymore. By virtue of the developed economic conditions in the North the intensification of selective working off of active stocks prevails. Continuation of such practice will inevitably lead to crisis of oil extracting.

Shortcomings of the model practically level effect from raw materials export as put economic development of regions and the countries in dependence on foreign manufacturers. Economy of the North, which potential is substantially directed to servicing exports of natural raw materials to the global market, cannot be for a long time in the condition of stable development. Also it should be noted, that export of resources causes low scientific and technical level of other industries.

The basic investments go to extraction of raw material. Taking into account that at the low level of technological security and bad working conditions, in many regions of the North there is outflow of skilled personnel, negative dynamics of traumatism and disease is noticed, the model of economic growth due to diversification of economy and expansions of resource-innovative sources of growth should replace the raw resource-export-oriented model of growth (Martsinkevich, 2006).

In other words for regions of the North vital transition from resource-export oriented models to resource-innovative ones is vitally important. Thus mineral raw material industries of the North as most financially provided, can serve as original "locomotive" for rise of domestic productions in mining, mineral processing, chisel equipment, manufacture of sea platforms and others high-tech productions.

Model of import substitution

The model of import substitution represents strategy of maintenance of the domestic market on the basis of development of national manufacture. Import substitution assumes carrying out of protectionist policy and maintenance of a steady rate of national currency. The import substituting model promotes improvement of structure of the balance of payments, normalization of internal demand, maintenance of employment, development of industrial production, scientific potential.

The negative parties of import substitution models of industrial policy are self-isolation from new tendencies in economic; an opportunity technological, and consequently, competitive backlog from the developed countries; danger of creation of hothouse conditions to national manufacturers; necessity, irrespective of the international division of labor to build completely industrial chains, which can be more capital and resource-intensive, than already existing in other countries (Fedoseev, 2003).

Besides, as the domestic production is noncompetitive and is not in demand at foreign markets, the state is compelled to market it, limiting sales of better imported production that goes on advantage neither to national manufactures, nor consumers. Such situation was characteristic for economies of the USSR and Northern Korea.

Until now the industrial policy of Russia carries strongly pronounced import substitution character: huge grants in an agriculture and branches of a manufacturing industry follow the account of operation profitable export-oriented raw material sector; the mechanism of monetary redistribution leans on restraint of the internal prices for the raw goods, fuel and energy, on direct deliveries to an agriculture and soft loans of the industry, on large creditor debts to the enterprises of thermal power station, on the cheap import which is present in the Russian market because of absence of protectionist measures inefficiencies of legislative base, the general degradation of a domestic production, on the rate of exchange overestimated, until recently.

It is necessary to use advantages of all models both export-oriented and import substitution on the basis of innovative development that will give the Russian economy a necessary push to industrial growth, growth of well-being of its citizens. It is necessary to note, that domestic commodity producers not in a condition to satisfy internal demand, assigning to its solid part to the imported goods. Therefore the problem of Russia is not in import substitution policy, and, more likely, in absence of a precise strategy of economic development including import substitution one (Matishov, 2005).

Resource innovative model

Now economies of industrially developed countries develop in many respects due to steady orientation to innovations and high technologies. The analysis of functioning of economy of regions of the North testifies to inevitability of transition of its development on the basis of use of innovations and new technologies that proves to be true positive experience of industrially developed countries. The potential of not innovative development is close to exhaustion then reduction of export of resources is inevitable, decrease in gross national product, deterioration of incomes of the population, decrease in a standard of life, growth of poverty and other negative consequences. The key characteristic defining a degree of economic and technological safety of any state, and the level of innovative development is formation of a system of maintenance and development of innovative making economy - it is the problem of the national

scale having complex, inter-sector character. Resource-innovative strategy is the basis of rational use of the mineral potential and is caused by following factors:

- a high level of total additional cost and profitability at sufficient volumes of processing of production and their delivery to export;
- qualitative improvement of structure of export due to increase in a share of finished goods;
- an opportunity of use of high technologies for deep processing resources. To number of the factors promoted realization of resource-innovative model of development of regions of the North, can be carried: - presence of the stocks of mineral resources significant reconnoitered and prepared for profitable extraction; - industrial potential of industries; - potentially capacious home market;
- significant territory, potential opportunities of investigation of the most valuable minerals;
- stabilized sociopolitical conditions. For transition to resource-innovative model it is necessary to create conditions for formation regional clusters around enterprises which manufacture production, competitive at the global markets; to render the state support to regions in attraction of foreign investments into hi-tech branches, to take into account their interests when forming foreign economic and customs policy (Larichkin, 2005).

Formation of industrial clusters promotes enough to fast transformation of results of scientific researches in the regional innovative industrial policy. Formation new industrial clusters is frequent thus is considered as base regional endogenous growth. Experience of the USA shows, those industrial clusters can be formed at a level of region where there is a high concentration of the interconnected branches. The important distinctive feature of a cluster is the factor of innovative orientation. Clusters, as a rule, are formed where promotion in the field of the "know-how" and the subsequent output on new segments of the market is carried out or expected. High competitiveness and stability of cluster economic systems is defined first of all with the factors stimulating distributions first of all of new technologies, Character and structure of interaction of a science and formation, the state bodies and the industries. The important role in development of clusters regions play science towns and centers of science. In regions of the North there are necessary conditions for the organization industrial clusters which activity is aimed at the further innovative development.

Technological innovations should be focused on solving the three main tasks:

- mobilization of the accumulated development potential;
- maintenance of conditions for increasing technological level of the domestic metal-working industry (first of all, decrease in metal consumption);
- strengthening position of the domestic metallurgy at the global market of metal products (Tsukerman, 2012).

The research conducted allows stating that in the future the resource-innovative model of economy of extraction and processing of mineral raw materials can transform to innovative-technological, in view of a real condition of industrial productions, implementation of domestic and foreign technologies and their subsequent development.

Innovative-technological model

The innovative-technological model of industrial development of the North represents the process of creation, expansion and exhaustion of the newest development, productive and economic and socially-organizational innovation potential. It also reveals perspective branches and sub-branches, accelerated development of which due to multiplicative effect will promote growth of gross national product.

The innovative-technological model promotes maintenance of scientific and technical potential of the country, and, hence, its competitiveness on the international scene; stimulates development of educational institutions and provides economy with highly educated and qualified staff; promotes creation of workplaces in the country, supports a stable and high rate of national currency and well-being of the

population, and focuses on productions with high value added. The basic mechanisms and conditions of for implementation of the innovative-technological model are as follows:

- the system state priorities, mechanisms of their performance, federal laws and departmental orders;
- regular evaluation of potential innovative and investment projects and programs;
- creation of the modern tax mechanisms not only stimulating innovative activities and supporting commercialization of research results, but also development and spread of technologies;
- further development of state-private partnership in business.

Meanwhile the innovative-technological model provides necessity of an expenditure of huge money resources on development of an innovative infrastructure and updating of the industrial device of the industry; state regulation and stimulation of innovative development of manufacture; preparation and retraining of the big number of the highly skilled staff, and, first of all, the technological managers, capable to operate innovative projects.

Realization of innovative model in many respects depends on regional regulation of innovative processes and innovative activity. The regional policy is formed depending on structural features of an economic complex, allocation of priorities and the purposes of social and economic development on the basis of an estimation of an available potential of concrete subjects. As a result for each of regions it accepts an individual orientation (Dolgunov, 2006). In this connection the federal authorities should incur development and introduction of effective mechanisms, which would stimulate innovative activities at a regional level and induce local authorities to implement the innovative model. Besides considering a huge capital intensity of the given process, efficient implementation of selective industrial policy on the basis of innovative development of separate priority competitive branches is represented. It will promote rapid development of these sectors and strengthen their competitive advantages at the global market. Also it will relieve from extra costs and inefficient development of sectors, which cannot “compete” similar sectors in other countries within the limits of the international labor division.

Besides when implementing any model of industrial policy, it is necessary to consider problems which have long-term character, such as deep structural crisis, low incomes of the majority of population, the limited financial resources of companies, significant deterioration of industrial equipment, and lack of highly skilled staff. It is necessary not only to identify and consider the problems but also to solve them.. Otherwise models and will remain just models.

It should be noted that the important condition of strengthening innovation level of the industries of the Arctic is closer partnership and cooperation between the regional government, industrial companies, higher schools, local authorities and other structures, which should adapt and compete successfully in the global economy. Now for regions of the North the primary problem is development of the education system, training new generation of innovators, specialists in the scientific and technical fields, capable to successfully compete at the labor market, which is also becoming global.

It should be noted, that there is a necessity of development of new indicators of innovative processes occurring in the real time. For this purpose the coordinated efforts of federal statistical agencies, trading associations, professional societies, research establishments, including international are required. The urgency to solve this problem is dictated by the fact that only new indicators are capable to reveal critically important problems, hindering innovations, and alternatives to signal about arising competitive potentialities and risks to prove criteria of estimation of the state innovative programs. Intensity of the global integration and progress in technology accelerates the necessity to solve these problems.

The economic effect from implementation of priorities of innovative development is not limited to increase of competitiveness of industrial companies. It is important, that during the development preconditions for structural reorganization of the economy are created. One of the priority problems of

innovative industrial policy in the near future should be maintenance of economic circulation of the country with financial resources and creation of a favorable investment climate. Within the limits of these directions it is necessary to implement the following:

- further reforming of the tax system of the country in order to decrease the general level of tax gatherings, introducing tax privileges for organizations carrying out investment and innovative activities;
- further expansion of budgetary and inappropriate state funds that will promote decrease in excessive congestion of the federal budget and rendering of its negative influence on a national economy;
- actions to be in full conformity with the general directions of reforms;
- improvement of measures directed to protection of domestic commodity producers at the domestic market,
- every possible support to national exporters at international markets.

We believe that implementation of the specified measures in the North will promote creation of favorable climate for economic growth and increase of competitiveness, resulting in growth of well-being of its population.

Acknowledgement

This paper is based on research carried out with the financial support of the grant of the Russian Science Foundation "The purposeful complex program of the Russian Arctic development(project №14-38-00009)". Peter the Great St. Petersburg Polytechnic University.

References

1. N.A. Petukhov Regional innovation systems: problems of cluster development // Management of innovations and strategy of innovative development of Russia – Moscow, 2007. – 168 p.
2. N.V. Konovalova Role of the state in institutionalization of processes of scientific and technological development of regional industry // Management of innovations. - Moscow, 2007. – 488 p.
3. V.I. Martsinkevich Efficiency Problems in the XXI century: the USA economy.- Moscow, 2006.-389p.
5. S.V. Fedoseev Strategic potential of basic industries. Series Apatity: KSC RAS, 2003. – p. 268.
6. G.G. Matishov, V.V. Denisov, S.L. Dzhenyuk. Strategy of rational nature management on the shelf an in coastal zones of the European North // Formation of bases of the modern strategy of nature management in Euro-Arctic region – Apatity: Publisher of the KSC RAS 2005 – p. 448-462.
8. F.D. Larichkin Problems of formation of a modern model of rational utilization of the entrails. // Formation of the bases of the modern strategy of nature management in Euro-Arctic region – Apatity: Publisher of the KSC RAS 2005 – p. 109-121. 1649
10. V. Tsukerman Growth Prospects Through Innovation Systems for Utilizing Mineral Wastes in Production //. Proceedings of Green Processing 2002. Australian Institute of Mining and Metallurgy – 2012 p.329-333.
11. K.A. Dolgunov, B.G. Sapozhnikov, V.N. Martirosyan The state, prospects and economic aspects of oil and gas prospecting on shelf of the Arctic Seas of Russia // Abstracts of the first Russian conference "National marine policy and economic activities in the Arctic" – Murmansk, June 1-2, 2006 p.53-54.

Understanding & Enabling Sustainability - Light Metals Recycling & Waste Valorization

REWAS 2016: Towards Materials Resource Sustainability
Edited by: Randolph E. Kirchain, Bart Blanpain, Christina Meskers, Elsa Olivetti, Diran Apelian, John Howarter, Anne Kvithyld, Brajendra Mishra, Neale R. Neelameggham, and Jeff Spangenberger
TMS (The Minerals, Metals & Materials Society), 2016

ELECTRODYNAMIC SORTING OF LIGHT METALS AND ALLOYS

Raj Rajamani[1], James Nagel[1] and Nakul Dholu[1]

1- Metallurgical Engineering Department, University of Utah, Salt Lake City, Utah-84112.

Keywords: Sorting, Metals, Alloys, eddy current, alternating magnetic field

Electrodynamic Sorting (EDX™), or variable-frequency eddy-current sorting, is an evolution of sorting technology aimed primarily at light-metal and aluminum alloy recycling. EDX™ is being developed by the Department of Metallurgical Engineering, University of Utah, under an ARPA-E (Advanced Research Projects Agency – Energy) contract. From a purely physical perspective, the EDX system operates by generating an alternating magnetic field in the gap of a toroidal ferrite core. As metallic particles pass through the gap, eddy currents are induced by the presence of the alternating field, which repel the particle from the gap. The velocity at which they exist then varies with distinct physical properties like electrical conductivity, mass density, excitation frequency, and geometry. In this presentation, we describe the fundamental physics of the phenomenon, including simulation data with CST software and results in pilot scale (100 kg/h) systems. Finally, the results on auto shredder scrap mix is presented.

Introduction

A typical source of scrap comes from end-of-life products like cars, household appliances, popular electronic devices, and waste products generated during the manufacturing process. The scrap mixture consists of ferrous and nonferrous metals, semiconductors, plastic, glass and rubber. Initially, the ferrous materials are removed through a magnetic separation process. The nonferrous scrap is then processed through mechanical eddy current sorters, optical sorters, and X-ray sorters to separate metallic scrap from nonmetallic. The sorted nonferrous metallic scrap is called Zorba, which generally constitutes aluminum, copper, nickel and brass. The Zorba product is further sorted by mechanical eddy current sorters to a product rich in aluminum, called Twitch. Due to the higher concentration of aluminum in Twitch, it has more economic value compared to aluminum sold as Zorba. Further economic value addition to Twitch can be achieved if it is sorted based on different alloy fraction such as cast alloys (e.g. 300 series) or wrought alloys (e.g. 1000 – 7000 series). Sorted Twitch adds 50% economic value, which is around 90% of the price of the pure Aluminum metal, compared to twitch if sold unsorted[i]. EDX is being developed to sort either Zorba or Twitch to recover metals as well as different metal alloys.

EDX core, coil, magnetic field, and particle deflection velocity simulation.

In the past, most of the theoretical foundation for EDX behavior has been tied to the physical models of Landau and Lifshitz[ii]. This was also the mathematical basis behind the Saveliev patent[iii] of 1998. However, due to the severity of assumptions made, such models are rather limited in scope and applicability. Analytical solutions therefore do not exist for the complex geometries being investigated, nor can they be easily derived.

When complex physical models exceed the capability of simple analytical methods, the most common solution is to resort to numerical simulation. Computer Simulation Technology (CST) is a software suite that specializes in complex electromagnetic simulation methods. Figure 1 shows a screen capture of a 44 cm core of NiZn ferrite before simulation. In particular, the simulation is focused on low-frequency electrical currents induced by time-varying magnetic fields. Once the electrical currents are computed, they can be used to solve for the net magnetic force on the particle they inhabit. This produces an acceleration,

which we can then track through the field to calculate the net work performed on the particle along the way. This in turn gives us the particle's kinetic energy, and hence its velocity and trajectory.

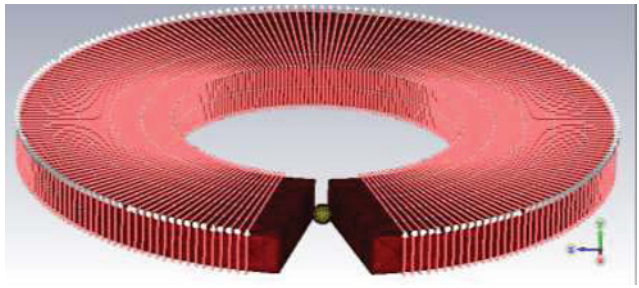

Figure 1: 44 cm core simulation model with 77 turns and tetrahedral mesh.

Although the scrap particles are generally random in their geometries, it is reasonable to presume a first-order approximation to the problem by treating all particles as perfectly uniform spheres. We also assume that particle diameters are generally limited to the range of 0.25 – 2.0 cm. The core itself was modeled as a rectangular toroid with inner diameter of 32 cm, outer diameter of 44 cm, and height of 3 cm. The magnetic permeability of the ferrite was set to μ_r = 1600 and then wound uniformly with 300 wire turns. The drive current was then fixed at 4.0 A_{pk} with a frequency of 5.0 kHz for all simulations. When a simulation is finally completed, CST then calculates the net force experienced by the particle.

To calculate the final velocity of the particle as it leaves the gap, we must perform several simulations. The first simulation begins with the particle placed as far into the gap as it can reasonably fit without making contact with the walls. Next, the particle is moved in tiny increments of 1.0 mm, repeating the simulation with each step. This generates an approximate force profile F(x) for the particle as a function of position. The physical work exerted on the particle as it leaves the gap may then be calculated using

$$W = \int F(x)dx \, .$$

Once we arrive at a numerical value for the physical work, we may assume that all of the energy will be converted directly into kinetic energy, as there is no significant source of friction acting on the particle. The final particle velocity as it leaves the gap is thus calculated as

$$v = \sqrt{\frac{2W}{m}} \, .$$

Typical Simulation result:

Figures 2 shows the comparison between CST and empirical measurement with a magnetic Hall probe. In general, the simulations appear to agree very well with the measured values and can be reliably used to model complex physical geometries. Figure 3 shows the resultant force profile on a spherical ball of copper with diameter 1.5 cm when driven to a frequency of 4.8 kHz. Superimposed on the data is an empirical measurement profile taken with a strain gauge. Again, simulation data shows excellent agreement with measurements, thus further boosting our confidence in the numerical model.

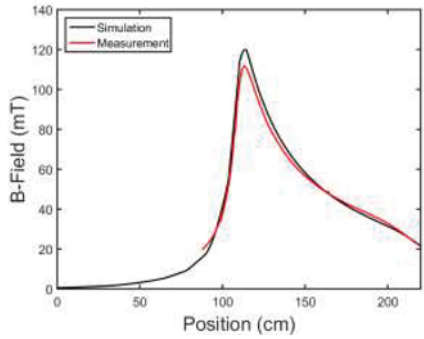

Figure 2: Measured and simulated field profile down the centerline of the magnetic core

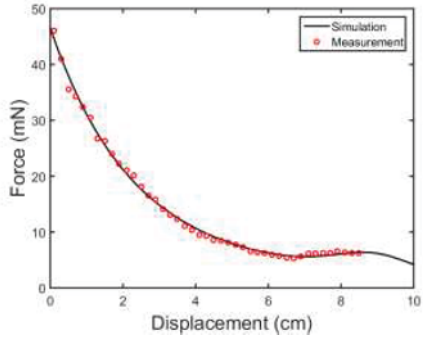

Figure 3: Force profile of a 1.5 cm copper sphere.

Sorting Experiments:

Finally, a number of sorting experiments were carried out with a lab scale and pilot scale EDX devices. The lab scale device ranged in core diameter between 7.5 cm to 20 cm while the pilot scale device used a core with 44 cm diameter. Throughput typically ranged between 10-30 kg/h, with a significant improvement in particle distribution due to sorting. A typical set of experimental results is shown in Table 1. These experiments were performed using synthetic mixture of 600 spherical particles with 6 mm diameter. The mixture varied in material composition, including copper, brass and titanium. Aluminum particles were also included using 200 oval-shaped aluminum particles with size ~8 mm x ~12 mm x ~3 mm. Ten consecutive runs of the whole sorting process were conducted for immediate precision and reproducibility assessment.

Table 1: Result of sorting experiments of the mixture of metals and alloys

Exp No	Recoveries				Grade			
	Al	Cu	Brass	Ti	Al	Cu	Brass	Ti
1	100.00%	93.00%	96.50%	97.50%	93.90%	98.41%	96.98%	97.99%
2	100.00%	96.00%	98.50%	98.50%	96.15%	98.46%	98.50%	100.00%
3	99.00%	98.50%	97.50%	98.00%	98.51%	96.57%	97.99%	100.00%
4	99.50%	99.00%	97.50%	98.50%	99.00%	98.02%	98.48%	98.99%
5	98.50%	99.00%	97.50%	97.00%	99.49%	97.54%	96.53%	98.48%
6	97.50%	98.50%	97.00%	96.00%	98.98%	97.52%	95.57%	96.97%
7	98.00%	98.50%	97.50%	97.00%	99.49%	96.57%	96.06%	98.98%
8	98.00%	97.00%	99.50%	97.00%	98.00%	97.98%	96.14%	99.49%
9	96.00%	100.00%	97.00%	97.50%	100.00%	94.79%	97.49%	98.48%
10	94.00%	99.50%	95.00%	98.50%	100.00%	93.43%	97.94%	96.10%
Average	**98.05%**	**97.90%**	**97.35%**	**97.55%**	**98.35%**	**96.93%**	**97.17%**	**98.55%**
Std dev	**1.88%**	**2.08%**	**1.18%**	**0.83%**	**1.93%**	**1.66%**	**1.06%**	**1.26%**

Experimental work on auto shredder scrap with a pilot scale EDX is underway. These results will be presented.

[i] Mike, R. and John, M., 2015. "Recycling twist cuts Ford truck costs". The wall street journal

[ii] L.D.; Lifshitz, E.M. and Pitaevskii, L.P., Landau and Lifshitz Course on Theoretical Physics, Volume 8, Electrodynamics of Continuous Media

[iii] Saveliev, V.L., 1995. “System and method for separating electrically conducting particles,” U.S. Patent 5,439,117, 1995.

REWAS 2016: Towards Materials Resource Sustainability
Edited by: Randolph E. Kirchain, Bart Blanpain, Christina Meskers, Elsa Olivetti, Diran Apelian, John Howarter, Anne Kvithyld, Brajendra Mishra, Neale R. Neelameggham, and Jeff Spangenberger
TMS (The Minerals, Metals & Materials Society), 2016

SCRAP CHARACTERIZATION TO OPTIMIZE THE RECYCLING PROCESS

Sean Kelly[1] and Diran Apelian[1]
[1]Center for Resource Recovery and Recycling (CR3), Worcester Polytechnic Institute
100 Institute Rd.; Worcester, MA, 01609, U.S.A

Keywords: Auto-shred aluminum, characterization, polymers, waste-to-energy

Extended Abstract

Managing the secondary production process for aluminum auto-shred scrap is of prime importance considering the projected demand increase for aluminum alloys in the transportation, electronic and packaging industries. Aluminum auto-shred scrap is a major end-of-life, mixed metallic stream that must be recovered and recycled effectively and efficiently to ensure infinite lifetime involving a broad distribution of re-use applications determined by specific alloy chemistry [1, 2]. Currently, secondary recyclers that dilute the melt chemistry using primary aluminum minimally only produce A380.1 as this alloy has broad alloy chemistry specifications [3]. Downgrading mixed auto-shred scrap streams is a significant waste of intrinsic value and re-use applicability. Downgrading here is defined as not utilizing all sortable chemistries within this mixed auto-shred. This, paired with scrap export, are the two major present day options for mixed aluminum scrap.

One issue preventing a wide secondary alloy spectrum is the lack of knowledge concerning sortable chemical compositions in these mixed scrap classes. In addition, proper commercial equipment capable of intelligently sorting into the consumer dictated chemistries while maintaining profitable throughput specific to aluminum and it's alloys needs to be properly developed and installed in the secondary recycling process. Steinert manufactures an XSS F (x-ray fluorescence sorting system) capable of sorting based on the heavy metals (Zn, Cu, Fe) in solid solution however more work needs to be completed to understand the extent of achievable sorting capabilities. Understanding of the varying scrap bulk chemistries as a function of time, region of origin, shredder feedstock and processing parameters will aid in proper allocation of scrap mixtures with or without intelligent sorting system exposure. Regardless of sorting mechanism, cleaning and removal of organic and polymeric content is necessary for proper downstream recycling [4]. These processes must be environmentally acceptable and exercise waste-to-energy removal methods of carbon-based impurities in the form of free polymers, oils, lubricants, paints and coatings. Another issue combating this industry is the unnecessary transport of recovered scrap particulates to be charged at external secondary smelting or casting facilities. The developing Aluminum Integrated Mini-mill process will utilize a proper inline process to sort, clean, re-melt and cast multiple secondary aluminum alloy types from this mixed scrap stream [5]. This work is focused on characterizing aluminum auto-shred in terms of metallic chemistry and through thermal analysis of the organic content to aid development of intelligent sorting systems and waste-to-energy cleaning processes, respectively.

Through a three phased approach, the research team will present an overview landscape of a complicated industry by: (i) investigating market relations domestically in the U.S. and with international consumers; (ii) financial fluctuations to expose margins for developing business

models; (iii) and auto-shred scrap composition characterization for intelligent sorting and cleaning systems. Automotive shredder scrap is an above ground aluminum ore that needs to be utilized in the USA as so much is produced with high amounts intrinsic energetic and metallic value. The export of scrap aluminum will continue to occur, but a higher volume should be maintained domestically so primary import and energy-intensive bauxite extraction can be avoided. The two auto-shred scrap classes analyzed in this work are Zorba and Twitch. Zorba is the non-ferrous auto-shred scrap containing aluminum, copper, zinc, magnesium, nickel, titanium and even some stainless steel. Twitch contains predominantly aluminum alloys (typically 90-98 wt. %) [6]. Twitch is derived from Zorba via sink-float separation or optoelectronic technology focusing on atomic density (*i.e. x-ray transmission*) [6].

Phase 1 of this project focuses on the market dynamics of the aluminum scrap industry and covers auto-shredder scrap specifically and aluminum scrap as a whole. The amount of auto-shred scrap, or Zorba/Twitch, that is exported from the USA to external markets is estimated. Upon further investigation, however, this estimation has been proven to be a significant underestimation and this will be discussed in the presentation. Due to the latter, a further analysis was conducted at a macro-scale covering the entire aluminum scrap market. One objective of this larger scale study is to compare scrap export with the international trade of other forms of aluminum (*i.e. mill products and ingots*). A second objective is to determine the amount of scrap consumed vs. how much is available for consumption in the U.S. and Canada; similar to the original auto-shred analysis. Finally, the amount of non-UBC (used beverage container) aluminum scrap metal traded to and from the U.S. on a country by country basis is to be determined for the most recent data available; 1996-2015 (YTD).

Phase 2 analyzes the margin between the cost of recovered auto-scrap classes and the value of secondary aluminum alloys. The value quantified is considered an initial margin as the calculation does not account for labor cost, capital cost, energy costs or any other accrued cost during the processing of this material.

Phase 3 seeks to quantify three distributions to support developing intelligent sorting systems. The distributions are: Major Category, Alloy, and Bin/Chemical. The six major categories are aluminum cast, aluminum wrought, other metals, mixed metals (*i.e. aluminum cast with a rusty steel bolt*), mixed material (*e.g. metal piece with significant amount of adhered polymer*), and free solid polymeric particulates. Oils, lubricants and paints are not considered to be significant adhesions. The alloy distribution includes cast 319, 356, 360, 380, 384, 390 and 413, specifically, and 2000, 3000, 4000, 5000, 6000, and 7000 series for the wrought portion. Distribution of the 6000 series to 6061, 6063 and the other 6000 alloys was achievable due the variance in the electrical conductivity measurements recorded, this was not possible for the 5000 series, however. The final distribution was determined based upon the chemical composition of the individual scrap pieces and a threshold criteria set by the research team upon discussions with professionals within the recycling industry.

Additionally, three thermal analysis techniques were performed on the organic and polymeric components found within these auto-shred scrap mixtures to aid in the optimization of proper cleaning techniques. Thermogravimetric analysis (TGA) to determine vaporization temperature and quantify residual mass values for free polymers, paints and coatings, adhered polymeric

materials and cutting oil in an inert atmosphere. Cone calorimetry was utilized to determine heat of combustion values and residual mass value for free polymers in air. Finally, a burn off study, in air, paired ultrasonic cleaning, in water, was conducted to quantify the amount of oils/paints/coatings/lubricants that can be removed as a function of temperature and char removal.

Finally, an evaluation of the sorting criteria set in Steinert's automated sorting systems, XSS T and F, was conducted. A 100 lb. Zorba sample was tested on the companies' XSS T (x-ray transmission) to determine its ability to sort Zorba into its material constituents. Also, a 100 lb. Twitch samples was run through the XSS F (x-ray fluorescence) system to determine the possible chemical composition outputs when sorting on the lowest sorting threshold for Cu, Zn and Fe.

References

[1] G. Gaustad, E. Olivetti, and R. Kirchain, "Toward sustainable material usage: evaluating the importance of market motivated agency in modeling material flows," *Environ Sci Technol,* vol. 45, pp. 4110-7, 2011.

[2] A. Gesing, "Assuring the Continued Recycling of Light Metals in End-of-Life Vehicles: A Global Perspective," *Journal of Materials,* vol. August 2004, pp. 18-27, 2004.

[3] M. E. Schlesinger, *Aluminum Recycling*. Hoboken: CRC Press, 2006.

[4] A. Kvithyld, C. E. M. Meskers, S. Gaal, M. Reuter, and T. A. Engh, "Recycling light metals: Optimal thermal de-coating," *Journal of Materials,* vol. 60, pp. 47-51, 2008.

[5] D. Apelian, "An Integrated Minimill to Produce Aluminum from Scrap," *Journal of Materials,* vol. 66, pp. 357-358, 2014.

[6] Institute of Scrap Recycling Industries, "Scrap Specifications Circular 2014," 2014.

REWAS 2016: Towards Materials Resource Sustainability
Edited by: Randolph E. Kirchain, Bart Blanpain, Christina Meskers, Elsa Olivetti, Diran Apelian, John Howarter, Anne Kvithyld, Brajendra Mishra, Neale R. Neelameggham, and Jeff Spangenberger
TMS (The Minerals, Metals & Materials Society), 2016

THE VALUE OF INTEGRATED PRODUCTION PLANNING FOR TWO-STAGE ALUMINUM RECYCLING OPERATIONS

Jiyoun C. Chang[1], Elsa A. Olivetti[1], Randolph E. Kirchain[2]

[1]Department of Materials Science and Engineering, Massachusetts Institute of Technology;
77 Massachusetts Ave.; Cambridge, MA 02139, USA
[2]Engineering System Division, Massachusetts Institute of Technology;
77 Massachusetts Ave.; Cambridge, MA 02139, USA

Keywords: Aluminum recycling, Dross reprocessing, Batch planning tool

Abstract

Recycling low-quality scrap and dross is of great interest in the aluminum industry due to its economic and environmental benefits. However, using these raw materials in alloy production requires reprocessing prior to the re-melting stage, leading to two-stage blending operations. In addition, there are energy saving opportunities through 1) immediately processing hot dross collected from alloy production and 2) delivering reprocessed scrap and dross as liquid to produce final alloys. This presentation will describe developing integrated production planning models that determine batch plans for reprocessing and re-melting stages simultaneously. Also, key drivers that maximize the benefits of integrated production planning will be presented. The results suggest that this approach enables aluminum producers to maximize incorporation of reprocessed low-quality raw materials.

Introduction

It is estimated that purchasing raw materials absorbs more than 70% of revenue in the aluminum industry [1]. If aluminum producers can replace primary aluminum with scrap materials to produce alloy products, this substitution can directly increase their profit margin, in addition to the environmental benefits offered by recycling. These benefits drive high demand for scrap materials. The tight scrap market has motivated aluminum producers to even recycle low-quality scrap and byproduct (i.e., aluminum dross), which require more intensive reprocessing. These materials are more available at relatively low prices in the market. In the past, using these raw materials was limited to production of low-end alloy products. However, the development of technology to reprocess these undervalued raw materials opens the possibility to use them even in higher-quality finished products.

These technologies include the preparation of scrap by effectively removing unwanted elements as well as improvement in yield during melting using furnaces specialized in processing low-quality raw materials. The rotary furnace is currently considered as the best way to recover metal from aluminum dross and is also able to process a wide range of feed stocks, including even highly contaminated ones at fairly good recovery rates [2]. Many studies have been devoted to find operational conditions to improve recovery rate in the rotary furnace. However, using reprocessed dross and scrap in high-end alloy products is still limited due to a complicated operational environment.

This paper will identify what causes limited usage of undervalued raw materials in finished alloy production and suggest a potential research opportunity to overcome these barriers.

Two-stage aluminum recycling operations

Using rotary furnaces to reprocess low-quality raw materials leads to a two-stage blending operation: 1) blending dross and post-consumed scrap into intermediate products in a rotary furnace and 2) blending intermediate products with primary and alloying elements into finished alloy products in a downstream re-melting furnace, as described in Figure 1. The recovered metal from dross and scrap (i.e., intermediate products) can be delivered to a downstream re-melter as either a molten metal or sow, depending on the layout or equipment of recycling facility.

The downstream re-melters must be able to incorporate intermediate products into final products as effectively as possible. Failure to use intermediate products effectively causes dramatic increases in raw material costs by requiring use of more expensive primary aluminum or high-quality scrap materials to meet demand.

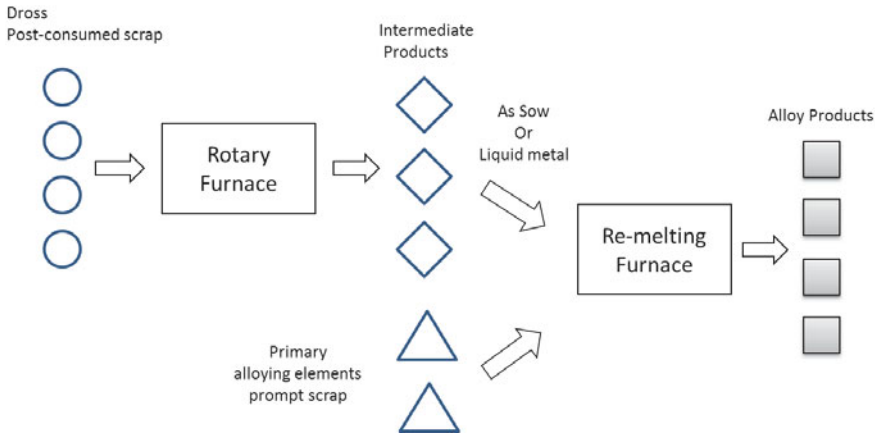

Figure 1. Schematic description of a two-stage recycling operation

Design of intermediate products

Since aluminum liquid metal is highly perishable, liquid metal must be cast as sows and be stored if it is not immediately used in alloy production. However, casting produced liquid metals as sows requires additional energy costs to remelt them. Other benefits of delivering reprocessed dross and scrap as molten metal are well reviewed [3]. For this reason, the benefits of delivering intermediate products can be maximized if all intermediate products can be immediately incorporated as liquid metals in finished alloy production. To achieve this goal, the chemistry of delivered liquid metal must fit the specifications of final alloy products produced in

a downstream re-melter. If the composition of delivered liquid metals from the reprocessing stage does not match the specifications of alloy products, casting them as sows is inevitable. Thus, the composition of intermediate products plays a critical role to determine how much of these intermediate products can be directly incorporated in final alloy production as liquid metals.

Although a two-stage recycling operation is common in practice, there has been little effort to design intermediate products. In many cases, the second-stage blending decisions are made while assuming that the composition of intermediate products delivered to a downstream re-melter is a given. The chemistry of intermediate products is not a part of decisions in such recycling operations. However, this is not an effective planning approach. To maximize the delivery of intermediate products as liquid metals, intermediate products must be designed to fit the specification of alloy products produced in a downstream re-melter. In other words, a rotary furnace operator must be aware of demand information for finished alloy products in downstream re-melter. Therefore, the integrated planning approach is required to coordinate the reprocessing and re-melting stages.

Integrated planning for two-stage recycling operations is particularly important when reprocessing is on-site. If reprocessing dross is done on-site, aluminum producers can save energy further by immediately processing hot dross collected from alloy production. Processing hot dross can prevent further oxidation of dross and reduce processing time in a rotary furnace. In this case, demand for final alloy products in the re-melting stage not only influences the design of intermediate products but also determines the chemistry of raw materials (dross) available to each batch of a rotary furnace.

Existing batch planning tools are applicable only one-stage blending process. These mathematical tools can be used to independently determine batch plans for individual stages of two-stage recycling operations. However, these tools are still lack of capability to determine the quality of intermediate products which is a key decision to maximize the delivery of intermediate products as liquid metal. Consequently, a different planning tool able to model two-stage recycling operations consisting of both a reprocessing stage and re-melting stage is needed. Such a tool would need to simultaneously consider the impact of decisions made at both stages of production.

Conclusion

To maximize the benefit of a two-stage recycling operation, integrated production planning for both reprocessing and remelting stages is necessary. However, there is no proper batch planning tool. There is clearly a need for developing a new batch planning tool to model two-stage recycling operations. Such a planning tool is expected to enables using more low-quality raw materials as well as improving energy efficiency in recycling practices.

1. Goddard, L., *Light is right: Globalization and the growing popularity of fuel-efficient cars will spur demand*, in *Aluminum Manufacturing in the US*2014, IBISWorld Industry Report.
2. Tzonev, T. and B. Lucheva, *Recovering aluminum from aluminum dross in a DC electric-arc rotary furnace.* Jom, 2007. **59**(11): p. 64-68.
3. Peterson, R.D. and G.G. Blagg, *Transportation of Molten Aluminum*, in *Recycling of Metals and Engineered Materials*2013, John Wiley & Sons, Inc. p. 857-866.

REWAS 2016: Towards Materials Resource Sustainability
Edited by: Randolph E. Kirchain, Bart Blanpain, Christina Meskers, Elsa Olivetti, Diran Apelian, John Howarter, Anne Kvithyld, Brajendra Mishra, Neale R. Neelameggham, and Jeff Spangenberger
TMS (The Minerals, Metals & Materials Society), 2016

SOLAR ALUMINUM RECYCLING IN A DIRECTLY HEATED ROTARY KILN

Martina Neises-von Puttkamer, Martin Roeb, Stefania Tescari, Lamark de Oliveira, Stefan Breuer, Christian Sattler

German Aerospace Center (DLR e.V.), Institute of Solar Research
Linder Höhe, 51147 Köln, Germany

Aluminum, Melting, Concentrated Solar, Recycling, Rotary Kiln

Abstract

South Africa currently is experiencing an electricity constraint due to economic growth and lack of investment in generation capacity, resulting in power blackouts in 2008. With increased electricity prices, the economic sustainability of energy intensive industries is threatened. The aluminum smelting industry is a significant consumer of electricity.
The consumption of electricity and the amount of emissions in the process of aluminum recycling can be reduced by the application of solar thermal technologies. A process concept for the solar thermal recycling of aluminum waste material was developed. The process takes place in a rotary kiln heated by concentrated solar radiation.
A directly absorbing rotary kiln receiver-reactor was tested on a lab-scale in the DLR high flux solar furnace. In this paper the design of the rotary kiln in the solar furnace is presented. A concept for a pilot-scale rotary kiln operated on a solar tower is shown.

Introduction

The feasibility of solar power generation via concentrated solar power systems on a technical scale has already been shown [1].
But concentrated solar radiation cannot only substitute the combustion of fossil fuels in power generation but also in chemical and metallurgical high temperature processes. In such a case, the heat provided by the solar concentrating system would be coupled into the process to provide the high temperature process heat. The high temperature treatments of metals are potential processes, because they require high temperatures and are very energy intensive. Substitution of fossil fuels through concentrated solar energy in such processes is especially interesting for countries with a large metal production industry on the one hand a vast capacity of solar radiation on the other. In this respect South Africa is an interesting candidate, because its metal industry is one of the largest industrial sectors of the country and it possesses a huge potential for use of solar energy due to its high annual incident solar radiation. The aluminum smelting industry, comprising aluminum alloy manufacturers and foundries (mostly SME's), is a significant consumer of electricity due to the widely-used electrical smelting furnaces. The use of concentrated solar energy implies the possibility to reduce overall electricity consumption and CO_2 emissions of South African aluminum foundries. Therefore the solar recycling of aluminum, delivering secondary aluminum to the automotive, construction and packing industry is proposed in this work.

The rotary kiln is widely used in industrial aluminum recycling plants, having high flexibility towards throughput and towards the kind and the metal content of the scrap. In a solar heated rotary kiln, the kiln would be directly heated by solar irradiation instead of fossil firing. Thus the kiln is used as a receiver-reactor: as a reactor for the remelting of aluminum scrap and at the same time as receiver for the incident irradiation.
Rotary kilns have been proven to be a suitable unit for use as a direct absorbing receiver reactor to provide high temperature process heat [2]. Applications include the heating of sand at a temperature level up to 940 °C at the solar furnace in Odeillo, France. A comprehensive overview on the options in terms of coupling solar radiation to the different applications is given by Alonso and Romero [3]. The use of a rotary kiln for solar lime production, its experimental proof by testing it in a solar furnace set-up [4, 5] and by evaluating the economic potential [6] is reported by Meier et al. Solar treatment of industrial residues and wastes [7] and wastes from mining [8] were reported in a rotary kiln. A solar assisted rotary coal dryer was analyzed in terms of exergy, economy and environment by Yilmazoglu et al. [9]. Bathen et al. compared different receiver and furnace technologies for solar aluminum smelting and recycling [10]. Ahmad et al. even extended such concepts towards much higher temperatures allowing the melting of glass [11]. Neises, Tescari et al. investigated the use of a solar heated rotary kiln for metal oxide reduction experimentally [12] and by numerical simulation [13, 14].
The implementation of a solar technology for aluminum recycling in South Africa will require a number of steps: beside the demonstration of technical feasibility in laboratory and pilot scale, industrial plant concepts have to be developed. Feasibility studies analyzing market and economic potential have to be developed along with the technology. At last the engagement of local foundries, stakeholders and policy makers will be an essential step.
The present work concentrates on the technological side and describes the lab-scale rotary kiln operated in the solar furnace of DLR to show the feasibility of the process in small scale. A concept of a scale-up rotary kiln is presented.

Lab-Scale Rotary Kiln

A lab-scale rotary kiln was developed and tested in the solar furnace of DLR in Cologne. It was designed for melting about one to two kilograms of aluminum waste. Figure 1 shows the scheme of the rotary kiln placed in the solar furnace.
The solar furnace enables a concentration of the direct solar beam up to 5000 times thus being able to deliver the energy required for the melting process. A heliostat of 57 m^2 mirror area tracks the sun throughout the day and reflects the solar radiation continually onto a fixed concentrator consisting of 150 spherical mirrors. The concentrator reflects and concentrates the sunlight on a focal area of 0.13 m diameter located in a special room for solar experiments, in which the rotary kiln established as an integrated receiver-reactor is installed. A peak flux density $I > 4.34$ MW/m^2 and a total beam power of 22 kW have been measured in the focal spot of the furnace at direct solar irradiance of 835 W/m [15].

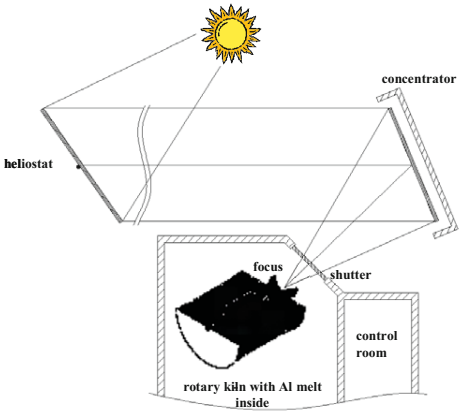

Figure 1: Scheme of the rotary kiln in the solar furnace.

The rotary kiln is designed as a cavity receiver with a small opening for the incoming solar radiation and a large vessel for absorption of the radiation. The concept of the rotary kiln is shown in Figure 2. A secondary concentrator is mounted in front of the rotary kiln to direct the incoming solar irradiation into the cavity. A quartz window located in the entrance plane of the secondary concentrator enables to work with adjustable compositions of the gas phase inside the chamber. The solar radiation enters through the aperture of the cavity (diameter of 0.08 m). Within the cavity the beam expands and hits the surface of the wall and the metal on the bottom of the kiln. The focus of the solar furnace is located about 10 cm behind the aperture of the secondary concentrator. The cavity (of 0.5 m length and 0.1 m radius) is made of siliconized silicon carbide, which has good heat conductivity. In order to reduce heat losses and to avoid thermal stresses the cavity is isolated by ceramic fiber plates. The entire equipment is enclosed in an insulated housing and the whole reactor is rotated on wheels driven by a motor. The rotational speed can be varied up to about 6 rpm. The capacity of the rotary kiln is one to two kilograms of aluminum plus additional salt slag, which is charged through the front opening into the SiSiC-crucible. The operation of the rotary kiln is batchwise. That means one test cycle includes different process steps: These are a) charging of scrap and flux, b) heating and melting, and c) discharging of aluminum smelting and slag. For allowing the discharge of molten metal and slag into molds, the kiln is mounted on a tiltable frame.

For the prevention of gaseous emissions through the front opening and for the combustion of organic component a slight stream of air can be sucked through the reactor. The reactor can also be closed by a quartz window mounted in front of the secondary concentrator. In this case a defined gas flow can be introduced through small holes positioned around the circumference of the secondary concentrator into the reaction chamber. The flow rate can be adjusted by volumetric gas flow controllers. The temperature distribution over the cavity surface is monitored by four thermocouples that are patched on the outer surface of the SiSiC wall. Temperature of the exhaust gas is monitored by one thermocouple placed in the off-gas duct. All temperatures are transferred to a data acquisition system.

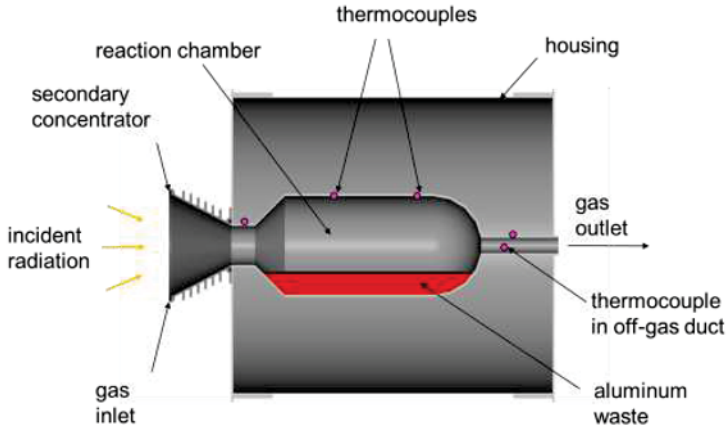

Figure 2: Scheme of the rotary kiln.

Melting of aluminum has been performed with the rotary kiln in previous campaigns [16, 17]. The solar power coupled into the reactor varied between 4.6 to 10 kW, resulting in cycle times between 1800 to 21600 s depending on the solar power input. Typically 1 kg of aluminum was melted at a temperature of about 1073 K. At this temperature a steady state was realized by a constant power into the reactor of 2.3 kW. Several cycles of charging, melting, and discharging of this amount of aluminum were performed even on days with less ideal weather conditions. A mathematical model for simulation of the transient behavior of the rotary kiln has been developed [18], which was validated by the experiments performed in the solar furnace.
Compared to fossil or electrically heated kilns the solar heating of a kiln will bring about exceptional and uncommon operation conditions due to alternating insolation, which requires at least one start-up and one shut-down period per day. A further test campaign will include operation at different operating conditions, such as varying solar flux densities and temperatures. The quality of the melt will be determined by taking samples at different operating conditions. The influence of operating conditions on the performance of the process and on the quality of the melt will be determined and serve as an input for the design of an industrial scale plant concept.

Concept of a Pilot-Scale Plant

After demonstrations of the lab-scale rotary kiln the next step is the development of a scale-up rotary kiln for operation on a solar tower. The pilot-scale rotary kiln will be designed for melting of up to 20 kg of aluminum.
To supply the large heat demand of the melting process the solar thermal recycling plant has been designed as central receiver system as shown in
Figure 3.
The plant will consist of the heliostat field, a solar tower and the pilot-scale rotary kiln. Several individually aligned mirrors, so-called heliostats, reflect and concentrate the direct solar irradiation toward a common fixed focal area. The heliostats are tracked throughout the day and the heliostat field has to be optimized for the intended annual yield of secondary aluminum at the

special site of interest. Like the lab-scale rotary kiln, the pilot-scale reactor will be realized as a cavity receiver-reactor with a capacity of 20 kg of aluminum waste. To achieve a control of the furnace atmosphere, the reactor will be designed as a closed reactor system. The solar radiation enters the kiln trough an aperture closed by a transparent quartz glass window. To avoid severe shadowing and blocking of the redirected beam by adjacent heliostats, the focal zone has to be elevated above the plane of the heliostats. Therefore the rotary kiln will be placed on top of a tower. Overall the design is similar to those of solar tower power plants [1].

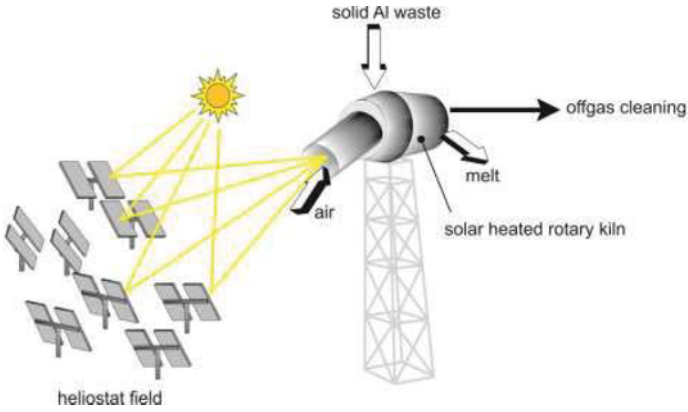

Figure 3: Concept of a solar thermal recycling plant.

Conclusion

Increasing electricity prices and the large amount of CO_2-emissions make the use of solar technologies interesting in a country like South Africa. The metal industry being one of the main electricity consumers of the country will need to look for alternative ways of energy supply. With excellent weather conditions, technologies like the directly heated rotary kiln could be used industrially.

The feasibility of solar thermal recycling of aluminum in a lab-scale reactor was demonstrated. A pilot-scale rotary kiln for melting of up to 20 kg of aluminum is under development and will be tested on a solar tower to proof the feasibility of the technology on larger scale

Beyond that rotary kilns are rather universal tools in high temperature processes. Thus the results of the technology development in solar thermal recycling of aluminum may be diversified and transferred to processes like pyrolysis, detoxification of filter residues, metal containing dust and foundry sands, as well as the production of iron oxide based pigments and the production of cement or lime.

Acknowlegement

This work was funded by the German Federal Ministry of Education and Research (BMBF) under the project “SOLAM”, grant identifier 033R121A.

References

1. M. Roeb, M. Neises, N. Monnerie, C. Sattler and R. Pitz-Paal, "Technologies and trends in solar power and fuels," *Energy & Environmental Science*, **4**(7) (2011), 2503-2511.
2. F. Kelbert and C. Royere. "Study of a Rotary Kiln as a Direct Receiver of Radiant Energy," in *Proc. of 5th Int. Symp. on Solar Thermal Technology-Research, Development and Applications*. June 1988. Santa Fe, NM, USA: Hemisphere, New York.
3. E. Alonso and M. Romero, "Review of experimental investigation on directly irradiated particles solar reactors," *Renewable and Sustainable Energy Reviews*, **41** (2015), 53-67.
4. A. Meier, E. Bonaldi, G.M. Cella, W. Lipinski, D. Wuillemin and R. Palumbo, "Design and experimental investigation of a horizontal rotary reactor for the solar thermal production of lime: SolarPACES 2002," *Energy*, **29**(5–6) (2004), 811–821.
5. A. Meier, E. Bonaldi, G.M. Cella, W. Lipinski and D. Wuillemin, "Solar chemical reactor technology for industrial production of lime," *Solar Energy*, **80**(10) (2006), 1355-1362.
6. A. Meier, N. Gremaud and A. Steinfeld, "Economic evaluation of the industrial solar production of lime," *Energy Conversion and Management*, **46**(6) (2005), 905-926.
7. M. Roeb, N. Monnerie, R. Schäfer and N. Rohner. "Thermal treatment of industrial residues using concentrated sunlight," in *Recycling and Reuse of Waste Materials, Proceedings of the International Symposium*. 2003.
8. A. Navarro, I. Cañadas and J. Rodríguez, "Thermal Treatment of Mercury Mine Wastes Using a Rotary Solar Kiln," *Minerals*, **4**(1) (2014), 37.
9. Y.M. Z. and A. E., "3E Analysis of a Solar Assisted Rotary Type Coal Dryer," *International Journal of Renewable Energy Research*, **2**(1) (2012), 16 - 22.
10. D. Bathen, M. Sonnenschein, T. Hahm and H. Schmidt-Traub. "Design and construction of a solar thermal miniplant," in *World renewable energy congress*. 2000.
11. S.Q.S. Ahmad, R.J. Hand and C. Wieckert, "Use of concentrated radiation for solar powered glass melting experiments," *Solar Energy*, **109** (2014), 174-182.
12. M. Neises, S. Tescari, L. de Oliveira, M. Roeb, C. Sattler and B. Wong, "Solar-heated rotary kiln for thermochemical energy storage," *Solar Energy*, **86**(10) (2012), 3040-3048.
13. S. Tescari, C. Agrafiotis, S. Breuer, L. de Oliveira, M. Puttkamer, M. Roeb and C. Sattler, "Thermochemical Solar Energy Storage Via Redox Oxides: Materials and Reactor/Heat Exchanger Concepts," *Energy Procedia*, **49** (2014), 1034-1043.
14. S. Tescari, M. Neises, L. de Oliveira, M. Roeb, C. Sattler and P. Neveu, "Thermal model for the optimization of a solar rotary kiln to be used as high temperature thermochemical reactor," *Solar Energy*, **95** (2013), 279-289.
15. A. Neumann and A. Witzke, "The influence of sunshape on the DLR Solar Furnace beam," *Solar Energy*, **66**(6) (1999), 447-457.
16. C. Glasmacher-Remberg, M. Roeb, J. Dersch, R. Schäfer and K.-H. Funken, "Solar thermal recycling of aluminium," *AL aluminium and its alloys*, **135** (2001), 73 - 77.
17. K.-H. Funken, M. Roeb, P. Schwarzboezl and H. Warnecke, "Aluminum Remelting using Directly Solar-Heated Rotary Kilns," *Journal of Solar Energy Engineering*, **123**(2) (2001), 117-124.
18. S.O. Alexopoulos, J. Dersch, M. Roeb and R. Pitz-Paal, "Simulation model for the transient process behaviour of solar aluminium recycling in a rotary kiln," *Applied Thermal Engineering*, **78**(0) (2015), 387-396.

REWAS 2016: Towards Materials Resource Sustainability
Edited by: Randolph E. Kirchain, Bart Blanpain, Christina Meskers, Elsa Olivetti, Diran Apelian, John Howarter, Anne Kvithyld, Brajendra Mishra, Neale R. Neelameggham, and Jeff Spangenberger
TMS (The Minerals, Metals & Materials Society), 2016

METAL RECOVERY FROM DROSS THROUGH ROTARY CRUSHING AND SEPARATION PRODUCING PRODUCTS INSTEAD OF WASTE

David J Roth
President, GPS Global Solutions, Downingtown PA, USA
David.roth@global-solutions.us.com

Introduction

There are many areas in the aluminum cast house and smelter operations that can benefit from efficient recycling and recovery of materials thru low cost, simple rotary processing operations. DIDION has the most widely developed uses and applications for rotary crushing and separation systems for the recycling and recovery of dissimilar materials that are often mechanically bonded together. The development of this technology was started in the foundry industry in the early 1970's. The first step was the separating of metal castings from the foundry sand mold pieces in which they were created. These hot, heavy castings required the development of a very durable machine. The equipment was next used for sand reclamation to keep these foundry materials in use and out of landfills.

The continued improvement of the DIDION RT/RS TUMBLERS has made mechanical processing of mixed materials a very cost effective and low maintenance alternative to other processing systems. These flexible systems can perform surface scrubbing, crushing, screening and sizing in one single piece of equipment. The DIDION systems take up far less space than conventional crushing and screening process facilities. While at the same time the system requires less maintenance and manpower to operate. The RT/RS TUMBLER systems contribute significantly to the aluminum industries potential ability to continue lowering its negative impact on the environment by this basic approach to bath, carbon, dross and the elimination of the need for salt cake processing.

Figure 1. Model RT 108 DIDION Crusher / Metal Separation

Basic Design Features:

There are three basic features of the DIDION RT Rotary Processing Systems.

First, the ability to process very large pieces of feed in the same processing step as finer material. Depending on the model, up to 1800 mm (72”) blocks can be processed at the same time as granulated fines.

Second, the ability to crush with controlled fines generation and full dust control.

Third, the ability to classify several sizes of material from bag house dust to 1800 mm (72”), within the same piece of equipment.

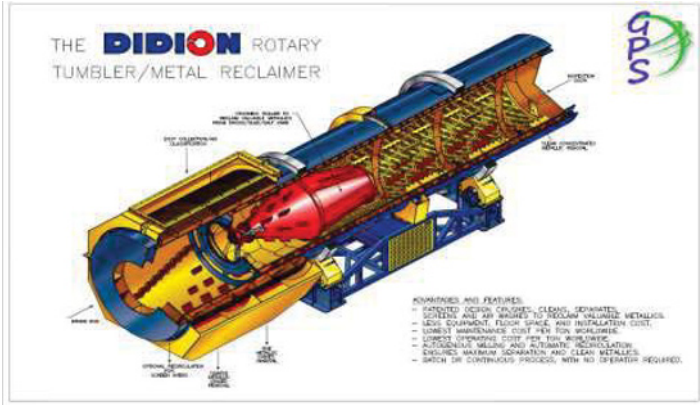

Figure 2. Material Flow Diagram and Fines Separation - **RT**

Crushing of Large Blocks of Material:

Handling large blocks of material can be particularly difficult for most processing systems. Most systems either use a primary jaw crusher or a mobile hydraulic hammer/crusher for this first breaking step.

The RT Systems process these blocks in the first section of the drum. The larger material is charged by end loader into a large hooded vibratory feed hopper that loads the drum. Hot materials can be charged with a vibratory cooling conveyor. Large cast steel teeth lift the blocks and then crash them down on hardened spikes for severe impact and size reduction.

This autogenous milling step that can handle any material used or produced in the cast house or smelter. Solid aluminum sows can be inadvertently charged into this section of the drum when processing dross for example and will not cause any damage to the DIDION unit. Large un-crushable pieces such as large of slabs of aluminum can be removed from the machine simply by backing out the feeder and reversing the rotation of the drum, discharging these large pieces into a waiting tub. This practice causes no damage to the equipment, which is often the case with impacting systems.

This is a valuable feature in bath, anode carbon crushing, pot cleanings and dross processing applications. Allowing one piece of equipment to handle these large pieces without significantly disrupting the process flow is unique to this material's processing steps.

Crushing with Controlled Fines Generation:

The impact action of the material falling on the cast steel flights in the pre-breaking and autogenous chambers combined with the action of the Concentric Crusher^{TM} , produce a for violent crushing action. Uniquely this system also immediately removes the fines that are being generated in the process. The impact breaking action of the system gives sharp fracture angles on the particles, which are preferred for most bath and carbon recycling process. In dross recycling this impact action liberates the aluminum particles without generating aluminum fines as a ball mill or hammer mill would. This step is critical to achieving process efficiency and success. The key technical challenge that the RT unit accomplishes is both removing these fines and preserving the preferred crushed material sizing, chosen by the liner slot openings.

Preselecting the correct liner opening and screen size determines the distinctiveness of materials, accomplishing the generation of the appropriate sized fines for further processing. This flexibility is a significant advantage of this process.

Classify several sizes of material in the same processing step:

This equipment has the ability to separate up to 8 (eight) different size fractions in the same processing unit simultaneously from bag house dust to1800 mm (72") blocks. This is achieved with the proper selection of the crushing chamber configuration, dam ring openings, liner openings and screen sizes.

> Fraction 1. Main feeder charge and discharge opening - solid metallic pieces up to the discharge opening size of the drum.
> Fractions 2 & 3. Double Screen capabilities discharge at the main screen hood area – course and fine materials sizes are determined by the process requirements, typically from 3 – 12 mm (1/8 – 1/2 ") in size range.
> Fraction 4. Recycled material discharge – sized to minus the liner slots to plus the largest screen size. Typically -35 mm + 7 mm (-1 3/8 + 1/4")
> Fractions 5 & 6. Oversized materials (metal) discharge at the end of the drum, that typically range from -250 mm +35 mm (-10 + 1 3/8"). An addition sizing rotary classifier

can be added to the end of the discharge point of the drum to get another solids separation. -250 + 75mm and -75 + 35mm for example.
Fractions 7 & 8. The pollution control unit can remove up to 1 mm particles in the air stream and can separate our the coarse particles in a cyclone collector. Sometimes this is also a valuable separation area for various materials.

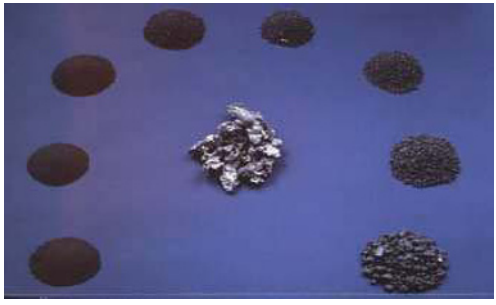

Figure 3. RT System Particle Size Control

All of these sizing steps occur inside the single RT DIDION system. The material processed determines to what lengths the process is set up to provide various fractions. Environmentally, dust is strictly controlled by the bag house/pollution control system installed with the unit or attached to the plant pollution control system.

Secondary and Primary Aluminum Plant Applications for Recycling Materials:

Bath:

The RT System can be used as rotary bath crusher and size separator in a single process with the ability to remove the tramp aluminum from this electrolyte and crush it to size in the same step. This process is normally done in multiple steps. The RT allows for metal removal and screen size selection as part of the crushing process. The unit originally designed for processing hot castings has no problem with hot bath.

The modified feed conveyor can pre-cool the hotter materials to below 400^{O}C for processing in the RT unit.

In bath recycling smelters require different screen sizes and minimal fines generation while crushing for optimal recyclability. RT Rotary crushing achieves these goals with a single main crusher and product classifier. The RT system provides a uniform product to put back on top of the pot cells.

Spent Carbon Anode:

The recycling process for spent anodes typically involves several crushers for sizing and magnetic separation units for the removal of tramp iron in the crushed carbon. If there are full size either green or baked anode blocks that are scrap, they have to be handled separately and manually crushed. The RT systems will handle full size baked carbon anodes and crush them without any problems. This is a very unique feature of this process. It will also replace the primary secondary and fine crushing steps and perform this job in one RT unit. Saving significant floor space, energy and maintenance dollars that would have been spent on the standard type of crushing system along with its many conveyors and screening systems.

The RT Rotary crushing approach to bath and carbon recycling gives a lower cost recycled product to be reintroduced into the recycling process that is high quality and from a system that is more flexible with anomalies that may occur.

Secondary and Primary Aluminum Plant Applications for Landfill Elimination:

Aluminum Dross

Dross processing has always produced more waste than the aluminum that is recovered. Salt cake is typically generated at an almost 2 to 1 ratio of the aluminum recovered in the rotary salt furnace process. Separation of metallics from oxides without the use of salt flux has a significant environmental impact. Instead of losing aluminum in the salt cake and producing significant amounts of landfill, the RT process separates the dross into its metallic, metallic oxide and oxide components all of which given enough effort can be recycled or sold as by products or used within the aluminum smelting process. Secondary aluminum dross can be recycled in the same method. Secondary black dross can be concentrated to higher aluminum levels not totally eliminating the landfill issues but significantly reducing the landfill of this material.

Spent Pot Liner

Another beneficial area that this system has proved capable of efficiently processing is spent pot liner. This material is a mixture of aluminum, iron, carbon and refractory materials. The RT system has proven capable of crushing the carbon phase and the refractory phase for further recycling and removing the tramp metals for recycling.

Due to the crushing and sizing characteristics of the RT System, these materials can be further processed for all or major elimination of the hazardous landfill items that are normally produced in the processing of SPL.

General Comments:

The installation space requirement for the largest unit is an envelope of approximately 6 x 30 meters (20 X 100'). This layout would assume that materials discharge into tubs. Conveyors can be added to the system for continuous removal of the products. These conveyors can be set up in

many configurations for additional separation steps such as eddy current processing, magnetic separation and/or product bulk bagging.

Stand alone systems that are used for dross or SPL processing typically require 2 people per shift for the operation of the entire system. The systems are very reliable. They were designed to be part of manufacturing lines in high production automotive foundries that run 24 hours a day seven days a week. Any unscheduled downtime is unacceptable to this industry. This reliable performance is achieved by the selection of simple dependable parts and extremely heavy duty components.

Operational costs are very low. The largest unit operates with a 200 Kw (275 Hp) drive motor, the smallest with a 22Kw (30 Hp) drive motor. Processing cost per ton will vary with the size of the unit but are considered very low for crushing/separation/screening systems system. Custom sizes, thru puts and processing configurations are part of the DIDION philosophy of equipment design and can always be evaluated and normally accomplished. Manpower requirements are also very low. Loading is typically done manually but the operation from that point is highly automated.

Summary:

The flexibility of the design configurations of the DIDION rotary processing equipment has many potential applications in the aluminum cast house and smelter environment. These dynamic systems can lower overall processing cost by reducing manpower, maintenance, energy consumption and lowering the plant area required for the above mentioned materials processing practices. The additional benefits of improving the recyclability of the dross and other aluminum containing materials is also of a benefit to reducing landfill cost and lowering the generation of green house gasses.

REWAS 2016: Towards Materials Resource Sustainability
Edited by: Randolph E. Kirchain, Bart Blanpain, Christina Meskers, Elsa Olivetti, Diran Apelian, John Howarter, Anne Kvithyld, Brajendra Mishra, Neale R. Neelameggham, and Jeff Spangenberger
TMS (The Minerals, Metals & Materials Society), 2016

A LABORATORY STUDY OF ELECTROCHEMICAL REMOVAL OF NOBLE ELEMENTS FROM SECONDARY ALUMINIUM

Ole S. Kjos, Sverre Rolseth, Henrik Gudbrandsen, Egil Skybakmoen, Asbjørn Solheim, and Trond H. Bergstrøm

SINTEF Materials and Chemistry, P.O. Box 4760 Sluppen, NO-7465 Trondheim, Norway

Keywords: Noble elements, Recycling, Electrorefining

Abstract

At present, recycled aluminium is "diluted" by primary metal to keep the impurity concentrations at acceptable levels. Future increase in recycling will require a new process for efficient removal of all impurities, including noble elements, from secondary aluminium. In the current preliminary laboratory study, an electrochemical method based on the well-known three-layer refining cell was explored. Metal with purity comparable to primary metal could be obtained from highly alloyed scrap feeds containing elements more noble than aluminium, such as iron, copper, manganese, and zinc. The energy consumption was as low as 8.5 kWh/kg Al, indicating that the process can be expected to be less expensive than for production of primary metal, but with higher costs than re-melting.

Introduction

Production of primary aluminium is power intensive. Still, aluminium is considered to be a "green" metal. This is due to its weight saving properties, but also because it requires very little energy for recycling to recycle once produced [1]. During recycling of aluminium there is a need to purify the metal, since many different alloys are often melted together, forming new alloys.

The removal of alloying elements less noble than aluminium can be easily achieved by oxidation. More noble elements, however, cannot be removed efficiently today. The current method for controlling the concentration of these elements in the final product is by sorting and selective picking of scrap, and if needed, by dilution with primary aluminium. This works well today as the share of recycled metal compared to primary metal is relatively small, and hence a high dilution ratio is possible. In the future this might be expected to change, as more and more produced aluminium will find its way back into the recycling loop. It is, therefore, a probable scenario that one ends up in a situation where certain scrap feeds are undesired because of its high content of noble alloys.

The purpose of the present work was to demonstrate a process for removing impurities from scrap aluminium, including noble elements, ending up with aluminium metal with purity similar or better than primary metal, but produced at a lower cost than primary metal. The process is based on the three-layer electrolysis process for producing super pure aluminium.

Theory

Electrorefining of aluminium is a well-known method for producing high purity aluminium from selected primary metal qualities. The Hoopes process [2] is basically a three-layered configuration with a heavy Al-Cu metallic layer at the bottom, a lighter molten salt (fluoride) electrolyte layer in the middle, and the purified produced aluminium floating on top. Aluminium is fed to the lower Al-Cu alloy at the bottom, and the purification of aluminium is achieved by applying a DC current which moves the aluminium to the top layer by oxidation and subsequent reduction of the aluminium. The anode and cathode reactions, respectively, can be written

$$Al_{alloy} + 3\,NaF(a) \rightarrow AlF_3(a) + 3\,Na^+ + 3\,e \quad (1)$$

$$AlF_3(c) + 3\,Na^+ + 3\,e = 3\,NaF(c) + Al_{pure} \quad (2)$$

The overall process is the sum of the electrode reactions,

$$Al_{alloy} + AlF_3(c) + 3\,NaF(a) = Al_{pure} + AlF_3(a) + 3\,NaF(c) \quad (3)$$

Since most of the current is transported by the Na^+ ion, AlF_3 and NaF are transported by diffusion close to the electrodes. The concentration differences due to diffusion give rise to concentration overvoltage, which is the second largest voltage component in the process. The total voltage is dominated by ohmic losses.

For elements more noble than aluminium, the following equilibrium will be shifted towards the right hand side,

$$Al + MF_n = M + AlF_3 \quad (4)$$

This means that a noble element present in the alloy must stay in its metallic form, and a noble impurity that approaches the alloy-electrolyte interface will not be oxidised, and hence can not transfer into the electrolyte. On the other hand, a less noble element will easily be oxidized to its fluoride, but it will virtually be rejected at the interface between the electrolyte and the pure metal because equilibrium (4) is shifted to the left hand side. This is illustrated in Figure 1.

After some time, the anode alloy will be enriched in noble elements. Some of these will form solid deposits that may be removed mechanically. The more noble elements will be enriched in the anode metal, which is a Cu-Al alloy. When the anode alloy is sufficiently enriched it can be recovered and there is a possibility of recovering noble and precious elements, but this is outside the scope of the current work. In an industrial process however it will be necessary to investigate recovery of both noble metals from the anode material, as well as the regeneration of the electrolyte by removing Zn and the other less noble metals. It might be advantageous to remove most of the less noble elements before subjecting the scrap to the present process.
As this process today is used for making high purity aluminium metal; the voltage, current density, and cell geometry are designed and optimized in such a way that the metal may have a

purity of 99.999%. Despite numerous modifications in order to improve the efficiency [3-5], the energy consumption in the Hoopes process is still comparable with primary metal production.

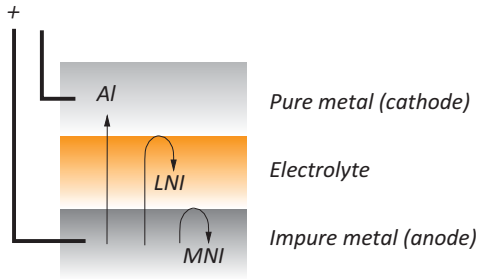

Figure 1. Principal sketch of the 3-layer cell (see the text). MNI – more noble impurities (than aluminium), LNI – less noble impurities.

By accepting a metal purity of around 99%, a lot of the restraints put on the process today can be relaxed, leading to reduced energy consumption and increased productivity. Research on modifying the process was undertaken by Sullivan [6], focusing on recovering aluminium and precious metals such as Au and Ag from old electronic scrap. They achieved promising results regarding the purity and amount of the aluminium recovered, as well as the concentration factor of noble metals in the anode alloy.

Experimental and Results

The current work involved the novelty of utilizing a solid TiB_2-graphite composite cathode, in order to reduce the cell voltage. With this arrangement; the purified metal forms droplets that are drained away from the cathode, enabling a large separation distance between the pure and impure metal layers, while at the same time, having a short anode-cathode distance. The cathode could also optionally be rotated, in order to control the convection and reduce concentration overvoltage at the cathode.

The experiments were run in two set-ups; three experiments were performed in a 100 mm dia. cell to gain experience with the process in general and the cathode arrangement in particular, followed by a long-term experiment with a cell allowing feeding of anode alloy. In all cases, the electrolyte was based on the system Na_3AlF_6-AlF_3-BaF_2 and the temperature was about 740 ^oC.

Test Experiments

The set-up used in the test experiments is shown in Figure 2.

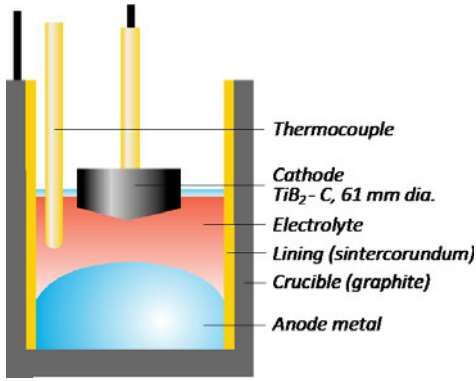

Figure 2. Experimental setup used in experiments 1-3.

Rotation. Figure 3 shows the cell voltage in an experiment with rotation of the TiB_2-C cathode (50 rpm). The effect of cathode rotation was not promising. It was not possible to observe any reduction in the cell voltage while the cathode was rotated; the only effect on the voltage measurements was increased noise levels. Also, the current efficiency (CE) was drastically reduced. The CE was only 14% in the experiment shown in Figure 3, compared to CEs up to around 95% obtained in experiments without rotating cathode. The reason for the low CE is probably destabilisation of the three liquid layers resulting in droplets from the pure metal re-alloying with the anode metal.

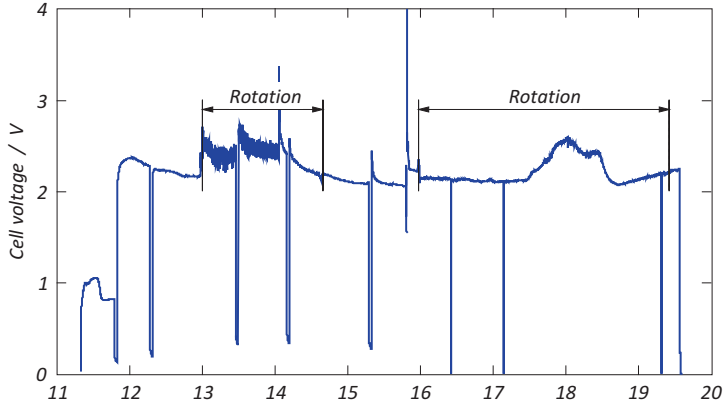

Figure 3. Cell voltage recorded during the experiment with rotating electrode.

The test experiments showed reasonable energy consumption and good purification effect, and good performance of the composite cathode. Therefore, a long term experiment was performed, but without using a rotating cathode.

Long Term Experiment

The long term experiment was conducted using the same process design in a scaled up configuration. The cell was equipped with a side chamber where more scrap metal could be fed to the anode during the experiment, as shown in Figure 4.

The experiment was run for 36 hours at currents to 100 A. In this timeframe, a total of 818 g metal was fed into the side chamber. The cell voltage was stable during the entire experiment (except periods where the current was varied or interrupted).

Metal Purity. The concentrations of all analysed impurity elements were very low after the electrorefining, as shown in Table I. In fact, the purity of the produced metal is so high that further process improvement in terms of efficiency and energy consumption at the expense of metal purity could be considered. The increase in Mg is within the analytical uncertainty; B appears to have a more defined increase, while still at a very low concentration level. 20 ppm of B is within acceptable limits for the metal. Probably, it originates from slow corrosion of the submerged cathode.

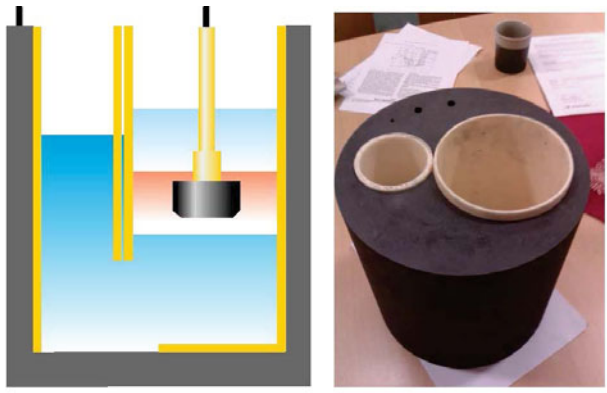

Figure 4. Setup for the long term experiment. A feeding chamber was located on the left hand side of the cell, but the basic principle is the same as for the setup described in Figure 2.

Table I. The composition of the elements in the starting alloy metal and the purified metal. All concentrations in µg/g (ppm).

	Si	Fe	Cu	Mn	Mg	Zn	Ti	B
Starting alloy	12000	2006	410000	5222	5	5327	1415	10
Purified metal	69	10	17	5	8	5	68	20

Stability of Titanium Diboride Cathode. After 36 hours of electrorefining, it was not possible to measure any wear of the TiB_2 electrode. 36 hour is a very short timeframe to determine wear on refractory parts. However, in an industrial process the cathode will be inserted from the top and easily changed without significant process interruptions. One of the key aspects, however, is that the produced metal should not be polluted by trace elements from the electrode. Although no accumulation of Ti was observed, there was a slight increase in the B content, averaging 20 ppm after the electrolysis as was shown in Table **I**. 20 ppm B in the end product corresponds to a cathode wear rate of 8 mg/kg produced metal. This is hardly a significant corrosion issue.

Energy Consumption. During the experiment 600 g of pure metal was produced, corresponding to 84 percent current efficiency. Even with the constraints of laboratory scale work it was possible to demonstrate electrorefining of Al at 8.5 kWh/kg Al. This is less than the energy required for primary metal production, but significantly more than the energy required for re-melting of the metal. It is probable that a scaled up cell will benefit from increased stability and might offer energy consumption down to 5-6 kWh/kg Al. If the price for certain scrap sources becomes low enough because it is not usable in re-melting processes, it will probably be possible to recover it in primary metal quality at a lower cost than producing primary metal.

Conclusions

The process to electrorefine aluminium scrap is feasible, and our experimental work has shown that primary metal quality can be achieved with significantly lower energy input than for primary metal production event in laboratory scale. It is, however, a requirement that the scrap aluminium to be used is significantly cheaper than regular scrap today. This can be the case in the future for certain scrap qualities that poses large requirements on dilution with primary Al, or scrap qualities that in other way gives large restrictions in the remelting process.

The electrorefining process today is tuned to allow for high purity, but has a very low throughput and high energy consumption. It is shown that by modifying this process with focus on higher throughput and lower energy consumption by using a different cathode design with a TiB_2 anode submerged in the electrolyte, and different operational parameters we demonstrate that it is possible to produce metal of primary metal purity with an energy consumption as low as 8.5 kWh/kg. Increased convection in the system had no measurable effect on the resistance, but a large negative impact on current efficiency. The main potential for increased efficiency is by reducing anode cathode distances and overall resistance.

References

1. L. Butterwick and G.D.W. Smith, *Conservation & Recycling* **9** (3), 293-307 (1986).
2. W. Hoopes *et al*., US patent No. 1,534,318, April, 1925.
3. R.A. Gadeau, US patent No. 2,034,339, 1936.
4. Guoha *et al*., Light Metals 1997 pp 417-420
5. Lu *et al*., Light Metals 2004 pp 303-305
6. T. Sullivan, "Recovery of aluminium base, and precious metals from electronic scrap", US Dept. of the Interior, Bureau of Mines, 1972.

REWAS 2016: Towards Materials Resource Sustainability
Edited by: Randolph E. Kirchain, Bart Blanpain, Christina Meskers, Elsa Olivetti, Diran Apelian, John Howarter, Anne Kvithyld, Brajendra Mishra, Neale R. Neelameggham, and Jeff Spangenberger
TMS (The Minerals, Metals & Materials Society), 2016

PRODUCTION OF MAGNESIUM AND ALUMINUM-MAGNESIUM ALLOYS FROM RECYCLED SECONDARY ALUMINUM SCRAP MELTS

Adam J.Gesing[1], Subodh K. Das[1], Raouf O.Loutfy[2]
[1]Phinix, LLC, P.O. Box 11668, Lexington, Kentucky, 40577, USA
[2]MER Corporation, 7960 S. Kolb Road, Tucson, Arizona, 85706, USA

Keywords: Magnesium and Aluminum-Magnesium Alloys Recovery / Production from Scrap

Abstract - An experimental proof of concept was demonstrated for a patent[1] and trademark[2]-pending RE-12^{TM} process for extracting a desired amount of Mg from recycled scrap secondary Al melts. Mg was extracted by electrorefining producing Mg product suitable as Mg alloying hardener additive to primary grade Al alloys. This efficient electrorefining process operates at high current efficiency, high Mg recovery and low energy consumption. Mg electrorefining product can meet all the impurity specifications with subsequent melt treatment for removing alkali contaminants. This economical and environmentally friendly chlorine-free RE-12^{TM} process could be disruptive and transformational for the Mg production industry by enabling the recycling of 30,000 tonnes of primary-quality Mg annually.

Introduction - North America produces only ~70,000 tonnes of primary Mg annually. The only practical recycling of post-consumer Mg is as alloying content in the Al-alloy recycling system. However, in that system over 30,000 tonnes is chlorinated or fluxed out to end up as Mg chloride contamination of dross.
The objective of this project was to develop a proof of concept on a laboratory scale of an electrorefining process to recover Mg from secondary Al alloy melts sourced from domestic Al alloy scrap feedstock and to produce primary-quality Al-Mg alloys.

The project was funded by the United States Department of Energy Advanced Research Project Agency (ARPA-e).

Process Concept - The process concept for extraction of Mg from Al scrap was designed to fit with existing Al remelting and recycling processes. Al is typically resmelted in a sidewell reverberatory furnace and the Mg is chlorinated out of the melt by continuous injection of Cl_2. In the RE12^{TM} process, Cl_2 injection and Mg chlorination is replaced by Mg electrorefining and Mg recovery for recycling.

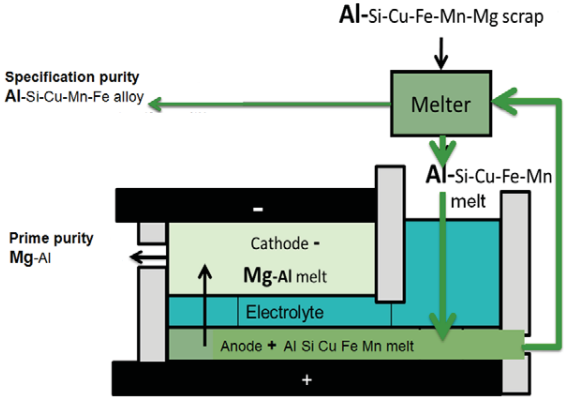

Figure: Illustrates the RE12™ process concept and its conceptual integration with an Al melter in an Al secondary smelter.

Experimental Results: Demonstrated performance of RE12™ electrorefining process

We characterized the refining cell performance and determined the optimum electrorefining configurations that resulted in a stable operation well below the target specific energy consumption of <10 kWh/kg Mg. We conducted a series of electrorefining experiments designed to measure key process operating parameters and milestone metrics as described below.

Metrics	Achieved	Target
Cell voltage @ CD 0.9 A/cm^2 (V)	1	<4
Energy consumption at 0.9A/cm^2 (kWh/kg Mg)	2.5*	<10
Current efficiency (%)	~100	>90
Cathode Mg recovery (%)	>93	>90
CO_2 emission (kg CO_{2eq} / kg Mg)	< 4	<1
Production cost ($/kg)	< $2	$1.7

* not including melting heat required from scrap and other external heat losses

Conclusion – Experimental results obtained indicate that the electrorefining process for extraction of Mg from Al melt is technically feasible. Our techno-economic analysis[3] indicates high potential profitability for applications in Al foundry alloys as well as beverage can and automotive sheet alloys.

References

1. Gesing, S. Das and M. Gesing, "Electrorefining of Mg from Scrap Metal Al or Mg Alloys", Patent Application US 2015/0225864 A1, 2015 (Phinix, LLC)
2. Phinix, LLC - Trade Mark RE12[12] Recycled Mg, 2014
3. Gesing, S. Das, and R. Loutfy, "Production of Mg and Al-Mg Alloys from Recycled Secondary Al Scrap Melts", full paper to be published in the Journal of Metals.

REWAS 2016: Towards Materials Resource Sustainability
Edited by: Randolph E. Kirchain, Bart Blanpain, Christina Meskers, Elsa Olivetti, Diran Apelian, John Howarter, Anne Kvithyld, Brajendra Mishra, Neale R. Neelameggham, and Jeff Spangenberger
TMS (The Minerals, Metals & Materials Society), 2016

RECOVERY OF ALUMINUM FROM THE ALUMINUM SMELTER BAGHOUSE DUST

Myungwon Jung[1] and Brajendra Mishra[2]

[1]Department of Metallurgical and Materials Engineering, Colorado School of Mines;
1500 Illinois St.; Golden, CO 80401, USA
[2]Department of Mechanical Engineering, Worcester Polytechnic Institute;
100 Institute Rd.; Worcester, MA 01609, USA

Keywords: Leaching, Hydrometallurgy, Waste recycling, Aluminum

Abstract

The extraction of metals from a primary or a secondary resource is achieved by pyrometallurgy and hydrometallurgy. Currently, most of metal production plants consist of both pyrometallurgical and hydrometallurgical processes. Dust generation during the processes is one of the disadvantages of pyrometallurgical plants. Therefore, dust collection systems are installed in metal production plants to capture the emission of air pollutants from their off-gases. Due to environmental problems associated with the dust and high cost of disposal, proper treatments are required to minimize these problems. Recycling some metals from the dust during waste treatment could be a good way to utilize metal resources. In this research, alkaline leaching on the aluminum smelter baghouse dust has been studied with different reagents, bath temperature and pulp densities. Based on the alkaline leaching tests, the recovery of aluminum is high with sodium hydroxide at high temperature and low pulp density. HSC chemistry analysis shows that the product of NaOH leaching on the aluminum smelter baghouse dust is the sodium aluminate.

Introduction

In pyrometallurgical plants, dust collection systems are often installed to control the emission of air pollutants from their off-gas and the air pollutants include particulate matters and harmful gases. In general, particulate matters which are collected in the dust collection systems may contain some amount of metal values. Thus, recycling metals from the dusts can be valuable in reducing the environmental issues and saving the metal resources.
In this research, hydrometallurgical processes are studied for the recovery of aluminum from smelter baghouse dusts from aluminum industry. Unit processes in hydrometallurgy generally consist of sample preparation, leaching, solid-liquid separation, concentration, and recovery. This research has mainly focused on the aluminum smelter baghouse dust leaching with variations of reagents, bath temperature, and pulp densities. Thermodynamic analysis of the sodium hydroxide leaching of aluminum smelter baghouse dust is also investigated with HSC chemistry.

Experimental

In hydrometallurgical processes, size of the samples generally affects the overall processing rates. When the size of the particle decreases, the surface area exposed by the solvent greatly increases

and it provides greater opportunity for the samples to be attacked by the solvent [1]. For this reason, particles which size is smaller than 45 μm are considered for the hydrometallurgical materials processing.

After the size classification, initial analysis of elemental compositions is conducted and it is one of the most important steps for efficient metal recovery from the waste streams. For the initial analysis, samples smaller than 45 μm are fused with mixture of lithium borate and lithium metaborate in a graphite crucible at 1000 ^{o}C for 1hr. The fusion process has several advantages over other methods. First, it readily dissolves minor refractory minerals which are not adequately attacked by hydrofluoric acid mixtures. Second, it needs no special equipment such as pressure vessel, Third, it provides a clear aqueous solution suitable for a variety of analytical procedures [2]. After the borate fusion process, the molten melt is dissolved in a 25 vol% nitric acid and is diluted with 2 vol% nitric acid for ICP-AES analysis.

For the alkaline leaching of aluminum smelter baghouse dust, 1M of NaOH and Na_2CO_3 are used for leaching with different bath temperatures and pulp densities. 100 mL of reagent is used and is agitated with magnetic stir bar at 250 rpm. The leaching is continued for 4 hours and the leachate is also analyzed with ICP-AES.

Results and Discussion

I. Initial analysis of as-received aluminum smelter baghouse dust

In general, leaching or dissolution of metals from the sample is the first step of hydrometallurgical process. If the size of the particle is increased, leaching step should take longer to dissolve metal ions. Thus, extraction of metals from the sample is separated by its size. Since the aluminum smelter baghouse dust shows relatively wide size distributions, less than 45 μm of sample is treated by hydrometallurgical processes since the smaller size of particles guarantee large surface areas to be attacked by the reagents. Therefore, ICP analysis on the sample smaller than 45 μm is conducted and the result is shown in Table I. Major elements of the aluminum smelter baghouse dust are Al, Si, Fe, Ca, and Mg and the amount of aluminum in the dust is about 13 wt%.

Table I. ICP analysis of aluminum smelter baghouse dust (<45μm)

Elements	Al	Ca	Fe	K	Mg	Si	Zn	Ti
Compositions (mg/g)	129.61	23.17	24.97	12.01	9.72	52.16	3.66	2.12

II. Effect of temperature and pulp density on leaching with Na_2CO_3

In the hydrometallurgical processing, several experimental parameters may affect the overall leaching kinetics such as temperature, pulp density, concentration of reagent, type of reagents, and agitation. For this research, two experimental conditions, bath temperature and pulp density, are changed. The bath temperature is changed from 25 ^{o}C to 60 ^{o}C and the pulp density is changed from 10 g/L to 50 g/L. 1M of sodium carbonate leaching of the dust is conducted for 4 hours and the bath is agitated by rotating magnetic stirrer at 250 rpm. After the leaching step, vacuum filtration is conducted for the solid-liquid separation and the leachate is analyzed with

ICP-AES. From Figure 1, the percent aluminum leaching is about 30 % and this value is not affected by the bath temperature when 1M sodium carbonate is used as a reagent. Pulp density is an important parameter as it can highly affect the leaching characteristics as well as economic feasibility of the process. Based on Figure 1, the leaching efficiency of aluminum is decreased from 30 % to 6 % when the pulp density is increased from 10 g/L to 50 g/L. Since the bath temperature does not affect the leaching efficiency of aluminum with sodium carbonate, another reagent, sodium hydroxide, was tested with same experimental procedures.

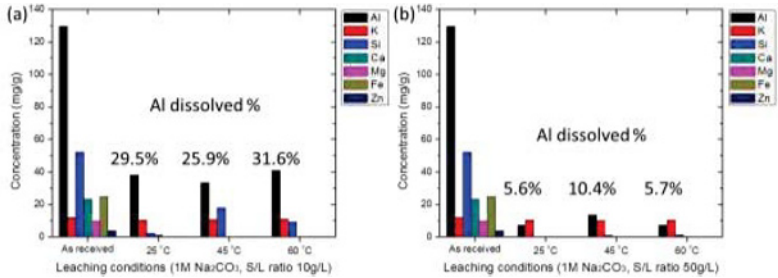

Figure 1. Effect of bath temperature and pulp density on Al smelter baghouse dust leaching with Na_2CO_3 (a) 10g/L, (b) 50g/L

III. Effect of temperature and pulp density on leaching with NaOH

From the previous results, aluminum leaching efficiency with sodium carbonate is only 6 % at 50 g/L pulp density and this indicates that sodium carbonate is not a proper reagent due to poor recovery. NaOH was tried for leaching since it is also used in the Bayer Process for pure Al_2O_3 production from bauxite. In the Bayer Process, after separating the insoluble red mud, the pure solution is then seeded to precipitate pure crystalline aluminum hydroxide which is subsequently filtered, washed, dried, and calcined to pure Al_2O_3 [3]. From Figure 2, aluminum leaching efficiency is only about 28 %, which is similar to the values of sodium carbonate leaching experiments. On the other hand, when the bath temperature is increased from 25 ºC to 60 ºC, most of aluminum in the dust is leached with 1M NaOH. Also, major elements of the dust remain in the residue after the leaching step. Therefore, selective leaching of aluminum from other elements in the dust is possible with NaOH as a reagent with high efficiency.

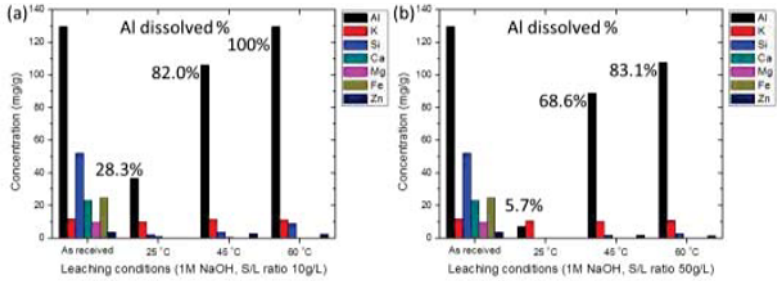

Figure 2. Effect of bath temperature and pulp density on Al smelter baghouse dust leaching with NaOH (a) 10g/L, (b) 50g/L

IV. Thermodynamic study of the NaOH leaching

Thermodynamic modeling of the NaOH leaching of aluminum smelter dust is also studied for the compatibility study of this process. In the smelter dust, both aluminum metal and aluminum oxide may be present. Therefore, several reaction equations of aluminum and alumina are proposed in Table II [4].

Table II. Reaction equations of aluminum and alumina during NaOH leaching

Reaction equations		ΔG^o (kcal)	
		0 °C	100 °C
Eqn.1	$Al + 3H_2O(l) + NaOH(l) = Na[Al(OH)_4] + 1.5H_2(g)$	-114.574	-116.350
Eqn.2	$2Al + 2NaOH(l) + 2H_2O(l) = Na_2O{\cdot}Al_2O_3 + 3H_2(g)$	-217.690	-221.893
Eqn.3	$Al + 3NaOH(l) = Al(OH)_3 + 3Na$	-3.950	-3.075
Eqn.4	$Al_2O_3 + 2NaOH(l) = Na_2O{\cdot}Al_2O_3 + H_2O(l)$	-10.636	-10.813
Eqn.5	$Al_2O_3 + 2NaOH(l) + 3H_2O(l) = 2Na[Al(OH)_4]$	-22.093	-21.621

For the thermodynamic study, the effects of other elements during leaching are ignored and the amount of aluminum and alumina in the sample is assumed at same mole fraction. Since the amount of the aluminum element in the dust is only 13 wt%, the total aluminum content in the leachate is maximum 0.048 moles at 10 g/L pulp density when the aluminum leaching efficiency is measured at 100 %. Based on this estimation, the amount of H_2O and NaOH can be considered enough for the reaction equations shown in Table II and also large amount of these solvents can promote the reaction goes in forward direction from the Le Chatelier's principle. Reaction equations which have lowest Gibbs free energy of formation are considered for the Gibbs free energy minimization. Based on this criterion, equations 2, 3, and 4 are not considered since their absolute values of standard free energy change are smaller than the values of equations 1 and 5. To compare the standard Gibbs free energy of formation between equations 1 and 2, the value for the equation 1 is doubled to calculate the free energy per mole of aluminum. In this case, equation 1 shows larger absolute value of Gibbs free energy of formation than that of equation 2.

Therefore, equations 1 and 5 are considered to form stable products after the leaching step and proposed reaction equations are as follows:

(1) $Al + 3H_2O(l) + NaOH(l) = Na[Al(OH)_4] + 1.5H_2(g)$
(5) $Al_2O_3 + 2NaOH(l) + 3H_2O(l) = 2Na[Al(OH)_4]$
(1) + (5) $Al + Al_2O_3 + 6H_2O(l) + 3NaOH(l) = 3Na[Al(OH)_4] + 1.5H_2(g)$

Based on the equations 1 and 5, the equilibrium composition diagram of the reaction is plotted and shown in Figure 3 [4]. In the final equation, the calculated Gibbs free energy of reaction is -137.971 kcal/mol and the equilibrium constant, K, is 7.035×10^{80} at 100 ºC. In this case, reaction tends to go in forward direction significantly since the Gibbs free energy of reaction shows negative value and the equilibrium constant is larger than 1. In Figure 3, the product after leaching step is sodium aluminate at lower temperature regions below 100 ºC. However, the formation of alumina is gradually increased with increasing bath temperature and it is the stable form at higher temperature over 700 ºC after dissociation.

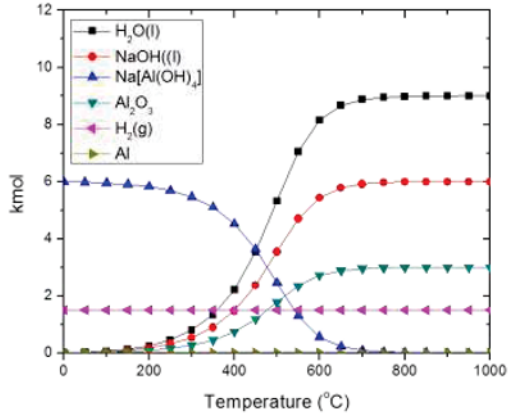

Figure 3. Equilibrium composition diagram of aluminum smelter baghouse dust leaching

The primary production of aluminum currently relies on the Bayer process which makes pure alumina from the bauxite. In the commercial processes, caustic leaching is used for the bauxite because titanium and iron minerals are soluble in acids. Therefore, in the Bayer process, aluminum hydroxide is extracted by sodium hydroxide leaching in steam-heated autoclaves and the main leach reactions are as follows: [5]

Gibbsite: $Al(OH)_3 + NaOH = Na[Al(OH)_4]$
Boehmite and Diaspore: $AlOOH + NaOH + H_2O = Na[Al(OH)_4]$

Based on the main leach reactions for the bauxite ore, the final product after the leaching step is also sodium aluminate which is same as the product obtained in smelted dust leaching. Thus, the

leached compound can be reverted back to produce high quality pure alumina making aluminum smelter baghouse dust a viable secondary source for aluminum industry.

Conclusions

In this research, alkaline leaching of the aluminum smelter baghouse dust is studied at different temperatures and pulp densities. With 1M of NaOH, aluminum leaching from the dust is effective when the bath temperature is high and the pulp density is low. Also, selective leaching is observed with caustic leaching. For the compatibility test of the NaOH leaching, thermodynamic study of the leaching is conducted and the final product form of the aluminum after the NaOH leaching is sodium aluminate which is identical to the Bayer process reactions. Therefore, aluminum smelter baghouse dust can be utilized as a secondary source for the Bayer process for alumina recovery. The residue after leaching can be a potential additive to make construction aggregate.

References

1. Hayes, P. C. (2003). *Process principles in minerals and materials production* (3rd ed.). Hayes Publishing co.

2. Verbeek, A. A., Mitchell, M. C., & Ure, A. M. (1982). *The analysis of small samples of rock and soil by atomic absorption and emission spectrometry after a lithium metaborate fusion/nitric acid dissolution procedure*. Analytica Chimica Acta, 135(2), 215-228.

3. Habashi, F. (2005). *A short history of hydrometallurgy*. Hydrometallurgy, 79(1), 15-22.

4. HSC Chemistry [Computer software]. Pori, Finland: Outokumpu.

5. Twidwell, L. G. (1980). *Unit Processes in Extractive Metallurgy: Hydrometallurgy : a Modular Tutorial Course Designed for Self-paced Learning*. Montana Tech of the University of Montana.

Understanding & Enabling Sustainability - Education Research Innovation

REWAS 2016: Towards Materials Resource Sustainability
Edited by: Randolph E. Kirchain, Bart Blanpain, Christina Meskers, Elsa Olivetti, Diran Apelian, John Howarter, Anne Kvithyld, Brajendra Mishra, Neale R. Neelameggham, and Jeff Spangenberger
TMS (The Minerals, Metals & Materials Society), 2016

THE MATERIAL LIFE CYCLE A STEERING WHEEL FOR EUROPE'S RAW MATERIALS ACADEMY

Eric Pirard[1], Jenny Greberg[2]

[1]Université de Liège, Sart Tilman B52, Liege, 4000, Belgium
[2] Lulea University of Technology, Lulea, Sweden

Keywords: Raw Materials, Education, Engineering, Europe

Abstract

EIT Raw Materials is a major European initiative supported by more than 120 core and associate partners from industry, research and academia. Among the core missions of this network is the establishment of a Raw Materials RM Academy to educate T-shaped professionals that will contribute to the development of a sustainable and resource efficient Europe.
Every T-shaped professional should combine an in depth knowledge of his own discipline with a sound understanding of the challenges of the full raw materials value chain and with a mindset for innovation and entrepreneurship. The main objective of the RM Academy is to connect all T-shaped professionals to help create the circular economy steering wheel. Therefore, the RM Academy has the following missions:

- Label and support educational programs.
- Promote a permanent offer of cross-disciplinary programmes, workshops and courses.
- Train T-shaped professionals into T-shaped entrepreneurs.
- Promote lifelong learning initiatives.
- Stimulate wider society learning initiatives aiming at raising social and political awareness.
- Closely collaborate with industry
- Enable a high degree of mobility of students and professionals

The cradle of engineering education

Europe is proud of its mining heritage. Many sites are now on the list of the UNESCO World Heritage from the very first flintstone (Spiennes, BE) and salt mines (Hallstatt, AT) to the fascinating Almaden (SP) mercury mine with its record of more than 2000 years of exploitation. Being a region of intense mining activity, Europe is also considered as the cradle of engineering education with several mining schools (Bergakademie) already well established in the middle of the XVIIIth century (Banska Stiavnica (SLO), 1763; Freiberg (DE), 1765).
Most of the traditional mining schools demonstrated throughout the last two centuries their ability to adapt to their environment and to evolve towards reputed electrical, biomedical or aeronautical engineering schools not to mention the ones who became merely business schools.
However, what is truly remarkable are the deep stigmas left by three decades of major disinterest for the raw materials sector between 1980 and 2010.
De Cuyper (1992) [1] in a report to the European Commission analysed the trend in Mining Engineering education in Europe and suggested that future programs should focus on

geotechnics, hydrogeology and environmental sciences as already exemplified by some existing Geological Engineering degrees (Liège (BE); Nancy (FR)). In about the same period, traditionally strong mining engineering schools anticipating what would prove to be a severe disinterest for extractive industries decided to create a European Mining Course (EMC) [2]. This European degree, established well before the arrival of Erasmus Mundus programs, included a mobility scheme (Delft (NL); Aachen (DE); London (UK); Helsinki (FI)) and close cooperation with industrial partners.
Within the same period, many universities struggled to maintain mining engineering degrees. Several specialized schools with a strong industrial support went through this period (Lulea (SE); Leoben (AT)), especially also in former Eastern Europe (Wroclaw (PL); Sofia (BG)) but many of them decided to close down all educational activities related to mineral resources exploration; extraction or processing. Dozens of Geological, Mining and even Metallurgical Engineering degrees dissapeared from the educational offer and many more academic positions were closed down to privilege investment in the so-called high technologies (computer sciences; biomedical engineering; aerospace; applied mathematics; etc.). It was crystal clear to many that Europe's future was to specialize into the very end of the value chain and to forsake the primary resource sector.

A sudden awakening

The decision, taken by the Chinese government in 2009, to apply export quota on Rare Earth concentrates seemingly surprised many actors in Europe. This decision had a temporary impact on the price of raw materials, but much more fundamentally it triggered a sudden awakening and a real concern about the security of supply of raw materials for the European industry. Cellphones, windmills and solar panels were among the objects treasured by the high-tech economy that could suddenly be threatened by a raw materials shortage. Also, the demand on raw materials for infrastructure and construction dramatically increased due to the upswing in European economy. In 2008, the European Union published a reference document "The Raw Materials Initiative" [3] quickly followed by a series of studies on "Critical Raw Materials for the EU" that set the scope and insisted on the urgent need to reconsider the raw materials strategy.
The Raw Materials Initiative prompted a series of expert meetings to develop a European Innovation Parnership (EIP) on Raw Materials to provide the necessary roadmaps for research, education and innovation [4]. In 2013, what had been neglected for almost thirty years suddenly reappeared as a priority. The Strategic Implementation Plan (SIP) of the EIP had three pillars, one which was technological and two non-technological. When referring to the skills shortage, the diagnosis was particularly explicit: *"There is a shortage of specialists in Europe in some of the areas related to raw materials production and processing (e.g. mineral processing), and the problem should be addressed at European level. The problems faced by the mining sectors are the lack of skilled workforce, no or sometimes bad image impacting interest in mining education and its relative unattractiveness, ageing workforce and lack of replacement." (EIP SIP Part II, p.46).*
But, probably the most important contribution of the EIP think tank has been to consider raw materials within the paradigm of the circular economy (Fig. 1). Instead of just stressing the importance of relaunching intense exploration, reopening mines and developing advanced solutions in mineral processing, the whole document is centered on the idea of resource

efficiency in the circular economy. The take-make-dispose linear economy thinking is definitely abandoned for a global vision of the value chain, putting the extraction of mineral and metal resources at the very beginning of a circle which ends by collecting end-of-life products and recovering valuable materials out of the urban mines. This systemic thinking considering the whole lifecycle of a metal in the production chain opens new perspectives in terms of research and innovation, but also in terms of education. The traditional cleavages between geology, mining or mineral processing can no longer be accepted. A new generation of engineers must hatch out with a clear entrepreneurial mindset and a better capacity to innovate by breaking barriers between disciplines. Europe's call in March 2014 for a unique Knowledge Innovation Community (KIC) in Raw Materials within the framework of the European Institute for Innovation and Technology (EIT) was the most tangible demonstration of this will to recover a leading position in raw materials education.

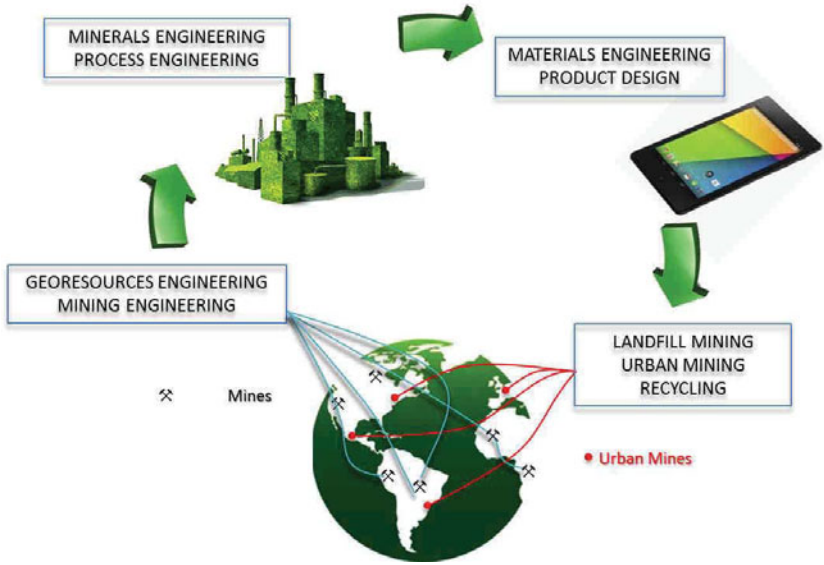

Figure 1. Engineering education needs along the whole lifecycle of a product.

Building a Knowledge Innovation Community

The EIT, launched in 2008, has the mission to reinforce Europe's innovation capacity by preparing the entrepreneurs and innovators of tomorrow. By fully integrating the three sides of the knowledge triangle (education, research and innovation), the EIT aims at boosting the innovation process: from idea to product; from lab to market and from student to entrepreneur. The EIT knowledge innovation community on Raw Materials was officially designated on December 9th 2014 after an open call for proposals. The EIT Raw Materials is an impressive consortium of 115 partners present in 22 countries. It was established as a legal entity on June

30th 2015 in Berlin and has the ambitious vision of turning the challenge of raw materials dependence into a strategic strength for Europe by acting at all stages of the materials value chain [5].
The desiloeing of the traditional activities of exploration, extraction, processing, recycling and substitution is a key objective of this KIC to be achieved, among others, by the establishment of a Raw Materials (RM) Academy. Such a RM Academy will coordinate a series of actions encompassing wider society learning, continuing professional education and master/doctoral schools. For these latter, the EIT has set a series of quality indicators and specific learning outcomes leading to a possible labelling. Quality indicators refer among others to a built-in European mobility scheme; the implication of business partners in the curriculum; a clear admission and selection procedure; the use of English as a teaching language and the adoption of strict ECTS, DS standards.

Educating T-Shaped raw materials professionals

The RM Academy aims at educating 4500 T-shaped professionals, who will be ready to provide their hands-on expertise to industry and research by 2022. What is key to the educational principles of T-shaped professionals is the idea of a holistic understanding of the raw materials value chain including interactions and trade-offs. The objective it to lead to the formation of T-shaped professionals having a deep understanding of their own discipline while keeping a broad and holistic view of the circular economy paradigm. The graduates are expected to act as change agents, intra- and entrepreneurs and be responsive to the needs of the raw materials sector.

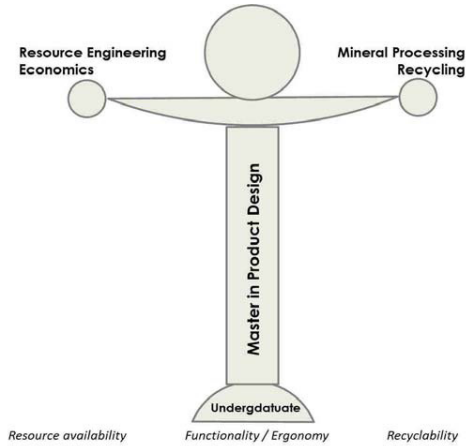

Figure 2. Simplified illustration of a T-shaped professional in product design.

As compared to traditional master degrees, the RM Academy will make sure that the proposed programs offer complementary training modules to understand the whole value chain. An example of this can be found in recently launched programs such as the EMerald Erasmus

Mundus Master in Georesources Engineering [6] organized by four leading universities in the field Liege (BE), Lulea (SE), Nancy (FR) and Freiberg (DE). This program specializes in Geometallurgy, a multidisciplinary approach which typically tries to bridge the gap between resource experts and process engineers, a program which considers both the material (ore, urban waste) and the machine (comminution, leaching, etc.) with the aim to better plan the mining operations and to optimize the energy and resource efficiency of industrial processes.
Another example of an innovative program could be a Master in Industrial Design focussing on design for recycling principles. Design engineers would be trained to optimize product design by considering their functionality and ergonomy but also by taking into account the resource availability and the potential recyclability of the product at the end of its lifecycle. This would require some basic modules in resource engineering and mineral processing to be offered in design schools (Fig. 2).
The RM academy will be particularly attentive to engineering programs being delivered using appropriate facilities and teaching methods. As much as possible, education activities include hands-on experience utilising real infrastructure and teaching using state of the art tools. Well equipped research laboratories and pilot plant facilities are of prime importance in training engineers in the raw materials sector. It is expected that the close cooperation with industrial partners in the knowledge triangle will broaden the opportunities for assignments, field visits, on site internships and master thesis research work closely linked to industrial problems.

In addition to the technical skills, all programs will include seminars given by industrial partners to develop the entrepeneurial mindset of students and business games or summer schools to develop innovation and entrepreneurship within a sustainable perspective. It will be the RM Academy's mission to bring together students covering the whole value chain to participate to innovation or business oriented workshops. It is expected that such cross-disciplinary initiatives will stimulate creativity and boost the raw materials and recycling sectors with ideas meeting the most stringent criteria of social acceptance and environmental footprint.

Conclusions

The European higher education in raw materials is back on tracks. Within the coming years a series of innovative programs will be launched with the aim to reposition Europe as a world leader in thematics such as exploration, mining, mineral processing, substitution and recycling.
Under the unbrella of the European Institute for Innovation and Technology (EIT) these programs will closely associate industrial partners, research institutions and major universities. A new generation of creative entrepreneurs with a holistic view of the raw materials value chain is expected to contribute to help closing the loop and improve process efficiency. This new community of engineers graduating from the Raw Materials Academy should be the steering wheel of a true circular economy.

References

1. De Cuyper J., *Analysis of mining engineering higher education and training in the European Community* (Commission des Communautés européennes, DGIII, Bruxelles, 1992).

2. European Mining, Minerals and Environmental Program (http://www.emmep.org/, 2015)

3. European Commission, *The Raw Materials Initiative – meeting our critical needs for growth and jobs in Europe* (http://ec.europa.eu/growth/sectors/raw-materials/policy-strategy/index_en.htm, 2008)

4. European Commission, *European Innovation Partnership (EIP) on Raw Materials: Strategic Implementation Plan* (https://ec.europa.eu/eip/raw-materials/en, 2010)

5. EIT Raw Materials Knowledge Innovation Community (http://eitrawmaterials.eu, 2015)

6. EMerald, European Master Program in Georesources Engineering (http://em-georesources.eu, 2015)

REWAS 2016: Towards Materials Resource Sustainability
Edited by: Randolph E. Kirchain, Bart Blanpain, Christina Meskers, Elsa Olivetti, Diran Apelian, John Howarter, Anne Kvithyld, Brajendra Mishra, Neale R. Neelameggham, and Jeff Spangenberger
TMS (The Minerals, Metals & Materials Society), 2016

EDUCATION PROGRAMS AND ACTIVITIES IN CHINA FOR THE SUSTAINABILITY OF METALLURGICAL INDUSTRY AND THEIR PERSPECTIVE

Guangqiang Li[1, 2]; Chengyi Zhu[2]; Junying Zhang[3]

[1]State Kay Lab. of Refractories and Metallurgy, Wuhan University of Science and Technology, No. 947 Heping Road, Wuhan, Hubei, 430081, China
[2]Key Laboratory for Ferrous Metallurgy and Resources Utilization of Ministry of Education, Wuhan University of Science and Technology, No. 947 Heping Road, Wuhan, Hubei, 430081, China
[3]School of Information Science and Engineering, Wuhan University of Science and Technology, No. 947 Heping Road, Wuhan, Hubei, 430081, China

Keywords: Steelmaking; Environmental Protection; Energy Saving

Abstract

The scale of the metallurgical industry of China is very huge. The energy consumption, resources supplying and environmental impaction of China are also causing severe challenges. The education programs and activities in universities towards undergraduate students and graduates concerning about the sustainability of metallurgical industry in China are introduced in this paper. Since the beginning of the 21centry, the courses related with environmental protection, energy saving, ecology, eco-materials were opened. Even the school of metallurgical engineering was changed to the school of metallurgical and ecological engineering and undergraduate students majoring in ecological engineering were cultivated. On the other hand, key laboratories related with metallurgical engineering and resources utilization which affiliated with Minister of Education were established in different universities. These laboratories provide platforms for educating and researching activities concerning sustainability of the metallurgical industry. The content of those courses, activities and achievements of education programs and research including international exchange will be reported in detail.

Introduction

The primary energy consumption of China in 2012 was 21.9% and that of USA was 17.7%. These two countries consumed 39.6% of the total energy in the world. Table I lists the top 10 countries of energy consumption by fuel. One can find that the ratios of coal in total energy consumption are quite different among different countries, that are 68.5% for China and 52.9% for India, but the highest one is South Africa, 72.8%. The combustion of coal will cause CO_2, SO_x and NO_x emission and needs investment to solve this problem. But the per capita energy consumption in China is only 29% and 54% of that of American and Japanese, respectively. The scale of metallurgical industry of China is very huge. The quantity of crude steel production has been increasing these years. The crude steel production in China reached 822.7 million tons in 2014, it takes almost half of the total world production. Thus the amount of energy and resources consumption is also very huge in China. Steel production needs energy, too. In 2010, steel

industry consumed 16% of the total energy in China and this is 23% of total industrial energy consumption in China

Table I Energy Consumption Top 10 Countries in 2012 (Million Tonnes of Oil Equivalent)*[1].

Country	Oil	Natural Gas	Coal	Nuclear Energy	Hydro Electricity	Renewables	Total
China	483.7	129.5	1873.3	22.0	194.8	31.9	2735.2
USA	819.9	654.0	437.8	183.2	63.2	50.7	2208.8
Russian Federation	147.5	374.6	93.9	40.3	37.8	0.1	694.2
India	171.6	49.1	298.3	7.5	26.2	10.9	563.5
Japan	218.2	105.1	124.4	4.1	18.3	8.2	478.2
Canada	104.3	90.6	21.9	21.7	86.0	4.3	328.8
Germany	111.5	67.7	79.2	22.5	4.8	26.0	311.7
Brazil	125.6	26.2	13.5	3.6	94.5	11.2	274.7
South Korea	108.8	45.0	81.8	34.0	0.7	0.8	271.1
France	80.9	38.2	11.4	96.3	13.2	5.4	245.4

* Oil consumption is measured in million tonnes; other fuels in million tonnes of oil equivalent.

Even as new processing technology for energy saving are adopted in many large steelmaking companies, the ratio of energy reuse in China steel companies is still lower, for example, the energy re-use ratio in about 50% of the steelmaking companies is less than 50%, Baosteel can re-use 77%, but this ratio in Nippon Steel & Sumitomo Metal is 92%.

China is the fourth largest iron ore producer in the world, it produced 1330 million tonnes iron ore domestically in 2011. But the average grade of iron ore produced is lower, the iron content is only about 33%. So China has to import about 70% of its iron ore demand abroad. By estimation, the needs for iron ore in China will decrease gradually from 850 million tonnes in 2015 to 500 million tonnes in 2030. The iron ore deposit in China can be used up after 26 years.

China steel industry has been facing on above mentioned energy, resource, and environmental problems, but in the same time we have also been contributing to the sustainable developing of steel industry. The efforts made by government including establishing policies, laws, training, and education. In this paper the education in university toward students majoring in metallurgy for sustainable development of steel industry in China will be introduced.

Sustainable Development Education for University Students Majoring in Metallurgical Engineering

There are 37 universities in China that have the major called metallurgical engineering, some of the name of these universities and numbers of their students per year are listed in Table II. By rough estimation, around 5000 undergraduate students major in metallurgical engineering graduate every year and more than 50% of them may work in ferrous or non-ferrous industries. Almost the same status can be observed in case of graduate students. The sustainable development education to these students is very important to face the challenge of energy, resource, and environmental crisis.

Table II Some Universities in China and Their Students per Year Major in Metallurgical Engineering

Rank	Name of University	Number of freshman per year
1	Central South University	180
2	University of Science and Technology Beijing	200
3	Northeastern University	270
4	Shanghai University	20
5	Kunming University of Science and Technology	200
6	Chongqing University	80
7	Wuhan University of Science and Technology	100
8	University of Science and Technology Liaoning	130
9	Inner Mongolia University of Science and Technology	160
10	Jiangxi University of Science and Technology	200
11	Xi`an University of Architecture and Technology	200
12	Jiangsu University	50
13	Taiyuan University Of Technology	120
14	Henan University of Science and Technology	70
15	Anhui University of Technology	175
16	North China University of Science and Technology	120
17	Guizhou University	120
18	Lanzhou University of Technology	120

The number of freshman in China whose major is non-environmental related is more than 99.5%. About 10% universities have environmental related courses for non-environmental related students [2]. The students majoring in metallurgical engineering will become policy makers, managers, and executors, their sense on environment protection and sustainable development will decide the tendency of sustainable development of metallurgical industry in future to a great extent.

As early as in 2002, University of Science and Technology Beijing (USTB) established the school of metallurgical and ecological engineering based on the previous school of metallurgical engineering. In this school, a new department with a new major named ecological engineering was opened. In other universities, some courses related with wastes treatment, resources utilization, energy saving, and environment protection were opened to undergraduate and graduate students. Table III and IV listed some representative course and text books.

The contents of the text book edited by two authors of present paper are as following [3]:

1 Introduction
1.1 Basic concepts of environment and environment protection
1.2 Fundamental processes and features of modern steelmaking
1.3 Resource, energy, and environment problems of steel industry
1.4 Current status of environment protection and energy saving of steel industry in China

2 Water pollution and water treatment in steel manufacture process
2.1 Status of water usage and pollution in steel plants
2.2 Water discharge standard and regular methods of water treatments

3 Waste gas treatment for steel industry

Table III Some Courses for Metallurgical Engineering Students in China

Course Name	University	Distinguishing feature
Introduction to Environmental Science	Central South University	Pollution caused by nonferrous metallurgy, Local area heavy metal pollution case study, water and slag treatment.
Metallurgical Ecology	University of Science and Technology Beijing	Emphasize in treatment and recycling of metallurgical wastes.
Introduction to Environmental Science	Northeastern University	Open to all undergraduate students; Contents including environment protection technologies for ferrous and non-ferrous metallurgical industries.
Environment Protection of Metallurgical Plants	Wuhan University of Science and Technology	Bilingual Teaching, introduce principles and examples of environment protection technologies of metallurgical industries.
Metallurgical Resources and Environment	Chongqing University	Teaching aim is make students having knowledge to response to the serious resources and environment problems in China and to reduce the pollution.
Introduction to Environmental Science	Jiangsu University	Focusing on the developing of responsibility and mission based on the peculiarity of metallurgical industries.

Table IV Some Text Books for Metallurgical Engineering Students in China

Text Book	Authors	Press and Published Year
Environment Protection and Wastes Reducing Technology for Metallurgical Industry	Xiaozhen Lang, Hongyi Yang	NEU Press, Aug. 2002, Shenyang, China
Environment Protection and Energy Saving for Steel Industry	Guangqiang Li, Chengyi Zhu	Metallurgical Industry Press, 2006, 2010. Beijing, China
Energy Saving and Emmision Reducing Technology for Metallurgical Industry	Qi Zhang, Jianjun Wang	Metallurgical Industry Press, 2013. Beijing, China

3.1 SO_x, NO_x and CO_2 in atmosphere
3.2 Sources, properties and emission standards of waste gases
3.3 Dusts control technologies
3.4 Cleaning technologies of coke oven gas
3.5 Desulfurization methods for sintering waste gas
3.6 Emission right trade of SO_x
3.7 Methods to reduce NO_x emission
3.8 Method to reduce emission and capturing of CO_2
3.9 Kyoto Protocol and Clean Development Mechanism

4 Slag treatment and valorization
4.1 Generation and properties of blast furnace, converter and electric arc furnace slags
4.2 Technologies for slag treatment
4.3 Routes of slag valorization and problems
4.4 Slagless steelmaking
4.5 Recovery of valuable elements from smelting slags of complex iron ores

5 Dusts and muds treatment and valorization

6 Noise pollution and control

7 Thermodynamic analysis of energy consumption process
7.1 General knowledges of energy
7.2 Quality evaluation of energy-Exergy
7.3 Examples of exergy analysis in steelmaking processes

8 Energy saving processes in steel industry
8.1 Introduction
8.2 SCOPE21 coke making new technology in Japan
8.3 Coke dry quench technology
8.4 Energy saving technology in sintering process
8.5 Energy saving technology in blast furnace
8.6 Power generation by blast furnace top gas pressure recovery turbine
8.7 Combined cycle power plant for steel industry
8.8 Recycling waste plastics by blast furnace and coke oven
8.9 Gas recovery technology from steelmaking converter

9 LCA and the environment protection, energy saving of steel industry
9.1 LCA and its development in the world
9.2 Technique frame and types of LCA
9.3 Application of LCA abroad
9.4 Studies of LCA to the environment protection, energy saving of steel industry
9.5 Some conclusions of LCA
9.6 Limits of LCA

Details of Chapters 5 and 6 are not listed. As can be seen, this book systematically introduced the basic concepts of environment, problems of steel industry in resource, energy, and environment. It also illustrated the generation of waste gas, water, slags, and methods of reuse, reduce and recycle of these waste resources, and the methods of emission control. Chapter 7 is very useful for students to understand how energy can be used more efficiently and how to evaluate the quality of a metallurgical process in energy consumption. They can also understand not only the quantity but also the quality of energy consumption both are important in an industry process.

Other Activities Related with Sustainable Development Education for University Students Majoring In Metallurgical Engineering in China

In addition to courses supplied to students, extracurricular activities concerning about sustainable development education are also selectable for students. Academic reports that introduce sustainable development of metallurgical industry is often given by professors abroad. Students can also join in a research group to do some experimental work related with recycling of wastes from metallurgical industry. For example, recovery of nickel and chromium from stainless steel slags, recovery copper from copper smelting slags, and so on. Students have the chance to visit steelmaking, copper or aluminum smelting plants to see how the scraps are recycled and how the waste gas, water are treated to fulfil the emission standards. Graduate students can have the opportunity to attend international conferences and visit metallurgical plants, by this way they can know the differences between China and developed countries in the way of sustainable development.

On the other hand, professors who are teaching metallurgy process paid more attention to sustainable development of metallurgical industry. They take part in various conferences with topic of sustainable development, such as the slag valorization symposium in Leuven, Belgium, special symposium organized by the Iron and Steel Institute of Japan. Thus, new ideas can be obtained by exchanging between different countries. Education can then be enhanced and improved. One of the present authors took four months last year as a guest professor in the University of Tokyo, joined their teaching of a course to graduate students with the name of Environmental Materials. I think that is a valuable experience to me. I also visited steel plants and R&D centers of Nippon Steel & Sumitomo Metal and JFE, which are first and second large steel company of Japan. Especially, I saw their slag treatment yards and their pilot scale unit for heat recovery from molten slag. I saw the waste plastics treatment by coke oven and blast furnace. These are what we do not do till now. Of course there are reasons but at least the thinking is quite different between China and Japan.

Summary

Education of sustainable development is in progressing toward students majoring in metallurgical engineering in universities in China. Various fundamental courses are opened and some text books are published. We hope that sustainable education for students major in metallurgical engineering can stimulate them to make revolution of metallurgical processes to reduce emission and energy consumption from metallurgical process itself.

References

1. BP Statistical Review of World Energy ed., BP Statistical Review of World Energy 2013, 22.

2. Yunyan Wang, Liyuan Cai, Zhixing Wang, “Teaching Reforming and Practicing on Introduction of Environmental Science Course for Students Major in Metallurgical Engineering”, *Education forum of China*, 2014, No. 4, 37-38.

3. Guangqiang Li, Chengyi Zhu ed., Environment Protection and Energy Saving for Steel Industry, (Beijing, China, Metallurgical Industry Press, 2010), V.

Understanding & Enabling Sustainability - Education Research Innovation + Electronic Equipment

REWAS 2016: Towards Materials Resource Sustainability
Edited by: Randolph E. Kirchain, Bart Blanpain, Christina Meskers, Elsa Olivetti, Diran Apelian, John Howarter, Anne Kvithyld, Brajendra Mishra, Neale R. Neelameggham, and Jeff Spangenberger
TMS (The Minerals, Metals & Materials Society), 2016

SUSTAINABILITY: OPPORTUNITIES FOR TEACHING OLD CONCEPTS VIA NEW PROBLEMS

Gabrielle Gaustad[1]

[1]Golisano Institute for Sustainability, Rochester Institute of Technology
111 Lomb Memorial Drive, Rochester, NY, 14623-5608, USA

Keywords: education, multi-criteria decision analysis, optimization, simulation

Abstract
The theoretical and methodological foundations of the sciences and technologies are essential to the removal of barriers to achieving sustainable systems. The teachings of these concepts still lie in traditional academic disciplines such as engineering, science, and mathematics. This structure can often manifest significant barriers to progress in tackling challenging sustainability issues due to an absence of a multi-faceted, interdisciplinary, systems approach. This work will explore approaches for using current sustainability issues and problems to introduce both systems thinking and traditional discipline specific learning objectives to the classroom. Specific examples will be illustrated for a diverse set of courses and curriculum. Assessment shows an improved rate of achieving teaching outcomes compared to traditional curricular techniques.

Introduction

Current sustainability issues have far-reaching impact and present a great challenge to be tackled by the next generation of thinkers. The current generation of educators is thereby tasked with ensuring these thinkers are equipped with the skillsets necessary to tackle these problems. The theoretical and methodological foundations of the sciences, technologies, engineering and math (STEM) are essential to the removal of barriers to achieving sustainable systems. While a majority of these concepts still lie in traditional academic disciplines such as material science, educators are challenged to integrate broader sustainability related concepts in the curriculum.

Besides the altruistic motivation above, integration of sustainability concepts is a key marketing opportunity for higher education. Keen interest in sustainability related issues by prospective students is becoming prevalent both in the US[1] and abroad[2]. Quantitative evidence is beginning to emerge to support this. The Princeton Reviews' 2009 survey showed that 66% of the 15,722 respondents value having information about a college's commitment to the environment; 24% said this would "strongly" or "very much" contribute to their decision to attend. Sustainability in the curriculum also provides a significant opportunity to attract under-represented female students into STEM degrees[3, 4] as research shows giving back and service learning to be key motivators for female students[5, 6].

Literature on integrating sustainability in higher education often highlight the need for new[7], multi-disciplinary[8], and even eclectic[9] approaches. There has also been much thought on the barriers present to achieving a cohesive integration of sustainability in current and new curriculums[10-13], not least of which is the definition of what constitutes sustainability itself[14-16]. A significant barrier to progress has been the absence of a multi-faceted, interdisciplinary, *systems* approach to solving seemingly intractable sustainability problems.

Local optimization approaches by researchers, corporations, and policy makers are destined to yield marginal positive impacts, or may even negatively impact other aspects of our global systems. True improvements in our global systems require a holistic systems view of both sustainability problems and potential solutions. The RIT degrees in Sustainability and Sustainable Systems aim to provide this systems perspective in our educational program.

Curriculum Development

The educational community at the Rochester Institute of Technology (RIT) has traditionally engaged and motivated students through a variety of stimulating and collaborative experiences and, because our mission as a university is to provide technology-based educational programs for personal and professional development, we rigorously pursue new and emerging career areas. In this context, a Ph.D. program encompassing advanced scholarship in the emerging field of sustainability was developed. This program is founded upon the increasingly demonstrated premise that the challenge of sustainability is beyond the scope of any single traditional discipline. The program, which admits students from a variety of educational backgrounds, consists of a unique core of interdisciplinary courses, a wide array of associated electives from multiple RIT departments, and original, systems-based research—all directed at graduating experts capable of bringing an integrative approach to sustainability research. The program will be a model for team-based graduate education in which team members with diverse backgrounds and complementary expertise will integrate multiple knowledge bases. The research questions that motivate these teams will be related to the understanding of systemic interactions and the integration of economic, social, and environmental context, content, and connectedness. Four key areas will be the focus of research within the Golisano Institute for Sustainability (GIS), housing the RIT PhD program in Sustainability: 1) sustainable production and manufacturing, 2) eco-IT (environmentally efficient information technology), 3) sustainable transportation and mobility, and 4) sustainable energy systems.

The curriculum combines required core courses in Sustainability; elective courses from the GIS and other RIT colleges as appropriate to the student's background and interests; a three quarter research seminar; and a research dissertation. The purpose of the core curriculum is to develop in the students a broad-based understanding of the interdisciplinary aspects of sustainable systems and to teach students to view both problems and solutions systemically. The following six courses constitute the program's core: Fundamentals of Sustainability Science, Risk Analysis, Industrial Ecology, Multi-criteria Sustainable Systems Analysis, Economics of Sustainability, Technology, Policy, and Sustainability.

Specific Course Examples

Many of the key core courses above are routed in traditional disciplines with fundamentally accepted ways of teaching certain problems. However, presenting these problems as sustainability dilemmas can provide a fresh perspective that re-invigorates the subject. In the multi-criteria decision analysis course that I teach, the learning outcomes all focus on traditional optimization and numerical simulation type problems, problem solving approaches, and algorithms. However, small adjustments to these foundational subjects make it easy to cast similarly structured sustainability problems in a way to teach these topics as illustrated in Table 1. For example, instead of focusing on a traditional modern portfolio theory example using

stocks or 401k plans, the students are tasked with programming and analyzing the risks and rewards associated with various energy sources from both renewable (eg. photovoltaics, wind, bio-mass) and non-renewable sources (eg. natural gas, petroleum, coal).

Table 1. Example sustainability problems used in multi-criteria decision analysis

Typical Optimization Problem	Sustainability Problem
Financial portfolio	Renewable energy portfolio
Reverse logistics supply chain	Reverse logistics MSW collection network
Utility maximization	Environmental welfare maximization
Traveling salesman	Micro-grid design
Nutrient blending	Recycled metal blending
Game theory	Circular economy
Genetic algorithms	Sustainable forest planning
Multi-criteria optimization	Economic and environmental trade-offs

Material science has a particularly relevant set of foundational courses that lend themselves to interesting sustainability integration. Material selection approaches and software have begun to incorporate both economic and environmental "properties" in the decision analysis, highlighting the tradeoffs made in real applications[17]. Thermodynamics and kinetics principles can be illustrated in interesting energy conversion examples for next-generation renewable energy storage and production technologies. Other important contributions exist in fundamentals of mining, processing, alloying, phase equilibria, material flow analysis, etc. A variety of recent research is available with additional innovative suggestions [18-20].

ACKNOWLEDGMENTS

All those affiliated with the Golisano Institute for Sustainability are thankful to the Henry Luce Foundation for providing a grant to support initial curriculum development. Special acknowledgement to the curriculum committee and working group members: John Albertini, Stefi Baum, Alex Bitterman, Marcos Esterman, Michael Haselkorn, Katherine Mayberry, Jacqueline Mozrall, Nenad Nenadic, Nabil Nasr, Ryne Raffaelle, Jennifer Schneider, William Stevenson, Michael Thurston, and James Winebrake. Thank you also to the external advisory board who provided tremendously helpful feedback and advice for the program: Joseph Allen, Robert Bechtold, Patricia Calkins, Edward J. Daniels, Joost Duflou, Mathew H. Fronk, V. Daniel R. Guide, Jr., Jack Jeswiet, Sami Kara, Hartmut Kaebernick, David M. Kiser, Edward Krause, Clare Lindsay, Jeffery Sama, Steve Schaffer, Gunther Seliger, and Ernst von Weizsaecker.

References

1. Marklein, M.B., *College hopefuls look for green universities*, in *USA Today*. 2011.
2. Thomas, I., *Student interest for environment/sustainability undergraduate programmes: recent Australian experience.* Journal of Education for Sustainable Development, 2014. **8**(1): p. 5-27.
3. Mihelcic, J.R., L.D. Phillips, and D.W. Watkins Jr, *Integrating a global perspective into education and research: Engineering international sustainable development.* Environmental Engineering Science, 2006. **23**(3): p. 426-438.
4. Oehlberg, L., R. Shelby, and A. Agogino, *Sustainable product design: Designing for diversity in engineering education.* International Journal of Engineering Education, 2010. **26**(2): p. 489.

5. Dahlberg, T., et al., *Applying service learning to computer science: attracting and engaging under-represented students.* Computer Science Education, 2010. **20**(3): p. 169-180.
6. Zimmerman, J.B. and J. Vanegas, *Using sustainability education to enable the increase of diversity in science, engineering and technology-related disciplines.* International Journal of Engineering Education, 2007. **23**(2): p. 242-253.
7. Moore, J., *Seven recommendations for creating sustainability education at the university level.* International Journal of Sustainability in Higher Education, 2005. **6**(4): p. 326-339.
8. Warburton, K., *Deep learning and education for sustainability.* International Journal of Sustainability in Higher Education, 2003. **4**(1): p. 44-56.
9. Fien, J., *Advancing sustainability in higher education: Issues and opportunities for research.* International Journal of Sustainability in Higher Education, 2002. **3**: p. 243-253.
10. Velazquez, L., N. Munguia, and M. Sanchez, *Deterring sustainability in higher education institutions.* International Journal of Sustainability in Higher Education, 2005. **6**(4): p. 383-391.
11. Thomas, I., *Sustainability in tertiary curricula: what is stopping it happening?* International Journal of Sustainability in Higher Education, 2004. **5**(1): p. 33-47.
12. Moore, J., *Barriers and pathways to creating sustainability education programs: policy, rhetoric and reality.* Environmental Education Research, 2005. **11**(5): p. 537 - 555.
13. Munson, K.G., *Barriers to ecology and sustainability education in US public schools.* Contemporary Education, 1997. **68**(3): p. 174-176.
14. Filho, W.L., *Dealing with misconceptions on the concept of sustainability.* International Journal of Sustainability in Higher Education, 2000. **1**(1): p. 9-19.
15. Wright, T.S.A., *Definitions and frameworks for environmental sustainability in higher education.* International Journal of Sustainability in Higher Education, 2002. **3**(3): p. 203-220.
16. Jucker, R., *"Sustainability? Never heard of it!".* International Journal of Sustainability in Higher Education, 2002. **3**(1): p. 8-18.
17. Ashby, M.F., H. Shercliff, and D. Cebon, *Materials: engineering, science, processing and design*. 2013: Butterworth-Heinemann.
18. Mainali, B., et al., *Integrating Sustainable Engineering Principles in Material Science Engineering Education.* Handbook of Research on Recent Developments in Materials Science and Corrosion Engineering Education, 2015: p. 273.
19. Gunister, E., et al., *Innovative Instructional Strategies for Teaching Materials Science in Engineering.* Handbook of Research on Recent Developments in Materials Science and Corrosion Engineering Education, 2015: p. 100.
20. Gipson, K.G. and R.J. Prins, *Materials and Mechanics: A Multidisciplinary Course Incorporating.* Handbook of Research on Recent Developments in Materials Science and Corrosion Engineering Education, 2015: p. 230.

REWAS 2016: Towards Materials Resource Sustainability
Edited by: Randolph E. Kirchain, Bart Blanpain, Christina Meskers, Elsa Olivetti, Diran Apelian, John Howarter, Anne Kvithyld, Brajendra Mishra, Neale R. Neelameggham, and Jeff Spangenberger
TMS (The Minerals, Metals & Materials Society), 2016

3D PRINTED ABS AND CARBON FIBER REINFORCED POLYMER SPECIMENS FOR ENGINEERING EDUCATION

Michael Golub[1], Xingye Guo[1], Mingyo Jung[2], Jing Zhang[1*]

[1]Department of Mechanical Engineering, Indiana University- Purdue University Indianapolis, Indianapolis, IN 46202, USA
[2]University High School, 2825 W. 116th Street, Carmel, IN 46032, USA

*Corresponding author: jz29@iupui.edu; 317-278-7186

Keywords: 3D Printing, Additive Manufacturing, ABS, ABS plus, Carbon Fiber Reinforced Polymer, Mechanical Property

Abstract

Three 3D printed plastic materials, ABS, ABS plus, and CFRP, have been studied for their potential applications in engineering education. Using tensile test, the stress strain curves of the materials have been measured. The Young's modulus, ultimate strength, and fracture toughness of the materials are calculated from the stress strain curve. The results show that CFRP has the highest stiffness or Young's modulus. ABS plus has strongest mechanical properties, with highest ultimate strength and fracture toughness. With the measured properties, the 3D printed samples are a viable solution for engineering students to learn mechanical properties of materials.

Introduction

Fused deposition modeling (FDM) is an additive manufacturing technology commonly used for modeling, prototyping, and production applications. It is one of the techniques used for 3D printing. FDM works on an "additive" principle by laying down material in layers; a plastic filament or metal wire is unwound from a coil and supplies material to produce a part [1]. 3D printers that run on FDM Technology build parts layer-by-layer from the bottom up by heating and extruding thermoplastic filament [2]. The process is simple: (1) Pre-processing: Build-preparation software slices and positions a 3D CAD file and calculates a path to extrude thermoplastic and any necessary support material. (2) Production: The 3D printer heats the thermoplastic to a semi-liquid state and deposits it in ultra-fine beads along the extrusion path. Where support or buffering is needed, the 3D printer deposits a removable material that acts as scaffolding. (3) Post-processing: The user breaks away support material or dissolves it in detergent and water, and the part is ready to use [2].

In this study, the study is focused on 3D printed ABS, ABS plus, and carbon fiber reinforced polymer. Their mechanical properties, including Young's modulus, ultimate strength, and fracture toughness, are characterized and compared using tensile test.

Methodology

Three plastic materials are used in this study: ABS from Stratasys (Eden Prairie, MN), ABS plus from the 3D Filament Shop Ltd. (the Swan Centre, Higher Swan Lane, Bolton, UK), and carbon fiber reinforced polymer (CFRP, 20 wt% of carbon fiber) from 3DXTech (Wyoming, MI). At least three samples of each material are used, and only the average mechanical properties are reported below. The specimens used in this study are designed in accordance with the ASTM standard test method for tensile properties of plastics. The printer used is FDM 3D printer developed by 3D Parts Manufacturing LLC (Indianapolis, Indiana).

The tensile testing is done using a MTS Systems universal testing machine according to ASTM standards for tensile properties of plastics. The model number of extensometer used in the test is 634.12E-54.

Before the tensile tests, the width and thickness of the center section of each of the specimens are measured then entered into the testing program. The tensile specimen is loaded into the testing machine by attaching the clamps to both ends and the distance between the clamps is measured and entered into the program. The tensile strain rate applied is 0.2 in/min (0.0847 mm/s). The program records tensile load and elongation, which can be converted to stress – strain curves.

Results and discussion

The fractured tensile samples are shown in Figure 1. In general, the samples show brittle fracture due to relatively small deformation. In order to evaluate the mechanical properties, the stress-strain curves of the three samples are plotted in Figure 2.

Figure 1: Optical images of the fracture tensile testing samples.

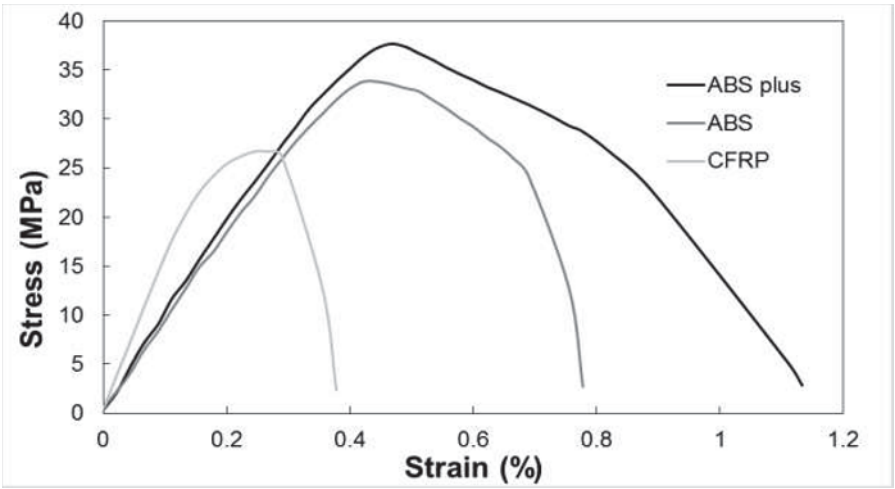

Figure 2: Representative stress-strain curves of tensile tests of three materials

The mechanical properties of the three materials, derived from the stress-strain curves in Figure 2, are summarized in Table 1. CFRP has the highest Young's modulus, due to its inclusion of high stiffness carbon fibers. However, its ultimate strength and fracture toughness are lower than those of ABS and ABS plus. So 3D printed CFRP is suitable for rigid applications. ABS and

ABS plus have similar Young's modulus, but ABS plus has much higher ultimate strength and fracture toughness. Therefore, ABS plus is suitable for large deformation applications, but more expensive than ABS. The order of cost of the three materials is: ABS < ABS plus < CFRP.

Table 1: Averaged mechanical properties of 3D printed ABS, ABS plus, and CFRP

	Young's modulus (GPa)	Ultimate strength (MPa)	Fracture toughness (MPa)
ABS plus	9.8	37.7	0.286
ABS	9.2	33.9	0.179
CFRP	17.1	26.7	0.073

Educational plan

With the measured materials properties, the educational plan of using the 3D printed plastics in engineering curriculums would be the following. The low cost of the 3D printed plastic samples allows student groups to print multiple samples each. They can use the built-in software to do the standard deviation of sample dimensions and manually check it. With steel, brass or aluminum the costs are too high to get enough samples to do a standard deviation.

Also because students can have more samples, they will gain experience performing the tensile tests. Previously only student teaching assistant used the tensile testing machine and extensometer since only one sample was available. Now the students can perform the experiment themselves since more samples are available. It is performed under close supervision. This is done so not to harm the equipment and to make sure that the multiple samples are done accurately.

As we acquire the technology to make different plastic samples we can add them to the lab session. We have not found a replacement for the metals, and are still doing a few of the metals per year so the students have comparison data. It is important that students understand the small differences in plastic deformation and fracture but they need to see and experience a larger spectrum of materials. Therefore, 3D printed plastic samples are a viable solution for engineering students to learn mechanical properties of materials.

Summary

Three 3D printed plastic materials, ABS, ABS plus, and CFRP, are investigated in this study:

1. CFRP has the highest stiffness or Young's modulus
2. ABS plus has strongest mechanical properties, with highest ultimate strength and fracture toughness.
3. 3D printed samples are a viable solution for engineering students to learn mechanical properties of materials.

Acknowledgements

JZ acknowledges the financial support provided by Walmart Foundation (project title: Optimal Plastic Injection Molding Tooling Design and Production through Advanced Additive Manufacturing).

References

1. Wikipedia. *http://en.wikipedia.org/wiki/*.
2. Stratasys. Available from: http://usglobalimages.stratasys.com/Main/Files/White%20Papers/WP_FDM_3D%20PrintingWithFDM.pdf?v=635786177472811876.

REWAS 2016: Towards Materials Resource Sustainability
Edited by: Randolph E. Kirchain, Bart Blanpain, Christina Meskers, Elsa Olivetti, Diran Apelian, John Howarter, Anne Kvithyld, Brajendra Mishra, Neale R. Neelameggham, and Jeff Spangenberger
TMS (The Minerals, Metals & Materials Society), 2016

WASTE MANAGEMENT OF PRINTED WIRING BOARDS: A LIFE CYCLE ASSESSMENT OF THE METALS RECYCLING CHAIN FROM LIBERATION THROUGH REFINING

Mianqiang Xue [1,2], Alissa Kendall [3], Zhenming Xu [1], and Julie M. Schoenung [3]

[1] School of Environmental Science and Engineering, Shanghai Jiao Tong University, 800 Dongchuan Road, Shanghai 200240, China
[2] Department of Chemical Engineering and Materials Science, University of California, Davis, One Shields Avenue, Davis, California 95616, United States
[3] Department of Civil and Environmental Engineering, University of California, Davis, One Shields Avenue, Davis, California 95616, United States

Keywords: Printed Wiring Boards, Recycling, Life Cycle Assessment

Due to economic and societal reasons, informal activities including open burning, backyard recycling, and landfill are still the prevailing methods used for electronic waste treatment in developing countries. Great efforts have been made, especially in China, to promote formal approaches. A formal recycling process can, however, engender environmental impact and resource consumption, although information is currently limited. To quantitatively assess the environmental impact of a formal printed wiring board (PWB) recycling chain, life cycle assessment (LCA) was applied to the steps from waste liberation through materials refining [1]. Scenario modeling was conducted, and results were compared to conventional primary metals production processes.

The goal of this study was to quantitatively assess environmental burdens and resource consumption associated with a formal recycling chain for waste PWBs, as implemented in China, including pilot pretreatment lines, heavy metals recovery and precious metals recovery. The LCA was carried out using GaBi 6 software. The CML 2001 method was used to evaluate the environmental impact of the processes in the PWB recycling chain. The chosen impact categories were as follows: global warming potential (GWP), acidification potential (AP), eutrophication potential (EP), abiotic depletion potential, fossil (ADP fossil), freshwater aquatic eco-toxicity potential (FAETP), human toxicity potential (HTP), marine aquatic eco-toxicity potential (MAETP), photochemical ozone creation potential (POCP), and terrestrial aquatic eco-toxicity potential (TETP). Global warming is evaluated considering a 100-year timescale. Normalization was conducted by means of CML2001-Nov. 2010, World.

The process flow diagram for the PWB recycling chain was divided into the beneficiation and refining stages. The beneficiation stage consisted of several liberation and separation processes. Specifically, waste PWBs are comminuted by multiple crushing systems; herein the metals and nonmetals are liberated. The circulating water system guarantees that the operation temperature in the crusher is maintained at a low level, avoiding hazardous emissions such as polychlorinated

biphenyls. Next, the metals are separated from the other materials through the application of a magnetic separator, an eddy current separator, an electronic separator, and three pneumatic separators. The mixed metals that remain after separation are refined through a sequence of steps that comprise heavy metal recovery, impurities leaching (leaching 1), targeted metals leaching (leaching 2), and an electrolysis processes. Lead and zinc are recovered first; the remaining mixed metals are then dissolved in sulfuric acid where impurities are removed; and the residuals are then dissolved by aqua regia. Electrolysis is used to recover the gold, silver, palladium, and copper from the liquid fraction derived from the leaching 2 process. The liquid fraction from the leaching 1 and electrolysis processes is assumed to be treated in industrial effluent plant. The residuals generated from the leaching 2 process are assumed to be discarded in a landfill.

The environmental impact of the baseline flow diagram was investigated. The metal leaching process engendered the most significant impact among the impact categories except for the category of acidification potential. This result can be attributed to the fact that the leaching process consumed significant quantities of hydrochloric acid and nitric acid, the production and consumption of which generate significant environmental loads. In contrast, the separation process had the minimum environmental impact, as the separators require relatively low amounts of power. Global warming potential was the most significant environmental impact category after normalization and weighting, followed by fossil abiotic depletion potential, and marine aquatic eco-toxicity potential. Scenario modeling results showed that variations in the power source and chemical reagents consumption had the greatest influence on the environmental impact. The environmental impact from transportation used for PWB collection was also evaluated. Results indicated that transportation distance is the most critical parameter for the collection process. The results were further compared to conventional primary metals production processes, highlighting the environmental benefit of metal recycling from waste PWBs.

There were several potential improvement strategies identified to make the recycling chain more environmentally friendly. The first strategy is to optimize the collection mode and to decrease the transportation distance, which will require a broad distribution of recycling facilities located near PWB waste sources. Relevant support should include motivational policies from government, establishment of collection stations, and education of citizens. The second strategy is to increase the liberating and separating efficiency in the beneficiation stage, so energy consumption decreases and more precious metals are recovered for the subsequent refining. The third strategy is to decrease the chemical reagent consumption in the refining stage through effective materials liberation and separation. The environmental impact would be greater if pretreatment of PWBs, i.e., the beneficiation stage, is not used to dramatically decrease the volume of the materials entering the leaching process. Not considered in this study, yet of environmental significance, are the nonmetals that are separated out during the dry pretreatment process. Because these retain most of the physical properties of resins and glass fibers, they could be reused as feedstock material, thus conserving both material and energy resources needed for primary polymer and glass production.

[1]. Mianqiang Xue, Alissa Kendall, Zhenming Xu, Julie M. Schoenung, “Waste Management of Printed Wiring Boards: A Life Cycle Assessment of the Metals Recycling Chain from Liberation through Refining,” *Environmental Science & Technology, 2015, 49 (2), pp. 940-947; doi:10.1021/es504750q.*

REWAS 2016: Towards Materials Resource Sustainability
Edited by: Randolph E. Kirchain, Bart Blanpain, Christina Meskers, Elsa Olivetti, Diran Apelian, John Howarter, Anne Kvithyld, Brajendra Mishra, Neale R. Neelameggham, and Jeff Spangenberger
TMS (The Minerals, Metals & Materials Society), 2016

UTILIZING ECONOMIC VALUE, RESOURCE AVAILABILITY, AND ENVIRONMENTAL IMPACT METRICS TO IMPROVE THE WEEE AND BATTERY DIRECTIVES AND PROMOTE ALIGNMENT WITH THE EUROPEAN COMMISSION CIRCULAR ECONOMY STRATEGY

Patrick Ford[1], Eduardo Santos[2], Paulo Ferrão[3], Fernanda Margarido[3], Krystyn J. Van Vliet[1,4], and Elsa Olivetti[1]

Departments of [1]Materials Science and Engineering and [4]Biological Engineering, Massachusetts Institute of Technology, Cambridge, MA 02139 USA; [2]3Drivers – Engenharia, Inovação e Ambiente, Lda, Lisbon, Portugal; [3]Department of Mechanical Engineering, Instituto Superior Técnico, Universidade de Lisboa, Lisbon, Portugal

Keywords: Waste Electrical and Electronic Equipment, WEEE Directive, Battery Directive, Recycling Economics, Circular Economy

Abstract

Waste electrical and electronic equipment (WEEE) provides complex challenges and unique opportunities for maximizing resource efficiency in the European Union (EU). This is due in part to the increasing volume, complexity, and value, and decreasing life cycles of such items. Current EU regulations, specifically the WEEE Directive and Battery Directive, focus on the end-of-life management of electronics and the impact of device design and material composition on environmental and human health. While these Directives are robust, the mass-based metrics on which they are focused can lead to a loss of materials that are impactful from an economic, resource availability, and environmental perspective. There is a need for increased research on the impact of these Directives on the availability of secondary raw materials and for an alignment of the WEEE Directive with the European Commission's Circular Economy Strategy. This can facilitate the development of more holistic policies based on the complete life cycle of devices and all stakeholders involved in its design, manufacturing, use, reuse, repair, and recycling.

Introduction

End-of-life waste electrical and electronic equipment (WEEE) represents one of the fastest growing waste streams in the EU, projected to increase by 3% to 5% each year [1, 2]. WEEE consists of a variety of devices, including mobile phones, computers, printers, white goods, and televisions, all of which must be responsibly managed at their end-of-life. The ten categories of WEEE are: large household appliances; small household appliances; IT and telecommunications equipment; consumer equipment and photovoltaic panels; lighting equipment; electrical and electronic tools; toys, leisure and sports equipment; medical devices; monitoring and control instruments; and automatic dispensers [3].

The materials contained within these devices include conflict minerals (gold, tantalum, tungsten, and tin), precious metals (gold, platinum, palladium, silver, and others), plastics, and glass [4]. These present a unique set of challenges and opportunities due to the potentially high value and demand of the materials, and the environmental dangers posed if managed incorrectly on a large scale [5].

All WEEE in the European Union (EU) must be handled according to two main regulations, the WEEE Directive and the Battery Directive. Each of these documents provide detailed guidelines and benchmarks geared towards increasing the mass of WEEE that is collected and recycled, while also decreasing the negative impact of potential toxins contained within the devices [3, 6]. However, the economic value, resource scarcity, and environmental impact of the materials within end-of-life electronics are not described explicitly in the directives. As a result, materials such as gold, silver, and platinum, which are more difficult to recover, but also more valuable than other metals on a per mass basis, may be lost to an outgoing waste stream [7]. Below we detail the policy objectives of the WEEE Directive and the Battery Directive, the opportunities for improving the directives through the inclusion of more robust metrics, and the research needed in order to address this gap.

EU Policies

The WEEE Directive was first established in 2003 (2002/96/EC), but was recast in 2012 as 2012/19/EU. This most recent version went into full effect in 2014. The overall goals of this directive are to minimize the mass of WEEE entering landfills each year, to protect environmental and human health, to increase the mass of commodity materials reused each year, and to hold producers responsible for the devices that they put on the market [3, 8]. More specifically, the target collection rate of end-of-life WEEE is 45% from 2016 – 2019 and 65% from 2019 going forward. The collection rates are measured by mass, and not by numbers of devices or the economic value of a given device [3]. Downstream of collection, targets are also established for the recovery and recycling of the waste materials. Recovery is defined as any operation in which waste serves "a useful purpose by replacing other materials which would otherwise have been used to fulfill a particular function." Recycling is defined as "any recovery operation by which waste materials are reprocessed into products, materials or substances whether for the original or other purposes [9]." Starting in August 2015, recovery targets range from 75% to 85% and recycling targets range from 55% to 80% depending on the category of waste in question [3]. The recycling process can vary by device and facility, but the directive mandates that printed circuit boards with surface areas greater than 10 square centimeters must be removed. However, this is only the case for "separately collected WEEE," which is defined as "collection where a waste stream is kept separately by type and nature so as to facilitate a specific treatment [9]." Although it was reported in 2008 that 65% of WEEE put on the market was collected separately, it is widely believed that much of this is still improperly handled

downstream of the collection process [3]. This can lead to large losses of the valuable materials detailed above, attributing to losses of capital and secondary resources, and negative environmental impacts.

The Battery Directive (2006/66/EC) went into effect in 2008, and mandates that all batteries be removed from devices prior to being recycled. It also requires that all member states achieve a collection rate of at least 45% by 26 September 2016. Further downstream of collection, this directive requires that recycling processes for lead-acid, nickel-cadmium, and other batteries and accumulators recover 65%, 75%, and 50% by weight, respectively [6]. These requirements have been put in place to reduce the negative environmental impacts of materials within batteries, both in use and at end-of-life [6].

Discussion

WEEE Directive Improvements. The regulations detailed above focus on two major objectives: to collect and recycle the highest percentage of end-of-life WEEE possible by mass; and to reduce the impact of the waste on environmental and human health. These goals have helped to shape electronic waste management policies for over a decade, but often lead to a loss of valuable and potentially scarce materials that would otherwise re-enter the market as secondary raw materials. This is due in large part to the processing steps, which often target the easier to access materials such as copper due to the high associated processing costs of other materials. As a result, more complex pieces such as the printed circuit boards may be lost to the waste stream [7]. Previous authors have noted the discrepancies between mass-based and value-based metrics and the impacts on the types of materials that are recovered [5]. From an economic standpoint, gold has been found to be the most important element contained in consumer electronics [5]. Therefore, even if a large percentage of the total mass of a device is recovered, the fraction that is lost can contain a high percentage of the value if gold remains in the unrecovered fraction [10].

Researchers have also studied the environmental and resource availability impacts of electronic devices and the materials of which they are comprised. Several of these studies have included an analysis of effective metrics for measuring impact on a large scale [2, 5, 11-16]. These studies are not confined to the economics of recycling, and therefore also identify and discuss critical materials such as certain rare earth elements (REE) that are oftentimes not recovered under present day policies and recovery infrastructures.

The WEEE and Battery Directives do point to the need for reducing toxins and protecting environmental health, but a more robust set of metrics that incorporate overall environmental impact in conjunction with the economic value and availability of those materials could help to strengthen the underlying goals of the directives. This could also help to lead to a cascading effect, where the directives help to inform future decision making around device design,

collection, and recycling. There are two key factors that will help to drive the success of any metric aimed at improving the WEEE or Battery Directives. The first is to utilize industry best practices to form robust and innovative metrics that not only aim at increasing recycling rates, but also evaluate and help to improve the overall system, from device design and manufacturing to its end-of-life. Secondly, the actual implementation of these potential changes would require buy in both from policymakers and the public, meaning that the inclusion of these stakeholders throughout the process would be vital to its ultimate success. Overall, there is a need for additional research on the value of the materials lost during the processing of WEEE due to the regulations as written, and the potential for reinvestment of this value back into the recovery process. In addition, it will be necessary to consider more holistic metrics, beyond only mass or value-based components, in local and national policies.

Circular Economy Strategy. An example of research that is currently underway in the EU, and is seeking to identify connections between more holistic WEEE end-of-life policies and material impacts, is the European Commission Circular Economy Strategy. In order to do this, the European Commission has carried out a series of proposals and reports aimed at analyzing the impact of the WEEE and Battery Directives, as well as other regulations on resource recovery and the European economy [17-25]. Much of this work has centered on the group's Circular Economy Strategy, which is projected to be fully laid out by the end of 2015 [25]. Among the findings listed, several relate to the connection between EU policies and the recovery of materials that can re-enter the market as secondary raw materials [23]. These reports stress the importance of considering the entire life cycle of the device when analyzing its environmental and economic impacts, and the role that metrics can play in the outcomes of implemented legislation [19, 20]. A specific example is discussed in relation to the Battery Directive, where mass-based targets that do not differentiate between chemical compositions can lead to the loss of lighter batteries that may contain more valuable, but difficult to recover materials [19]. In addition, a separate analysis of mobile phones stressed the importance of connecting market forces with appropriate policies in order to ensure that devices can be repaired, reused, and recycled as effectively as possible [24]. Lastly, progress towards the implementation of the Circular Economy in the EU has been aided by the WEEE and Battery Directives, but a focus on resource efficiency is needed in order to catalyze system-wide improvements in device design, manufacturing, use, and recycling [21, 22].

Conclusions

The current framing and implementation of the WEEE and Battery Directives guide EU WEEE policies, but the present focus on mass-based metrics do not sufficiently target specific materials of importance. There are several steps that could be taken to increase the recovery of targeted materials, while continuing to carry out the present day objectives of lawmakers in the EU and the Circular Economy Strategy. Therefore, we offer the following two recommendations: (1) to

better align the WEEE Directive and Battery Directive with the European Commission Strategy on the Circular Economy; and (2) to increase research on the impacts of the WEEE Directive on the availability of secondary materials resources, the profits generated from recycled goods, and the environmental impact of key materials. Aligning the WEEE and Battery Directives with the Circular Economy Strategy could allow for newly designed targets that focus on specific materials that can be cycled from end-of-life devices back to the secondary raw materials market. Lastly, increased research on materials availability, and economic and environmental impacts would aid more informed policy decisions about the metrics used in the directives, and the devices that should be analyzed in most detail.

References

1. Cucchiella, F., et al., *Recycling of WEEEs: An economic assessment of present and future e-waste streams.* Renewable and Sustainable Energy Reviews, 2015. **51**: p. 263-272.

2. Georgiadis, P. and M. Besiou, *Environmental and economical sustainability of WEEE closed-loop supply chains with recycling: a system dynamics analysis.* International Journal of Advanced Manufacturing Technology, 2010. **47**(5): p. 475-493.

3. *Directive 2012/19/EU Of The European Parliament And Of The Council of 4 July 2012 on waste electrical and electronic equipment (WEEE)*. 2012, European Union: European Union. p. 1-34.

4. Fitzpatrick, C., et al., *Conflict Minerals in the Compute Sector: Estimating Extent of Tin, Tantalum, Tungsten, and Gold Use in ICT Products.* Environmental Science & Technology, 2015. **49**(2): p. 974-981.

5. Chancerel, P., et al., *Estimating the quantities of critical metals embedded in ICT and consumer equipment.* Resources, Conservation & Recycling, 2015. **98**: p. 9-18.

6. *Directive 2006/66/EC Of The European Parliament And Of The Council of 6 September 2006 on batteries and accumulators and waste batteries and accumulators and repealing Directive 91/157/EEC*, E. Council, Editor. 2006, European Union. p. 14.

7. Chancerel, P., et al., *Assessment of Precious Metal Flows During Preprocessing of Waste Electrical and Electronic Equipment.* Journal of Industrial Ecology, 2009. **13**(5): p. 791-810.

8. *Impact Assessment of the Recast Directive 2012/19/EU on Waste Electrical and Electronic Equipment (WEEE)*. 2013, Department for Business, Innovation and Skills (BIS): United Kingdom.

9. *Directive 2008/98/EC Of The European Parliament And Of The Council of 19 November 2008 on waste and repealing certain Directives*. 2008, European Commission: European Union. p. 1-28.

10. Hageluken, C. *Improving metal returns and eco-efficiency in electronics recycling - a holistic approach for interface optimisation between pre-processing and integrated metals smelting and refining*. in *Proceedings of the 2006 IEEE International Symposium on Electronics and the Environment (IEEE Cat. No. 06CH37796)*. 2006. Place of Publication: Piscataway, NJ, USA; Scottsdale, AZ, USA. Country of Publication: USA.: IEEE.

11. Nicolli, F., N. Johnstone, and P. Söderholm, *Resolving failures in recycling markets: the role of technological innovation.* Environmental Economics & Policy Studies, 2012. **14**(3): p. 261-288.

12. Geyer, R. and V.D. Blass, *The economics of cell phone reuse and recycling.* International Journal of Advanced Manufacturing Technology, 2010. **47**(5-8): p. 515-525.

13. Olivetti, E., F. Field, and R. Kirchain, *Understanding dynamic availability risk of critical materials: The role and evolution of market analysis and modeling.* MRS Energy & Sustainability - A Review Journal, 2015. **2**: p. 1-16.

14. Alonso, E., *Material scarcity from the perspective of manufacturing firms : case studies of platinum and cobalt*. 2010: c2010.

15. Bauer, D., et al., *U.S. Department of Energy Critical Materials Strategy*, D.o. Energy, Editor. 2011, U.S. Department of Energy Office of Policy and International Affairs (PI). p. 196.

16. Atlee, J. and R. Kirchain, *Operational Sustainability Metrics Assessing Metric Effectiveness in the Context of Electronics-Recycling Systems.* Environmental Science & Technology, 2006. **40**(14): p. 4506-4513.

17. *Commission Staff Working Document Impact Assessment Accompanying the document Proposal for reviewing the European waste management targets*. 2014, European Commission: Brussels, Belgium. p. 1-128.

18. *Proposal for a Directive Of The European Parliament And Of The Council amending Directives 2008/98/EC on waste, 94/62/EC on packaging and packaging waste, 1999/31/EC on the landfill of waste, 2000/53/EC on end-of-life vehicles, 2006/66/EC on batteries and accumulators and waste batteries and accumulators, and 2012/19/EU on waste electrical and electronic equipment*. 2014, European Commission: Brussels, Belgium. p. 1-32.

19. *Ex-Post Evaluation of Five Waste Stream Directives*. 2014, European Commission: Brussels, Belgium. p. 1-89.

20. *Progress Report on the Roadmap to a Resource Efficient Europe*. 2014, European Commission: Brussels, Belgium. p. 1-19.

21. *Communication From The Commission To The European Parliament, The Council, The European Economic And Social Committee And The Committee Of The Regions Towards a*

circular economy: A zero waste programme for Europe. 2014, European Commission: Brussels, Belgium. p. 1-14.

22. *Annex To The Communication From The Commission To The European Parliament, The Council, The European Economic And Social Committee And The Committee Of The Regions Towards a circular economy: A zero waste programme for Europe*. 2014, European Commission: Brussels, Belgium. p. 1-3.

23. *Analysis of an EU target for Resource Productivity*. 2014, European Commission: Brussels, Belgium. p. 1-30.

24. Vanner, R., et al., *Scoping study to identify potential circular economy actions, priority sectors, material flows and value chains*. 2014, European Union: Luxembourg. p. 1-321.

25. *Roadmap - Circular Economy Strategy*. 2015, European Commission: European Union. p. 1-9.

REWAS 2016: Towards Materials Resource Sustainability
Edited by: Randolph E. Kirchain, Bart Blanpain, Christina Meskers, Elsa Olivetti, Diran Apelian, John Howarter, Anne Kvithyld, Brajendra Mishra, Neale R. Neelameggham, and Jeff Spangenberger
TMS (The Minerals, Metals & Materials Society), 2016

HIGH TEMPERATURE CHARACTERISATION AND TECHNO-ECONOMICS OF E-WASTE PROCESSING

Michael A Somerville[1] and Paul Kolton[1]

CSIRO Mineral Resources
Private Bag 10, Clayton South, Victoria, 3169, Australia

Keywords: e-waste, high temperature, Melbourne, value recovery, characterisation

Abstract

The elemental composition of selected e-waste materials has been determined through fusion in a metal and slag bath. During this process the elemental components of the inhomogeneous pulverized material distributed to the copper, slag and fume process streams. Through the analysis and mass of these streams the composition of the original e-waste was calculated.

This characterization information was used as the basis of a techno-economic study of the collection and processing of e-wastes in the Melbourne (Australia) metropolitan area. Four consumer electronic items were considered in the study and included: mobile phones, DVD players, televisions and personal computers. In this, the first part of the study, the value contained in these representative items of e-waste was calculated based on the composition, the e-waste disposal rate, the population of the Melbourne region, and the proportion of PCB's to the total mass of the consumer item.

The results showed that the total contained value of elements in the e-waste disposed in the Melbourne region was $19.8 million/year. The consumer item which had the largest contribution was to the total was personal computers at about $9.8 million/year. Most of the value contained in the e-waste is associated with precious metals ($9.0 million/year) and with transition elements ($8.8 million/year).

Introduction

In recent years the recycling of and value recovery from waste electric and electronic materials (e-waste) has gained much attention. This has been driven through the twin goals of limiting waste disposal in landfill and recovering valuable precious and base metals. E-waste is a valuable resource and the concentration of precious and base metals in most kinds of e-waste are higher than in most primary ore deposits. At present there is no process in Australia to extract the value contained in e-wastes and these materials are shipped overseas for processing. The collection, handling and processing of e-waste materials to recover the contained value is not without cost. This project attempts to determine if the dollar value of elements contained in four samples of typical e-waste materials will cover the required collection, handling transport and processing costs. The first part of the project is reported here and covers the calculation of contained value of elements contained in e-waste which could be recovered from disposed consumer electrical equipment from the Melbourne (Australia) metropolitan region per year.

E-waste characterisation

The printed circuit boards (PCB) of typical e-waste materials have been analysed using a high temperature fusion process to determine their elemental composition.

The four e-waste materials considered in this study were sourced from common consumer electronic items and include: mobile phone (MP), television (TV), DVD player (DVD) and personal computer (PC). The printed circuit boards from these items were removed and pulverized in a large ring mill and then sized at two mm to remove large pieces of plastic, metal casings plugs etc. The -2mm fraction was used in the characterisation studies. One hundred gram aliquots were prepared by riffling the pulverized and sized raw e-waste materials.

The e-waste was fused in a molten bath of 98.5 % copper and a conventional fayalite type slag used in copper smelting. The experiments were performed in porcelain crucibles which were heated by electro-magnetic induction. Characterisation experiments were conducted by melting 100 or 25 g of pulverized e-waste along with 400 g of copper and 400 g of slag. The crucible and contents were heated to 1250 °C, over 4 hours under a protective blanket of nitrogen gas. When the experimental temperature was reached samples of the copper was collected using a suction bulb connected to a silica tube. The slag was sampled using a steel dip rod. Following the collection of samples the furnace was turned off and the crucible contents cooled under a flowing nitrogen stream. When cool the crucible was removed from the furnace and the slag and copper recovered, weighed. Fume which was collected in a baghouse was also recovered, weighed and analysed along with the copper and slag samples.

Major components of the copper and fume samples were determined using conventional acid digestion and ICP-OES analysis. Major components of the slag samples were determined using XRF analysis of fused glass disks. Minor and trace elements of the slag, copper and fume samples were determined using ICP-MS analytical techniques. Samples of the original slag and copper were also analysed to determine background compositions of the elements of interest.

The amount of major, minor and trace elements of the pulverized e-waste was determined by first calculating the amount in the final copper, slag and fume products. The background amounts from the original materials was then subtracted. Finally the net amount of elements was divided by the amount of original e-waste used in the fusion experiment to obtain the fraction of each element in the pulverized e-waste.

Table 1 shows the mass of the raw materials used in the fusion experiments and the output masses. The input materials included: anode copper, slag and e-waste. Output materials included: slag, copper and fume. The recovery of masses to the output streams was 106%, 93%, 99% and 98 % for Test EW-1, EW-2, EW-3 and EW-4 respectively.

Table 1: Masses of input and output materials used in the four fusion experiments

Test No.	E-waste type	Input masses (g)			Output masses (g)		
		Anode copper	Slag	E-waste	Slag	Copper	Fume
EW-1	MP	400	400	25	507	363	1
EW-2	DVD	400	400	100	330	498	5
EW-3	TV	400	400	100	391	491	7
EW-4	PC	400	400	100	425	454	6

Table 2 shows the calculated concentration of the major components of pulverised e-waste in Wt. %. Table 3 shows the concentration of minor and trace components of the pulverised e-waste materials in ppm.

Table 2: Concentration of major components in different e-waste materials (Wt %)

Element	MP	DVD	TV	PC
Bi	0.00	0.06	0.03	0.03
Mn	0.27	2.13	2.12	0.16
Ni	6.25	0.22	0.25	1.11
Sn	2.49	3.96	3.95	6.47
Cu	60	50	55	62
Pb	3	2.38	0.56	4.47
Sb	0.18	0.11	0.18	0.39
Zn	5.03	4.99	3.86	1.56
As	0.49	0.06	0.12	0.05

Table 3: Concentration of minor and trace elements in different e-waste materials (ppm)

Element	MP	DVD	TV	PC
Ag	1705	409	389.2	468.4
Au	97	1	1.7	106.9
Ga	179	21	30.5	16.9
Hf	45	4	12.2	2.6
In	95	115	123.6	189.5
Li	144	9	47.3	64.0
Nb	201	29	222.1	190.0
Nd	3585	28	26.4	400.8
Pd	43	1	3.4	92.0
Sr	1989	217	228.9	232.4
V	266	94	62.4	113.2

E-waste materials in Melbourne

In this study the four categories of consumer electronics were assumed to represent the majority of e-waste materials. The average mass of each unit and the mass of the PCB's within the units was estimated based on data from the US EPA and from a number of sample weights from a range of model sizes [1]. Table 4 shows the average mass of units in each category, proportion of PCB's to the total mass and the mass of the PCB's in each category.

Table 4: Mass of PCB's in each consumer electronic category.

Category	Average mass of complete unit (kg)	Contribution of PCB to mass (%)	Mass of PCB (kg)
PC	5.5	23	1.3
TV	25.2	21	5.3
MP	0.2	50	0.1
DVD	7.9	20	1.6

The number of units of consumer electronics disposed of in Australia was estimated from Australian and USA data [1, 2]. The number of units disposed in the Melbourne metropolitan area was based on the Melbourne population as a proportion of the Australian population which is about 19 % [3]. The rate of consumer electronic recycle was estimated to be 60 % per year based on current and projected rates of consumer electronic recycle in Australia, [4]. Table 5 shows the estimated generation of PCB's for the four e-waste categories from the Melbourne area.

Table 5: Mass of PCB's from each consumer electronic category disposed from the Melbourne region per year.

Category	Number of units disposed in Australia (10^6)	Number of units disposed in Melbourne (10^6)	Mass of PCB's (kg)	Mass of PCB's disposed (T/y)
PC	4	0.76	1.3	570
TV	1.5	0.23	5.3	904
MP	14	2.66	0.1	159
DVD	3	0.57	1.6	540

Value of e-wastes

The value of e-waste material which could be collected from the Melbourne region per year, can be calculated from the composition of the pulverised PCB's (Tables 2 and 3), the value of the element [5], and the amount of disposed PCB's for each categories (Table 5). This information, is shown in Tables 6 and summarised in the different element groups in Table 7. The element groupings include: precious elements (Ag, Au, Pd), transition metals (Mn, Ni, Cu, Zn, V, Sr), heavy metals (Bi, Sn, Pb, Sb, Nb) and rare earth elements (Nd).

Table 6 shows that the e-waste category with the biggest contained value is PC at $9.7 million/year. The lowest value is contained in the DVD at $2.6 million/year. The total value of the elements contained in the e-waste was about $19.8 million/year. Table 7 shows that most of the value of the e-waste is contained in the precious elements and the transition elements, at $9 and $8.8 million/year respectively. There is much less value contained in the heavy elements and non-metals. The rare earth elements is represented by a single element (neodymium). This elements category probably requires further analysis.

Table 6: Value of elements contained in waste consumer electronic items from the Melbourne area.

Element	element value ($/kg)	Contained value ($/year)			
		MP	DVD	TV	PC
Bi	18.7	0	6,059	5,071	3,198
Mn	1.5	644	17,253	28,747	1,368
Ni	25	248,438	29,700	56,500	158,175
Sn	15	59,387	320,760	535,620	553,185
Cu	6	572,400	1,620,000	2,983,200	2,120,400
Pb	3	14,310	38,556	15,187	76,437
Sb	6	1,717	3,564	9,763	13,338
Zn	3	23,993	80,838	104,683	26,676
As	1.43	1,114	463	1,551	408
Ag	1,022	277,059	22,5719	359,577	272,862
Au	53,000	817,419	28,620	81,450	3,229,449
Ga	525	14,942	5,954	14,475	5,057
Hf	1,200	8,586	2,592	13,235	1,778
In	590	8,912	36,639	65,923	63,729
Li	270	6,182	1,312	11,545	9,850
Nb	180	5,753	2,819	36,140	19,.494
Nd	20	11,400	302	477	4,569
Pd	58,330	398,802	31,498	17,283	3,058,825
Sr	1,000	316,251	117,180	206,926	132,468
V	14.3	605	726	807	923
total		2,787,913	2,570,554	4,710,162	9,752,188

Table 7: Value contained in waste consumer electronic items from the Melbourne region, by element group.

Element group	Value in PCB's from consumer electronic categories ($/year)				
	MP	DVD	TV	PC	Total
Precious elements	1,493,280	285,837	620,311	6,561,136	8,960,564
Transition elements	1,162,330	1,865697	3,380,863	2,440,010	8,848,900
Heavy metals	81,166	371,758	601,782	665,652	1,720,358
Non metals	39,736	46,960	106,729	80,822	274,247
Rare earth element	11,400	302	477	4,569	16,749

Conclusions

The results showed that the contained value of elements in the e-waste was $19.8 million/y. The consumer item which had the largest contribution was to the total was personal computers at about $9.8 million/y. Most of the value contained in the e-waste is associated with precious metals ($9.0 million/y) or with transition elements ($8.8 million/y).

Future work

Melbourne, Australia is a large city of 4.4 million people spread over a geographical area of nearly 10,000 km^2. The relatively low population density of this city provides particular difficulties in the economical collection of waste materials such as e-wastes. Options for e-waste collection and processing include a municipal collection system or a consumer deposit system or combination. Options for processing the e-wastes and extracting the contained value include a greenfield facility close to Melbourne or processing at the nearest primary base metal smelter at Port Pirie which is 1000 km distant. The second part of this project will attempt to estimate the costs of e-waste collection, handling and transport and the costs of extracting contained value using the two main scenarios.

The project will also consider other processing issues of how the different elements can be separated and extracted. This is performed in other parts of the world with higher population density, e,g, Europe, North America and east Asia. However establishing the financial feasibility of a similar facility in Australia has particular difficulties.

References

1. US EPA, 2011, Electronics waste management in the United States through 2009, report 530-R-11-002, May 2011, 'http://nepis.epa.gov/Exe/ZyPURL.cgi?Dockey=P100BKKL.txt'.

2. J. Angel, Tipping point: Australia's e-waste crisis, Report http://www.tec.org.au/recent-tec-reports (2008)

3. ABS 2012, Australian bureau of statistics, Population by age and sex, regions of Australia, http://www.abs.gov.au/ausstats/abs@.nsf/Products/3235.0~2012~Main+Features~Main+Features?OpenDocument#PARALINK0

4. ABS 2013, Australian bureau of statistics, Waste account Australia, Experimental estimates, http://www.abs.gov.au/ausstats/abs@.nsf/Products/4602.0.55.005~2013~Main+Features~Electronic+and+Electrical+Waste?OpenDocument

5. Value of elements, 'https://en.wikipedia/wiki/prices of elements and their compounds'

REWAS 2016: Towards Materials Resource Sustainability
Edited by: Randolph E. Kirchain, Bart Blanpain, Christina Meskers, Elsa Olivetti, Diran Apelian, John Howarter, Anne Kvithyld, Brajendra Mishra, Neale R. Neelameggham, and Jeff Spangenberger
TMS (The Minerals, Metals & Materials Society), 2016

ENABLING ENERGY EFFICIENT ELECTRONICS THROUGH THERMALLY CONDUCTIVE PLASTIC COMPOSITES: NOVEL SURFACE MODIFICATION TECHNIQUES FOR BORON NITRIDE IN EPOXY

Alex N. Bruce[1], Holly Avins[1], Inez Hua[2,3], John A. Howarter[1,3]

[1]Materials Sci & Engr, Purdue University, 701 W Stadium Ave, West Lafayette, IN 47901, USA
[2]Lyles School of Civil Engr, Purdue Univ, 550 W Stadium Ave, West Lafayette, IN 47901, USA
[3]Environmental & Ecological Engr, Purdue Univ, 500 Central Dr, West Lafayette, IN 47901, USA

Keywords: high thermal conductivity, dielectric, polymer composite, boron nitride, polydopamine

Abstract

Thermal management is an ongoing concern in electronics largely because of the challenging specifications of the substrate materials. Substrates *must* be electrically insulating so as to not interfere with devices or circuits, and so historically have had very poor thermal conductivity. These low thermal conductivity substrates cause heat to build up around devices, raising the local operating temperature and decreasing energy efficiency and device lifetime.

This work focuses on creating thermally conductive, electrically insulating epoxy/boron nitride composites. Past work has been limited by the necessity of very high loading levels of BN required to achieve acceptable thermal conductivities (>5W/mK).

1. Introduction

Polymer composites are used in a diverse set of applications such as aerospace, electronics, and packaging due to their ease of manufacturing, low cost, and highly tunable range of properties. In the electronics field, there is a large demand for polymer composites with high electrical resistivity and good thermal conductivity for use as substrates for passive thermal management. These are commonly known as high thermal conductivity dielectric polymer composites and are desired in application such as printed circuit boards and LEDs[1]. These composites would be used to conduct heat output from devices away from the lights and devices on the substrate, increasing device efficiency and lifetime[2].

The most electrically resistive, thermally conductive homogenous materials are generally very hard ceramic materials, making them very difficult or expensive to process into useable forms for electronic substrates[3]. Using these materials as fillers in polymer composites is a logical next step because of the ease of polymer processing and the good electrical resistivity and dielectric properties of many polymers. The field of high thermal conductivity dielectric polymer composites has largely focused on a few target fillers: aluminum oxide, silicon dioxide, aluminum nitride, and boron nitride[4–14]. This is due to many factors including thermal conductivity, dielectric constant, and cost. Hexagonal boron nitride (h-BN) is the most commonly studied form as a filler material

because of the platelets' high aspect ratio character and relative softness when compared to zincblende boron nitride. In addition to this, boron nitride does not readily absorb water, making it attractive in applications such as printed circuit boards where water can interfere with device functions.

Other properties besides filler type have been intensively studied, including filler morphology, size, surface modification, and optimum mixtures of all of these factors[11,15,16]. In general, mixtures of sizes of high aspect ratio particles has been shown to achieve the highest possible thermal conductivity while surface modification has had less effect. This seems to be due to the fact that high aspect ratio fillers are more likely to form a connected, percolated network inside the matrix than low aspect ratio fillers at comparable volumetric loading levels[17]. Surface modification has not been shown to have as large of an effect on thermal conductivity as filler size or morphology, and studies have varied on the efficacy of various types of surface treatments showing slight or no improvement in thermal conductivity of the composite after treating the surface of the filler material. This is particularly pronounced in the case of boron nitride due to the lack of functional groups on the surface, preventing easy attachment of other molecules. Unlike carbon, boron nitride has few intrinsic defects and is stable when exposed to heat and water. The only native defects are on the edges of the h-BN plates, consisting of hydroxyls and primary and secondary amine groups. Recently, a new surface modification technique has emerged utilizing a non-covalent strategy. Dopamine (Fig. 1) has been shown to attach to the surface of boron nitride, the method proposed being a relatively strong pi-pi interaction between the dopamine and boron nitride rings followed by subsequent polymerization of the dopamine on the surface[18–20].

This works focuses on surface modification of larger boron nitride particles than previously reported for thermal conductivity enhancement in an epoxy matrix for use as a printed circuit board material.

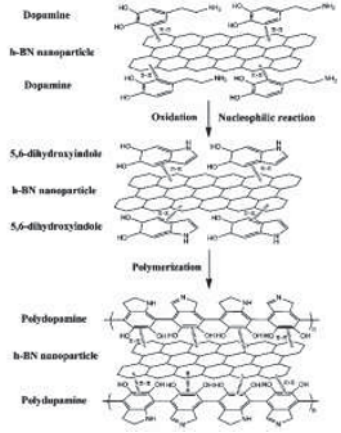

Fig. 1, from [21], a proposed mechanism for non-covalent attachment of polydopamine to boron nitride.

2. Experimental methods

2.1 Materials

Nanopure purified deionized water (DI water) with a resistivity of 18.3 μΩ(cm) was used. Hexagonal boron nitride (h-BN) powders with an nominal average particle size of 1.5μm from MK Impex/Lower Friction (Mississauga, Ontario, Canada) were used. Dopamine hydrochloride (DOPA), 2-amino-2-(hydroxymethyl)-1,3-propanediol (Trizma® base), paraffin wax with a melting point range from 53-57°C (ASTM D 87), and and triethylenetetramine were used from Sigma Aldrich (St. Louis, Missouri, USA). HCl, chloroform. Epoxy resin EPON 825, high purity bisphenol A epichlorohydrin with an epoxide equivalent weight of 175-180g/eq was used from Hexion (Columbus, Ohio, USA).

2.2 h-BN particle surface functionalization

To homogenously modify h-BN with polydopamine, a buffer solution of 10mM Tris was made by adding 0.606g Trizma base to 500ml dionized water. Diluted HCl was added until pH reached 8.5, then 1g of dopamine hydrochloride was dissolved into the solution. When the solution became dark brown in color, 10g of h-BN was added and the solution was bath sonicated for 1.5hr while periodically being removed and shaken to prevent sedimentation of the particles. The solution was then set in an oil bath at 60°C with a magnetic stirrer for four days. The particles were then washed and centrifuged several times until the supernatant appeared clear, generally taking four wash (diluted 100% with DI water) and centrifuge (5000 rpm for 60min) steps. After drying in an oven, the particles were ball milled for one day on a rotary ball mill and sieved through a 325 mesh size (nominally 45μm) sieve. The particles were then dried in a vacuum oven at 110°C overnight and stored in sealed chamber with desiccant until further characterization or use.

2.3 Characterization techniques

An Accupyc 1330 (Micromeritics, Norcross, Georgia, USA) helium pycnometer was used to characterize density. A Q50 thermogravimetric analysis (TGA) (TA Instruments, New Castle, Delaware, USA) was used with a testing procedure as follows: heating the sample to 30°C and holding for ten minutes followed by heating to 900°C at a rate of 10°C/min. An XL40 (FEI, Hillsboro, Oregon, USA) scanning electron microscope (SEM) was used to image particles at an accelerating voltage of 10keV, a spot size of 3, and a working distance of 15.1mm. A TriStar3000 surface area analyzer (Micromeritics, Norcross, Georgia, USA) was used to determine surface area of powder samples after degassing overnight at 150°C.

3. Results & Discussion

Fig. 2, h-BN powders before (left) and after (right) surface modification

Surface modification of the h-BN powder was observed as a visible color change from bright white to a dark gray (Fig. 2) as well as a mass loss difference of 1.3% at 800°C compared to unmodified h-BN. Powder morphology and surface area remained relatively unchanged after surface modification as seen in Fig. 3 and Table 1.

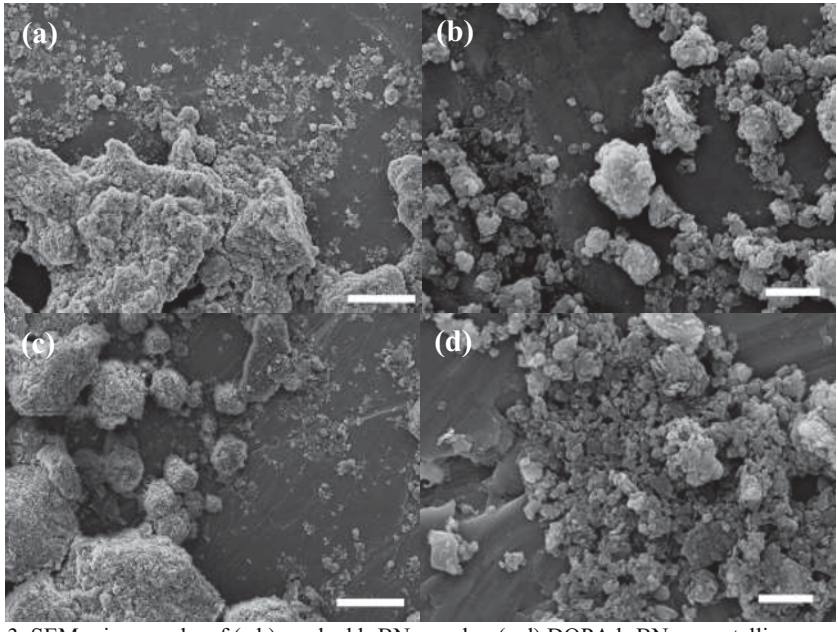

Fig. 3, SEM micrographs of (a,b) washed h-BN powder, (c,d) DOPA h-BN on metallic substrates. Scale bars are (a,c) 20µm and (b,d) 2µm.

Table I, surface area, density, and mass loss at 900°C for h-BN and polydopamine modified h-BN

Powder	Surface area (m^2/g)	Density (g/cm^3)	Mass change at 800°C in air (%)	Surface coverage (g/m^2)*
h-BN (washed)	28.0	2.23	+0.23%	-
DOPA h-BN	24.7	2.29	-1.1%	0.05

*Calculated from measured DOPA h-BN mass loss plus the h-BN mass gain at 800°C

4. Conclusions

Hexagonal boron nitride particles were successfully modified with polydopamine through a surface functionalization technique which has previously been applied to nanoparticles. This work has shown that a TGA measureable mass of polydopamine has been attached to the surface of particles in a size range of 1.5 to 45µm. This size range of particle is promising for the application of increasing thermal conductivity in polymer composites as nano-fillers have not been shown to be effective. Further work on incorporating these particles into an epoxy matrix and studying the thermal conductivity of different filler levels is needed to confirm this hypothesis.

5. References

1. Huang, X., Jiang, P. & Tanaka, T. A review of dielectric polymer composites with high thermal conductivity. *IEEE Electr. Insul. Mag.* (2011).

2. Yung, K. C., Liem, H. & Choy, H. S. Heat dissipation performance of a high-brightness LED package assembly using high-thermal conductivity filler. *Appl. Opt.* **52,** 8484–93 (2013).

3. Kasap, S. *Principles of electronic materials and devices*. (2006).

4. Xu, Y., Chung, D. D. . & Mroz, C. Thermally conducting aluminum nitride polymer-matrix composites. *Compos. Part A Appl. Sci. Manuf.* **32,** 1749–1757 (2001).

5. Fang, L. *et al.* Nano–micro structure of functionalized boron nitride and aluminum oxide for epoxy composites with enhanced thermal conductivity and breakdown strength. *RSC Adv.* **4,** 21010 (2014).

6. Xu, Y. & Chung, D. D. L. Increasing the thermal conductivity of boron nitride and aluminum nitride particle epoxy-matrix composites by particle surface treatments. *Compos. Interfaces* **7,** 243–256 (2000).

7. Hong, J.-P. *et al.* High thermal conductivity epoxy composites with bimodal distribution of aluminum nitride and boron nitride fillers. *Thermochim. Acta* **537,** 70–75 (2012).

8. Kochetov, R. *et al.* Preparation and dielectric properties of epoxy - BN and epoxy - AlN nanocomposites. *2009 IEEE Electr. Insul. Conf. EIC 2009* 397–400 (2009). doi:10.1109/EIC.2009.5166378

9. Kim, K. & Kim, J. Fabrication of thermally conductive composite with surface modified boron nitride by epoxy wetting method. *Ceram. Int.* **40,** 5181–5189 (2014).

10. Hong, J. *et al.* Interphase control of boron nitride / epoxy composites for high thermal conductivity. **22,** 259–264 (2010).

11. Kemaloglu, S., Ozkoc, G. & Aytac, A. Thermally conductive boron nitride/SEBS/EVA ternary composites:'processing and characterization'. *Polym. Compos.* (2010). doi:10.1002/pc

12. Huang, X. *et al.* Thermal conductivity and dielectric properties of epoxy composites with hyperbranched polymer modified boron nitride nanoplatelets. *2012 IEEE Int. Conf. Cond. Monit. Diagnosis* 1089–1092 (2012). doi:10.1109/CMD.2012.6416347

13. Wattanakul, K., Manuspiya, H. & Yanumet, N. The adsorption of cationic surfactants on BN surface: Its effects on the thermal conductivity and mechanical properties of BN-epoxy composite. *Colloids Surfaces A Physicochem. Eng. Asp.* **369,** 203–210 (2010).

14. Kozako, M., Okazaki, Y., Hikita, M. & Tanaka, T. Preparation and evaluation of epoxy composite insulating materials toward high thermal conductivity. *2010 10th IEEE Int. Conf. Solid Dielectr.* 1–4 (2010). doi:10.1109/ICSD.2010.5568250

15. Wattanakul, K., Manuspiya, H. & Yanumet, N. Thermal conductivity and mechanical properties of BN-filled epoxy composite: effects of filler content, mixing conditions, and BN agglomerate size. *J. Compos. Mater.* **45,** 1967–1980 (2011).

16. Yung, K. C. & Liem, H. Enhanced Thermal Conductivity of Boron Nitride Epoxy-Matrix Composite Through Multi-Modal Particle Size Mixing. *J. Appl. Polym. Sci.* **106,** 3587–3591 (2007).

17. Nejad, S. A review on modeling of the thermal conductivity of polymeric nanocomposites. *E-Polymers* 1–38 (2012). at

18. Roy, A. K., Park, B., Lee, K. S., Park, S. Y. & In, I. Boron nitride nanosheets decorated with silver nanoparticles through mussel-inspired chemistry of dopamine. *Nanotechnology* **25,** 445603 (2014).

19. Thakur, V. K. *et al.* Novel polymer nanocomposites from bioinspired green aqueous functionalization of BNNTs. *Polym. Chem.* **3,** 962 (2012).

20. Shen, H., Guo, J., Wang, H., Zhao, N. & Xu, J. Bio-inspired Modification of h-BN for High Thermal Conductive Composite Films with Aligned Structure. *ACS Appl. Mater. Interfaces* 150224074733007 (2015). doi:10.1021/am507416y

21. Wu, H. & Kessler, M. R. Multifunctional Cyanate Ester Nanocomposites Reinforced by Hexagonal Boron Nitride after Noncovalent Biomimetic Functionalization. *ACS Appl. Mater. Interfaces* **7,** 5915–5926 (2015).

REWAS 2016: Towards Materials Resource Sustainability
Edited by: Randolph E. Kirchain, Bart Blanpain, Christina Meskers, Elsa Olivetti, Diran Apelian, John Howarter, Anne Kvithyld, Brajendra Mishra, Neale R. Neelameggham, and Jeff Spangenberger
TMS (The Minerals, Metals & Materials Society), 2016

Environmental and economic evaluation of cathode ray tube (CRT) funnel glass waste management options in the United States

Qingbo Xu [1,2,3], Mengjing Yu [3], Alissa Kendall [4], Wenzhi He [1,2], Guangming Li [1,2], Julie M. Schoenung [3]

[1] College of Environmental Science and Engineering, Tongji University, Shanghai 200092, China
[2] State Key Laboratory of Pollution Control and Resource Reuse, Tongji University, Shanghai 200092, China
[3] Department of Chemical Engineering and Materials Science, University of California, Davis, CA 95616, USA
[4] Department of Civil and Environmental Engineering, University of California, Davis, CA 95616, USA

Keywords: Cathode Ray Tubes, Recycling, Life Cycle Assessment

Electronic waste (e-waste) contains a wide variety of heavy metals that are detrimental to human and environmental health if they are not disposed of properly. Cathode ray tube (CRT) funnel glass is an important component of the growing volume of end-of-life CRT television and computer monitor waste. CRT glass contains 14-23% of lead (Pb) by weight, which is necessary for protecting monitor users from the cathode ray radiation and for connecting various glass pieces together. However, the large amount of lead contained in the CRT funnel glass creates a serious problem when the CRT glass products reach their end-of-life because lead can escape into the environment and cause severe damage to humans and the environment. Small amounts of lead exposure can result in adverse central nervous system damage that leads to headaches, behavior problems, reproductive issues, and cognitive deficits in children. Despite these well-known health effects, CRT funnel glass still faces improper disposal fates. In recent years, various researchers have investigated the environmental or economic impacts related to CRT glass recycling. These investigations have focused on the collection, dismantling, and materials recovery of various CRT glass recycling processes. Despite these previous investigations, a systematic evaluation of the economic and environmental attributes of various waste management options for CRT funnel glass specifically, especially at the detailed process level, does not exist. In this paper, environmental impacts and economic feasibility of four currently available and one novel CRT funnel glass waste management options are compared and discussed [1].

Five waste management options were evaluated from environmental and economic standpoints: hazardous waste landfill, municipal waste landfill, pyrometallurgy, closed-loop recycling, and hydrometallurgy. Two life-cycle assessment (LCA) methodologies: CML2001 and Eco-Indicator 99, were utilized. With CML2001 the following impact categories were considered: (1) depletion of abiotic resources (abiotic depletion potential,

ADP), (2) acidification (acidification potential, AP), (3) eutrophication (eutrophication potential, EP), (4–6) eco-toxicity (marine aquatic, freshwater aquatic and terrestrial eco-toxicity potential; MAETP infinite, FAETP infinite and TETP infinite, respectively), (7) climate change (global warming potential, GWP 100 years), (8) human toxicity (human toxicity potential, HTP infinite), (9) stratospheric ozone depletion (ozone layer depletion potential, ODP steady state) and (10) photo-oxidant formation (photochemical ozone creation potential, POCP). With Eco-Indicator 99, human health, ecosystem and resources depletion impacts were analyzed. Life-cycle assessment is conducted using GaBi 4. Economic feasibility was analyzed using technical cost modeling (TCM). Overall costs for each waste management option consisted of two categories: variable costs and fixed costs. Variable costs included labor, utilities and material costs. Fixed costs included equipment and facility costs. Transportation costs were investigated separately due to variations in transportation distances. Revenues derived from fees charged to customers and sales from recovered materials were considered.

LCA results showed that all five CRT funnel glass waste management options contribute to greenhouse gas emissions because of the need to transport CRT funnel glass to disposal and recycling sites. Sensitivity analysis results highlighted that transportation distances for the three recycling options need to be reduced by approximately 75% for these effects to become negligible. LCA results also show that landfill options have harmful impacts on human health while the recycling options reduce human health impacts. Sensitivity analysis showed that the HTP inf. value for the pyrometallurgy and landfill options exhibit higher sensitivity to key process parameters because of the potential for lead emissions. TCM analysis showed that the transportation cost accounts for approximately 26-45% of the overall waste management cost. The recycling options are more profitable than the landfill options. Sensitivity analysis showed that closed-loop recycling and pyrometallurgy options are more sensitive to changes in transportation distance than the hydrometallurgy option. However, closed-loop recycling and pyrometallurgy options remain profitable across the spectrum of -75% to +75% variations in baseline distance, while hydrometallurgy is no longer profitable after transportation distance increases to more than 75% of the baseline. Overall, landfill options are the least environmentally friendly and least profitable options. Closed-loop recycling is the best option in countries where CRT glass still has a market, but it is not a feasible option for U.S. recyclers. Both environmental and economic evaluation showed that transportation has a large impact on the sustainability and profitability of the CRT funnel glass waste management options. Overall, pyrometallurgy and hydrometallurgy are the most feasible recycling options to implement in the United States. While pyrometallurgy appears to be more sustainable and economical, hydrometallurgy has more opportunities for improvements in process sustainability and for use on-site further improving sustainability and profitability.

[1]. Qingbo Xu, Mengjing Yu, Alissa Kendall, Wenzhi He, Guangming Li, Julie M. Schoenung, “Environmental Life Cycle and Economic Assessment of CRT Funnel Glass Waste Management Options,” *Resources, Conservation and Recycling 78 (2013) 92-104; doi:10.1016/j.resconrec.2013.07.001*

Poster Session

REWAS 2016: Towards Materials Resource Sustainability
Edited by: Randolph E. Kirchain, Bart Blanpain, Christina Meskers, Elsa Olivetti, Diran Apelian, John Howarter, Anne Kvithyld, Brajendra Mishra, Neale R. Neelameggham, and Jeff Spangenberger
TMS (The Minerals, Metals & Materials Society), 2016

Recovering of Carbon Fiber Present in an Industrial Polymeric Composite Waste through Pyrolysis Method while Studying the Influence of Resin Impregnation Process: Prepreg

Thiago Ribeiro Abdou[1], Denise Crocce Romano Espinosa[2], Jorge Alberto Soares Tenório[3]

[1, 2, 3]Escola Politécnica of the University of São Paulo; 580 Professor Lineu Prestes Avenue; São Paulo, São Paulo, 05434-070, Brazil

Keywords: Carbon fiber, Prepreg, Composite material, Thermal degradation

Abstract

The present work aims to recover carbon fiber from industrial polymeric composite waste so as to determine the optimum process parameters of pyrolysis. It is also part of the scope of this study to evaluate the influence of the resin impregnation methods (Prepreg) on the recovered carbon fiber morphological properties. Thermal degradation behavior of the composites and of the virgin carbon fiber was investigated by thermogravimetric analysis (TGA) and pyrolysis was held under an inert atmosphere. The samples were heated up to isotherms of 300, 450 and 550 for 1 hour. To assess the morphological properties and chemical composition of the recovered carbon fiber surface, visual inspection was performed with scanning electron microscope (SEM) and energy dispersive spectroscopy (EDS), respectively, before and after the recovering process. Virgin carbon fiber was used as means of comparison to indicate that the recovered reinforcement material had its structural integrity maintained.

Introduction

Composite materials, in particular those with carbon fibers, have been used increasingly in the aerospace, automotive and wind turbines industry, as engineers seek for alternative to minimize the weight of components and maximize the mechanical resistance.
Every year, Europe and the United States produces about 1 million tons of polymeric composites [1]. Disposal, which is sent to landfills as Class 2 waste, costs about $ 90 million per year [1].
The polymeric matrix is responsible for the geometrical shape of the final product, protection from external agents, chemical resistance, maintain the orientation of the reinforcement material and transfer the request load to the reinforcement elements are fibers. The purpose of the fibers, among others, is to give mechanical strength to the composite [2, 3]

Polymeric Matriz

The polymeric matrix, which is commonly confused with the term resin, is constituted by combining a resin and additives, the latter can be, curing agents, initiators and curing promoters or accelerators. The resin may either be referred to the polymer itself or the polymer matrix. When curing process happens, the polymer matrix acquires mechanical properties and chemical resistance [2]. The most used as a composite resins are polyester resins, epoxy and vinyl ester [2, 4, 5].

Some composites use glass fibers as a reinforcement material and are combined with thermoplastic resins. The thermoplastic resins are those that soften and flow under temperature and pressure effect [2,5]. However, commercial carbon fiber polymeric composites use thermosetting resin as the polymeric matrix. Figure 1 shows an example of an epoxy resin molecule. Epoxy resin is more commercially used in polymer composites reinforced with carbon fiber.

When curing occurs in thermoset polymers, a three-dimensional structure is formed due to cross-links that were established between the polymer chains in the thermoset. This structure is, however, insoluble and infusible, meaning that once cured, the thermosetting resin will not return to liquid state if heated. However, studies show that it is possible to promote a chemical reaction capable of reducing macromolecules in oligomers [2,6,7,8, 9]. Examples of thermosets are epoxy resins, unsaturated polyester, vinyl ester and phenolic [2,4,5].

The thermosets exhibit superior mechanical and elastic properties to the thermoplastics. By contrast, compared with metallic materials, their use temperature range is lower [2, 4].

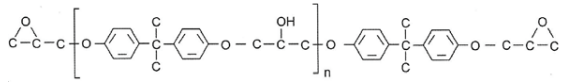

Figura 1. Epoxy resin molecule representation [2, 10]

Carbon Fiber Reinforcement

The carbon fiber is produced from a raw material precursor. The most used are polyacrylonitrile (PAN), the Rayon and the mesophase pitch, however, for economic reasons, the PAN is the most used among all. Most carbon fibers found in the market are manufactured from [2, 11].

The carbon fibers have become valorized for the composite materials industry, not only due to the low density and high mechanical strength as shown by a comparison with other materials in Table 1, but also due to the elasticity modulus and deformation resistance. In the fabrication of structural composites, such properties are an attractive; causing the carbon fiber reinforcement to be the predominant material in this application [2].

Table 1. Mechanical Properties of carbon fiber compared to metallic materials [2].

Material	Density (g/cm^3)	Tensile Strength (MPa)	Young Modulus (GPa)
Carbon steel annealed	7.86	400	210
Maraging steel	7.86	2000	210
Aluminum	2.63	600	73
Titanium	4.61	1900	115
Glass fiber	2.54	3448	72
Carbon fiber	1.77	3400	238

Objectives

The objectives of this study are as follows: Check the degradation of the polymer matrix of the composite in an inert atmosphere; evaluate the weight loss of the composite as a function of temperature; check the surface integrity of the carbon fiber composite after degradation to verify the possibility of reuse of the carbon fiber.

Experimental

Materials

For this study, samples of polymer composites reinforced with carbon fiber were acquired by donation from Texiglass. The composite were manufactured as prepregs and samples are from company's production line. The dimensions of the prepreg were 4 plates of 15 cm^2 length.
The polymeric matrix of the samples was composed of epoxy resin and carbon fiber used in the composite corresponds to HTS40 E13 3k Toho Tenax manufacturer.

Thermogravimetric analysis and Mass Spectrometer

To analyze the degradation of the polymeric matrix of the composite, this test was performed with a thermogravimetric balance NETZSCH STA 449 F1. The sample was cut with the aid of a hand saw in a piece of about 3 x 3 x 5 mm due to the size of the container going on the thermogravimetric balance, where the sample is placed. The test took place with controlled heating, with a heating rate of 5 °C/min from room temperature (20 °C) to 700 °C. Upon the final temperature, it was maintained at that temperature for one hour. The heating was done under inert atmosphere conditions (N_2) with a gas flow of 50 ml/min.
A mass spectrometer NETZSCH QMS 403C was connected to the thermogravimetric balance and while the heating occurred, all the gases of the resultant mass loss was analyzed to verify which components were being eliminated from the composite sample.

Scanning Electron Microscope (SEM) – Energy Dispersive Spectroscopy (EDS)

The analysis and morphological study of the surface of the carbon fiber after pyrolysis was performed using scanning electron microscopy techniques with the Phenom Pro X equipment manufactured by Phenom World. It was also carried out an inspection in the composite prior to degradation of the polymeric matrix stage in order to make it possible to verify the degradation of the matrix. In both cases it was also made an estimate of the chemical components present on the surface analyzed by the method of energy dispersive spectroscopy (EDS).

Pyrolysis

The samples were placed at each time inside an electric furnace. Three pyrolysis temperatures were studied: 300ºC, 450ºC and 550ºC under an inert atmosphere of argon. When the furnace reached the temperature, it was held an isotherm for 1 hour. After this time the furnace was shut down and the samples were only removed when the inside temperature reached 20ºC under inert atmosphere.

Results and Discussions

Thermogravimetric analysis and Mass Spectrometer

The TG curves were plotted in function of temperature. Figure 3 shows the variation in mass percentage in function of time (green curve) and represented by the blue curve is the derivate.

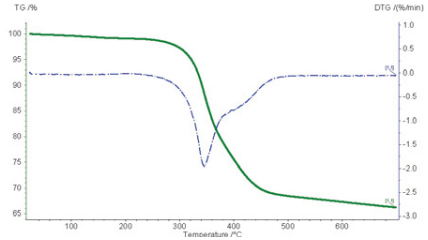

Figure 2. Thermogravimetric curves

From Figure 2 it is possible to see that from the moment the temperature reached 500 °C, the mass loss rate (green curve) decreased almost tending to zero. This suggests that the weight loss is reduced, requiring a new supply of energy to continue the degradation of the polymer matrix.
Figure 2 also shows the derivative curve, from this, it is possible to note again that, at the instant that the temperature reached 500 ° C, the derivative remained zero.
By analyzing those curves, one can estimate the temperature in which the composite mass loss started. From a point of the derivative curve (blue curve) for the start of the slope, it can determine that the beginning of mass loss occurred around 250 °C. According to the literature [12,13], a pure epoxy resin sample begins to suffer weight loss around 300 °C. This discrepancy can be explained due to the regions in the polymeric matrix that, during the manufacturing process, did not suffer a complete cure in its structure, facilitating weight loss.
The Figure 3 represents the molecule mass that was detected while the thermogravimetric analyses were performed. According to that, from around 300ºC to 500ºC, occur emissions of the following components which can be found in literature [14]: Carbon dioxide (44), carbon (12), acetone (58), cyclopentadiene (66), pyridine complex (79), aniline (93), phenol (94) and p-toluidine (107). This suggests the eliminations of the polymeric matrix under these temperatures.

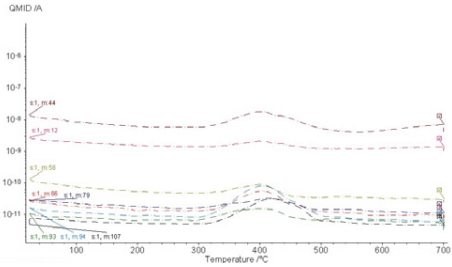

Figure 3. Mass spectrometer curve

Scanning Electron Microscope (SEM) – Energy Dispersive Spectroscopy (EDS)

After the pyrolysis method used on prepregs composites, samples of the recovered carbon fiber were analyzed by SEM and the regions represented in Figure 4 were also exanimated using EDS analysis. Virgin carbon fiber was also used as a reference to study the efficiency of pyrolysis. The random points in the regions of Figure 4 have been chosen to analyze both the fiber so as the residual polymer matrix. In the case of virgin carbon fiber, the selected points correspond only to the carbon fiber.

The photo, on the top right, shows that the polymeric matrix is still present. However, it is noticeable the shape of carbon fibers, suggesting the initiation of the process of degradation.

The polymeric matrix is comprised essentially of carbon and oxygen, as shown in Figure 1 and the result of EDS test of this region presents the elements of carbon and oxygen.

In the bottom left photo, although there is still a residual presence of the polymeric matrix in that sample, it is easily to perceive that the surface morphology of the carbon fibers remained unchanged, when compared to virgin carbon fiber. EDS test for this recovered carbon fiber indicate the presence of oxygen in less proportion.

The area represented in the bottom right photo shows a composition, through EDS analyses, in which only carbon is present, suggesting that the whole polymeric matrix has been eliminated. In addition to that, morphological aspects of the surface of the recovered carbon fiber at 550ºC are quite visually similar to virgin carbon fiber, this way, it is possible to affirm that prepreg composites, under these conditions of pyrolysis, can yield a carbon fiber free of the polymeric matrix.

Figure 4. Backscattered electron image obtained by SEM (top left) virgin carbon fiber (top right) recovered carbon fiber at 300ºC (bottom left) recovered carbon fiber at 450ºC and (bottom right) recovered carbon fiber at 550ºC.

Conclusions

From the tests performed in this study, it can be concluded that by heating a carbon fiber reinforced polymeric composite manufactured as Prepreg to temperature of 550 °C in an inert atmosphere, occurs degradation of the polymer matrix, leaving the reinforcing material

untouched. Also no reaction with the environment was detected and it has the same surface morphology of the composite fibers before pyrolysis. It was determined that the onset of thermal degradation occurs at 250 ° C and to verify total elimination of the polymer matrix heating should exceed the temperature of 500 °C.
The time of treatment, kept in constant temperature did not favor the degradation of the polymeric matrix.

Acknowledgements

We acknowledge the support of the CNPq, CAPES and Texiglass.

References

1 Abmaco, Associação Brasileira de Materiais Compósitos. Compósitos 1 - Materiais, Processos, Aplicações, Desempenho e Tendências. (São Paulo: Abmaco;2013).
2 Gerson Marinucci, *Materiais compósitos poliméricos: fundamentos e tecnologia* (São Paulo: Artliber Editora; 2011).
3 William D. Callister Jr., *Ciência e Engenharia de Materiais: Uma Introduçã*o (Rio de Janeiro: Livros Técnicos e Científicos Editora Ltda; 2012).
4 Bunsell AR, Renard J. *Fundamentals of Fibre Reinforced Composite Materials* (Bristol: Institute of Physics Series in Materials Science and Engineering; 2005).
5 Chawla K.K., *Composite Materials Science and Engineering* (New York: Springer; 2012).
6 Pimenta S, Pinho ST. "Recycling Carbon Fibre Reinforced Polymers for Structural Applications: Technology Review and Market Outlook". *Waste Management* (2011) 378–392.
7 López FA, Rodríguez O, Alguacil FJ, García-Díaz I, Centeno TA, García-Fierro JL, et al. "Recovery of Carbon Fibres by the Thermolysis and Gasification of Waste Prepreg". *Journal of Analytical and Applied Pyrolysis*. (2013) 675-683.
8 Meredith J, Cozien-Cazuc S, Collings E, Carter S, Alsop S, Lever J, et. al. "Recycled Carbon Fibre for High Performance Energy Absorption" *Composites Science and Technology*. (2012) 688-695.
9 Morin C, Loppinet-Serani A, Cansell F, Aymonier C. "Near- and Supercritical Solvolysis of Carbon Fibre Reinforced Polymers (CFRPs) for Recycling Carbon Fibers as a Valuable Resource: State of the art" *The Journal of Supercritical Fluids* (2012) 232– 240.
10 Chen KS, Yeh RZ. "Pyrolysis Kinetics of Epoxy Resin in a Nitrogen Atmosphere". *Journal of Hazardous Materials* (1996) 105-113
11 Berardine RC, ALMACO Associação Latino-americana de Materiais Compósitos. *Compósitos 5 Alto Desempenho* (São Paulo: ALMACO, Associação Latino-americana de Materiais Compósitos;2013).
12 El Gouri M, El Bachiri A, Hegazi SE, Rafik M, El Harfi A. "Thermal Degradation of a Reactive Flame Retardant Based on Cyclotriphosphazene and its Blend with DGEBA Epoxy Resin" *Polymer Degradation and Stability* (2009) 2101-6.
13 Rodrigues GGM, de Paiva JMF, do Carmo JB, Botaro VR. "Recycling of Carbon Fibers Inserted in Composite of DGEBA Epoxy Matrix by Thermal Degradation" *Polymer Degradation and Stability*. (2014) 50-58.
14 Pickering S.J. "Recycling technologies for thermoset composite materials – current status" *Composites Part A* (2006) 1206-1215

REWAS 2016: Towards Materials Resource Sustainability
Edited by: Randolph E. Kirchain, Bart Blanpain, Christina Meskers, Elsa Olivetti, Diran Apelian, John Howarter, Anne Kvithyld, Brajendra Mishra, Neale R. Neelameggham, and Jeff Spangenberger
TMS (The Minerals, Metals & Materials Society), 2016

EVALUATION OF ADDING GRITS IN THE MANUFACTURE OF SOIL-CEMENT BRICKS

Rita de Cássia S. S. Alvarenga[1], Délio Porto Fassoni[1], Larissa de Almeida Miranda[1], Márcia Lana Pinheiro[1]

[1]Federal University of Viçosa
Av. Peter Henry Rolfs, s/n-Campus Universitário, Departamento de Engenharia Civil, Viçosa – MG 36570-000, Brazil

Keywords: Soil-Cement bricks, Industrial solid waste (grits), Construction and habitation.

Abstract

The production of residues in pulp and paper industry is continuously increasing, which generates storing expenses and greater environmental impacts. The grits is an inorganic solid waste generated during the Kraft process by the pulp and paper industry, which presents in its composition the main ingredients of Portland cement. Therefore this paper aims to evaluate the feasibility of incorporating grids to the manufacture of soil-cement compressed bricks. To set the ideal amount of waste to be used, various samples with varying contents of cement, soil and grits were carried. The materials were characterized by mechanicals, physical and environmental tests and the results are consistent with the prescriptive requirements. Regarding the compressive strength at 28 days, all samples had their mean values higher than the normalization, which is 2.0 MPa. The bricks produced with higher amount of grits showed better performance in compressive strength.

Introduction

The global manufacture of pulp, paper and paperboard have been increasing at constant rates since 1960. In 2012 a production of 204 million tons of pulp and 507 million tons of paper and paperboard were registered. Brazil, for instance, produced 14 million tons of pulp and 10 million tons of paper and paperboard generating 240 thousand tons of grits in 2012. Hence, Brazil is positioned as the fourth worldwide producer of pulp and the eleventh producer of paper and paperboard [1]. Grits are yellowish solid and granulated residues from calcined green liquor, composed of sintered and vitrified lime.

In this context, the pulp and paper industries are faced with the challenge of increasing the production and, simultaneously, solving the problems related to the final disposal of residues. In the search for a solution to the final destination of these residues, innumerous researches are being developed in order to minimize the economic and environmental impacts of its final disposal. An interesting alternative is the utilization of these residues as a construction material to produce new technologies to the civil construction [2, 3, 4, and 5]. The incorporation of grits residue to the manufacture of soil-cement compressed bricks is a feasible solution from the technical and economic perspectives. This is due to the facts that grits have similar granulometry of a soil considered adequate to the production of soil-cement bricks and it presents two of the most abundant components in cement (lime and silica) in great quantity.

Therefore, the aim of this paper is to evaluate the feasibility of incorporating grits residue to the manufacture of soil-cement compressed bricks, obtaining the maximum consumption of residue and respecting the regulatory requirements.

Materials and Methods

The following materials were used to produce this research paper: Portland cement type CP II – E 32, potable water from the supply network, industrial residue (grits) supplied by the company Fibria Celulose e Papel from Aracruz – ES, Brazil, and soil from the field at Nô da Silva, Viçosa region (Cajuri) – MG, Brazil.

Initially, a base mixture was used with proportion in mass of 1:10 cement to soil, respectively. Furthermore, the portion of the soil was gradually substituted by grits in relation to the mass, in the percentages of soil to grits 100-0; 75-25; 50-50; 25-75 and 0-100, respectively. The intention was to use a maximum amount of residue respecting the regulatory requirements [6]. Consequently, the soil should present the following characteristics: 100% passing the 4.8 mm mesh sieve, 10% to 50% passing the 0.075 mm mesh sieve, liquidity limit equal or lower than 45% and plasticity index equal or lower than 18%.

The physical characterization of the various soil-grit mixtures were undergone through the subsequent testing: Dry specific weight [7], particle size analysis [8], Atterberg limits [9] and compaction [10].

Once the materials characterization phase was concluded, the next procedure was the manufacture of bricks with the various mass contents of soil-grits. The bricks were produced in accordance with [6]. Initially, the intention was to produce bricks with the mass contents of 100-0, 75-25, 50-50, 25-75 and 0-100 soil to grits, respectively. However, during the production process, it was noticed that it was not possible to remove the bricks with 75% and 100% of grits in substitution to soil from the press. Consequently, a new mixture with mass content of 37.5% soil and 62.5% grits was added.

After the cure, compressive strength and water absorption tests were undertaken [11]. According to this regulation, bricks must not present an average value for compressive strength lower than 2.0 MPa nor individual values lower than 1.7 MPa at 28 days of age. Regarding the water absorption, the tested sample must not present average values of water absorption greater than 20% nor individual values greater than 22% at 28 days of age.

The experimental trials were undergone at the Soil Mechanics and Construction Materials Laboratory of the Civil Engineering department of the Federal University of Viçosa in Viçosa, MG, Brazil.

Results and Discussion

Physical characterization of the soil and mixtures

Particle size analysis

The tested soil and grits presented dry specific weight equal to 2.75 g/cm³ and 2.76 g/cm³, respectively. Figures 1 and 2 show the respective granulometric curves. It is noticeable that 13.17% of the soil passed through the 0.075 mm mesh sieve, as well as 26.78% of the grits also passed this sieve.

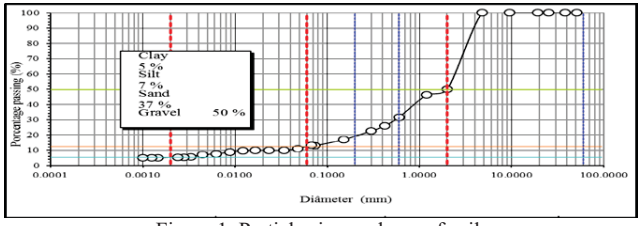

Figure 1. Particle size analyses of soil.

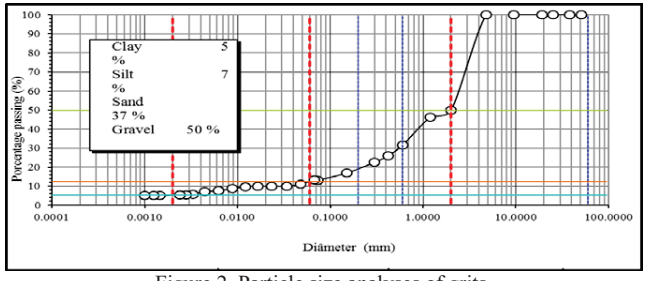

Figure 2. Particle size analyses of grits.

Regarding the granulometric distribution of soil and grits, it is possible to observe from Figures 1 and 2, respectively, that both comply with the requirements of [6]. Therefore, all of the soil-grits compositions will comply with the requirements established by the regulation.

Atterberg limits

On Table 1 the test results for liquidity limit (LL), plasticity limit (LP) and the plasticity index (IP) values are presented to the various compositions of soil-grits analyzed.

Table 1. LL, LP and IP Results

Test	Percentage of grits in the mixture				
	0%	25%	50%	75%	100%
Liquidity Limit (LL)	32.45	25.70	23.70	18.85	15.63
Plasticity Limit (LP)	17.31	12.05	10.60	13.30	15.27
Plasticity Index (IP)	15.14	13.65	13.10	5.55	0.36

It is noticeable from Table 1 that by increasing the grits content there was a reduction in the liquidity limit (LL), which is due to the grits sandy characteristics. Furthermore, it is clear that all the analyzed mixture compositions comply with the requirements regarding the LL, given that all

the values obtained for LL were below 45%, which is the maximum allowed. It was also detected that by increasing the grits content there was a reduction in the plasticity index (PI). This fact is due to the reduction that occurred in the LL, considering that the plasticity limit (LP) only had a small alteration for increasing grit contents. All the analyzed soil-grit compositions comply with the requirements of [6] regarding the plasticity index, since all the values obtained for IP were lower than the maximum allowed of 18%.

Compaction of the soil and mixtures

The results obtained in the compaction test of optimum moister content and dry density for the soil-grits mass composition of the percentages 100-0; 75-25; 50-50; 25-75 and 0-100, respectively, can be observed on Table 2.

Table 2. Summary of the compaction results.

Result of Compaction test	Percentage of grits in the mixture				
	0%	25%	50%	75%	100%
Optimum Moisture Content (%)	13.90	12.93	12.30	13.00	11.90
Dry Density (g/cm^3)	18.92	19.48	20.05	19.88	20.20

The analysis of the compaction test results shows that the increase in grits content leads to the reduction of optimum moisture content and an increase in the dry density.

Mechanical and physical characteristics of the soil-cement-grits bricks

This section presents the results of water absorption, compressive strength and leaching and solubilization tests.

Water absorption

The results for the bricks on the 28th day are shown on Table 3.

Table 3. Average absorption of the soil-grits bricks with different grits contents

Result of Water absorption test	Percentage of grits in the mixture				
	0%	25%	50%	62,5%	Maximum allowed
Average absorption (%)	15	14	14	14	22

As it is seen on Table 3 all the samples comply with the requirements of [11] regarding water absorption, as all of them regardless of the soil-grits composition presented individual water absorption values lower than the maximum allowed of 22% and average lower than 20%.

Compressive strength

The results obtained from the Simple compression test of the individual samples at 28 days old with the soil-grits mass composition of the percentages 100-0; 75-25; 50-50 and 62.5-37.5, respectively, can be observed in Figure 3. By evaluating the picture, it is verified that all the analyzed samples comply with the requirements of [11] regarding simple compression, as they present individual values of compressive strength at 28 days old greater than the minimum allowed of 1.7 MPa and average greater than 2.0 MPa.

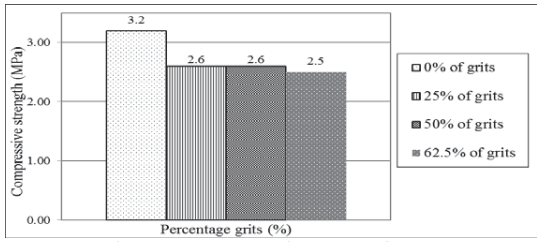

Figure 3. Compressive strength test.

Leaching and solubilisation tests

For the optimum sample (62.5% of grits) a leaching test was undertaken according to the procedures from [12]. Based on the chemical analysis of the grits, the metals in the leached extract of this mixture were determined. The results obtained for the leached extract comply with the requirements of [12] regarding the toxicity, as all the elements contents found in the mixture had values lower than the maximum allowed. Therefore, the soil-cement with the addition of grits is characterized as non-toxic and can be used with no restriction.

Similarly, the metals in the leached extract of the optimum mixture were determined. It was observed that this extract does not comply with the requirements of [12] regarding the standards of potability of water, considering that the contents of Pb, Fe, Na and Cr showed values greater than the maximum allowed. However, the mixture with soil-grits mass content correspondent to the percentages of 37.5 and 67.5 did not present characteristics of inflammability, reactivity, toxicity nor pathogenicity. On the other hand, it presented components that are solubilized in concentrations greater than that allowed by [12], being therefore classified as class II A. Nonetheless, this fact does not make it unfeasible to use it for the intended purposes, as long as it is used with the applicable precautions. The suggestion is to use a painted coating to avoid that the soluble elements cause water contamination and/or bring any harm to humans' health.

Conclusions

In regard to the physical characterization, it can be concluded that all the soil-grits mass contents correspondent to the respective percentages of 100-0; 75-25; 50-50; 25-75 and 0-100 comply with the requirements of [6]. However, in practice, it is known that to remove the brick from the press and transport it to the cure location a minimum amount of plasticity to the soil is required. Hence, it was only possible to manufacture bricks with the following percentages of soil-grits mass content, respectively: 100-0; 75-25; 50-50 and 37.5-62.5.

With respect to the compressive strength and water absorption tests, all the soil-grits mass contents complied with the requirements of [11]. Nevertheless, the sample correspondent to the percentages 37.5-67.5 of soil-grit, respectively, was defined as optimum, considering that it uses the greatest amount of residue and has the minimum plasticity required to permit the manufacture of bricks, its removal of the press and transportation to the cure location, respecting all the regulatory requirements.

Therefore, it is concluded that the use of grits in the production of soil-cement bricks is shown as a feasible alternative, in addition to minimizing the environmental degradation caused by the landfills and the use of natural resources, such as soil fields.

Acknowledgements

The authors thank the Brazilian agencie Fapemig for the support provided to this investigation.

References

1. M. Funchal, Worldwide outlook in the sector of pulp paper and paperboard. <http://www.painelflorestal.com.br/noticias/artigos/panorama-mundial-do-setor-de-celulose-papel-e-papelao>. Accessed in 16th of December, 2014.

2. A.P.Ribeiro, "Evaluation of usage of inorganic solid residues from the pulp manufacture in ceramic materials" (Ph.D. thesis, Universidade Federal de São Paulo, Brazil, 2010), 149 p.

3. Zanella B.P. et al., "Durability of mixed mortar lining containing dregs-grits", *American Journal of Environmental Science* 10 (2014), 44–47.

4. M.L.L. Garcia et al., "Grits as a Partial Cement Replacement for Concrete. *Second International Conference on Sustainable Construction Materials and Technologies* (2010).

5. R. Modolo et al. "Pulp and paper plant wastes valorization in bituminous mixes." *Waste Management* 30 (2010), 685–696.

6. Brazilian Association of Technical Regulation. Soil-cement compact brick using manual pressing. Rio de Janeiro: ABNT 1989. (NBR 10832) (In Portuguese)

7. Brazilian Association of Technical Regulation. Soil - #4,8mm sieve passing- Determination of specific mass. Rio de Janeiro: ABNT 1984. (NBR 6508). (In Portuguese)

8. Brazilian Association of Technical Regulation. Soil – Granulometric analysis. Rio de Janeiro: ABNT 1984. (NBR 7181). (In Portuguese)

9. Brazilian Association of Technical Regulation. Soil – Determination of liquidity limits. Rio de Janeiro: ABNT 1984. (NBR 6459). (In Portuguese)

10. Brazilian Association of Technical Regulation. Soil – Determination of plasticity limits. Rio de Janeiro: ABNT 1984. (NBR 7180). (In Portuguese)

11. Brazilian Association of Technical Regulation. Bloco vazado de solo-cimento sem função estrutural – Determinação da resistência à compressão e da absorção de água. Rio de Janeiro: ABNT 1994. (NBR 10836). (In Portuguese)

12. Brazilian Association of Technical Regulation. Procedures for obtainment of leaching extract from solid residues. Rio de Janeiro: ABNT 2004. (NBR 10005). (In Portuguese).

REWAS 2016: Towards Materials Resource Sustainability
Edited by: Randolph E. Kirchain, Bart Blanpain, Christina Meskers, Elsa Olivetti, Diran Apelian, John Howarter, Anne Kvithyld, Brajendra Mishra, Neale R. Neelameggham, and Jeff Spangenberger
TMS (The Minerals, Metals & Materials Society), 2016

THE EXPERIENCE IN DEVELOPMENT OF TECHNIQUE AND TECHNOLOGY OF ELECTRIC PULSE DISINTEGRATION OF ROCKS AND ORES

Anatoly Usov[1]; Vyacheslav Tsukerman[2]; Alexander Potokin[1]; Daniil Ilin[1]

[1] Centre of Physical and Technological Problems of Energy of North of Kola Science Centre of RAS, Fersman street, 14, Apatity, Murmansk region, 184209, Russia
[2] Institute of Economic Problems of Kola Science Centre of RAS Fersman street, 24a, Apatity, Murmansk region, 184209, Russia

Keywords: electric pulse disintegration, disintegration machines, chambers of comminution, high-voltage pulse generating; pulse transformer

Abstract

Unique technical means of electric pulse method of disintegration of material and the prospects assessment of the practical realization of new technology are submitted. Analysis of development experience physical bases, unique technical means and prospects assessment the practical realization of electric pulse (EP) method disintegration ores are submitted. The ways which could significantly improve the specific characteristics of high voltage pulse generators are determined and analysed. The experiments have proved the possibility to adapt these technological solutions for EP devices, and a further strategy of the EP technologies development and application has been suggested on this base.

Introduction

The studies carried out by the Russian researchers and those carried out jointly within some contracts with scientific organizations and companies of other countries, show that the electric pulse disintegration of materials (EPD), proposed and investigated in detail in Russia [1-7] has been widely recognized and developed abroad [8-12]. The international journals and the proceedings of the conferences dealing with the electric pulse disintegration pay great attention to the principal principals of selective disintegration of materials. However, any information concerning both the technical means and the assessment of their performance is limited, which would be necessary in objective assessment of possibility of the industrial use of the technology. For the first time, the results of long-term studies of the technique and technologies of electric pulse disaggregation and grinding, carried out by Russian researchers from Research Institute of High Voltages (Tomsk), Kola Science Centre of RAS (Apatity), Institute "Mekhanobr"(S.Pertersburg) are described in [4] in publications of the international symposium in S. Pertersburg in 1989 [13] and more fully represented in [7]. In the research papers the stands, the technological installations, the results of experimental tests in work mode are described. Earlier, by [14] basic circuits and classification of technical means electric pulse disintegration of the materials are proposed, the analysis of transportation schemes and classification of the material in the disintegration apparatus are given, construction of chambers

for continuous stadial disintegration of ores and materials are presented. The results of special researches of issues of hardware of electrical pulse technology are presented.

A continuous stand (1 t/hr) (EDUN-1)

The stand was developed by RIHV jointly with Mekhanobr to test both hardware components and high capacity disintegration schemes, as well as determine their applicability to the tasks of industrial apparatus development for non-ferrous metallurgy. The stand EDUN-1 allowed testing various working chambers, various schemes of material processing, with the amount of the initial raw materials and the finished product being of 1-1.5 t/hr. Also stand EDUN-1 allowed the testing of four types of 1 t/hr machines developed by RIHV jointly with Mekhanobr.

A grinding-jigging machine (272US)

The unit allows to combine the processes of classification and gravity concentration could be carried out simultaneously in one and the same apparatus, allowing grains liberated from useful minerals leave, readily and continuously, the grinding medium. Moreover, if grinding and gravity concentration processes are organized in such a way that at the last stage the ore passing through the active zone of the working chamber with continuous liberation of grains, has the useful minerals content similar to that of tailings, allowing it to go to waste, the principle “not to crush anything superfluous” is observed, which essentially improves energy indices of disintegration. The principles stated above are implemented in grinding-jigging machine 272US. (Figure 1)

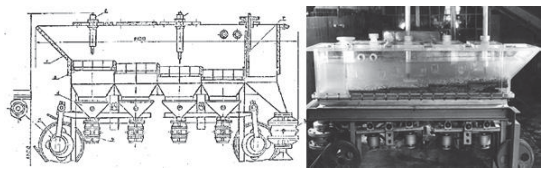

Fig. 1. A Grinding-jigging machine 272US

The machine has been tested on tin-bearing ore from the Solnechny deposit, with energy indices estimated. The total amount of ore processed in the grinding-jigging machine was 57.5 ton. The maximum productivity of the machine was 1250 kg/hours with power consumption of 20kWh/t. The technological tests and examination of the products of grinding have shown that ore minerals disintegration in the grinding-jigging machine (the stand EDUN-1) is the same as the size distribution of the product obtained in laboratory apparatus; the degree of disintegration is essentially higher than that in the mechanical apparatus.

A grinding machine, with a drum screen (275US “sizing trammel”)

The product classification efficiency in the working chamber depends on the degree of over grinding of the material and the energy indices of electric pulse grinding machines. To do that, a new grinding machine distinguished by that an earthed electrode was made in a kind of a perforated slowly rotating drum, has been developed and tested. In this machine ("sizing trommel") the grinding process is effectively combined with that of screening.

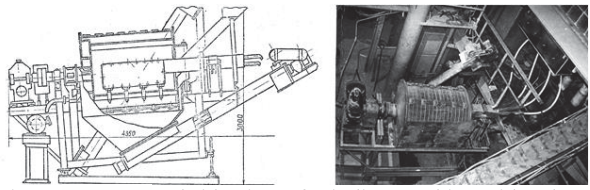

Fig. 2. Cutaway and side view of grinding machine with a drum screen

In the course of grinding, due to drum rotation, the finished product is screened, and a new batch of the initial material is fed under the electrode. Rotation increases the efficiency of size separation of the material. The machine allows both a closed and open cycle of operation. The granulometric characteristics of the finished product speaks for the best efficiency of material classification in comparison with that of other types of apparatus tested, as well as the minimum material over grinding due to the fast removal of the finished product from the active zone of disintegration. The total amount of material processed on the "sizing trommel" was 17.0 t, with the average output of 960 kg/hours and power consumption of 30kWh/t. Of greater advantage was the reliable operation of the earthed electrode in the "sizing trommel". It should be noted that the construction tested does not allow considering an opportunity to develop apparatus with productivity higher than 1 t/hour. To eliminate the disadvantages mentioned and preserve advantages of the construction is possible if, instead of the drum, a semi-cylinder is used, which vibrates about the axis on which high-voltage electrodes are fixed.

A grinding-classifying stage chamber (280US)

The examination of the electric pulse disintegration at each stage has shown that it is possible to reduce power consumption and produce the finished product with a smaller amount of fine grains by selecting both the size of sieves at the intermediate stages and the regime of material disintegration at each stage. The grinding-classifying stage chamber 280US has been developed, which is distinguished by the presence of three working compartments and an opportunity of installation of 3-6 electrodes.

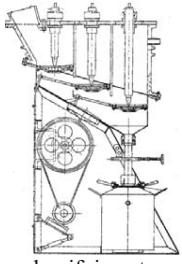

Fig. 3. A grinding-classifying stage chamber 280 US

This type of the machine designed for quartz glass grinding with consequent production of super pure quartz glass powder with a certain granulometric composition (80 % - 2+0,5 mm), is

distinguished by that all the metal parts are made of duralumin. The system provides consecutive stage-to-stage size reduction, with the product of the size required being removed from the process through control classifying sieves in due time. In the bottom of the chamber there is a pulser, whose diaphragm, 200-500 pump/min frequency and 0-10mm amplitude, provides the necessary hydraulic mode of operation of the machine. The chamber has been tested on the tin-bearing ores from the Solnechny deposit. Using three pulse generators and six forming elements, the productivity of the machine was 900 kg/hours with the specific energy consumption of 26.3 kWh/t, i.e. the productivity per one electrode makes 150 kg/hours.

A crushing-grinding machine, with a vibrating drive unit (244US)

One of the disadvantages of «stage» working chambers is low efficiency of material classification on a stationary earthed electrode-classifier. If a vibration drive is used, like in chamber 244US (Fig. 3), complex vibrations of the earthed electrode-classifier result in continuous motion of the material on the electrode and, accordingly, in a more effective classification of the finished product both under a high-voltage electrode and in space between them. The finished product is transported and dewatered by a bucket elevator.

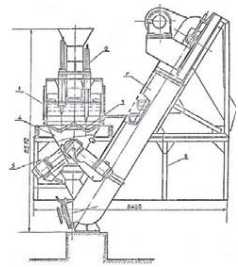

Fig 4. A crushing-grinding machine, with a vibrating drive unit

Tests were carried out on slugs produced at Krastsvetmet plant. To produce charge for smelting, the secondary slug was ground from 100-150mm to -30mm, and to recover entrapped cold shots by gravity, slug was ground to -1mm. The productivity, with size -30mm and size -1 mm, was 1170 kg/hour and 420 kg/hour, respectively.

Pilot devices for electric pulse disintegration

Development and successful laboratory tests of devices for electric pulse disintegration of materials encouraged the Russian scientists to carry out pilot tests in order to interest industry in the developments suggested, to get greater experience in industrial operations of electric pulse devices.

Devices for rock crushing to liberate rough diamond

A complex device for rough diamond raw materials disintegration and liberation of rough diamonds from various productive rocks has been developed by the order of the production

association Soyuzkvartssamotsvet, Mingeo, the USSR. The device has been developed by KSC RAS jointly with RIHV and Mekhanobr (Fig. 5).

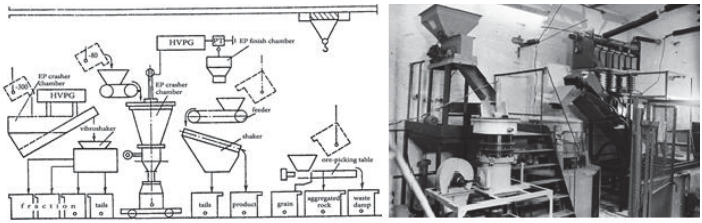

Fig. 5. The scheme of apparatus of the device for rock disintegration and liberation of rough diamonds and a view of complex device for rough diamond raw materials disintegration and liberation of rough diamonds (on experimental stand in KSC RAS)

The flowsheet allowed the product of 300-100mm to -3mm (tailings size) to be processed in four stages. The first stage of crushing is carried out in the chamber with a slot discharge gap (development of KSC RAS), which is capable to accept ore pieces of to 300 mm and crush them in one step up to size -90+6 mm. The second and third stages of grinding are carried out in the electric pulse working chamber 288US (developments of RIHV and Mekhanobr) equipped with replaceable electrodes-classifiers allowing production of the finished product of various size.

To test the device, over 10 tons of productive rocks were processed. Garnet grains revealed no failures. All ruby crystals revealed schistose jointing normal to the axis of the crystal but even such attenuated grains revealed no failures. Some transparent individuals of spinel were liberated well enough.

An installation for disintegration of emerald-bearing rock has been developed by KSC RAS for Malyshev mine (the town of Asbest). The disintegration of crystal raw materials was carried out on the installation in two stages by six electrode devices: 2 at the 1st stage of grinding and 4 – at the 2-nd stage, and, accordingly, these electrode systems were connected to six separate pulsers charged from one charger. The installation could operate for a long time with optimal loading of the sections due to regular control of loading in the section of the 1st stage of grinding by the change in ore feeding by the feeder. The peculiarity of water treatment was in use of cooled steam-condensate of higher specific resistance (2-6) 10^4 Ohm cm. The intermediate product output (growths with visible crystals, crystals and parts of crystals) is 2,75 times higher in electric pulse disintegration than that in the existing production technology. The crystal-bearing raw materials output is on the average 1.8 times higher (both in separate size and in total amount) after application of the electric pulse disintegration than that in the conventional technology.

The problems of manufacturing EPD technology (conclusion)

The studies have shown the opportunity of electric pulse disintegration chambers of productivity to 1 t/hour for - 2 mm and to 5-10t/hour for for ores with coarse-grained inclusions of minerals. However, the use of these plants is limited by small production volumes.

For many types of raw mineral, enriched by gravity and flotation the industrial scales of use of electric pulse plants can be possible only under the condition while the performance will be increased up to several tens or even hundreds of tons per hour, and mass-dimensional parameters of the units will not be significantly lower than the traditional devises of grinding. However, it is difficult to achieve the significant increase in the throughput performance of electric pulse grinding technology. The classifying ability of the chambers (the output of a product with specified size) close to the limits of optimization. Applied to disintegration installations, mechanical mills and crushers surpass by an order of magnitude electric-pulse installations in specific capacity. For example, a complex (GMC), used in selective disintegration of geological samples, has the performance of the order of 1kg/hr per $1m^3$ of the volume of the installation and of 20 kg/hr per 1kg of the weight of the installation. Given in Table 1 for comparison are technical characteristics of industrial laboratory grinding units.

Table 1. Technical characteristics of industrial laboratory grinding units

Type	Weight, [kg]	Dimensions, [mm]	Initial finer size class, [mm]	Final finer size class, [mm]	capacity, [kg/hr]	specific capacity, per 1 m^3 of the volume [kg/hr m^3]	specific capacity, per 1 t of the weight of the installation [kg/hr t]
Jaw crusher	133	650x330x580	to 55	1…20	30…300	250...2500	225...2255
Roll crusher	210	640x480x780	15…30	0,5…8	100…500	476...2381	416...2083
Hammer crusher	200	1200x640x800	to 90	0,3…8	50…100	250...500	82...124
Cone inertial crusher	26	380x190x330	to 6	0,2…2	to 10	384,6	500

Low specific energy characteristics of electric pulse disintegration depends on large size and weight of electrical equipment for realization of method. Electrotechnological block of the installations are disproportionately large in comparison with the technological block what does not allow to increase the performance of electrotechnological complexes by the organization of parallel operation of single blocks. The improvement of electrical equipment is a priority task of the present period of development of electric pulse technologies [15-17]. The real progress in the evolution of highvoltage electronics and electrical technology in the turn of the centuries created a real technical prerequisites to solve this problem. Chargers of high frequency voltage conversion, developed on modern element base, allows to reduce the size and weight of devices two by two orders, in comparison with rectifiers of AC voltage of industrial frequency with the magnetic core of iron devices. A pulse generators based on pulse voltage conversion (instead of the previously used Marx generators) also allows significantly reduce the size and weight of the electric pulse installations, reducing the cost of energy on the formation of high-voltage pulses and the process of destruction of the material. A noticeable disadvantage, limited the application of EP disintegration, due to physical factors is the significantly decreasing of energy efficiency in fine grinding of material [7]. However the problem of power-consuming can be substantially reduced by the weakening electric discharge effect. In different variants of electric discharge weakening of ores the task of selective weakening, carried out by electro-hydro pulse effect or by or incomplete channels of electrical discharges in material with nanosecond high-voltage pulses is placed instead of grinding. Technological effect of electric pulse weakening is realized in the following directions/forms: as an activator of hydrometallurgical processing of processing

mineral raw materials. For example, while the autoclave leaching of spodumene the temperature and pressure, at which the process is implemented, can be reduced; as a factor that increases the selectivity of the subsequent mechanical regrinding of the ore material by improving the liberation of useful minerals.

High technological effectiveness of electrohydraulic weakening is proved by the example of pretreatment of loparite ores [18]. By the increasing the output of the productive class and the best liberation of useful mineral the extraction in loparite concentrate is increased by 10-12% in absolute energy consumption on the weakening in 3-4 kWh/t. There are indications that the total energy consumption of ore pretreatment cycle can be even reduced in comparison with the traditional scheme of ore enrichment. Pre-weakening with use voltage pulses of nanosecond duration is confirmed by impressive results of operations in preparation for leaching of pyrite wastes [19] IEP UD RAS and auriferous concentrates [20] (IPKON RAS). It is technologically important that the mode of weakening with using multiwave microwave generators can be realized in the air.

In the future ore treatment the combination of the positive properties of several methods of disintegration will be used with maximum technological effect– high-performance crushing in a mechanical way, the high selectivity of breaking ores by destruction of electric pulse method and a combination of electric discharge weakening with the mechanical grinding of the material. The realization of this scheme with the optimal ratio of energy consumption on the stage of process of grinding ore will slightly reduce the severity of the problems, associated with the size and weight of electrical equipment, and will improve the performance of electrotechnological complexes to the required parameters according to the criteria of technical and economic efficiency.

References

1. A. A. Vorob'ev, *Destruction of rocks by pulsed electric discharges*, (Tomsk: Publishing house of the Tomsk state University, 1961), 150 (in Russian).

2. A.A.Vorob'ev, et all., *Pulse breakdown and the destruction of dielectrics and rocks* (Tomsk: Publishing of the Tomsk University, 1971), 225 (In Russian).

3. I.I. Kalyatsky et all. “The principle of elecrtric pulse disintegration and prospects for its application in industry,” (*Obogashcheniye Rud*, Vol. 1, 1980), 6-11 (in Russian).

4. A.F. Usov.et all., *Transients in plants of electric pulse technology* (Len.: LO Nauka, 1987), 189 (2nd ed. 2000), 160 (in Russian).

5. B.V. Siomkin et all., *The principle of electric pulse Destruction of materials (*Apatity: KSC RAS, 1995), 276 (In Russian).

6. Usov, A.F. and Tsukerman, V.A. “Prospective of electric impulse processes for the study of the structure and processing of mineral raw materials,” *Proceedings of the XXI International Mineral Processing Congress*, (Rome, Italy, July, 23-27, 2000), 8-15.

7. V.I Kurets et all., *Electric pulse disintegration of materials* (Apatity: KSC RAS, 2002), 324 (In Russian).

8. U.Andres, "Electrical disintegration of rock," *Mineral Proc. Extractive Metallurgy Rev*.(14, 1995), 87- 110.

9. H. Inoue et all., "Drilling of hard rocks by pulsed power,". *In Electrical Insulation Magazine, IEEE* (Volume: 16, Issue 3, 2000), 19-25.

10. H. Bluhm, *Pulsed power system: principles and applications*. (Springer, Berlin, 2006).
11. J. Biela, et al., "Electric Discharge Drilling of Conrete," *Proceeding of the IEEE International Power Modulator Conference*, (Las Vegas, NV, 2008).

12. Jörg Giese et al., "Electrodynamic Disaggregation: Does it Affect Apatite Fission-Track and (U-Th)/He Analyses?" *Geostandards and Geoanalytical Research* (Volume 34 Issue 1, 2009), 9 – 48.

13. *Proceedings of international symposium in St. Petersburs*, Obogashcheniye Rud, (Leningrad, Vol. 4, 1989), 33-46 (in Russian).
14. A.F. Usov and V.A. Tsukerman, "Electric pulse disintegration: russian experience and prospects," *Proceedings of the 2008 Global Symposium on Recicling, Waste Treatment and Clean Technology (REWAS-2008,* 12-15 October 2008, Cancun, Mexico), 221-226.

15. A.F. Usov and V.V. Borodulin, "Electrotechnical aspects of a problem of creation of installations for electric pulse disintegration of materials," *Proceedings of the XXIV IMPC* (Beijing, 24-28 sep. 2008), 467-471.

16. A.F. Usov and A.S. Potokin, "Conceptual solutions to create compact, electrical equipment for technology electropulse fracture of materials," *Proceedings of the 15th Conference on Environment and Mineral Processing*, (VŠB - Technical University of Ostrava, Czech Republic, p.2), 8-10 (6, 2011), 393-398.

17. A.F. Usov and A.C. Potokin, "Electric pulse disaggregation of materials – russian experience". *XXVI International Mineral Processing Congress, IMPC (*New Delhi, India. 24 - 28 sep. 2012. Conference Proceedings), 05618-05626.

18. A. F. Usov and A. I. Rakaev, "Electrical impulse crushing and disintegration of ores and other materials", *Obogashcheniye Rud*, (the typography of Leningrad, 1989) 48 (in Russian).

19. Y. A. Kotov. et all. "Complex processing of pyrite wastes of mining and processing plants by nanosecond pulse impacts," (DOKL. 2000. T. 372, No. 5), 654-656 (in Russian).

20. V. A. Chanturia et all., "The liberation of refractory auriferous ores by high-power electromagnetic pulses.," (DOKL. 1999. T. 366, No. 5.), 680-683 (in Russian).

REWAS 2016: Towards Materials Resource Sustainability
Edited by: Randolph E. Kirchain, Bart Blanpain, Christina Meskers, Elsa Olivetti, Diran Apelian, John Howarter, Anne Kvithyld, Brajendra Mishra, Neale R. Neelameggham, and Jeff Spangenberger
TMS (The Minerals, Metals & Materials Society), 2016

PRECIPITATION OF METALS FROM LIQUOR OBTAINED IN NICKEL MINING

Mónica M. Jiménez Correa[1], Paula Aliprandini[1], Jorge A. Soares Tenório[1], Denise Crocce Romano Espinosa[1]

[1]Chemical Engineering Dep., Polytechnic School, University of São Paulo;
158 Av. Prof. Luciano Gualberto, Trav. 3; Caixa postal 61548, São Paulo, SP 05424-970, Brazil.

Keywords: Nickel, selective precipitation, lateritic ore, ferric ion, ferrous ion

Abstract

In recent years, alternative treatment processes of nickel low-grade ores have been studied for nickel mining. The present work intends to study the precipitation of metals such as nickel, aluminum, cobalt, iron, zinc and copper from liquor obtained in the atmospheric leaching of a limonite nickel waste. Initially, synthetic solutions were prepared to simulate the sulfuric leach liquor. The iron in the first solution was found in the form of ferrous ions (Fe^{+2}), while in the second solution was found as ferric ions (Fe^{+3}). Precipitation tests were carried at 25ºC and pH was varied with KOH additions. Metal concentration in aqueous and solid samples were analyzed by energy-dispersive X-ray (EDX) and a scanning by electron microscope (SEM) and energy dispersive X-ray spectroscopy (EDS), respectively. Around 100% of iron, 60% of cobalt and 10% of copper were precipitated at pH 3,0 from the solution with ferric ions, while in the solution with ferrous ions, the highest metal precipitation were achieved at pH 5,5.

Introduction

Sulphide and lateritic nickel ores are the main sources of nickel metal. Lateritic ores contain about 60% world's know nickel resources, whereas 40% of world's nickel are found in sulphide ores. Limonite, (Fe,Ni)O(OH)·nH2O, is a part of nickel laterite and can be processed through pyrometallurgical, hydrometallurgical or a combination of both techniques (Mudd, 2010; USGS, 2014).

In general, the first hydrometallurgical stage is the leaching process, which can be performed using sulfuric acid, ammonia or chloride acid at atmospheric or high pressure. The resulting leach liquor containing mainly iron is treated with separation techniques such as precipitation, solvent extraction and electrowining (McDonald and Whittington, 2008; Moskalyk and Alfantazi, 2002).

Precipitation is used to remove impurities from liquor and can be divided in chemical or physical. In the hydrometallurgical field selective precipitation is used to purify solutions by addition of reagents to form an insoluble metallic compound (Heck, 2010; Lewis, 2010). Iron precipitation is the most widely used method to obtain a solution without high iron concentration level. The solid precipitated can form jarosite, goethite and hematite (Chang et al., 2010).

The present work aims to investigate the precipitation of metals such as nickel, aluminum, cobalt, iron, zinc and copper from liquor obtained in the atmospheric leaching of a limonite nickel waste. Particular interest was devoted to iron precipitation that affects the metals loss during its precipitation process.

Materials and methods

The solutions used in this study were based on the leaching from nickel limonite ore. Two solutions were prepared to reproduce the limonite solution. Reagents used were of analytical grade of the metals as sulfates. The composition used containing 4.5g/L Al [as Al2(SO4)3.xH2O], 0.07g/L Co [as CoSO4.7H2O], 0.13g/L Cu [as CuSO4.5H2O], 8.09g/L Mg [as MgSO4.7H2O], 0.37g/L Mn [as MnSO4.H2O], 2.52g/L Ni [as NiSO4.6H2O] and 0.04g/L Zn [as ZnSO4.7H2O]. In the first solution was added 21.40g/L ferrous ions (Fe+2) as FeSO4.7H2O, while in the second solution was added 21.40g/L ferric ions (Fe+3) as Fe2(SO4)3.xH2O. In both solutions, the liquor was prepared with deionized water. The pH was adjusted to 1.5 at room temperature (25ºC).

The experiments were carried out in batch scale by stirring of the synthetic solutions for 5 minutes after a constant pH was obtained by a drop-wise addition of 1 molar potassium hydroxide (KOH) as precipitant. To study the influence of pH on the precipitation of metals, both solutions ranged pH at: 2.0, 2.5, 3.0, 3.5, 4.0, 4.5, 5.0 and 5.5. The choice of pH values was determined considering the metals concentration and pH at which precipitation occurs at 25˚C when a hydroxide is used as the precipitant. The relationship of these two factors is shown in Figure 1.

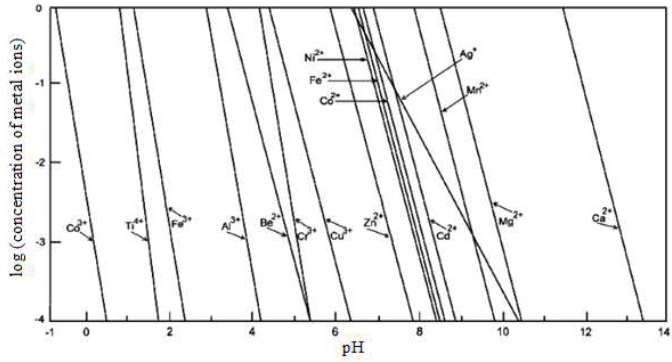

Figure 1: Relationship between concentration of metal ions and pH to precipitation at 25˚C using hydroxide as the precipitant (Gupta, 2003).

After the reaction, the solid residues were filtered, washed and dried in oven at 50ºC for 24 hours. The precipitated were subsequently analyzed by scanning electron microscope and energy dispersive X-ray spectroscopy (SEM-EDS) to determine the morphology and composition of the precipitate formed. The final liquor concentration was determined by energy-dispersive X-ray (EDX).

Results

Metals precipitation

Metals precipitation from liquors after leaching steps has been studied by several authors in order to separate metals and to purify solutions (Dorella and Mansur, 2007; Lewis, 2010; Provazi et al., 2011).

Iron precipitation is an interest topic in metallurgy and mining fields, since iron removal is an important stage to recover other metals. Then, precipitation of metals from liquor obtained in the atmospheric leaching of a limonite nickel waste was studied in the present work. Figure 2 shows precipitation percent of metals obtained by EDX chemical analysis of both liquors (solution with ferrous ions and solution with ferric ions) after experiments.

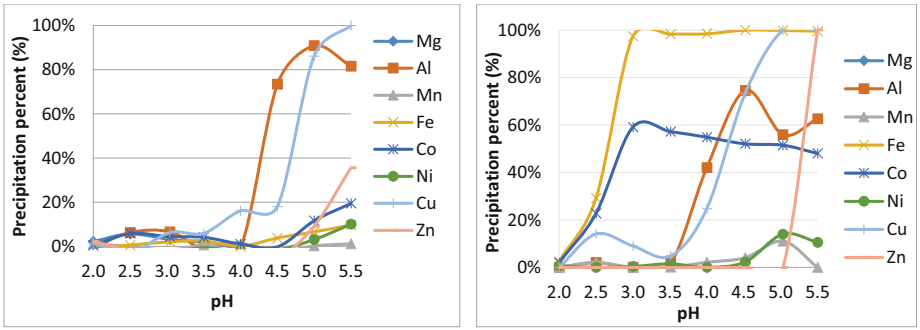

(a) (b)

Figure 2. Metals precipitation percent after experiments using solution with (a) ferrous ion and (b) ferric ion.

Metals precipitation was promoted by pH increment using KOH. Reaction 1. defines metals precipitation using hydroxide reagents.

$$M^{+z} + nOH^{-} \leftrightarrow M(OH)_n \qquad \text{Reaction 1}$$

Where, M^{+z} is metallic cation.

For the solution with ferrous ion, aluminum and copper significant precipitation occurred since pH 4.5, whereas a lower iron precipitation (10%) was obtained at pH 5.5. The best aluminum precipitation was achieved at pH 5.0, in which around 90% aluminum was deposited. Already, copper was effectively precipitated at pH 5.5, in which 100% copper was attained. The solid morphology obtained after the tests that used pH 5.5 was examined by SEM and EDS. Figure **3** shows elements presents in the sample. Analysis by EDS showed peaks corresponding to the main elements of solid like iron and aluminum, which ones were expected to be present in solid sample.

For the solution with ferric ion, precipitation of iron, cobalt and copper started at pH 2.5. Iron achieved 100% of precipitation at pH 3, at the same pH 60% cobalt was precipitated that value corresponds to the best cobalt precipitation. Still, aluminum and copper precipitation in the ferric solution was similar than precipitation in the ferrous solution. Nevertheless the best aluminum precipitation was at pH 4.5, where precipitation percent was 78%, while 100% copper was precipitated at pH 5.0.

Precipitation of iron and cobalt had a similar behavior in the solution with ferric ion. According to Gupta (2006) cobalt precipitation for low metal concentration only take place on pH around

8.5(Gupta, 2003). However, in precipitation cobalt was started at pH 3.0 This effect could be induced for the high iron concentration and chemical affinity. Ions that are more concentrated can drag and co-precipitate other metals in selective precipitation (Farley et al., 1985; Silva and Afonso, 2008). Also the atomic ratio for both ions are close to each other, then metal co-precipitation occurs(Jackson, 1986).

After precipitation experiments at pH 3.0, the solid morphology obtained was examined by SEM and EDS. Elements presents in the solid sample can be observed in Figure **4**. The main elements of solid like iron and aluminum were found by EDS, which one showed peaks corresponding.

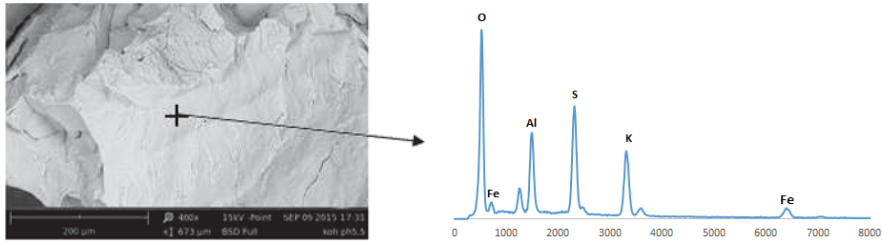

Figure 3. Scanning electron micrographs and EDS of solid precipitate for a solution with ferrous ion.

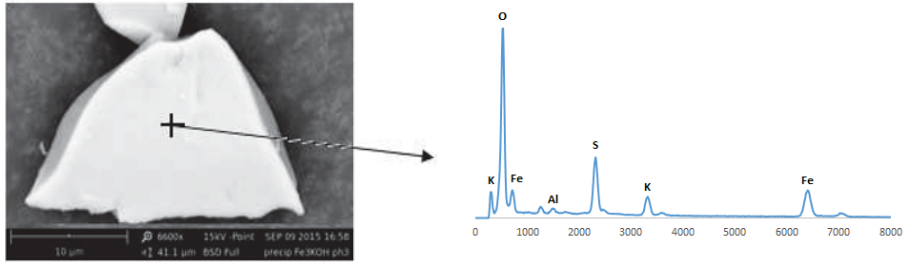

Figure 4. Scanning electron micrographs and EDS of solid precipitate for a solution with ferric ion

Comparison between ferrous ion and ferric ion precipitation

According to Gupta (2003), ferrous ion precipitation ion occurs at pH 8.0, while ferric ion the pH of precipitation is 3.5. The difference between iron ions behavior is due especially to: i) the size of the atomic radius, ii) the number of valence electrons and iii) the chemical activity.

The ferrous ion is greater than the ferric ion since ferrous ion has one electron more than the other one. When valence electrons are removed, remaining electrons are attracted strongly by the nucleus. Smaller ions have more available space than bigger ions, then its interaction with other chemical species is also higher. The opposite happens on ions that have huge nuclei atomic. Figure 5 shows the comparative between ionic radius and electron configuration for zero-valence iron and its ions (Feltre 1996; Santana, 2015).

Considering valence electrons, ferrous ion (Fe^{+2}) is more stable than Ferric ion (Fe^{+3}). As it can be observed in ferric electron configuration (Figure 5-c), one orbital in the 3d sublevel is not

complete with electrons, while in ferrous configuration three orbitals in the 3d sublevel are filled. Therefore, bond formation between OH^- and Fe^{+3} ion is preferred (Feltre, 1996) .

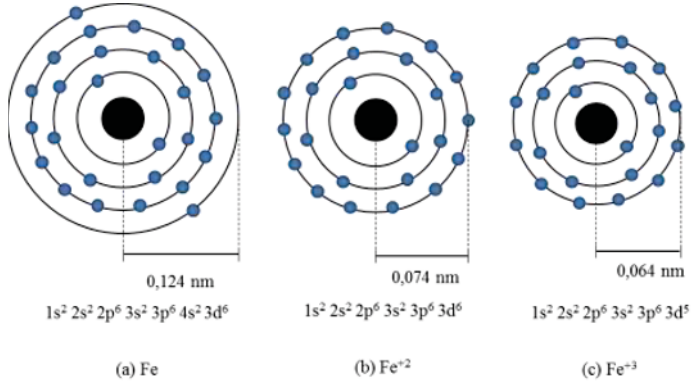

Figure 5. Ionic radius and electron configuration for (a) Fe; (b) Fe^{+2} and (c) Fe^{+3} (Adapted from Feltre, 1996)

For a given ionic strength, when ion charge increases the difference between activity coefficient and the unit also increases. For ferric ion the activity is farther from ideality (activity = 1) than for ferrous ion. On acid pH ferric activity achieves a value where precipitation occurs, however for ferrous ion attains the same activity value, the pH have to be raised at 8 (Jackson, 1986; Santana, 2015).

Conclusions

Precipitation experiments with constant agitation, at 25ºC using KOH were performed. After analysis of results obtained can be concluded that:

- For the solution with ferrous ion, aluminum and copper significant precipitation occurred since pH 4.5, whereas a lower iron precipitation (10%) was obtained at pH 5.5. The best aluminum precipitation was achieved at pH 5.0, in which around 90% aluminum was deposited. Already, copper was effectively precipitated at pH 5.5, in which 100% copper was attained.
- For the solution with ferric ion, precipitation of iron, cobalt and copper started at pH 2.5. Iron achieved 100% of precipitation at pH 3, at the same pH 60% cobalt was precipitated that value corresponds to the best cobalt precipitation. Still, aluminum and copper precipitation in the ferric solution was similar than precipitation in the ferrous solution. Nevertheless the best aluminum precipitation was at pH 4.5, where precipitation percent was 78%, while 100% copper was precipitated at pH 5.0.
- Ferric ion has a different precipitation behavior when compared with ferrous ion, because their chemical characteristics are particular of each one. Ion in ferric form began its precipitation at pH 3.0, while iron in ferrous form had its precipitation at pH 5.5.

Acknowledgements

To the Counsel of Technological and Scientific Development (CNPq) for the financial support through doctorate grant.

To the Coordenação de Aperfeiçoamento de Pessoal de Nível Superior (CAPES) for the financial support through master grant.
To the Fundação de Amparo à Pesquisa do Estado de São Paulo (FAPESP) for financial support through the research project 2012/51871-9 ,

References

Chang, Yongfeng, Xiujing Zhai, Binchuan Li and Yan Fu 2010. Removal of iron from acidic leach liquor of lateritic nickel ore by goethite precipitate. Hydrometallurgy 101: 84-87.

Dorella, Germano and Marcelo Borges Mansur 2007. A study of the separation of cobalt from spent Li-ion battery residues. Journal of Power Sources 170: 210-215. doi: http://dx.doi.org/10.1016/j.jpowsour.2007.04.025

Farley, Kevin J, David A Dzombak and François MM Morel 1985. A surface precipitation model for the sorption of cations on metal oxides. Journal of Colloid and Interface Science 106: 226-242.

Feltre, Ricardo 1996. Fundamentos da Química . São Paulo, Ed Moderna :p67.

Gupta, Chiranjib Kumar 2003. Chemical Metallurgy: Principles and Practice. India.

Heck, Nestor Cezar 2010. Precipitação In Precipitação Rio Grande do Sul.

Jackson, E. 1986. Hydrometallurgical extraction and reclamation. New York: Ellis Horwood Limited.

Lewis, Alison Emslie 2010. Review of metal sulphide precipitation. Hydrometallurgy 104: 222-234. doi: http://dx.doi.org/10.1016/j.hydromet.2010.06.010

McDonald, R. G. and B. I. Whittington 2008. Atmospheric acid leaching of nickel laterites review: Part I. Sulphuric acid technologies. Hydrometallurgy 91: 35-55. doi: http://dx.doi.org/10.1016/j.hydromet.2007.11.009

Moskalyk, RR and AM Alfantazi 2002. Nickel laterite processing and electrowinning practice. Minerals Engineering 15: 593-605.

Mudd, Gavin M. 2010. Global trends and environmental issues in nickel mining: Sulfides versus laterites. Ore Geology Reviews 38: 9-26. doi: http://dx.doi.org/10.1016/j.oregeorev.2010.05.003

Provazi, Kellie, Beatriz Amaral Campos, Denise Crocce Romano Espinosa and Jorge Alberto Soares Tenório 2011. Metal separation from mixed types of batteries using selective precipitation and liquid–liquid extraction techniques. Waste Management 31: 59-64. doi: http://dx.doi.org/10.1016/j.wasman.2010.08.021

Santana, Genilson Pereira 2015. Equlíbrio químico. Brazil.

Silva, Cristiano Nunes da and Júlio Carlos Afonso 2008. Processamento de pilhas do tipo botão. Química Nova 31: 1567-1572.

USGS, United States Geological Survey 2014. Mineral Commodity Summaries-Nickel 2014. In Mineral Commodity Summaries-Nickel 2014.

REWAS 2016: Towards Materials Resource Sustainability
Edited by: Randolph E. Kirchain, Bart Blanpain, Christina Meskers, Elsa Olivetti, Diran Apelian, John Howarter, Anne Kvithyld, Brajendra Mishra, Neale R. Neelameggham, and Jeff Spangenberger
TMS (The Minerals, Metals & Materials Society), 2016

GREEN STRUCTURAL CERAMIC WITH ADDITION OF RAW CLAY WASTE

Alessandra Savazzini dos Reis[1,3], Viviana P. Della-Sagrillo[2], Francisco R.Valenzuela-Diaz[3]

[1]IFES Colatina; Av. Arino Gomes Leal, 1700; Colatina, Espírito Santo,CEP 29700-660, Brasil
[2]IFES Vitória; Av. Vitória, 1729; Vitória, Espírito Santo, CEP 29040-780, Brasil
[3]PMT/EPUSP; Av. Prof. Mello Moraes, 2463; Cidade Universitária, São Paulo, CEP 05508-030, Brasil

Keywords: Raw clay waste, Green structural ceramic, Sustainability, Waste.

Abstract

Raw clay waste is generated in the products conformation stage in the structural ceramic industry. Incorporation of raw clay waste is an alternative to make the structural ceramic sector more environmentally sustainable while reducing the consumption of clayey raw material. The Brazilian structural ceramic industry consumes 10.3 million tons of clay per month. This work aims to study the technical feasibility of raw clay waste addition in clayey mass used in the structural ceramic production. Samples of raw clay waste and clay were tested for chemical, physical and mineralogical characterization. Specimens containing waste contents, varying from 10% to 90% (wt.), were produced and burned in an industrial tunnel at 850°C. The technological properties evaluated were: water absorption, apparent porosity, apparent density, loss on ignition, firing shrinkage and mechanical strength. The results show that the addition of waste improves the evaluated properties significantly. With this, the reuse of raw clay waste in the clayey mass for production of ceramic roof tiles and blocks can contribute to the sustainability of ceramics sectors, reducing raw materials consumption and avoiding waste disposal in landfills. It becomes a feasible alternative to aim the ceramic industry comes to be a "green structural ceramic".

Introduction

The Brazilian structural ceramics industry has 6903 companies with the majority of micro, small and medium size operating in various technological levels, which generate 293,000 jobs according to ANICER - Associação Nacional da Indústria Cerâmica [1]. The sector presents a monthly production of 4.0 billion blocks and 1.3 billion roof tiles serving the building industry. Consumption of clay, the main raw material of the industry, is 10.3 million tons per month [1]. The extraction of clay to supply the industry is made, usually, in small mines, from 1,000 to 20,000 t/month, with low unit value of the raw material, but with high cost of transport [2]. The extraction and transportation activities generate significant environmental impacts [2]. The main problems faced by small and medium structural ceramics industries are: generation of waste without adequate treatment, lack of product quality control, high level of losses in mining and processing steps and lack of technology, among others [2]. The structural ceramic industry generates waste during the production of roof tiles and blocks causing environmental impact, which added to the impact of clay extraction, make the industry not sustainable environmentally. One of the ways to change this reality is to improve the technology involved in the productive process and the incorporation of waste in clayey mass.

The use of wastes may reduce consumption of non-renewable raw materials and the volume of waste disposed in landfills. There are many academic papers on the use of waste from various industries in the clayey mass production of structural ceramics, but the large-scale production of

products with incorporated waste is low. With this, technological innovation does not happen in the industry. This problem could be solved with the approach of academic research to the productive sector involved. This study aimed the interaction between research in the laboratory and the test industry to streamline the technological innovation process. The survey was conducted in a ceramics industry using the variables involved in the productive process of the ceramic products, such as local temperature and humidity conditions in the molding of the specimens. It was used the industry tunnel furnace, which utilizes a maximum temperature in the burning zone of 850°C for about 6 h with a total cycle of 24 h. In this sense, the aim of this research is to study the technical feasibility of the addition of raw clay waste to the clayey mass for structural ceramics production. The waste called as raw clay waste (Figure 1) is generated in the ceramic industry itself in the step of conformation the ceramic bodies. It consists of burrs of the pressing of roof tiles, and roof tiles and freshly pressed blocks discarded because of visual defects, such as cracks. The waste is taken out the process and stored in storage piles. It is estimated that the raw waste clay represents 40% of clay mass that enters the process.

Figure 1. Raw clay waste

In the literature, there are no studies (to our knowledge) on the characterization and the addition of raw waste clay (not burned) in the clayey mass production of structural ceramics. There are several studies [3, 4] about the use of "chamotte", which is burned ceramic waste. When the industries in Brazil incorporate raw clay in the process it is generally without any previous study of characterization of the waste clay and verification of its ceramics properties. The waste volume which returns to the process is not usually controlled, so products can be made from waste only when the disposal of waste clay is high.

Materials and methods

The clay is extracted from a quarry located in Baixo Guandu-ES-Brazil. The raw clay waste is generated in a structural ceramic industry located in Colatina-ES-Brazil. Samples of clay and raw clay waste were collected in the storage of the structural ceramic industry located in the State of Espírito Santo using waste sampling procedures specified by ABNT – Brazilian Association for Technical Standards NBR 10007/2004 [5]. The raw clay waste consists of the clay and granite waste, both are raw materials used by the industry for the production of ceramic roof tiles and blocks After that, the samples were air-dried, broken with the aid of a pounder, quartered and homogenized. Part of the material was used for characterization tests, and part for preparing the specimens. The materials were characterized by X-ray fluorescence (XRF) in a Philips PW2400 spectrometer; X-ray diffraction (XRD) with copper source (K α radiation) in a Philips X- Pert MPD equipment; scanning electron microscopy (SEM) in a Philips XL-30 electron microscope; particle size analysis by laser diffraction in a Malvern Mastersizer 2000 equipment. The plasticity was evaluated using Atterberg's limits [6, 7]. The identification of the samples in XRD was made by comparison with the Crystallographic Open Database – COD standard files.
Molded spheres specimens were made for evaluation of ceramic properties after firing at the ceramic industry. The spheres were made with a mixture of clay and raw clay waste (sieved in #

40 of ABNT). The specimens were manually molded with an average diameter of 2 cm, 10 g dry mass, with enough water to allow molding, according to the methodology developed in Laboratório de Materiais Não-Metálicos Prof. Persio Souza Santos (LPSS) of PMT/EPUSP/BR.
The spherical specimens have been used in other studies [8, 9], which were compared to the results of pressed bars. The authors observed that the results found in ceramic properties of bars and spheres have coherence and often the values are similar. The spheres preparation method is simpler than the bars; and can be made in any structural ceramic industry for an initial analysis of low cost characterization of raw materials for use in ceramic bodies.
The raw clay waste content in the clayey mass varied from 10% to 90% (in weight) for making of specimens. The spheres were dried in a drying oven for 24 h at 110°C. Compressive strength was measured in part of the specimens, and part of the specimens was burned in an industrial tunnel-type furnace in a structural ceramic industry for 24 h, at a maximum temperature of 850°C in the burning zone for about 6 h. After firing, the following properties were evaluated: water absorption, apparent porosity, apparent specific mass, loss on ignition, according to the methodology proposed by Souza Santos [10], besides compressive strength.

Results and discussion

The chemical analysis result (Table 1) is shown in terms of percentage through the weight of constituent oxides and loss on ignition. By analyzing the data, the clay was verified to present a typical chemical composition of common clay raw material, with 40.85% silica, 33.56% alumina; and 14.29% loss on ignition obeying ranges of values, from 6.80% to 38.00% for Al_2O_3 and from 6.00% to 15.70% for the loss on ignition, respectively, as specified by Souza Santos [10] for ceramic raw materials. The silica content is located next to the range from 43.20% to 77.60% specified for SiO_2 [10]. The high value of loss on ignition of clay may cause porosity in the ceramic bodies. The percentage of 7.41% iron oxide is responsible for the reddish color after firing. The concentration of Na_2O (0.16%) and K_2O (0.77%) is not high; therefore, even being fluxing oxides, they contribute little to the formation of the glassy phase. Clays with these characteristics (aluminous silica, with high iron content and low content of fluxing oxides) demand high sintering temperature, as reported by Hildebrand et al. [11]. As seen in the table, the raw clay waste presents chemical composition similar to clay, with a high silica content (44.70%) and alumina (27.57%); and high value of loss on ignition (12.85%). These values obey to the specified by Souza Santos [10] for raw material of structural ceramic.
As the raw clay waste has granite waste in its composition, there is the presence of fluxing alkali oxides Na_2O (0.65%) and K_2O (1.56%), which may contribute for burning the ceramic bodies, reducing the need of high temperature in the formation of the glassy phase of the clay in question. The presence of Fe_2O_3 is associated with steel shot, and CaO is associated with lime, both used in the mud from which the granite waste originates.

Table 1. Chemical composition of materials by XRD (wt%)

	SiO_2	Al_2O_3	Fe_2O_3	TiO_2	K_2O	MgO	CaO	Na_2O	P_2O_5	MnO	LOI
Clay	40.85	33.56	7.41	1.51	0.77	0.63	0.21	0.16	0.14	<0.05	14.29
Waste	44.70	27.57	8.96	1.22	1.56	0.72	1.01	0.65	0.16	0.06	12.85

Note: LOI – loss on ignition

Figure 2 shows the X-ray diffraction of the clay and the raw clay waste. The XRD analysis of clay indicates that the predominant minerals are kaolinite, quartz, illite and goethite. The analysis of the X-ray diffractogram of the raw clay waste identifies the presence of crystalline phases associated to mica, feldspar and quartz; the latter confirms the high value of SiO_2 (44.70%) in the

XRF detected. In addition, orthoclase was also detected. The raw clay waste also shows characteristic peaks of kaolinite and quartz, originated from clay.

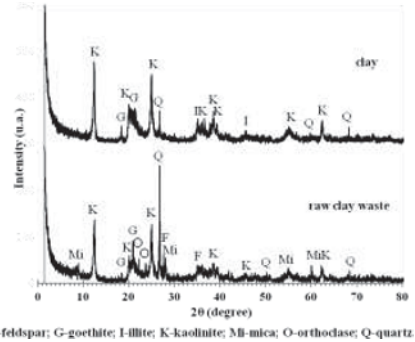

Figure 2. XRD of materials

Figure 3 presents images showing the material morphology and particle size obtained by electron microscopy. The images indicate that the grains of materials are irregular in shape tending to form lamellar and slender particles, some scattered and others in clumps forming larger particles. The formation of these clumps between very thin particles may increase the porosity. The particles size ranged from 2 μm to 45 μm in the clay; and from 2 μm to 50 μm in raw clay waste.

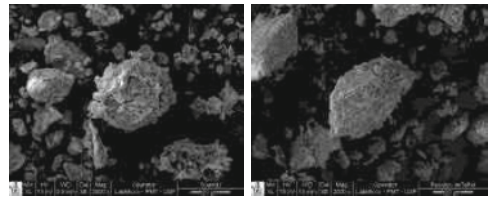

(a) Clay (b) Raw clay waste

Figure 3. SEM of materials

Atterberg limits of the raw materials are presented in Table 2. The clay plasticity index (PI) is 25.46% and the raw clay's waste is 20.75%, above 15.0%, indicating high plasticity, which makes them suitable for molding by extrusion. Regarding the plasticity limit (PL) of clay, the 42.00% value is within the range from 9.0% to 56.0% specified by Souza Santos [10] for kaolinitic clay, confirming the predominance of the kaolinite mineral identified in XRD. It is found that the values of the Atterberg limits of the raw waste clay are within the ranges suitable for the structural ceramic products, 30 to 60% for the LL, 15 to 30% PL and 10 to 30% for PI [12]. Thus, it can be said that the raw clay waste has adequate plasticity for extrusion.

Table 2. Atterberg limits of materials

	Plasticity Limit-PL (%)	Liquid Limit-LL (%)	Plasticity Index-PI (%)
Clay	42.00	67.46	25.46
Waste	29.45	50.22	20.75

The particle size distribution of the clay and the raw clay waste are shown in Figure 4. The effective diameter of the clay is 2.06 μm and the raw clay waste is 2.10 μm. These are very close

values, indicating that both raw materials have similar particle size distribution. The clay and the raw clay waste have about 25% grains larger than 20 µm; 64% grains between 2 µm and 20 µm, and less than 11% grains smaller than 2 µm. The clay and raw clay waste have low "clay fraction" (grains smaller than 2 µm), presenting plasticity due to the organic matter contained in the clay and the raw clay waste.

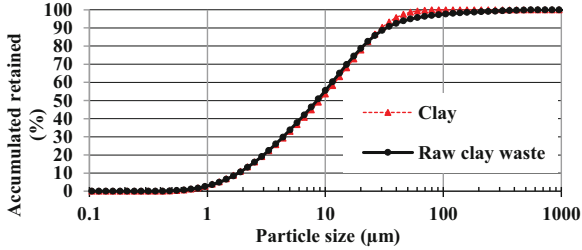

Figure 4. Particle size distribution curve of materials

The results of ceramics properties from the spheres made with solely clay and with mixture of clay and raw clay waste are shown in Table 3. For the fired spheres the highest value of compressive strength (2.93 MPa) was obtained with the 90% content of waste, which resulted in improvement of this property, since the clay without waste presented a lower value (2.16 MPa). The highest compressive strength value (0.69 MPa) in dry spheres also occurred for 90% of waste content. The values of water absorption, apparent porosity, loss on ignition and firing shrinkage decreased by increasing the raw clay waste content, while the value of apparent density increased with the waste content, indicating that the raw clay waste promotes the densification of ceramic bodies. The fluxing oxides contained in waste helped burn the specimens, because they minimize the effects of adverse conditions, such as, the low temperature 850ºC practiced in the industry and the use of the kaolinitic clay, which is more refractory. And the fine granulometry of the waste promoted the filling of the interstices between the clay grains promoting the physical packaging; and with that, there was the increase of strength in the specimens.

Table 3. Average values of the ceramic properties of spheres

Waste(%)	LOI(%)	WA(%)	AP(%)	AD(gcm^{-3})	FS(%)	σ_D(MPa)	σ_B(MPa)
0	14.34	25.38	37.92	1.54	12.03	0.61	2.16
10	14.35	24.93	39.25	1.54	10.45	0.56	1.50
20	13.76	24.83	38.19	1.54	9.34	0.56	1.54
30	13.32	23.97	37.60	1.57	9.09	0.56	1.69
40	13.14	23.86	37.39	1.57	8.79	0.59	2.00
50	12.26	22.47	36.47	1.64	8.39	0.65	2.07
60	12.21	22.13	36.25	1.64	7.95	0.65	2.27
70	11.65	21.65	35.99	1.64	7.39	0.68	2.35
80	11.65	21.41	35.31	1.67	7.21	0.68	2.52
90	11.35	21.09	34.76	1.67	6.83	0.69	2.93
Reference*	6.00 to 15.70	≤ 25.00	≤ 35.00	1.50 to 2.00	2 to 17	-	-

Note: LOI= loss on ignition; WA= water absorption; AP= apparent porosity; AD= apparent density; FS=firing shrinkage; σ_D=compression strength after drying; σ_B= compression strength after burning.
Note:*Souza Santos [10].

Considering the referential limits [10] described in Table 3, the water absorption, apparent density, loss on ignition and firing shrinkage values met the limits at all the raw clay waste

contents. The porosity met the limit with 90% of waste. The porosity values were influenced by the properties of clay (main component of waste), such as, high value of loss on ignition.

Conclusions

Chemical and mineralogical characterization showed that clay is predominantly kaolinitic, containing adequate amounts of quartz and iron. The clay and the raw clay waste may be considered silica aluminous materials. In all the compositions studied, the values of ceramic properties (less apparent porosity) meet the requirements for structural ceramic. Apparent porosity only meets these limits with 90% of waste content. The results show that the addition of waste improves the evaluated properties significantly. It can thus be concluded that the raw clay waste especially influences the formation of the glassy phase of the ceramic body, reducing water absorption, increasing the densification, including the comparison of the values obtained from clay without waste. The reuse of raw clay waste in the clayey mass can contribute to the sustainability of ceramics sectors, reducing raw materials consumption and avoiding waste disposal in landfills. It becomes a feasible alternative for the ceramic industry becomes a green industry. The paper shows the technical feasibility of using spheres, and industrial firing, in studies about the incorporation of industrial wastes in the ceramic industry.

Acknowledgments

The authors thank Federal Institute of Espírito Santo, Departament of Metalurgical and Materials Engineering of Polytechnical School of State University of São Paulo, and CAPES (Coordination for the Improvement of Higher Level Education Personnel) for the financial support.

References

[1] ANICER. Dados oficiais. RJ. 2014. [Access on 12 mar. 2015] available in:<http://www. anicer.com.br/index.asp?pg=institucional.asp&secao=3&categoria=60&selMenu=4>.
[2] Cerâmica Vermelha – Ministério do Desenvolvimento do BR. Termo de referência. [Access on 20 aug. 2015] Available in: < http://www.mdic.gov.br/arquivos/dwnl_1295436730.pdf>.
[3] F.P. Gouveia, R.M. Sposto . "Incorporação de chamote em massa cerâmica para a produção de blocos. Um estudo das propriedades físico-mecânicas". *Cerâmica*, 55 (2009), 415-419.
[4].D.C. Fastofski et al. "Metodologia de caracterização de resíduo de cerâmica vermelha para emprego como material pozolânico em pasta de cimento" (Paper presented at the 5th Fórum Mundial de Resíduos Sólidos, São Leopoldo, Rio Grande do Sul, 2014).
[5] Associação Brasileira de Normas Técnicas. NBR 10007, Sampling of solid waste. RJ. 2004.
[6] _____. NBR 6459, Soil - Determination of the liquid limit. RJ. 1984.
[7] _____. NBR 7180, Soil - Determination of the plastic limit. RJ. 1984.
[8] R.Y. Miyahara, G.H.R.H.Furlan, F.R.Valenzuela-Diaz, S.M.Toffoli. "Correlação entre medidas de resistência mecânica de corpos de prova de argila conformados manualmente e por prensagem uniaxial" (Paper presented at the 48ºCongresso Brasileiro de Cerâmica, PR, 2004).
[9] A.S. Reis, V.P. D.Sagrillo, F.R. V.Diaz. "Caracterização de resíduo de massa cerâmica crua para aproveitamento em cerâmica vermelha" (Paper presented at the 70º ABM, RJ, 2015).
[10] Persio S. Santos. *Tecnologia das argilas* (São Paulo, SP: Edgard Blucher,1975), v.1 e 2.
[11] E.A. Hildebrando, J.A.S. Souza, R.S. Angelica, R.F. Neves. "Application of bauxite waste from Amazon region in the heavy clay industry". *Materials Research*,16, n.6 (2013), 1418-1422.
[12] R.S. Macedo et al. "Study of clays in red ceramic". *Cerâmica*. 54 (2008), 411-417.

AUTHOR INDEX
REWAS 2016

W

X

Y

Z

SUBJECT INDEX
REWAS 2016

T

U

V

W

Z